THEORETICAL INVESTIGATIONS IN HELIOSEISMOLOGY

by

EUGENE M. LAVELY

B.S., Physics
Columbia University
(1983)

SUBMITTED TO THE DEPARTMENT OF EARTH,
ATMOSPHERIC AND PLANETARY SCIENCES
IN PARTIAL FULFILLMENT OF THE REQUIREMENTS
FOR THE DEGREE OF

DOCTOR OF PHILOSOPHY

at the

MASSACHUSETTS INSTITUTE OF TECHNOLOGY

FEBRUARY 1990

Signature of Author _____
Department of Earth, Atmospheric and Planetary Sciences
February 9, 1990

Certified by _____
Thomas H. Jordan
Department of Earth, Atmospheric and Planetary Sciences
Thesis Supervisor

Accepted by _____
Thomas H. Jordan
Chairman, Department Committee

THEORETICAL INVESTIGATIONS IN HELIOSEISMOLOGY

by

EUGENE M. LAVELY

Submitted to the Department of Earth, Atmospheric and Planetary Sciences
on February 9, 1990 in partial fulfillment of the requirements for the
Degree of Doctor of Philosophy

ABSTRACT OF THE THESIS

The observable frequencies, amplitudes, and linewidths of the normal modes of the Sun depend on a variety of factors. The degenerate frequencies of the modes are determined by the radial variation of the thermodynamic variables. The split frequency spectrum depends primarily on the differential rotation, but is also affected by aspherical structures such as the velocity field of large scale convection, and magnetic fields. Modal energies are determined by, among other things, the mode excitation mechanism and nonlinear modal interactions. The latter can lead to exchange of energy among modes. Modal lifetimes are controlled by dissipative processes such as radiative damping. A major goal of helioseismology is to devise theories which connect the the observable properties of the modes (and their time variation) to physical processes and structures in the Sun. In this way the Sun can be used as a laboratory in which to test the theory of stellar structure, the physics of the equation of state, theories of convection (including mixing length theory), and conditions in the core relevant to neutrino production.

The solution to helioseismological problems can generally be separated into two principal categories; the forward problem and the inverse problem. The forward problem consists of identifying a physical variable (or process) of interest and deriving a theory which relates observable properties of the modes to model parameters which fully characterize the variable (or process) . The inverse problem consists of applying

inverse theory to the data to estimate relevant variables and processes. Subsequently, conclusions are drawn pertaining to the physics of the problem.

Solar oscillations can be described with classical physics, but mathematical and physical analogues with quantum mechanics are pervasive. Information about the aspherical structure of the Sun is mathematically encoded in an object called the supermatrix. It is composed of the general matrix elements familiar to workers in atomic physics. Each mode is identified by a set of quantum numbers: radial order n, harmonic degree l, and azimuthal order m. Each mode $k = (n, l, m)$ is a member of a multiplet ${}_nS_l$ which is $(2l + 1)$ dimensional since $-l \leq m \leq l$. For a spherically symmetric Sun, the $(2l + 1)$ modes are degenerate (*i.e.*, they all have the same frequency ω_{nl}). Deviations from spherical symmetry, such as differential rotation, convection, and magnetic fields, breaks the symmetry, and induces splitting of the multiplet and coupling among the modes. The strength of coupling between modes k and k' is determined by the general matrix element. The new frequency and displacement pattern associated with the modes for the aspherical Sun is determined by the eigenvalues and eigenvectors of the supermatrix. Helioseismologists typically parameterize the frequency splittings in terms of the splitting coefficients a_i. The latter are defined by the relation $\omega_k = \omega_{nl} + l\sum_{i=0}^{N} a_i P_i(-m/l)$, where the P_i are the Legendre Polynomials. Bulk rotation is fully parameterized by the a_1 coefficient.

In Chapter (2), we present a theory which may be used to determine the influence of long-wavelength convection on modal frequencies and amplitudes. The principal theoretical result is the general matrix element for convection. Extensive numerical calculations were performed using a realistic convection model provided to us by Dr. Gary Glatzmaier. There are two principal numerical results. The first result is that poloidal and toroidal velocity fields can together generate an even component to the frequency splitting of a given multiplet. This effect could partially explain the even component observed in the data *i.e.*, the non-zero a_2 and a_4 coefficients. To date, this component has been attributed to magnetic fields. The second result is that convection induced self-coupling of the modes gives rise to fluctuations in

the differences $a_1 - a_1^{bulk}$ comparable in magnitude to the fluctuations measured by observers. Estimates obtained to date of the radial variation of the bulk rotation may be biased since observers ignore the effect of convection on the frequencies. The spatial and temporal basis functions of the oscillatory modes for a Sun with nonaxisymmetric flow fields do not separate in the observer's or inertial frame. This effect depends quadratically on the bulk rotation rate and the convective flow field. We ignored this complicated effect in the numerical calculations. Therefore, the numerical results are accurate only to first order in the bulk rotation rate and the convective flow field.

In Chapter (3) we derive the kinetic equation for p modes to determine the time evolution of modal energies due to nonlinear p mode coupling. An expression for modal frequency shifts is also given. Kumar and Goldreich have used the theory of three mode coupling to argue against overstability mechanisms as the source of the p modes. Their calculations were in planar geometry with an idealized atmosphere. Our results are in spherical geometry, and can be used for a star with arbitrary thermal stratification.

In Chapter (4) we investigate the influence of perturbations to the spherically averaged structure of the Sun on modal degenerate frequencies, and the dependence of these frequencies on important free parameters in stellar evolution theory such as the mixing length.

Thesis Supervisor: Professor Thomas H. Jordan

Title: Professor of Geophysics

Members of the Thesis Committee:

Professor Thomas Jordan

Professor Edmund Bertschinger

Professor Steven Stahler

Professor Thomas Herring

Dr. Michael Ritzwoller

Dr. Adriaan Van Ballegooijen

TABLE OF CONTENTS

- ABSTRACT OF THE THESIS 1
- ACKNOWLEDGEMENTS 11
- DEDICATION 14
- PREAMBLE 15

CHAPTER 1

INTRODUCTION

- I. OVERVIEW 17
  - a) The Significance of Helioseismology 17
  - b) p Mode Phenomenology 17
  - c) Stable and Unstable g modes 19
  - d) Mode Excitation 19
  - e) Turbulent Motions 20
  - f) The Granules and Supergranules 22
  - g) The Giant-cells 22
  - h) The Helium Abundance 23
  - i) Convective Overshoot 25
  - j) Mixing Length Theory 25
  - k) The Mean Radial Structure of the Convection Zone 26
  - l) The Solar Neutrino Problem 27
  - m) The Solar Differential Rotation 27

• II. SUMMARY OF THE MAJOR CHAPTERS OF THE THESIS 28

a) Chapter 2; The influence of convection on p modes 28

b) Chapter 3; Nonlinear interactions among p modes 30

c) Chapter 4; The influence of perturbations to spherical structure on p mode frequencies 31

• REFERENCES 32

CHAPTER 2

THE EFFECT OF LARGE SCALE CONVECTIVE FLOWS ON HELIOSEISMIC OSCILLATIONS

• ABSTRACT 35

• I. INTRODUCTION 37

a) An Overview of Heliseismology 37

b) The Influence of Convection on Oscillation 38

c) Velocity Fields in the Convection Zones 40

d) An Overview of this Paper 42

• II. JUSTIFICATION OF ASSUMPTIONS 43

a) The Assumptions of Our Approach 43

b) Physical Justification of the Assumptions of our Approach 43

i) Convection-Oscillation Coupling is not Significant below the Top Few Scale Heights 43

ii) The Convection is Anelastic 45

iii) A Linearized Treatment Suffices 47

iv) The Flow Field is Steady 49

- c) Frequency Splitting from Small-scale Structure....49
- d) Summary Remarks....50
- III. REFERENCE FRAMES....50
- IV. THE EQUATION OF MOTION....52
  - a) The Equilibrium Model....53
  - b) The Perturbed Equilibrium Model....54
  - c) The Reference Model....55
  - d) The Perturbed Reference Model....57
  - e) The Equations of Motion for a General Model Perturbation....62
- V. PERTURBATION THEORY....63
  - a) The normal modes....63
  - b) Notation and Terminology....64
  - c) Quasi-degenerate Perturbation Theory....65
  - d) The Perturbation Equation for Convection....69
- VI. THE GENERAL MATRIX ELEMENT FOR CONVECTION....70
  - a) The Flow Field and the Thermodynamic Variables....70
  - b) The General Matrix for a General Flow Field....72
  - c) The General Matrix with the Incorporation of the Anelastic Constraint74
  - d) The General Matrix for Terms Linear in $\mathbf{u}_0$ and Ω....75
  - e) The General Matrix for Perturbations to the Thermodynamic Variables76
  - f) The General Matrix....78
- VII. QUALITATIVE INTERPRETATION OF QUASI-DEGENERATE PERTURBATION THEORY....78

a) Selection Rules 79

b) Qualitative Discussion of Sensitivity 80

c) The Hybrid Eigenfunctions 81

- VIII. SELF-COUPLING 82

a) General Toroidal Flows 82

b) Differential Rotation 83

- IX. NUMERICAL RESULTS 85

a) The Velocity Models 85

i) The Differential Rotation Model 87

ii) The Convection Model 87

b) The Numerical Implementation of Self and Full Coupling 88

i) The Determination of the Eigenspace 88

ii) Assembling the Supermatrix 90

c) The Effect of the Flow Field on Frequencies 90

d) The Effect of the Flow Field on the a_i Coefficients 94

e) The Effect of the Flow Field on the Eigenfunctions 95

- APPENDIX 2A: THE EQUATIONS OF MOTION IN THE SOLAR FRAME 97

- APPENDIX 2B: CALCULATING THE GENERAL MATRIX 98

- APPENDIX 2C: AN ALGORITHM FOR THE CALCULATION OF WIGNER 3-j SYMBOLS 102

- APPENDIX 2D: INCORPORATING THE ANELASTIC CONSTRAINT INTO THE GENERAL MATRIX 105

• APPENDIX 2E: THE HERMITICITY OF THE GENERAL MATRIX ... 107

• ACKNOWLEDGEMENTS ... 109

• REFERENCES ... 109

• Table 1 ... 113

• FIGURES (1A)-(10B) ... 114-138

CHAPTER 3

THREE MODE COUPLING OF SOLAR OSCILLATIONS 1. THEORY

• ABSTRACT ... 140

• I. INTRODUCTION ... 141

• II. COHERENT MODE COUPLING ... 145

a) Derivation of the Dynamical Equation ... 145

• III. WEAK TURBULENCE THEORY ... 149

a) The Random Phase approximation ... 149

b) Derivation of the Kinetic Equation ... 151

c) Determination of the Frequency Shift ... 158

• IV. DERIVATION OF THE NONLINEAR INTERACTION COEFFICIENT 162

a) Equations of Motion of the Quiescent State ... 162

b) The Perturbed Equation of Motion ... 162

c) Calculation of First and Second Order quantities ... 163

e) The Nonlinear Interaction Coefficient ... 167

• APPENDIX 3A: CALCULATION OF WIGNER 3-j SYMBOLS 169

• ACKNOWLEDGEMENTS 171

• REFERENCES 172

CHAPTER 4

HELIOSEISMOLOGICAL APPLICATIONS OF RAYLEIGH'S PRINCIPLE

• ABSTRACT 174

• I. INTRODUCTION 175

• II. ENTROPY AND DENSITY STRATIFICATION 177

a) The Stratification Parameter η 180

b) The Stratification Parameter as an Instability Criteria 181

• III. THE FORWARD PROBLEM 184

• IV. THE THEORETICAL RELATIONSHIP OF THE STRATIFICATION PARAMETER TO PREDICTIONS OF MIXING LENGTH THEORY 191

a) Overview of Mixing Length Theory 191

b) Inferring the Mixing Length Ratio from Helioseismic Data 197

• APPENDIX 4A: DERIVATION OF PERTURBATION EQUATIONS 198

a) Derivation of equation (4.82) 198

b) Derivation of equation (4.83) 199

c) Derivation of equation (4.84) 199

d) Derivation of equation (4.85) 199

e) Derivation of equation (4.86) 201

f) Derivation of equation (4.87) 202

g) Derivation of equation (4.88) 204

- ACKNOWLEDGEMENTS 205

- REFERENCES 205

CHAPTER 5

CONCLUSION

- CONCLUSION 208

ACKNOWLEDGEMENTS

The transformation from a student to a scientist is not an easy one. Young scholars are taught the scientific method from grade-school onwards. However, if my experience is any guide, I believe the only way to acquire the qualities necessary to become a scientist is by apprenticeship. I have been most fortunate to work closely with three scientists: Don Forsyth who patiently initiated me into the world of research, Tom Jordan whose work in geophysics has always been an inspiration to me, and Mike Ritzwoller who has had a fundamental influence on me since we met in 1987. It is to Mike that I am most grateful. I have benifitted greatly from his outstanding generosity, personality, and scientific qualities. The daily scientific conversations I have had with Mike, and his criticism of my scientific ideas and scientific writing have led to great improvements in the work presented here. In addition, I have benefited by observing the clarity of his thought, the logic of his approach to science, and the high standards he has set for himself in his scientific work.

I have been fortunate in many ways. I have the advantage of a sister and loving parents who have always encouraged me to excel, and the example of a literary father who is fundamentally responsible for instilling in me the appreciation of an intellectual life. My mother has always experienced my every failure and success just as vividly if not more so than I. It pleases me greatly to acknowledege her here.

My first exposure to the scientific life was at Columbia College. Two professors there have made a deep impression on me. They are Professor Isadore Epstein (now retired) of the astronomy department, and Professor Duong H. Phong of the math department. Professor Epstein is the only true Renaissance man I have ever had the fortune of knowing. I am very grateful to him and his wife for their friendship. Professor Phong is a brilliant mathematician from whom I learned almost all of my math. I still remember his outstanding lectures vividly, not to mention his words of wisdom and witicisms.

I have benefited greatly from the academic excellence at M.I.T. I have had interac-

tion with faculty members from my own department and from the physics department. I am particularly grateful to Edmund Bertschinger and Steve Stahler for the interest they have taken in my work. I have never met anyone who understands astrophysics and the practice of science as profoundly as Edmund Bertschinger does. I am indeed fortunate that his generosity is as great as his intellect. I have enjoyed my conversations with Steve and have benefited from his papers and public talks. I am grateful to my advisor, Tom Jordan, for allowing me to do astrophysics in a geophysics department. He has supported me continuously and particularly during critical junctures of my career. Tom was generous enough to allow me to pursue my own ideas. The freedom and encouragement he has given me, and the trust he has had in me have been crucial to the completion of this thesis. Tom's work in free oscillation theory is what initially attracted me to subject of normal modes. A course he taught on free oscillations of the earth is one of the most outstanding courses I have ever taken and continues to serve me well to this day. He presented the subject with such generality and mathematical elegance that most of the material was equally applicable to the Sun.

I would like to thank the members of my thesis committee Tom Jordan, Tom Herring, Steve Stahler, Edmund Bertschinger, Mike Ritzwoller, and Ad Van Ballegooijen. I am grateful to Ad for the many conversations we have had over the last three years. He has helped me to overcome several serious stumbing blocks in my work.

The pleasure of working in helioseismology is due in no small part to the members of the community. My colleagues have become my friends and I would like in particular to mention Pawan Kumar, Steve Tomcyzk, Sylvain Korzennik, and Bill Jeffrey. It has always been a pleasure to interact and socialize with Tim Brown, Tom Bogdan, Peter Gilman, Ken Libbrecht, Bob Noyes, and Ad Van Ballegooijen.

From the first time I indicated an interest in helioseismology, Juri Toomre has encouraged me and has made available opportunites to work with the community. I am deeply grateful for his generosity. Aside from his scientific work, his personality and wit are accomplishments in themselves and have greatly enriched the commu-

nity. Douglas Gough, the godfather of helioseismology is an amazing person. I am constantly in awe of his voice, his scientific prowess, and his wit. His accute mind easily unearths even subtle errors or inconsistencies even as one speaks in public. Suspecting that some day he may read some of the material in this thesis, I wrote every sentence and derived every equation with great care, and constantly asked myself "What would Douglas say?". However, I know there are some things with which he will take exception to; these items were included nonetheless.

My fellow graduate students from M.I.T. and Harvard have made my tenure as a graduate student most rewarding. I would like in particular to mention Mark Murray, Kurt Feigl, Mike Bergman, Justin Revenaugh, Jeff Love, Andy Jackson, Lind Gee, Greg Beroza, Julianna Hsu, and Phillip Podsialwonski.

I am grateful to NASA for supporting me for three years through their graduate student fellowship program. I am grateful to Katherine Ware for making life here at M.I.T. so easy.

Bob Noyes has played a pivotal role in my life. His *Scientific American* article on helioseismology led to my thesis topic, and he introduced me to my fiance. Last, but not least, I wish to mention Julie Stiffler and our dog Merckx who make it all so much more worthwhile.

DEDICATION

This thesis is dedicated to the memory of my grandmother, Emma Fernandez de Rodriguez (1907-1990).

PREAMBLE

In those Hyperborean regions, to which enthusiastic Truth, and Earnestness, and Independence, will invariably lead a mind fitted by nature for profound and fearless thought, all objects are seen in a dubious, uncertain, and refracting light. Viewed through that rarefied atmosphere the most immemorially admitted maxims of men begin to slide and fluctuate, and finally become wholly inverted; the very heavens themselves being not innocent of producing this confounding effect, since it is mostly in the heavens themselves that these wonderful mirages are exhibited.

But the example of many minds forever lost, like undiscoverable Arctic explorers, amid those treacherous regions, warns us entirely away from them; and we learn that it is not for man to follow the trail of truth too far, since by so doing he entirely loses the directing compass of his mind; for arrived at the Pole, to whose barrenness only it points, there, the needle indifferently respects all points of the horizon alike.

Pierre (1852)

Herman Melville

CHAPTER 1

INTRODUCTION

Not to want to say, not to know what you want to say, not to be able to say what you think you want to say, and never to stop saying, or hardly ever, that is the thing to keep in mind, even in the heat of composition.

Molloy (1947)

Samuel Beckett

INTRODUCTION

In §I of this introduction, we briefly review p mode phenomenology, describe certain aspects of the internal structure and dynamics of the Sun, and provide specific suggestions on how helioseismology can be used to probe the solar interior. In §II, we summarize the major results of this thesis.

I. OVERVIEW

a) The Significance of Helioseismology

Until the emergence of helioseismology, data to verify the theory of stellar structure was confined to a small set of observable parameters such as stellar masses, radii, luminosities, and effective surface temperatures. Even these parameters are not always available. The neutrino flux of a star can constrain core conditions, but such a measure is available for the Sun only. Though the theory of stellar structure and evolution is able to rationalize the observed relations between mass, radius, luminosity, and age of the Sun, there are important details of physics which can only be investigated with the diagnostic power of helioseismology. Since the degenerate frequencies of the normal modes of the Sun are integral measures of its spherically averaged internal structure, it is possible to obtain a detailed picture of the interior by application of inverse theory. Moreover, the fine frequency structure is a measure of the internal dynamics and departures from spherical symmetry. Even though the Sun is an ordinary G2 main sequence star, determination of the structure and processes operating in its interior will have implications for much of astrophysics. For example, a helioseismological determination of the Helium abundance would have cosmological significance.

b) p Mode Phenomenology

The resonant modes are confined to the solar interior. They have an upper reflection point near the surface due to the rapidly decreasing density there, and they

decay exponentially in amplitude beneath their classical turning point. The depth of the turning point is determined approximately by the condition

$$\frac{\omega}{\sqrt{l(l+1)}} = \frac{c(r_{t.p.})}{r_{t.p.}} \tag{1.1}$$

where ω is the angular frequency of the mode, l is its harmonic degree, c is the adiabatic sound speed, and $r_{t.p.}$ is the radius of the turning point (see Christensen-Dalsgaard *et. al.* 1985). The vertical component of wave motion vanishes at $r = r_{t.p.}$. The number of zero crossing of the eigenfunctions describing the mode displacement is given by the radial order n. The energy of low n and high l modes is confined primarily near the surface. The high n and low l modes propagate through the center of the star. The frequency of each mode is an integral measure of the structure of the star where its amplitude is appreciable; it is asymptotically related to the travel time between the turning point and upper reflection point.

The observable modes with the most power have periods which range between three and seven minutes. The power of p modes is confined to ridges (overtone branches) on an $\omega-k$ dispersion diagram where k is the wavenumber. The wavenumber of a p mode at the surface with harmonic degree l is $\sqrt{l(l+1)}/R_{\odot}$, where $R_{\odot}$ is the solar radius. Those modes which have an upper reflection point beneath the atmosphere where the measured line spectra are formed can also be found on $\omega - k$ dispersion diagrams produced to date. Their signal is detectable since they are able to tunnel some distance beyond their resonant cavity. Highly accurate measurements of the frequencies of the modes have recently become available (*e.g.*, Duvall *et al.* 1988). Libbrecht and Kaufman (1988) report frequency measurements up to at least $l = 1320$. The observed frequencies generally match the frequencies predicted for standard solar models to within 1% (the observational uncertainties are as low as 1 part in 10000).

The amplitude of an individual p mode at the solar surface is typically 15 cms^{-1}. The collective velocity of the p modes near the surface is ~ 0.5 kms^{-1}. The theory of helioseismology is considerably simplified since the amplitudes of individual acoustic

modes are very small. In many applications, it suffices to use linearized, adiabatic theories. The energy of a typical p mode is $\sim 3 \times 10^{27}$ ergs , and there are ~ 10 million modes, so the total p mode energy is $\sim 10^{34}$ ergs (Libbrecht 1988). A p mode can only propagate in a region if its frequency is greater than the radius-dependent acoustic cut-off frequency $\omega_{a.c.}$. For an isothermal atmosphere, $\omega_{a.c.} = c/H_p$ where H_p is the pressure scale height. For an ideal gas, $\omega_{a.c.}$ varies with the inverse square root of the temperature, and therefore, the highest $\omega_{a.c.}$ occurs at the temperature minimum in the solar atmosphere, which corresponds to a period of about 185 seconds.

c) Stable and Unstable g modes

There are several types of motion in the Sun including acoustic modes of §*b* (often referred to as p modes since pressure is their restoring force), and stable and unstable g modes. The energy of the stable g modes is concentrated in the core and the radiation zone; they are evanescent in the convection zone. These modes have not been observed to date since they have nearly vanishing amplitudes near the surface. The unstable g modes are confined to the convection zone and correspond to the convective motions themselves. When their amplitude reaches a certain level, nonlinear effects begin to dominate and they degenerate into turbulence. The p mode motions can be separated from the unstable g mode motions by applying temporal and spatial filters to the Dopplergrams since the power of the p modes is confined to distinct ridges on an $\omega - k$ dispersion diagram, whereas the g modes have lower frequencies and all wavenumbers for a given frequency. Most often, investigators ignore the coupling between p modes and g modes. For the stable g modes, wave propagation is possible only in the atmosphere above the photosphere and in regions below the convection zone where buoyancy can be restoring rather than destabilizing. They are confined to regions where their frequency is less than the Brunt-Väisälä frequency. The stable g modes have long periods (exceeding forty minutes).

d) Mode Excitation

The excitation of the p modes is still an unresolved issue. The excitation mechanisms fall into two broad classes, excitation by turbulent fluctuations and self-excitation (*e.g.*, the κ mechanism). In the latter process, acoustic waves modulate the opacity and tap energy from the radiation field. This is analogous to the κ-mechanism which drives the large-amplitude pulsations of the Cepheids. Such driving is probably weaker in the Sun. Linear stability calculations involving this mechanism are ambiguous because of the uncertainty involved in including turbulent viscous damping of the modes.

Recent results suggest that solar p modes are driven stochastically by turbulence (Goldreich and Keeley 1977a, b; Goldreich and Kumar 1988; Kumar and Goldreich 1989). The treatment of this problem is interesting in itself, but since the frequencies of the p modes are slightly affected by the turbulence (see Brown 1984; Goldreich and Kumar 1988), it is an important step in the diagnosis of solar structure.

Goldreich and Kumar (1988) have calculated the emissivity and absorptivity of acoustic radiation by a turbulent fluid. The processes which generate acoustic waves from turbulence lead dominantly to monopole, dipole, and quadrupole acoustic radiation. When a fluid blob loses its heat at the solar surface, it shrinks in size and sinks. The shrinking changes the volume of the blob which leads to monopole radiation. The action of gravity on the blob results in dipole radiation. If two blobs push against one another, then the force on one is equal and opposite to the reaction force on the other, and the two blobs together emit quadrupole radiation, and this is the dominant process (see Lighthill 1952, 1954). The acoustic radiation which is emitted by the blobs can also be reabsorbed by them, which limits the amplitudes of the modes. Since the absorption and emission processes depend strongly on the Mach number (the ratio of the convective speed to the sound speed), it is straightforward to show that convection-oscillation coupling is significant only in a very thin shell near the solar surface (see Chapter 2).

e) Turbulent Motions

The power of turbulence is spread over a wide range of k for fixed ω. The total

energy of the p modes is small compared to the total kinetic energy in the convective motions, the latter being $\sim 5 \times 10^{38}$ ergs. Approximately 5×10^{34} ergs of this energy resides in the top scale height of the convection zone where the characteristic overturn time is ~ 5 minutes. The overturn time for the longest wavelength g modes is $\sim$ one month. The average convective velocity below the top few scale heights varies from ~ 15 ms^{-1} to ~ 100 ms^{-1}.

Turbulence is usually described in terms of characteristic length and time scales. The largest energy bearing eddies have length-scale $\sim H$, velocity magnitude $\sim v_H$, and lifetime $\tau_H \sim H/v_H$. The eddies cascade to scale l where they are dissipated by molecular viscosity. Energy dissipation is negligible in the inertial range $l \leq h \leq H$. Therefore, assuming the flow of energy per unit volume for eddies of size h in the range l to H is constant, one obtains $\rho v_h^2/\tau_h = \rho v_H^2/\tau_H$. This implies the Kolmogoroff scaling $v_h \sim (h/H)^{1/3} v_H$ and $\tau_h \sim (h/H)^{2/3} \tau_H$. The Mach number of an eddy of size h is given by $M_h \sim v_h/c$ where c is the adiabatic sound speed $(P\Gamma_1/\rho)^{1/2}$. We denote M_H simply by M. The pressure fluctuations arising from the Reynolds stresses have magnitude $\sim \rho v_h^2$. Assuming perturbations in entropy can be neglected, the perturbations in density may be obtained from the pressure perturbation by using $\Delta P = (\partial P/\partial \rho)_s \Delta \rho$ so that the density fluctuations have magnitudes $\sim \rho M_h^2$.

To determine the smallest scale of turbulent motion we require the Kolmogoroff length, time, and velocity microscales which are given respectively by $\eta = (\nu^3/\epsilon)^{1/4}$, $\tau = (\nu/\epsilon)^{1/2}$, and $v = (\nu\epsilon)^{1/4}$ where ϵ is the dissipation rate per unit mass in units of m^{2}s^{-3}, and ν is the kinematic molecular viscosity in units of $m^2 s^{-1}$ (Tennekes and Lumley 1972). The Reynolds number for an eddy of size H is given by $\mathcal{R}_e = v_H H/\nu$. The cascade of eddies to smaller scales has a termination point because viscosity dissipates the energy of small scale motions into heat. The Reynolds number in the Sun is huge but dissipation nonetheless occurs because the nonlinear terms in the equation of motion always generates scales of motion small enough to be affected by the viscosity, the smallest scale η always adjusting to the value of ν. Tennekes and Lumley (1972) argue that in a turbulent flow, the rate of energy supply to the largest

eddies should be equal to the rate of dissipation so that we obtain $\epsilon \sim v_H^3 / H$. Using the above definitions it can be shown the smallest scale of motion is given by $l \sim H/\mathcal{R}_e^{3/4}$.

f) The Granules and Supergranules

The scales of motion in the Sun range from the Kolmogoroff microscales to the differential rotation. In between are the granules, supergranules, giant cells, and energy-bearing eddies.

The granular velocities are ~ 1 km s^{-1}, their horizontal scales are ~ 1400 km and they lifetimes $\sim 6-15$ minutes (Bray *et al.* 1984). The Hydrogen ionization in the top scale heights liberates ionization energy which is converted to thermal energy. This enhances the convective instability by contributing to the buoyancy of the gas. Also ∇_r becomes very large because of the large opacity there. Therefore, the convective instability is very large but the convective efficiency is low due to the very low density in this region, radiative losses, and the collisional disspation of kinetic energy. Thus, the convective velocities become very large to transport the heat flux from below.

The supergranules are a cellular pattern with a horizontal divergence from a central point in each cell. The supergranules have mean horizontal velocities $\sim 0.3 - 0.5$ kms^{-1}, mean vertical velocities $\sim 0.1 - 0.2$ kms^{-1}, mean cell sizes of ~ 35000 km, and their mean lifetimes are ~ 20 hours (Bray *et al.* 1984). The scale of the supergranules may be related to the depth of the He ionization zone. The granulation and supergranulation patterns appear to be uniform from the poles to the equator.

g) The Giant-cells

The existence of giant-cells has not been directly confirmed. If they do exist at the surface of the Sun, their amplitudes are less than 10 ms^{-1} (Howard and Labonte 1980; Labonte *et. al.* 1981; Brown and Gilman 1984). However, the Sun displays a number of features which are suggestive of sustained large-scale motions (Gilman 1987). These include the persistent large-scale patterns in the solar magnetic field,

the coronal holes which survive several solar rotation periods without being sheared apart by differential rotation, and the existence of active longitudes where new active regions preferentially arise. Observation of the distinct cellular motions of granules and supergranules suggests that for thermal convection there are preferred scales of motion. This trend may continue deeper in the convection zone. In the mixing length picture of convection, the scale of the convecting eddies is set by the pressure scale-height so that one would expect layers of convection with ever decreasing vertical scale as the surface is approached. However, both linear and nonlinear models (Gough *et al.* 1976; Grahm 1975) show that even when the fluid is compressible, and the stratification includes several scale heights, convection which spans the entire unstable layer is favored. Thus, for the Sun, patterns of motion with horizontal dimensions up to $\sim 200,000$ km would be expected. In addition, the space-lab experiment of thermal convection (Hart *et al.* 1986), and the numerical simulations of Glatzmaier (1984) and Gilman and Miller (1986) suggest that large and sustained patterns of motion may exist in the Sun with scales approaching the depth of the convection zone.

h) The Helium Abundance

Theoretical solar models do not place clear constraints on the abundances. Models can be built over a wide range of hydrogen abundance X and Helium abundance Y, with little basis for preferring one over another. The equation of state is largely determined by these two elements. It would be of interest to determine their radial variation within the Sun. There are several inverse problems which can be posed to address this issue. To determine the Helium abundance, one may use the fact that the first adiabatic exponent Γ_1 is sensitive to the degree of ionization of the gas. There is virtually no overlap between the H and HeI ionization zones. Therefore, the radial profile of Γ_1 in the HeI ionization zone is a strong function of the Helium abundance. In chapter four we derive forward perturbation problems involving the model parameter combinations (ρ, Γ_1), and (c, Γ_1) which can serve as the basis for

an inversion of Γ_1. This would involve a sequence of nonlinear iterative calculations. First an inversion would be performed in which the model parameters are adjusted from their starting values to minimize the difference between the observed and predicted frequencies. The forward problem is intrinsically nonlinear, and therefore the solution to the inverse problem will require several iterations. The next step could be one of several possibilities. First, one could compute in a monte-carlo type calculation a suite of solar models with different Helium abundances each with a slightly different Γ_1 profile to see which one best matches the profile required by the inversion. Alternatively, one could derive an equation relating perturbations in Helium abundance to perturbations in Γ_1 for each knot in the HeI ionization zone, and use the inversion results to determine the required perturbation to the Helium abundance. Such an equation is likely to be nonlinear, and will only implicitly determine the Helium abundance perturbation so that it must be solved iteratively. With this value in hand, a solar evolution calculation must then be performed to determine a self-consistent radial profile of the solar structure, and to determine which mixing length is required to match the surface boundary conditions (where the newly determined Helium abundance remains fixed). Of course, the constraint ($X + Y + Z = 1$) must also be satisfied where Z is the metal abundance. The heavy element abundance Z influences heavily the opacity. This is an important effect in the radiation zone since the radiative temperature gradient there depends on the opacity, but is almost of no consequence in the convection zone since the bulk of the convection zone convects very efficiently and therefore its temperature gradient is well approximated by the adiabatic gradient. Whichever method is used, the inverse problem is nonlinear, and therefore a new set of degenerate frequencies should be computed with the new solar model and the process outlined above should be repeated. Knowledge of the solar Helium is important to cosmologists. According to stellar evolution theory, the material in the convection zone has not been mixed with the products of the nuclear transformations in the core. Thus, the Helium abundance in convection zone should be the same as in the proto-sun.

i) Convective Overshoot

The large-scale dynamics of the convection zone is capable of being studied by using low and intermediate degree normal modes. These motions affect not only the fine frequency structure of any given multiplet ${}_nS_l$, but can change the radial stratification of the Sun, and thus, affect the degenerate frequencies ω_{nl} as well. For example, convective overshoot into the stably stratified radiation zone below the convection zone alters the thermal stratification there. The stratification parameter η is sensitive to this type of perturbation. An inversion for the radial profile of η would shed light on the problem of convective overshoot (which is often ignored in stellar structure codes). Chapter four contains a detailed discussion on how perturbations in η affect helioseismic frequencies. We also show there the dependence of η on the predictions of mixing length theory. One simplifying aspect of stellar structure theory as applied to the Sun, is the assumption that the core is unmixed. It could be that nonlinear g modes, or large-scale meridional circulations act to mix the chemical species in the core. Deduction of the stratification parameter from helioseismic data could be used to determine the validity of the no-mixing assumption (see Chapter 4).

j) Mixing Length Theory

The primary application of mixing length theory is to calculate the temperature gradient in convectively unstable regions of a star. Excellent descriptions of mixing length theory can be found in Cox and Giuli (1968), Gough and Weiss (1976), Gough (1977a, 1977b). By analogy with gas kinetic theory, mixing length approaches consider the fluid to be composed of turbulent 'eddies', 'parcels', or 'elements' which advect heat through a mean free path or mixing length l and then merge with their surroundings. An element is created as a result of instability, with the same properties on average as its immediate enviroment; it is accelerated by an imbalance between buoyancy forces, pressure gradients, and nonlinear advection processes, and may gain or lose mass by entrainment or erosion. It is as a result of ignoring different combinations of these processes, approximating the remaining ones in slightly different

ways, and making different assumptions about the geometry of the flow that different mixing length models have emerged. Mixing length contains free parameters not determined by the theory, the most important being the mixing length which is usually taken to be a constant times the pressure scale height. Mixing length theory can be calibrated since any formula used to evolve the Sun must match the present age, luminosity, and radius. In chapter 4 we show how the mixing length and the thermal stratification is related to helioseismic frequencies.

Near the surface of the Sun, the density is very low, and the radiative losses of the buoyant blobs are very high. The latter is true because the temperature differences between the blobs and the ambient medium are very high, and because the medium is optically thin. Therefore, the heat capacity of the blobs becomes very small. The same luminosity must be transported and therefore two things happen. The velocity of the blobs becomes very high to enhance the heat flux, and there is a transition from dominant convective transport to dominant radiative transport.

k) The Mean Radial Structure of the Convection Zone

The mean radial structure of the convection zone depends only on the integrated properties of the super-adiabatic region as we argue in the following. Below the strongly super-adiabatic boundary layer the Sun convects very efficiently and, thus, $\nabla = \nabla_{ad}$ to a high degree of accuracy where ∇_{ad} is the adiabatic temperature gradient. It follows from the definition of the second adiabatic exponent Γ_2 that

$$P = KT^{\frac{\Gamma_2}{(\Gamma_2 - 1)}} \tag{1.2}$$

in the adiabatic part of the convection zone where P and T, denote respectively the pressure and temperature, and K is a constant (in those regions where Γ_2 is a constant). For the Sun, at least, the primary use of mixing length theory is to determine the entropy jump across the super-adiabatic region. The entropy jump defines the adiabat of the convection zone and implicitly determines K in equation (1.2). The strength of convective instability is measured by $\nabla_r - \nabla_{ad}$ where ∇_r is

the radiative gradient. The radiative opacity κ_r becomes quite large in the H, He, and HeI ionization zones and the pressure there increases dramatically compared to the temperature because Γ_2 approaches unity in an ionizing region. Since ∇_r is proportional to $\kappa_r P/T^4$ the radiative gradient becomes very large. It reaches a peak value at the base of the HeI ionization zone and decreases roughly as $1/T^3$ until the depth where $\nabla_r = \nabla_{ad}$ (the base of the convection zone). Since P and T have been on an adiabat since the transition point to efficient convection (just beneath the strongly super-adiabatic layer), the peak value of ∇_r depends on the value of P and T at the transition point. These P and T values depend in turn on the entropy jump. Thus only the integrated properties and not the detailed structure of the super-adiabatic region are relevant to the structure of the rest of the Sun.

Since the Sun convects so efficiently, the temperature gradient through the bulk of the convection zone is determined by the adiabatic temperature gradient and is insensitive to the opacity. Of course, the particular adiabat depends on the mixing length. The radiation zone, on the other hand, has a temperature gradient given by the the radiative gradient ∇_r. Therefore, its structure depends strongly on the opacity.

l) The Solar Neutrino Problem

Helioseismology may someday yield estimates of the density ρ, sound speed c, and composition in the solar core. The low l and high n modes are sensitive to this part of Sun. Since the temperature can be calculated from the equation of state once ρ and c are known, the estimates of ρ and T can be used to calculate the neutrino flux (for a given composition). Current theories predict a flux three times larger than that observed. Before theories of nuclear and particle physics are adjusted to account for this discrepancy, it is essential to obtain accurate estimates of core conditions.

m) The Solar Differential Rotation

The Solar rotation varies with depth and latitude in the Sun. How it does so is crucial for testing theories of angular momentum transport and the solar dynamo.

The interaction between rotation and convection has a bearing on the latter. The mechanisms for $\alpha-\omega$ dynamo action require a radial gradient of the rotational rate Ω to convert poloidal to toroidal magnetic fields, and a radial gradient of Ω together with helicity (the scalar product of velocity and vorticity) to convert toroidal to poloidal field. The direction of motion of the resulting dynamo waves (and hence the direction of migration of magnetic flux) depends on the sign of the product of $d\Omega/dr$ and the helicity. The latter arises from the interplay of buoyancy and Coriolis forces. The sense of helicity in the bulk of the convection zone is such that $d\Omega/dr$ must be negative in order to reproduce the equatorword migration of low-latitude magnetically active regions.

Recent results by Brown *et. al.* (1989) indicate that a latitudinal variation of $\Omega(r,\theta)$ similar to that observed at the solar surface exists throughout the Sun's convection zone. The near constancy with depth of the latitudinal variation of $\Omega(r,\theta)$ confronts the $\alpha-\omega$ dynamo theory with severe difficulties. We show in chapter 2 how the long-wavelength convection can possibly bias the interpretation of frequency splittings which workers use to recover the rotation profile.

II. SUMMARY OF THE MAJOR CHAPTERS OF THE THESIS

Chapters two, three, and four were written in the style of the *Astrophysical Journal* since they are intended for publication.

a) Chapter 2; The influence of convection on p modes

Solar p modes are split and coupled by convective velocity fields and thermodynamic perturbations in the solar interior. We applied quasi-degenerate perturbation theory to calculate the influence of time-independent, global, long-wavelength, anelastic, laminar convection on p mode frequencies and amplitudes. The investigation was motivated by the many studies which have connected the solar dynamo, the observed surface magnetic activity, and the solar differential rotation profile with large-scale convective flows deep in the interior of the Sun. Models of the interaction between

p modes and convection are useful in that they provide theoretical predictions of the split frequency spectrum, amplitudes, and linewidths of the p modes, all quantities needed by observers to constrain the structures affecting their data. The convective velocity field was decomposed into a sum over poloidal and toroidal fields. The principal theoretical result is the general matrix element $K^{m'm}_{n'n,l'l}$ which governs the interaction between modes with quantum numbers $k = (n, l, m)$ and $k' = (n', l', m')$ due to convection. In the case of self coupling (coupling among singlets of a single multiplet) the general matrix element vanishes for poloidal velocity fields and for even degree toroidal flows. Therefore, in the self coupling approximation, only odd degree toroidal fields contribute to frequency splitting. Both poloidal and toroidal flows contribute to full coupling (coupling between singlets of different multiplets). Forward numerical calculations using a realistic convection model were performed to assess quantitatively the influence of convection on the modes. The numerical results indicate that convection systematically perturbs the singlet eigenfrequencies, sometimes by as much as 0.65 μhz for the sectoral ($m = \pm l$) singlets. This is a measurable quantity and ignoring its effect leads to erroneous estimates of the solar differential rotation profile. Unfortunately, to date, the effect of global, non-axisymmetric structure on helioseismic oscillations has been otherwise ignored.

In the self coupling approximation, frequency splitting of a multiplet is purely odd about the degenerate frequency ω_{nl}, but in the full coupling case aspherical convection generates a frequency spectrum with an even component about ω_{nl}. Thus, an expansion of the spectrum in terms of Legendre Polynomials requires even-ordered expansion coefficients. It has been conventional wisdom to ascribe even-ordered expansion coefficients required by actual data to large-scale axisymmetric magnetic fields. Our finding that convection can also contribute to the even coefficients can be understood ray theoretically. In an axisymmetric Sun, frequencies are uniquely associated with one mode, but this does not hold for an aspherical Sun. Instead the displacement pattern (which we call the hybrid eigenfunction), is a linear combination of modes. The set of modes which couple to the mode $(n, l, |m|)$ in the full coupling

case, is quite different from the set of modes which couple to the mode $(n, l, -|m|)$. Thus the hybrid eigenfunctions associated with these modes no longer possess the symmetry in the n, l, and m quantum numbers that they did in the self coupling approximation. They sample the Sun in a manner quite different from the axisymmetric case. It is this non-symmetric sampling which introduces the even component to the frequency splitting. It is important to examine full coupling systematically since we have found, for many individual test cases, that singlets can undergo extensive hybridization perturbing their frequencies and amplitudes significantly from that predicted by the self-coupling approximation. Uncovering a systematic signal in the hybridization may allow observers to infer the existence of giant-cells and perhaps even constrain their size and geometry.

b) Chapter 3; Nonlinear interactions among p modes

The lowest order nonlinear interaction among solar p modes is three mode coupling. Kumar and Goldreich (1989) have used the theory of three mode coupling to argue that p modes are excited by stochastic fluctuations associated with turbulence rather than by an overstability mechanism. Nonlinear interactions can lead to transfer of energy from trapped resonant modes to propagating modes that leak into the solar atmosphere; this process damps the trapped modes. Since the p modes have finite amplitudes, there must be some nonlinear mechanism which quenches their growth rate if they are overstable. Three mode coupling is a leading candidate. It would be an argument against the overstability hypothesis, if it could be shown that three mode coupling is unable to limit the amplitudes of the overstable modes. Kumar and Goldreich (1989) were not able to unambiguously demonstrate this since the calculation requires accurate knowledge of the energies of high degree modes. They performed three mode coupling calculations for a plane layered analog to the Sun (with an isothermal atmosphere and adiabatic convection zone) using a Hamiltonian formalism, and found energy transfer rates which range from 10 to 100 per cent of the products of the mode energies and linewidths (depending on the input energies of

the high degree modes). However, they conclusively demonstrated that f modes are damped by three mode coupling. Due to the incompressibility of f modes, it is not likely that they are excited by the κ mechanism. Further, since the f modes can not be excited by nonlinear transfer of energy, they are probably excited by turbulence. As a first step toward addressing this issue for a spherically symmetric Sun with a realistic thermal and density stratification, we have used methodologies from weak turbulence theory of plasma physics to derive the dynamical and kinetic equations for p modes. These equations are coupled first order differential equations which govern the time rate of change of the amplitudes and energies of the modes. The p modes can nonlinearly interact if the interaction conserves energy and angular momentum. These requirements are embodied by a frequency resonance condition and by selection rules on the Clebsch-Gordon coefficients. Three mode coupling can also systematically shift the phases of the modes and thus slightly alter their apparent frequencies. An expression quantifying this effect is provided.

c) Chapter 4; The influence of perturbations to spherical structure on p mode frequencies

The degenerate frequencies of solar p modes are integral measures of the radial structure of the Sun. We have applied Rayleigh's principle to derive sensitivity kernels that relate frequency perturbations $\delta\omega$ to small model perturbations $\delta m(r)$. The frequencies depend on two independent model parameters so that the perturbations relations are of the form $\delta\omega = \int[K_1(r)\delta m_1(r) + K_2(r)\delta m_2(r)]r^2dr$. These relations can be used as the basis for inverse problems in which model parameter perturbations are adjusted to minimize the differences between observed and predicted frequencies. The pairs of thermodynamic variables considered include (ρ, κ) (c, κ), (c, ρ), (ρ, Γ_1), (c, Γ_1), (c, η), and (ρ, η), where ρ, κ, c, Γ_1, and η denote, respectively, the density, adiabatic bulk modulus, adiabatic sound speed, first adiabatic exponent, and stratification parameter. The variable Γ_1 is sensitive to the He, He^+, and He^{++} fractions in the first and second Helium ionization zones. Application of inverse

theory to determine the radial profile of Γ_1 in these ionization zones could be used to place a constraint on the Helium abundance of the Sun. Knowledge of the radial variation of the stratification parameter could be used to constrain the depth of the convection zone and the entropy jump from the photosphere to the adiabatic part of the convection zone. We derive an asymptotic theory that establishes the connection between η and the mixing length in regions of low and high convective efficiencies.

REFERENCES

Bray, R.J., Loughhead, R.E., Durrant 1984, *The Solar Granulation* (Cambridge: Cambridge University Press)

Brown, T.M., 1984, *Science*, **226**, 687.

Brown, T.M., and Gilman, P.A. 1984, *Ap. J.*, **286**, 804.

Brown, T.M., Christensen-Dalsgaard, J., Dziemowski, W.A., Goode, P., Gough D.O., and Morrow, C.A. 1989, preprint.

Christensen-Dalsgaard, J., Duvall, T.L., Jr., Gough, D.O., Harvey, J.W., and Rhodes, E.J., Jr. 1985, *Nature*, **315**, 378.

Cox, J.P., and Giuli, R.T. 1968, *Principles of Stellar Structure* (New York: Gordon and Breach).

Duvall T.L., Jr., and Harvey, J.W. 1984, *Nature*, **310**, 19.

Duvall, T.L.Jr., Harvey, J.W., Libbrecht, K.G., Popp, B.D., and Pomerantz, M.A. 1988, *Ap. J.* **324**, 1158.

Gilman P.A. 1987, in *Physics of the Sun* ed. P.A. Sturrock, (Reidel), 95.

Gilman, P.A. and Miller, J. 1986. *Ap. J. Supp.* **61**, 585.

Glatzmaier, G.A. 1984 *J. Comp. Phys.*, **55**, 461.

Goldreich, P., and Keeley, D.A. 1977a, *Ap. J.*, **211**, 934.

Goldreich, P., and Keeley, D.A. 1977b, *Ap. J.*, **212**, 243.

Goldreich, P., and Kumar, P. 1988, *Ap. J.*, **326**, 462.

Gough, D.O., and Weiss, N.O. 1976. *M.N.R.A.S.*, **176**, 589.

Gough, D.O., Moore, D.R., Spiegel, E.A., and Weiss, N.O. 1976, *Ap. J.*, **206**, 536.

Gough, D.O., 1977a, in *Problems of Stellar Convection* eds. E.A. Spiegel and J.P. Zahn (Berlin: Springer Verlag), 15.

Gough, D.O., 1977b, *Ap. J.*, **214**, 196.

Grahm. E. 1975, *J. of F.M.*, **70**, 689.

Hart, J.E., Toomre, J., Deane, A.E., ... 1986 *Science*, **234**, 61.

Howard,R., and Labonte, B.J. 1980 *Ap. J.*, **239**, 738.

Kumar, P., and Goldreich, P. 1989, *Ap. J.*, **342**, 558.

Labonte, B.J., Howard,R., and Gilman, P.A. 1981, *Ap. J.*, **250**, 796.

Libbrecht, K.G. 1988, Caltech Astrophysics Preprint, BBSO no. 0281.

Libbrecht, K.G., and Kaufman, J.M. 1988, *Ap. J.*, **324**, 1172.

Lighthill, M.J. 1952, *Proc. Roy. Soc. London, A* **211**, 564.

Lighthill, M.J. 1954, *Proc. Roy. Soc. London, A* **222**, 1.

Tennekes, H., and Lumley, J.L. 1972, *A First Course in Turbulence* (Cambridge: The M.I.T. Press).

CHAPTER 2

THE EFFECT OF LARGE SCALE CONVECTIVE FLOWS ON HELIOSEISMIC OSCILLATIONS

> It was a clear steel-blue day. The firmaments of air and sea were hardly separable in that all-pervading azure; only, the pensive star was transparently pure and soft, with a woman's look, and the robust and man-like sea heaved with long, strong, lingering-swells, as Samsom's chest in his sleep.
>
> Hither, and thither, on high, glided the snow-white wings of small unspeckled birds; these were the gentle thoughts of the feminine air; but to and fro in the deeps, far down in the bottomless blue, rushed mightly Leviathans, sword-fish, and sharks; and these were the strong, troubled, murderous thinkings of the masculine sea.
>
> *Moby Dick* (1851)
>
> *Herman Melville*

THE EFFECT OF LARGE SCALE CONVECTIVE FLOWS ON HELIOSEISMIC OSCILLATIONS

EUGENE M. LAVELY

Massachusetts Institute of Technology, Department of Earth, Atmospheric, and Planetary Sciences

MICHAEL H. RITZWOLLER

Harvard University, Department of Earth and Planetary Sciences

ABSTRACT

Solar p modes are split and coupled by convective velocity fields and thermodynamic perturbations in the solar interior. We apply quasi-degenerate perturbation theory to calculate the influence of time-independent, global, long-wavelength, laminar convection on p mode frequencies and amplitudes. The convective velocity field is decomposed into a sum over poloidal and toroidal terms. The flow satisfies the unperturbed mass continuity equation and therefore does not generate acoustic waves. The principal theoretical result is the general matrix element $K^{m'm}_{n'n,l'l}$ (eq. 2.143) which governs the interaction between p modes with quantum numbers $k = (n, l, m)$ and $k' = (n', l', m')$ (defined for a spherically symmetric, non-rotating, isotropic Sun (SNRIS)).

The Wigner-Eckart theorem implies that $K^{m'm}_{n'n,l'l}$ can be separated into a reduced matrix element independent of m and m' times a Clebsch-Gordon coefficient. Selection rules immediately follow from both factors. In the case of self coupling (coupling among singlets of a single multiplet), only odd degree toroidal fields contribute to frequency splitting since the reduced matrix element vanishes for poloidal velocity fields and for even degree toroidal flows. The Clebsch-Gordon coefficient is nonvanishing only if l, l', and s satisfy the triangle inequalities, and if $-m' + t + m = 0$ (where s and t denote, respectively, the harmonic degree, and azimuthal order of a component of the flow field). In the full coupling case (coupling between singlets of different

multiplets) $K^{m'm}_{n'n,l'l}$ is nonvanishing only if: (1) $l+l'$ is even, the poloidal component s is even, or the toroidal component s is odd, or (2) $l+l'$ is odd, the poloidal component s is odd, or the toroidal component s is even.

To couple, the modes must satisfy the above selection rules. To interact strongly, their frequencies must be neary degenerate. In our numerical work we chose a particular singlet of the spherical Sun (the target singlet) and used the frequency and quantum number selection rules to cull all singlets with which it could significantly interact; we then assembled the supermatrix (eq. 2.86) (whose elements are composed of the various $K^{m'm}_{n'n,l'l}$), and performed an eigenvalue-eigenvector decomposition to obtain the hybrid eigenfunction and hybrid eigenfrequency associated with the selected singlet. We performed this operation using a realistic flow model provided to us by Gary Glatzmaier for a suite of singlets covering a broad region of the ω-k dispersion diagram.

The self coupling calculations show that the difference $a_1^{self} - a_1^{d.r.}$ (see eq. 2.168) can be as large as 7.8 nhz, where a_1^{self} and $a_1^{d.r.}$ denote, respectively, the a_1 coefficients calculated for a velocity model of convection in the self coupling approximation, and for a differential rotation model. Similarly, the difference $a_3^{self} - a_3^{d.r.}$ can be as large as .27 nhz. For sectoral ($m = l$) singlets, the largest frequency difference is $\omega^{self} - \omega^{d.r.} =$ .65 μhz. The fluctuations in the a_1 coefficients in the self coupling case with respect to the a_1 coefficients predicted by bulk rotation alone are comparble in magnitude to the fluctuations measured by observers. The largest frequency difference between $\omega^{full} - \omega^{self}$ a full coupling and self coupling calculation for a suite of singlets with $m = -.8l$ is .27 μhz. The difference $\omega^{full} - \omega^{self}$ tends to increase with increasing l and is largest for low n, high l singlets. The latter singlets can undergo significant hybridization. The nearly zonal singlets ($m \sim 0$) are virtually unaffected by Glatzmaier's flow model since most of the power of his model is in the sectoral components. The frequencies of oscillation are nearly insensitive to radial flow. The horizontal sensitivity kernels of poloidal flow in the full coupling case tend to be larger than those of the toroidal flow. We performed a full coupling calculation for every singlet of

several multiplets. A regression revealed that the a_2 coefficient of these multiplets were comparable in magnitude to the a_2 coefficients estimated by Libbrecht (1989). The even a_i coefficients are obtained only in the case of full coupling; frequencies in the self coupling approximation depend only on odd azimuthal order m. Modes contributing to the hybrid eigenfunctions often have amplitudes that are $\sim$ 10 % of the amplitude of the target mode.

The spatial and temporal basis functions of the oscillatory modes for a Sun with nonaxisymmetric flow fields do not separate in the observer's or inertial frame. This effect depends quadratically on the bulk rotation rate and the convective flow field. We ignored this complicated effect in the numerical calculations. Therefore, the numerical results are accurate only to first order in the bulk rotation rate and the convective flow field.

I. INTRODUCTION

a) An Overview of Heliseismology

Helioseismology, the study of the seismic oscillations of the Sun, has recently emerged as a major field of solar physics. The frequencies and amplitudes of the oscillations are dependent on the structure and dynamics of the Sun. Oscillation frequency estimates have been used to estimate the depth of the Sun's convection zone (Ulrich and Rhodes 1977), the solar Helium abundance (Dappen and Gough 1986), the sound speed profile through much of the solar interior (Christensen-Dalsgaard *et. al.* 1985), the radial profile of the radiative opacity (Korzennik and Ulrich 1988), the strength of the magnetic field at the base of the convection zone (Dziembowski and Goode 1988), the velocity profile of the solar differential rotation (Brown *et al.* 1989), and to test the physics of the equation of state (Christensen-Dalsgaard *et. al.* 1988). These advances have been made possible by the precision instruments (*e.g.* Brown 1981; Libbrecht and Zirin 1986; Tomcyzk 1988) and high quality data (*e.g.* Duvall *et. al.* 1984, 1986; Brown 1985; Libbrecht and Kaufman 1988; Tomcyzk 1988) that have recently become available. The raw data are a time sequence of Doppler images

of the visible surface of the Sun for a particular spectral line. The Doppler shifts are the surface manifestation of millions of resonant normal modes in the solar interior. The images are spatially and temporally filtered to yield measurements of oscillation frequencies and amplitudes (see Libbrecht and Kaufman (1988) and Tomcyzk (1988) for a review of data analysis procedures).

With the Global Oscillations Network soon to be installed by the National Solar Observatory, a vast amount of high quality data is forthcoming. In addition, the SOHO satellite, scheduled to be launched in 1995, will contain the Michelson Doppler Interferometer which will measure the solar oscillations free from the distortions of the Earth's atmosphere. To utilize effectively the information contained in these data will require an understanding of the way in which various solar structures affect helioseismic data. It is upon an understanding of these forward problems that any future inversions will rest.

b) The Influence of Convection on Oscillations

The goal of this paper is to present a theory which governs the splitting and coupling of solar p modes by global, steady-state, laminar convection. In this contribution we consider only the forward problem. However, in a later paper we will discuss the observational consequences of the theory.

It is important to distinguish between convection-oscillation coupling (see Gough 1977), and coupling among p modes due to convection. In the latter (which is the subject of this paper), the convection breaks the spherical symmetry of the Sun which leads to p mode coupling. We seek to model the interaction among p modes in a regime where the convection-oscillation coupling is very weak. The flow model we use satisfies the unperturbed continuity equation (which we refer to as the anelastic condition) so that p modes cannot be generated by the flow. The convection zone extends over many pressure scale heights and thus the characteristic temporal and spatial scales of the convection and turbulence varies widely. The most vigorous convection is located in the top few scale heights where the the characteristic lifetimes are the shortest and

length scales are the smallest. This paper is concerned with the influence of convection on modes below the top few scale heights where the convection is likely to be more coherent in space and in time. Strong, long-lived features of the convection leave characteristic signatures in p mode frequencies and amplitudes. Helioseismological inference of such features would be valuable since many studies (see Gilman 1980) have connected the existence of large-scale convective flows with the structure of the differential rotation and with the solar dynamo (see Stix 1981). Also, magnetic activity observed at the solar surface is probably controlled by flows at depth.

The work to date on convection-induced p mode coupling is sparse. In an asymptotic treatment, Gough and Toomre (1983) calculate the frequency shift of a mode due to advection by a horizontal flow. Hill (1983) has attempted to infer convective velocities near the solar surface using helioseismic data. The scattering of sound by a steady laminar compact vortex was considered by Bogdan (1989). Brown (1984) has calculated the influence of turbulence on modal degenerate frequencies.

In this paper we argue that the problem of convection-oscillation coupling and p mode coupling in the Sun can be separated into two distinct processes, each process dominating the physics in one of the shells. The top shell occupies the top few scale heights where the Mach number is relatively large and where the time scales of the turbulence and the acoustic radiation are nearly similar and where the amplitudes of the p modes and the convective modes are peaked. Goldreich and Keely (1977a, b) and Goldreich and Kumar (1988, 1989) have calculated the amplitudes and energies of the p modes under the assumption they are excited by stochastic turbulent convection. Using the results of Goldreich and Kumar (1988), one may show that seismic wave emission and absorption in the Sun principally take place through interaction with turbulence in the top few scale heights of the convection zone. The region of significant interaction between the p modes and the convection defines the radial extent of the top shell. Processes in the top shell such as convection-oscillation coupling, three-mode coupling (Kumar and Goldreich 1989), and radiative damping are primarily responsible for the amplitudes and line widths of the modes, but can also perturb

modal degenerate frequencies since the turbulent pressure alters the radial structure. The bottom shell is much larger and is directly below the top shell occupying $\sim$ 99% of the convection zone. The emission and absorption of seismic waves in the bottom shell by turbulence is negligible and can, therefore, be ignored. The exchange of energy between long-wavelength coherent velocity structures and the p modes is quite accurately set to zero in the anelastic approximation as long as it is applied in the bottom shell alone. The solar medium in the bottom shell is optically thick and therefore radiative damping is negligible. Since the amplitude of the p modes are so strongly peaked near the surface in the top shell, the contribution to the interaction coefficient describing three-mode coupling from the bottom shell relative to the top shell is negligibly small (Kumar and Goldreich 1989). Therefore, in the bottom shell the most significant coupling process involving p modes is coupling among them due to long-wavelength and long time-scale convective structures. In this paper we derive expressions for the perturbations to the frequencies and amplitudes of the p modes caused by this coupling. We state and defend the assumptions which have led us to the above conclusions in §II.

To date, helioseismologists have generally neglected the effect of the complicated physical interactions in the top shell on the split frequency spectrum of the normal modes. However, some investigators (*e.g.* Brown 1984; Christensen-Dalsgaard and Fransden 1983; Christensen-Dalsgaard *et. al.* 1989) have attempted to account for the effect of first-shell physics on the degenerate frequencies. Our interest in this paper is the description of the split frequency spectrum rather than perturbations to the degenerate frequency. However, in §II.c we do attempt to justify ignoring top shell physics on the split frequency spectrum.

c) Velocity Fields in the Convection Zone

The scales of convective motion in the Sun range from the Kolmogoroff microscales to the differential rotation. In between are the granules, supergranules, giant cells, and energy-bearing eddies. The solar p modes have scales which range in size from the

smallest to the largest of the convective motions. See Tennekes and Lumley (1972) and Goldreich and Kumar (1988) for a review of turbulence. Bray *et. al.* (1984) and Gilman (1987) provide overviews of the physics and morphology of granules, supergranules, and giant cells. For a review of p mode phenomenology, see Libbrecht (1988a). In the following, we briefly summarize the evidence for giant-cells since it is the influence of motions of this scale we seek to model.

The existence of giant-cells has not been directly confirmed. If they do exist at the surface of the Sun, their amplitudes are less than 10 ms^{-1} (Howard and Labonte 1980; Labonte *et. al.* 1981; Brown and Gilman 1984). However, the Sun displays a number of features which are suggestive of sustained large-scale motions (Gilman 1987). These include the persistent large-scale patterns in the solar magnetic field, the coronal holes which survive several solar rotation periods without being sheared apart by differential rotation, and the existence of active longitudes where new active regions preferentially arise. Observation of the distinct cellular motions of granules and supergranules suggests that for thermal convection there are preferred scales of motion. This trend may continue deeper in the convection zone. In the mixing length picture of convection, the scale of the convecting eddies is set by the pressure scale-height so that one would expect layers of convection with ever decreasing vertical scale as the surface is approached. However, both linear and nonlinear models (Gough *et al.* 1976; Grahm 1975) show that even when the fluid is compressible, and the stratification includes several scale heights, convection which spans the entire unstable layer is favored. Thus, for the Sun, patterns of motion with horizontal dimensions up to $\sim 200,000$ km would be expected. In addition, the space-lab experiment of thermal convection (Hart *et al.* 1986), and the numerical simulations of Glatzmaier (1984) and Gilman and Miller (1986) suggest that large and sustained patterns of motion may exist in the Sun with scales approaching the depth of the convection zone. Glatzmaier (1984) probably over-predicts vertical velocities near the surface since he does not model the small pressure scale height regions where the ionization zones are (see below).

A possible explanation of the small vertical velocities of the supergranules and the absence of a strong signature of giant-cells in the data of Howard and Labonte (1981) may be found in the work of Latour *et al.* (1981) and Ballegooijen (1986). Latour *et al.* (1981) have used an anelastic modal approach to model convection in A-type stars. They find that buoyancy breaking may occur in upward directed flows which have horizontal scales large compared to vertical scale height of the region into which they penetrate. This leads to lateral deflection and strong horizontal shearing motions. If this result applies to G-type stars as well, it may be the explanation of why giant-cells are not observed at the surface. This is an ionization zone effect since from the definition of the second adiabatic exponent it can be shown that the vertical scale height rapidly decreases in an ionizing region. Ballegooijen (1986) finds that density stratification screens out periodic components of the near surface flow pattern in his convection model.

d) An Overview of this Paper

In §II, we state and attempt to justify the assumptions used in this study. we present all equations intended for practical application in the observer's frame. Reference frames are discussed in §III. The equations of motion governing the seismic oscillations in the presence of a time independent large-scale velocity field and the associated thermodynamic perturbations are derived in §IV. We present in §V the quasi-degenerate perturbation theory needed to calculate the influence of a time-independent, but otherwise general, aspherical perturbation on solar oscillations. In §VI, we derive the interaction matrices which determine the strength of coupling between oscillations due to a specified convection model using the perturbation operator derived in §IV and the perturbation theory derived in §V. The application of quasi-degenerate perturbation theory to the normal modes of the Sun and the interpretation of the coupling phenomenon is discussed in §VII. In §VIII, we consider a special case in which only modes that are members of a single multiplet couple. In §IX, we present preliminary numerical results in which the theory derived in this paper is applied to

a convection model provided to us by Gary Glatzmaier (see Gilman and Glatzmaier 1981; Glatzmaier and Gilman 1981a,b; Glatzmaier 1984). Helioseismologists often use the technique of Cuypers (1980) to reduce integrals on the unit sphere which arise from complex vector calculus calculations. In Appendix 2B, we present an alternative technique adapted from Phinney and Burridge (1973) which considerably simplifies evaluation of such integrals. We used this technique to calculate the general matrices presented in §VI. Appendices 2A, 2C, 2D, and 2E relate to technical discussions in the chapter.

II. JUSTIFICATION OF ASSUMPTIONS

a) The Assumptions of Our Approach

We seek to calculate accurately the influence of long-wavelength, long-lifetime convection on p mode frequencies and amplitudes. We adopt the following assumptions. (1) Convection-oscillation coupling below the top one or two pressure scale heights (the top shell) does not significantly affect p mode frequencies and amplitudes. A corollary assumption is that the convective velocity field $\mathbf{v}$ and the thermodynamic perturbations associated with convection in the second shell are small enough so that the anelastic approximation (Gough 1969) is justified. (2) It suffices to retain terms in the equation of motion to first order only in the p mode amplitude. (3) The general features of the long-wavelength convective flow remain approximately steady during the interval over which helioseismic observations are made.

b) Physical Justification of the Assumptions of our Approach

i) Convection-Oscillation Coupling is not Significant below the Top Few Scale Heights

Recent results suggest that p modes are excited by turbulent convection (Goldreich and Keely 1977a, b; Kumar & Goldreich 1988; Goldreich and Kumar 1988, 1989). The extent of energy exchange between oscillations and turbulent convection depends on their relative time and velocity scales. Convenient measures of the coupling are given by the spectral emissivity $\epsilon(\omega)$ and absorptivity $\alpha(\omega)$ of acoustic radiation by

a turbulent fluid and the flux F_p pumped into to the modes from the convective energy. These quantities have been calculated by Goldreich and Kumar (1988, 1989). The emissivity and absorptivity depend on the manner in which the turbulence is generated. *Turbulent pseudoconvection* is the model most relevant model to the Sun considered by Goldreich and Kumar (1988). The emissivity for this type of turbulence is given by

$$\begin{aligned}
&\epsilon(\omega) \sim \rho_o v_H^2 \, M^3 (\omega\tau_H)^2 \text{ for } \omega\tau_H \leq 1, \\
&\epsilon(\omega) \sim \rho_o v_H^2 \, M^3 (\omega\tau_H)^{-9/2} \text{ for } 1 \leq \omega\tau_H \leq M^{-2}, \\
&\epsilon(\omega) \sim \rho_o v_H^2 \, M^5 (\omega\tau_H)^{-7/2} \text{ for } M^{-2} \leq \omega\tau_H \leq \mathcal{R}_e^{3/4} \\
&\epsilon(\omega) \sim 0 \text{ for } \mathcal{R}_e^{3/4} \leq \omega\tau_H \,,
\end{aligned} \tag{2.1}$$

and the absorptivity is given by

$$\begin{aligned}
&\alpha(\omega) \sim \frac{M^2}{\tau_H} \text{ for } \omega\tau_H \leq \mathcal{R}_e^{3/4}, \\
&\alpha(\omega) \sim 0 \text{ for } \mathcal{R}_e^{3/4} \leq \omega\tau_H \,.
\end{aligned} \tag{2.2}$$

The variables in equations (2.1)-(2.2) have the same meaning as in §I. Goldreich and Kumar (1989) derive an expression for F_p given by

$$F_p = M^{\frac{15}{2}} F_c \tag{2.3}$$

where F_c is the convective flux. In the mixing length picture of convection one would choose

$$H \sim \alpha H_p \tag{2.4}$$

$$M \sim \left[\frac{g F_c \alpha H_p Q \rho^{1/2}}{4(\Gamma_1 P)^{3/2} c_p T}\right]^{1/3} \tag{2.5}$$

$$\tau_H \sim \frac{\alpha H_P}{cM} \tag{2.6}$$

where $H_p = P/(\rho g)$ is the pressure scale height, α is the ratio of the mixing length to H_p g is the gravity, Γ_1 is the first adiabatic exponent, and c_p is the specific heat. We have set $Q = (4 - 3\beta)\beta^{-1}$ where β is the ratio of the gas pressure to the total

pressure. The convective flux was calculated using

$$F_c = \frac{L_\odot}{4\pi r^2}\left[\frac{\nabla_r - \nabla}{\nabla_r}\right] \tag{2.7}$$

where $L_\odot$ is the solar luminosity. We have used equation (14.58) of Cox and Giuli (1968) to obtain the Mach number $M \sim v_H / c$.

We can show that convection-oscillation coupling is not significant below the top few scale-heights by calculating the radial dependence of $\epsilon(\omega)$, $\alpha(\omega)$, and F_p. The Mach number decreases and τ_H increases with increasing depth so that the emissivity and absorptivity decrease with depth. Figure (1a) is a plot of the characteristic length, velocity, and time scales of convection predicted by mixing length theory (see equations (2.4), (2.5), and (2.6)). These plots were made using the solar model of Podsiadlowski (1989) and α was taken to be 1.305. The predicted time and velocity scales near the surface correspond well with observations of granulation. Figure (1b) is a plot of $\epsilon(\omega)$, $\alpha(\omega)$ and F_p versus depth for a 3.5 mhz mode. Equations (2.5) and (2.6) were used to compute M and τ_H , and we have set $v_H = cM$. The values of $\epsilon(\omega)$ and $\alpha(\omega)$ are plotted for a single eddy. The period corresponding to 3.5 mhz is similar to the overturn time of a typical solar granule. From Figure 1b, it is clear that wave emission, absorption, and flux of energy going into the p modes occurs primarily in the top $\sim .15\%$ of the convection zone. These quantities depend on the Reynolds stresses which scale as $\rho_o v_H^2$ and which generate quadrupole emissions, and the buoyancy forces which arise from entropy fluctuations that scale as $c_p v_H^2 / (gH)$ (Goldreich and Kumar 1988) and which generate dipole emissions. The Reynolds stresses and entropy fluctuations act far more efficiently in the top few scale heights as a mode-turbulence coupling mechanism than in the deeper layers where the characteristic velocities are smaller and the length scales are larger, as can be seen from Figure 1b.

ii) The Convection is Anelastic

The p modes, and g modes (both stable and unstable), are solutions to the general equations of hydrodynamics. If the convective speeds of the unstable g modes are much smaller than the sound speed of the p modes there will be a mismatch in

either the time scales or the length scales, or both, and the coupling between the two types of motion will be small. To decouple the short-period acoustic waves from convection, only those terms in the equations of motion with scales appropriate to long-wavelength, long-lifetime convection should be considered. The coupling between acoustic waves and convective motions (or turbulence) cannot in general be ignored. However, as far as the general description of the convective dynamics is concerned, the coupling can safely be neglected as long as the amplitudes of the acoustic modes are sufficiently small. This filtering forms the basis of the anelastic approximation.

The anelastic approximation excludes density perturbations on acoustic time scales. However, density perturbations on the much longer time scales associated with convective overturn times in the deeper parts of convection zone are allowed. The primary reasons that the anelastic approximation has been used in the past (*e.g.* Latour *et al.* 1976; Toomre *et al.* 1976; Gilman and Glatzmaier 1981) are: (1) the high frequency acoustic waves are filtered out so that the small time-scale associated with these waves need not be resolved in numerical simulations of convection, and (2) the convection can be modelled over many density scale heights which is much more realistic than the single scale height required in the Boussinesq approximation. The anelastic approximation is justified when the frequencies and Mach numbers of the convection are not too high. Its basic effect is to suppress terms which are nonlinear in the horizontal fluctuations of the thermodynamical variables yet allows large vertical variation in the mean density and preserves the dynamical nonlinearities in the equations governing convection. From the argument in the previous subsection, this implies that the emission and absorption of acoustic modes by anelastic convection are very weak processes.

We retain the anelastic approximation in this paper for several reasons. First, we use a perturbative theoretic approach (see §V) which requires that the perturbations from spherical symmetry (including the velocity field and thermodynamic variations) are small enough so that accurate estimates of frequency perturbations can be obtained by retaining terms first-order only in the perturbation variable. A flow which

satisfies the conditions of linearization in our perturbation theory is likely to satisfy the anelastic approximation as well. Second, the interaction matrix which describes the coupling of the p modes due to a given flow field is Hermitian only if the flow is anelastic. This result implies that the eigenfrequency of a normal mode of oscillation is complex in the presence of a flow which is not anelastic. The physical interpretation is that such a flow field has a non-zero mass-flux in or out of a finite volume which means within the context of the anelastic approximation that if the density is not allowed to change on the acoustic time scale, then there are mass-sources, mass-sinks, and cavitation in the flow field. A flow which is anelastic satisfies the unperturbed continuity equation, $\nabla\cdot(\rho_o\mathbf{v}) = 0$ which clearly, is a condition that eliminates sources, sinks, and cavitation. Therefore, to examine self-consistently the influence of a flow with time-scales far longer than the acoustic time scale and to satisfy the linearization requirements of our theory, we use the anelastic approximation. The principal physical effect of an anelastic flow on the p modes is that energy may be scattered between any two p modes provided that the angular momentum is conserved *i.e.*, the modes must satisfy certain selection rules which we enumerate in §VII.

iii) A Linearized Treatment Suffices

Helioseismologists ordinarily retain mode displacement terms to first order only in perturbed equations of motion that govern frequency splitting caused by aspherical structures. We adopt this approximation as well. The convective velocities and the p mode amplitudes are peaked in the top few scale heights (the first shell) and diminish with depth. Thus, the most significant nonlinear interactions between p and g modes, or among p modes alone, are largely confined to the first shell. In the linear approximation, p modes are coupled by convective structures (energy is scattered among them). There are several nonlinear energy transfer mechanisms whose efficiency depends on the finite amplitude of the p modes alone, or on the finite amplitudes of the p modes and the unstable g modes. Retaining terms to second order in the displacement fields, the various scenarios are: (1) one p mode may couple to two g modes, (2) two p modes may couple with one g mode, (3) three

p modes may couple with one another, or (4) three g modes may couple with one another.

The two important classes of interaction involving the p modes alone are two mode coupling and three mode coupling. There are two types of two mode coupling and these are self and full coupling. Self coupling occurs when two modes that share the same degenerate frequency (modes with the same radial order n and harmonic degree l) couple. More generally, two modes with different degenerate frequencies may couple and this is called full coupling. In self and full coupling, the energy is scattered by an asphericity in the Sun such as convection. We show in §VI that full coupling can be induced by both poloidal and toroidal velocity fields and that in the self coupling approximation only toroidal velocity fields couple modes. Three mode coupling (Kumar and Goldreich 1988) is important if the p modes have significant finite amplitude. In this case, nonlinear terms in the equation of motion cannot be ignored. Energy can be exchanged between the three modes if the interaction conserves energy and momentum. Kumar and Goldreich (1989) have shown that the most significant nonlinear interactions among p modes occurs in the top few scale heights. Although, the convective velocities are large in the first shell, the scale of the aspherical structure there is so small, that to first order in the velocity field, coupling between modes with harmonic degrees $1 \leq l \leq 100$ is zero. We argue this point in §II.e.

The amplitudes and energetics of the p modes depend strongly on turbulence (which is intrinsically nonlinear) and on the finite amplitude of the p modes themselves (Goldreich and Keely 1977b, Kumar and Goldreich 1988). Turbulence and three-mode coupling inappreciably change the frequencies (Brown 1984; Kumar 1989, personal communication). Thus, the influence of internal structure on the frequencies is relatively divorced from complicated nonlinear interactions. Since the amplitudes of the p and unstable g modes are small below the top few scale heights, it suffices to solely consider self and full coupling to calculate the frequency splitting due to convective structures in this shell.

iv) The Flow Field is Steady

As a first step toward modelling convection-induced p mode interaction, we derive in this paper a perturbation theory for a steady flow field. At each instant in time, the frequency shift of a mode due to an asphericity is a function of global properties. If the asphericity changes in time, the peak of the resonance function associated with a given mode also varies. The peak instantaneously traces a trajectory in frequency space. The peak of a resonance function in the frequency domains represents a time average of the trajectory of the modal frequency. Thus, an asphericity which changes during the data collection interval leads to line broadening. These are complicated effects which we do not address in this paper.

The coherence time of large-scale flows beneath the turbulent boundary layer is not known since the flows cannot be directly observed. Clearly though, slower velocity and larger length-scale convective eddies have longer lifetimes than the small length-scale and time-scale granules and supergranules observed at the surface as can be seen from Figure 1a. The lifetime of active longitudes and coronal holes may be related to the lifetime of large-scale motions in the interior. Glatzmaier and Gilman (1981, 1982) find in their numerical simulations that some components of the flow have lifetimes on the order of weeks.

c) Frequency Splitting from Small-scale Structure

We are interested in the fine frequency structure of modes and not their degenerate frequencies. Our goal is to describe the interaction of p modes with harmonic degrees l between 1 and 100. The turbulence in the turbulent boundary layer will affect the degenerate frequency (see Brown 1984) but not the fine structure. The latter observation follows from the conservation of angular momentum. The harmonic degree l of structure with horizontal wave-number k_h is given by $l \sim R_\odot k_h$ where $R_\odot$ is the radius of the Sun. Taking a typical horizontal wavelength of granules to be 1400 km implies a harmonic degree $s \sim 3140$. Suppose two modes interact which have harmonic degrees l and l'. The angular momentum is conserved only if $\mid l' - s \mid \leq l$

and $| l - s | \leq l'$. Modes with l and l' between 1 and 100 cannot satisfy these triangle inequalities and therefore their fine structure will not be affected by the small-scale structure in the turbulent boundary layer. This result follows from the discussion in §VII.

d) Summary Remarks

We have argued that mode coupling between p modes and unstable g modes is important only in the first shell (the top few scale heights), and that the principle effect of convection on p modes in the second shell (which comprises the vast majority of the convection zone) is to induce two mode coupling among them (a process which we call self and full coupling and which is the subject of the rest of this paper). We have argued that it is justifiable to use the anelastic approximation ($\nabla \cdot (\rho_o \mathbf{v}) = 0$) in the second shell by using the results of Goldreich and Kumar (1988) and standard results of mixing length theory. The wave emission and absorption by a single convective eddy at depth is down by many orders of magnitude relative to the first shell which is consistent with the anelastic approximation which filters out coupling between acoustic modes and convective modes. Our perturbation theory is derived for a stationary flow field. The large scale flow in the second shell may be steady for a time approaching the coherence time of observed large-scale magnetic features.

III. REFERENCE FRAMES

Current measurements of helioseismic oscillations are generally made from the surface of the Earth. Space-based measurements will soon exist, but whether measurements are obtained from a natural satellite such as the Earth or future man-made satellites, observers require theoretical results reported in a frame other than the Sun's. So that observers can more easily use the results in this paper, all equations intended for practical application will be set up and solved in what we call the observer's frame. Let us denote the origin of the observer's frame as $\mathcal{O}_0$, and the origin of the Sun's frame, the Sun's center of mass, as $\mathcal{O}_s$, as is shown in Figure 2. The

position vector $\mathbf{R}$ connects the origins of the two frames. Positions in the solar frame are taken relative to a set of orthonormal unit vectors $\{\mathbf{e}_1, \mathbf{e}_2, \mathbf{e}_3\}$ which rotate about $\mathbf{e}_3$ with rotation rate Ω, the bulk rotation of the Sun. Thus, the position vector in each frame is given by

$$\begin{aligned} \mathbf{r}_s &= r_i \mathbf{e}_i, \\ \mathbf{r}_0 &= \mathbf{R} + r_i \mathbf{e}_i, \end{aligned} \tag{2.8}$$

the velocity vectors by

$$\begin{aligned} \mathbf{v}_s &= \dot{r}_i \mathbf{e}_i, \\ \mathbf{v}_0 &= \dot{\mathbf{R}} + \dot{r}_i \mathbf{e}_i + r_i \dot{\mathbf{e}}_i, \end{aligned} \tag{2.9}$$

and accelerations by

$$\begin{aligned} \mathbf{a}_s &= \ddot{r}_i \mathbf{e}_i, \\ \mathbf{a}_0 &= \ddot{\mathbf{R}} + \ddot{r}_i \mathbf{e}_i + 2\dot{r}_i \dot{\mathbf{e}}_i + r_i \ddot{\mathbf{e}}_i, \end{aligned} \tag{2.10}$$

where the overdot signifies the local time derivative $\frac{\partial}{\partial t}$. For our purposes the rate of bulk rotation of the Sun can be considered constant and the orientation of the rotation axis fixed relative to the observer's frame. With these assumptions, a simple geometric argument shows that

$$\dot{\mathbf{e}}_i = \boldsymbol{\Omega} \times \mathbf{e}_i. \tag{2.11}$$

The vectors $\dot{\mathbf{R}}$ and $\ddot{\mathbf{R}}$ account for the fact that the origin of the solar frame may itself translate and accelerate relative to the observer's frame.

We assume that the reference model undergoing convection exhibits a stationary flow field $\mathbf{u}_0$ superimposed on the equilibrium solar model. We identify this velocity field with $\dot{r}_i \mathbf{e}_i$ so that

$$\mathbf{u}_0 = \dot{r}_i \mathbf{e}_i. \tag{2.12}$$

Thus, with equations (2.11) and (2.12), we rewrite the velocity and acceleration in the observer's frame as

$$\begin{aligned} \mathbf{v}_0 &= \dot{\mathbf{R}} + \mathbf{u}_0 + \boldsymbol{\Omega} \times \mathbf{r}, \\ \mathbf{a}_0 &= \ddot{\mathbf{R}} + 2\boldsymbol{\Omega} \times \mathbf{u}_0 + \boldsymbol{\Omega} \times \boldsymbol{\Omega} \times \mathbf{r} + \mathbf{u}_0 \cdot \nabla \mathbf{u}_0 \end{aligned} \tag{2.13}$$

where we have used the assumption that the velocity field and rotation rate are steady; *i.e.*, $\dot{\Omega} = \dot{u}_0^i = 0$. The velocity and acceleration in the solar frame are then given by

$$\begin{aligned} \mathbf{v}_s &= \mathbf{u}_0 \,, \\ \mathbf{a}_s &= \mathbf{0}. \end{aligned} \tag{2.14}$$

The solar rotation dominates the Doppler shifts of spectral lines. However, the orbital motion of the earth and its rotation also contribute. Henceforth, we assume that the Doppler images have been processed to remove these latter motions and, therefore, we set $\dot{\mathbf{R}} = \ddot{\mathbf{R}} = 0$. We also assume that the images have been rotated to account for the inclination of the solar rotation axis out of the plane of the sky (the B angle). Other operations that are usually performed include multiplication by the factor $\mu = sin(\theta)cos(\phi)$ to obtain the projection onto the line of sight and multiplication by an additional factor of μ to reduce the weight of the polar regions (see Tomczyk 1988 for a detailed discussion). Assuming the application of these data corrections and neglecting the acceleration of the solar system with respect to the rest of the universe, we can identify the observer's frame with the inertial frame so that $\mathbf{v}_0$ and $\mathbf{a}_0$ can be identified with the inertial velocity $\mathbf{v}_I$ and acceleration $\mathbf{a}_I$ referred to in §IV. We have

$$\begin{aligned} \mathbf{v}_I &= \mathbf{u}_0 + \mathbf{\Omega} \times \mathbf{r}, \\ \mathbf{a}_I &= 2\mathbf{\Omega} \times \mathbf{u}_0 + \mathbf{\Omega} \times \mathbf{\Omega} \times \mathbf{r} + \mathbf{u}_0 \cdot \nabla \mathbf{u}_0 \end{aligned} \tag{2.15}$$

IV. THE EQUATION OF MOTION

We derive in this section the equation of motion governing p modes in the presence of global, long-wavelength, steady state, laminar convection and is given in equation (2.70) The perturbation operator is derived in the observer's frame so that our numerical results are more easily comparable to observations. The equation of motion governing oscillations in an otherwise static and spherically symmetric Sun is given in equations (2.21) and (2.22). The equation of motion governing oscillations in the

presence of convection is given by equation (2.70) with equations (2.61), (2.68), and (2.69).

To derive these equations, it is necessary to define precisely four solar models. These are: (a) equilibrium model, (b) the perturbed equilibrium model, (c) the reference model, and (d) the perturbed reference model. The equilibrium model is the standard solar model. In §IV.a we prescribe the minimal set of characteristics the equilibrium model must possess. The perturbed equilibrium model is the equilibrium model undergoing helioseismic oscillations. The reference model is the equilibrium model with the addition of rotation and convection and, therefore, has a prescribed set of departures from spherical symmetry taken relative to the equilibrium model; it is not seismically disturbed. The perturbed reference model is the reference model undergoing helioseismic oscillations. In the following, we prescribe the properties of each of these models in greater detail.

a) The Equilibrium Model

The equilibrium model is the spherically symmetric, non-rotating reference model to which convective structural perturbations will be added. For our purposes, we require only knowledge of its mass $M_\odot$, radius $R_\odot$, and the radial profile of two independent thermodynamic state variables for $0 \leq r \leq R_\odot$ (the density ρ and adiabatic bulk modulus κ, for example). We refer to these variables as the equilibrium model parameters. They smoothly vary with position and display no internal discontinuities. The equilibrium model which we have used in this paper was calculated with the stellar evolution code of Gilliland (see for example, Gilliland, 1985). We evolved the sun to age 4.6 billion years and used $X = 0.75$, $Y = 0.23$, and $Z = 0.02$ for the initial hydrogen, helium, and metal abundances, and chose $\alpha = 1.368$ for the ratio of the mixing length to the pressure scale height.

Let ρ_0, ϕ_0, and P_0 denote the density, gravitational potential, and pressure of the equilibrium model. The equilibrium equations are:

$$\rho_0 \nabla\phi_0 = -\nabla P_0 , \tag{2.16}$$

$$\nabla^2\phi_0 = 4\pi G\rho_0 \,. \tag{2.17}$$

Equations (2.16) and (2.17) must be solved in the volume of the model subject to the jump conditions at $r = R_\odot$:

$$[\phi_0\,]^+_- = 0, \tag{2.18}$$

$$[\hat{\mathbf{r}} \cdot \nabla\phi_0\,]^+_- = 0, \tag{2.19}$$

$$[\hat{\mathbf{r}} \cdot P_0\,\mathbf{I}]^+_- = \mathbf{0}, \tag{2.20}$$

where G is the constant of gravitation, $\hat{\mathbf{r}}$ is the unit vector in the radial direction, and $\mathbf{I}$ is the identity tensor. The notation $[Q]^+_-$ denotes the jump discontinuity of quantity Q across the surface $r = R_\odot$, the positive contribution arising from that side toward which $\hat{\mathbf{r}}$ is directed. Both ρ_0 and P_0 are defined to be zero for $r > R_\odot$, and ϕ_0 is required to vanish at infinity.

b) The Perturbed Equilibrium Model

The perturbed equilibrium model is an equilibrium model subjected to seismic oscillations. The equations governing this model result directly, as a special case, from the more general equations derived in detail in §IV.d (see eq. 2.66) Consider a single normal mode of oscillation, with angular eigenfrequency ω and associated displacement eigenfunction $\mathbf{s}(\mathbf{r})$ so that $\mathbf{s}(\mathbf{r},t) = \mathbf{s}(\mathbf{r})e^{i\omega t}$. The linearized momentum equation which governs oscillations of the equilibrium model is given by

$$\mathcal{L}(\mathbf{s}) + \rho\omega^2\mathbf{s} = 0, \tag{2.21}$$

where

$$\mathcal{L}(\mathbf{s}) = \nabla\cdot[P_0\,\{(\Gamma_1 - 1)(\nabla\cdot\mathbf{s})\,\mathbf{I} + 2\mathbf{e} - \nabla\mathbf{s}\}] - \rho_0\,\nabla\delta\phi - \rho_0\,\mathbf{s}\cdot\nabla\nabla\phi_0 \tag{2.22}$$

and Γ_1 is the first adiabatic exponent, $\nabla\nabla$ is the dyadic derivative, $\mathbf{e}$ is the incremental strain tensor defined by

$$\mathbf{e} = \frac{1}{2}(\nabla\mathbf{s} + (\nabla\mathbf{s})^T) \tag{2.23}$$

and, $\delta\phi$ is the eulerian perturbation in gravitational potential governed by

$$\nabla^2\delta\phi = -4\pi G\nabla\cdot(\rho_0\,\mathbf{s}). \tag{2.24}$$

In equation (2.22) we have assumed the oscillations are adiabatic. The boundary conditions for $\delta\phi$ at $r = R_\odot$ can be written

$$[\delta\phi]^+_- = 0, \tag{2.25}$$

$$[\hat{\mathbf{r}}\cdot\{(4\pi G)^{-1}\nabla\delta\phi + \rho_0\,\mathbf{s}\}]^+_- = 0, \tag{2.26}$$

where equation (2.26) can be derived from equations (2.52) and (2.53) with an application of the divergence theorem. An additional surface boundary condition is that the Lagrangian pressure variation must vanish:

$$\Delta P = -P\Gamma_1\nabla\cdot\mathbf{s} = 0. \tag{2.27}$$

The inner boundary conditions can be obtained by approximating the innermost region of the star as a small homogeneous sphere and by solving analytically for the eigenfunction displacements. The inner boundary conditions can be obtained by evaluating ratios of the eigenfunctions at the surface of the sphere (see Pekeris *et. al.*, 1958). We have used a computer code written by John Woodhouse to calculate the eigenfunctions and eigenfrequencies of the oscillations. See Woodhouse (1988) for a detailed description of the code.

c) The Reference Model

The reference model is an aspherical rotating and convecting model. Perturbations in structure (such as density perturbations) are referred to the equilibrium model. The reference model rotates with bulk rotation rate Ω and includes $\mathbf{u}_0$, the velocity field $\mathbf{u}_0$ of long-wavelength convection (referred to from the rotating frame). The velocity field satisfies the anelastic condition (see eq. 2.29) which insures that seismic waves are not generated by the convection.

The general velocity field $\mathbf{v}$ introduced below includes $\mathbf{u}_0$ and contributions due to reference frame effects. The anelastic condition insures that seismic waves are not

generated by the convection. The reference model is fully characterized by Ω, $\mathbf{v}_I$, and a parameterization of the convective perturbations to two independent thermodynamic state variables (*e.g.* ρ and κ).

The unperturbed mass continuity equation of the reference model is written

$$\frac{\partial \rho}{\partial t} + \nabla \cdot (\rho \mathbf{v}_I) = 0 \tag{2.28}$$

where $\mathbf{v}_I = \mathbf{\Omega} \times \mathbf{r} + \mathbf{u}_0$, and $\mathbf{u}_0$ satisfies the anelastic condition

$$\nabla \cdot (\rho_0 \, \mathbf{u}_0 \,) = 0. \tag{2.29}$$

The conservation of energy is given by

$$\rho T \frac{DS}{Dt} = \text{ entropy production terms,} \tag{2.30}$$

where the total time derivative is defined by

$$\frac{D}{Dt} = \frac{\partial}{\partial t} + \mathbf{v}_I \cdot \nabla. \tag{2.31}$$

The right hand side of equation (2.30) represents the production of entropy through dissipative processes such as heat conduction, viscous shearing and expansion, emission and absorption of radiation, divergence of the convective flux, and so on. Even in the absence of entropy production terms, equation (2.30) states that entropy must be conserved along streamlines of the motion in steady state. In general, such a velocity field cannot be designed *ab initio* and this requirement is not naturally incorporated into the Lagrangian describing the oscillations. Rather, we assume in the sequel that the flow fields in the reference model are determined *a priori* from a self-consistent dynamical calculation in which equation (2.30) holds. We will later assume that the Lagrangian and Eulerian variations of the entropy are zero, and, therefore, drop any further consideration of the energy equation (2.30).

Ignoring magnetic fields, the Reynolds stresses generated by turbulence, and the effects of external body forces, the conservation of linear momentum becomes

$$\frac{D\mathbf{v}_I}{Dt} = -\frac{\nabla P}{\rho} - \nabla \Phi. \tag{2.32}$$

The gravitational potential is governed by Poisson's equation:

$$\nabla^2\phi = 4\pi G\rho. \tag{2.33}$$

The equation of state is given by

$$P = P(S,\rho) \tag{2.34}$$

which for our purposes need not be given an explicit form.

d) The Perturbed Reference Model

In this section we seismically perturb the reference state defined in §IV.c to obtain the equations of motion governing small elastic-gravitational oscillations of the Sun in the presence of a time independent velocity field. As argued in §III, we identify the observer's frame with the inertial frame. Therefore, we make the indentification $\frac{D\mathbf{v}_I}{Dt} = \mathbf{a}_I$.

The response of the reference state to an oscillation can be determined by perturbing the momentum equation (eq. 2.32). The resulting equation includes terms perturbed in ρ, ϕ, and P; these terms can be obtained by perturbing equations (2.28), (2.33), and (2.34), respectively. In the rotating frame, the temporal and spatial basis functions of the oscillatory modes conveniently separate. They also separate in the observer's frame if the rotating body has an axisymmetric flow field. However, the temporal and spatial basis functions do not separate in the presence of a flow field that is more general than an axisymmetric flow if the measurements are taken in the observer's frame. Ignoring this effect introduces errors that are quadratic in the bulk rotation rate, the nonaxisymmetric flow, and products between them (personal communication, Ad Van Ballegooijen). To avoid this problem, the perturbation calculations could be performed in the rotating frame. To make comparisons with the data, the Doppler images would have to be transformed to the rotating frame for reduction and analysis. To avoid these complications, we have chosen to assume the modal basis functions separate *i.e.*

$$\mathbf{s}(\mathbf{r},t) = \mathbf{s}(\mathbf{r})e^{i\omega t} \tag{2.35}$$

and perform the calculations in the observes frame to first order accuracy in the bulk rotation rate and flow field. In future work, we will perform the calculation in the rotating frame and determine the appropriate transformation.

Since the oscillations are assumed to be small, all perturbed quantities calculated in the following are linearized in $\mathbf{s}(\mathbf{r})$. In the observer's frame, the first and second time derivatives of (2.35) are given by:

$$\frac{\partial \mathbf{s}}{\partial t} = \frac{\partial (s_i \mathbf{e}_i)}{\partial t} = i\omega \mathbf{s} + \mathbf{\Omega} \times \mathbf{s}, \tag{2.36}$$

$$\frac{\partial^2 \mathbf{s}}{\partial t^2} = -\omega^2 \mathbf{s} + 2i\omega \mathbf{\Omega} \times \mathbf{s} + \mathbf{\Omega} \times \mathbf{\Omega} \times \mathbf{s}, \tag{2.37}$$

where we have used equation (2.11). The Lagrangian change operator is denoted by Δ and is defined by the operation

$$\Delta(Q) = Q(\mathbf{r} + \mathbf{s}(\mathbf{r}, t), t) - Q_0(\mathbf{r}, t) \tag{2.38}$$

where Q and Q_0 are the values of a scalar or vector quantity in the perturbed and unperturbed flows, and $s(\mathbf{r}, t)$ is the displacement suffered by that fluid element which would have been at $\mathbf{r}$ at time t in the unperturbed flow. Lynden-Bell and Ostriker (1967) show that the total time derivative and the Lagrangian change operator commute:

$$\left[\frac{D}{Dt}, \Delta\right] = 0. \tag{2.39}$$

The Eulerian change operator is defined by the operation

$$\delta(Q) = Q(\mathbf{r}, t) - Q_0(\mathbf{r}, t) \tag{2.40}$$

Comparing equations (2.38) and (2.40), we see that the two operators are related to first order in $\mathbf{s}$ by

$$\Delta = \delta + \mathbf{s} \cdot \nabla. \tag{2.41}$$

To obtain the Lagrangian governing the oscillations, we need to take the variation of equation (2.32). Since the operator δ does not commute with the total time derivative, variational calculations are greatly simplified if we take the Lagrangian rather

than the Eulerian variation of the equations of motion. Applying equation (2.38) to equation (2.32) yields

$$\Delta\left(\frac{D\mathbf{v}_I}{Dt}\right) - \frac{\Delta\rho}{\rho^2}\nabla P + \frac{\Delta(\nabla P)}{\rho} + \Delta(\nabla\phi) = 0. \tag{2.42}$$

The Lagrangian change operator may be brought inside the total time derivative operator with commutation relation (2.39). It may also be brought inside the gradient operators with the the commutation relation

$$[\Delta, \nabla_i] = -(\nabla_i s_j)\nabla_j, \tag{2.43}$$

which can be derived from the discussion in Cox (1980). Thus, we require the perturbed quantities $\Delta\mathbf{v}_I$, $\Delta\rho$, ΔP, and $\Delta\phi$ which are given by

$$\Delta\mathbf{v}_I = \frac{D\mathbf{s}}{Dt} \tag{2.44}$$

$$\Delta\rho = -\rho\nabla\cdot\mathbf{s} \tag{2.45}$$

$$\Delta\phi = \delta\phi + \mathbf{s}\cdot\nabla\phi \tag{2.46}$$

$$\Delta P = -P\Gamma_1\nabla\cdot\mathbf{s} \tag{2.47}$$

where Γ_1 is the first adiabatic exponent. The product $P\Gamma_1$ can be identified with the inverse of the adiabatic compressibility κ_s. Equations (2.44)-(2.47) are derived in the following.

By the definition of the the Lagrangian change operator in equation (2.38), the Lagrangian variation of velocity in the inertial frame is given by

$$\Delta\mathbf{v}_I = \frac{D(\mathbf{r}_0 + \mathbf{s})}{Dt} - \frac{D\mathbf{r}_0}{Dt} = \frac{D\mathbf{s}}{Dt}, \tag{2.48}$$

which follows from the linearity of the total derivative. This establishes equation (2.44).

The Lagrangian perturbation to the density is given by

$$\Delta\rho = \delta\rho + \mathbf{s}\cdot\nabla\rho. \tag{2.49}$$

To determine $\delta\rho$ we take the Eulerian variation of the mass conservation equation

$$\delta\left(\frac{\partial\rho}{\partial t}+\nabla\cdot(\rho\mathbf{v}_I)\right)=0. \tag{2.50}$$

Dropping terms second order in small quantities, noting that $\nabla\cdot(\rho\boldsymbol{\Omega}\times\mathbf{r})=0$, and using the commutation relations from Cox (1980)

$$\left[\frac{\partial}{\partial t},\delta\right]=[\nabla,\delta]=0, \tag{2.51}$$

we obtain

$$\delta\rho=-\nabla\cdot(\rho\mathbf{s}), \tag{2.52}$$

which, together with equation (2.49), yields equation (2.45).

Equation (2.46) results simply from the application of equation (2.41) to ϕ. The Eulerian perturbation in gravitational potential $\delta\phi$ can be obtained by solving the perturbed Poisson equation

$$\nabla^2\delta\phi=4\pi G\delta\rho, \tag{2.53}$$

which is

$$\delta\phi=-G\int\frac{\delta\rho(\mathbf{r}')}{|\mathbf{r}-\mathbf{r}'|}d^3\mathbf{r}'=G\int\frac{\rho(\mathbf{r}')\mathbf{s}(\mathbf{r}')}{|\mathbf{r}-\mathbf{r}'|}\cdot d\mathbf{S}-G\int\rho(r')\mathbf{s}(\mathbf{r}')\cdot\nabla'\frac{1}{|\mathbf{r}-\mathbf{r}'|}d^3\mathbf{r}' \tag{2.54}$$

where we have used equation (2.52) and the divergence theorem. The Lagrangian perturbation in pressure ΔP can be determined from the equation of state. Taking the total derivative of equation (2.34) yields

$$\Delta P=\left(\frac{\partial P}{\partial\rho}\right)_S\Delta\rho+\left(\frac{\partial P}{\partial S}\right)_\rho\Delta S. \tag{2.55}$$

Under the assumption that the oscillations are adiabatic (*i.e.*, $\Delta S=0$):

$$\Delta P=\left(\frac{\partial P}{\partial\rho}\right)_s\Delta\rho=\frac{P}{\rho}\left(\frac{\partial\ln P}{\partial\ln\rho}\right)_s\Delta\rho=\frac{P\Gamma_1}{\rho}\Delta\rho=-P\Gamma_1\nabla\cdot\mathbf{s}, \tag{2.56}$$

completing the derivation of equations (2.44)-(2.47).

The inertial term in equation (2.42) may be reduced by application of equations (2.39) and (2.48) which yields

$$\Delta\left(\frac{D\mathbf{v}_I}{Dt}\right)=\frac{D^2\mathbf{s}}{Dt^2}=\frac{\partial^2\mathbf{s}}{\partial t^2}+2\mathbf{v}_I\cdot\nabla\left(\frac{\partial\mathbf{s}}{\partial t}\right)+\mathbf{a}_I\cdot\nabla\mathbf{s}+\mathbf{v}_I\cdot\nabla(\mathbf{v}_I\cdot\nabla\mathbf{s})=$$

$$-\omega^2\mathbf{s} + 2i\omega\boldsymbol{\Omega}\times\mathbf{s} + \boldsymbol{\Omega}\times\boldsymbol{\Omega}\times\mathbf{s} + 2(\mathbf{u}_0 + \boldsymbol{\Omega}\times\mathbf{r})\cdot\nabla(i\omega\mathbf{s} + \boldsymbol{\Omega}\times\mathbf{s}) +$$
$$(2\boldsymbol{\Omega}\times\mathbf{u}_0 + \boldsymbol{\Omega}\times\boldsymbol{\Omega}\times\mathbf{r} + \mathbf{u}_0\cdot\nabla\mathbf{u}_0)\cdot\nabla\mathbf{s} +$$
$$(\mathbf{u}_0 + \boldsymbol{\Omega}\times\mathbf{r})\cdot\nabla((\mathbf{u}_0 + \boldsymbol{\Omega}\times\mathbf{r})\cdot\nabla\mathbf{s}). \tag{2.57}$$

Substituting equations (2.44)-(2.47) and equation (2.57) into equation (2.42) yields

$$\rho\left(\frac{D^2\mathbf{s}}{Dt^2}\right)_i = \mathcal{L}_{ij}s_j \tag{2.58}$$

where

$$\mathcal{L}_{ij}s_j = \nabla_i(P\Gamma_1\nabla_j s_j) - (\nabla_j s_j)\nabla_i P + (\nabla_i s_j)\nabla_j P - \rho s_j\nabla_j\nabla_i\phi - \rho\nabla_i\delta\phi. \tag{2.59}$$

Using equations (2.15), (2.57), and (2.59), equation (2.58) can be rewritten

$$-\rho\omega^2\mathbf{s} + \rho\mathbf{T}(\mathbf{s}) = \mathcal{L}(\mathbf{s}) \tag{2.60}$$

where

$$\mathbf{T}(\mathbf{s}) = \mathbf{B}(\mathbf{s}) + \mathbf{C}(\mathbf{s}) + \mathbf{D}(\mathbf{s}) + \mathbf{E}(\mathbf{s}). \tag{2.61}$$

The operators $\mathbf{B}(\mathbf{s})$, $\mathbf{C}(\mathbf{s})$, $\mathbf{D}(\mathbf{s})$, and $\mathbf{E}(\mathbf{s})$ are defined as

$$\mathbf{B}(\mathbf{s}) = 2i\omega\boldsymbol{\Omega}\times\mathbf{s} + 2i\omega(\boldsymbol{\Omega}\times\mathbf{r})\cdot\nabla\mathbf{s} + 2i\omega\mathbf{u}_0\cdot\nabla\mathbf{s}, \tag{2.62}$$

$$\mathbf{C}(\mathbf{s}) = \boldsymbol{\Omega}\times\boldsymbol{\Omega}\times\mathbf{s} + \boldsymbol{\Omega}\times\boldsymbol{\Omega}\times\mathbf{r}\cdot\nabla\mathbf{s} + \boldsymbol{\Omega}\times\mathbf{r}\cdot\nabla(\boldsymbol{\Omega}\times\mathbf{s}) + \boldsymbol{\Omega}\times\mathbf{r}\cdot\nabla(\boldsymbol{\Omega}\times\mathbf{r}\cdot\nabla\mathbf{s}), \tag{2.63}$$

$$\mathbf{D}(\mathbf{s}) = 2\boldsymbol{\Omega}\times(\mathbf{u}_0\cdot\nabla\mathbf{s}) + 2\mathbf{u}_0\cdot\nabla(\boldsymbol{\Omega}\times\mathbf{s}) +$$
$$\boldsymbol{\Omega}\times\mathbf{r}\cdot\nabla(\mathbf{u}_0\cdot\nabla\mathbf{s}) + \mathbf{u}_0\cdot\nabla(\boldsymbol{\Omega}\times\mathbf{r}\cdot\nabla\mathbf{s}), \tag{2.64}$$

$$\mathbf{E}(\mathbf{s}) = 2\mathbf{u}_0\cdot\nabla(\mathbf{u}_0\cdot\nabla\mathbf{s}). \tag{2.65}$$

The operator $\mathbf{B}$ is linear in $\mathbf{u}_0$ and $\boldsymbol{\Omega}$, $\mathbf{C}$ is quadratic in $\boldsymbol{\Omega}$, $\mathbf{D}$ is of order $\boldsymbol{\Omega}\cdot\mathbf{u}_0$, and $\mathbf{E}$ is quadratic in $\mathbf{u}_0$ which for the Sun is a progression from the most to the least significant contribution to the perturbed equation of motion. The equation of motion in the solar frame is given in appendix 2A; it is identical to the corresponding result of Lynden-Bell and Ostriker (1967).

For a spherical non-rotating, non-convecting Sun the perturbation term $\mathbf{T}(\mathbf{s}) = 0$ and

$$-\rho\omega^2\mathbf{s} = \mathcal{L}(\mathbf{s}) \tag{2.66}$$

which is identical to equation (2.21). As we have mentioned earlier, the assumption that the temporal and spatial basis functions separate in the observer's frame is accurate only to first order in the bulk rotation rate and nonaxisymmetric flow field. Therefore, in the rest of this paper, we neglect contributions from the higher order terms in the operators **C**, **D**, and **E**.

e) The Equations of Motion for a General Model Perturbation

Thus far we have accounted for the velocity field of convection and the reference frame effects. It remains to introduce convective perturbations of the thermodynamic state variables. In a fluid there are only two independent state variables, the equilibrium model parameters. A variety of model parameter combinations can be chosen; the density ρ and incompressibility modulus κ are convenient choices. The latter is also known as the adiabatic bulk modulus and is defined

$$\kappa = \rho\left(\frac{\partial P}{\partial \rho}\right)_S = P\Gamma_1. \tag{2.67}$$

In the following, any scalar quantity with the subscript o denotes the value of that quantity in the equilibrium model. It is solely a function of radius. The operator δ applied to a quantity Q without the subscript o signifies the eulerian perturbation of that quantity due to seismic motion. The operator δ applied to a quantity Q with the subscript o signifies the structural perturbation of that quantity referenced to the equilibrium model.

Therefore, using equation (2.22), the operator $\mathcal{L}$ may be written

$$\mathcal{L}(\mathbf{s}) = \nabla\cdot\left[\kappa_0\left(\nabla\cdot\mathbf{s}\right)\mathbf{I} + P_0\left\{2\mathbf{e} - \nabla\mathbf{s} - \left(\nabla\cdot\mathbf{s}\right)\mathbf{I}\right\}\right] - \rho_0\,\nabla\delta\phi - \rho_0\,\mathbf{s}\cdot\nabla\nabla\phi_0 \tag{2.68}$$

Clearly, ϕ_0 and P_0 are functions of density alone so that $\mathcal{L}$ is a function of the model paramaters κ_0 and ρ_0.

We now present the equations of motion for the perturbed reference model in the observer's frame when the perturbations include bulk rotation, velocity field $\mathbf{u}_0$, and perturbations $\delta\kappa_0$ to κ_0 and $\delta\rho_0$ to ρ_0. We use the notation $\delta\mathcal{L}$ to indicate the perturbation to the operator $\mathcal{L}$ due to perturbations in the scalar model parameters and the concomitant perturbations δP_0 to P_0 and $\delta\phi_0$ to ϕ_0. Thus, $\delta\mathcal{L}$ can be written

$$\delta\mathcal{L}(\mathbf{s}) = \nabla\cdot[\delta\kappa_0\,(\nabla\cdot\mathbf{s})\,\mathbf{I} + \delta P_0\,\{2\mathbf{e} - \nabla\mathbf{s} - (\nabla\cdot\mathbf{s})\,\mathbf{I}\}] -$$
$$\delta\rho_0\,\nabla\delta\phi - \delta\rho_0\,\mathbf{s}\cdot\nabla\nabla\phi_0 - \rho_0\,\mathbf{s}\cdot\nabla\nabla\delta\phi_0 \qquad (2.69)$$

where we have linearized the perturbation operator in the structural perturbations. In general $\delta\kappa_0 = \delta\kappa_0\,(r,\theta,\phi)$ and $\delta\rho_0 = \delta\rho_0\,(r,\theta,\phi)$. Thus, the equation of motion given by equation (2.60) for the perturbed reference model in the observer's frame becomes

$$-\rho_0\,\omega^2\mathbf{s} + \rho_0\,\mathbf{B}(\mathbf{s}) = \mathcal{L}(\mathbf{s}) + \delta\mathcal{L}(\mathbf{s}) \qquad (2.70)$$

where we have ignored the higher order terms in the operators $\mathbf{C}$, $\mathbf{D}$, and $\mathbf{E}$.

V. PERTURBATION THEORY

In this section we present the quasi-degenerate perturbation theory (*e.g.* Dahlen 1969; Luh 1974; Woodhouse 1980) and show that degenerate perturbation theory (Mathews and Walker 1970) is a special case. We consider a small, but otherwise general perturbation to the equilibrium model and seek expressions for the eigenvalues and eigenfunctions of the perturbed system. The particular perturbations we consider are the rotation, the convective velocity field, and perturbations to κ_0 and ρ_0. The parameterizations of these perturbation are given in §VI.a. In §§V.a-V.c, no references is made to the form of the perturbing operator; in §V.d, the operator is specialized to the perturbations considered in §IV. We present the normal mode eigenfunctions of the equilibrium model in the following subsection.

a) The normal modes

The p modes are spheroidal; their displacement may be written in the form

$$\mathbf{s}(\mathbf{r}) = {}_nU_l(r)Y_l^m(\theta,\phi)\hat{\mathbf{r}} + {}_nV_l(r)\nabla_1\,Y_l^m(\theta,\phi) \qquad (2.71)$$

where ${}_nU_l(r)$ and ${}_nV_l(r)$ denote, respectively, the radial and horizontal eigenfunctions for harmonic degree l and radial order n. The surface gradient operator is given by $\nabla_1 = r(\nabla - \hat{\mathbf{r}} \cdot \nabla)$. We use the notation $\mathbf{s}_{k'}(\mathbf{r})$ to indicate a mode with indices $k' = (n', l', m')$. The function Y_l^m is a spherical harmonic of degree l and azimuthal order m defined using the convention of Edmonds 1960:

$$\int_0^{2\pi} \int_0^{\pi} [Y_{l'}^{m'}(\theta, \phi)]^* Y_l^m(\theta, \phi) \sin\theta d\theta d\phi = \delta_{mm'}\delta_{l'l} \tag{2.72}$$

where integration is over the unit sphere. The coordinates (r,θ,ϕ) are spherical polar coordinates (where θ is colatitude) and $\hat{\mathbf{r}}, \hat{\theta}, \hat{\phi}$ denote unit vectors in the coordinate directions. Henceforth, we will drop the subscripts n and l in equation (2.71) and use instead $U={}_nU_l(r)$, $V={}_nV_l(r)$, $U'={}_{n'}U_{l'}(r)$ and $V'={}_{n'}V_{l'}(r)$. The modes satisfy an orthogonality condition given by

$$\int \rho \mathbf{s}_{k'}^* \cdot \mathbf{s}_k d^3r = N\delta_{m'm}\delta_{n'n}\delta_{l'l} \tag{2.73}$$

where

$$N = \int_0^{R_\odot} \rho_0 \left[UU' + l(l+1)VV'\right] r^2 dr. \tag{2.74}$$

The scalar normalization constant N depends on the normalization convention of the eigenfunctions U and V. This varies among codes commonly in use so we retain N. To facilitate discussion we introduce in the following subsection notation and terminology.

b) Notation and Terminology

A *multiplet* of the equilibrium model is uniquely specified by n and l and is denoted by ${}_nS_l$. The range of m for a multiplet with radial overtone n (where $n = 0$ corresponds to the fundamental mode) and harmonic degree l is $-l \leq m \leq l$. Thus, the dimension of the eigenspace associated with multiplet ${}_nS_l$ is $(2l+1)$. The $(2l+1)$ eigenfrequencies associated with each multiplet are ω_{nl}^m. In the equilibrium model, these frequencies are all identical and therefore the degenerate frequency ω_{nl} is said to be $(2l+1)$ degenerate. Each member of the multiplet ${}_nS_l$ will be called a *singlet.*

Two singlets whose eigenspaces are orthogonal do not interact and are said to be *isolated* from one another. A multiplet composed of singlets whose combined eigenspace is orthogonal to the combined eigenspace of the singlets composing all other multiplets is said to be *isolated* or *self-coupled.* The effect of rotation and other asphericities in the sun is to destroy the $(2l+1)$ degeneracy of ${}_nS_l$ and split the multiplet. The split eigenfrequencies of an isolated multiplet are given by $\omega_{nl}^m = {}_n\omega_l + \delta\omega_{nl}^m$ for $-l \leq m \leq l$ where the $\delta\omega_{nl}^m$ are the eigenvalues of a $(2l+1) \times (2l+1)$ hermitian matrix called the *splitting matrix.*

Two or more singlets which are not isolated, interact and are said to be *coupled.* The degree of coupling between singlets is a function of a number of factors, among which are the strength and geometry of the asphericity producing the coupling, and the similarity of the radial eigenfunctions. When two singlets k and k' couple, the strength of interaction is described by the so-called *general matrix element* $H_{n'n,l'l}^{m'm}$. The matrix $\mathbf{H}_{n'n,l'l}$ is of dimension $(2l'+1) \times (2l+1)$ and is called the *general matrix.* The square general matrix $\mathbf{H}_{nn,ll}$ is just the splitting matrix. The eigenfrequencies of non-isolated singlets which couple within or across n or l are the eigenvalues of an assemblage of block diagonal splitting matrices and off-block diagonal general matrices. The entire assemblage is called the *supermatrix.*

In general, the eigenfunction of an aspherical Sun is a linear combination of the basis functions of the unperturbed system; we call it the *hybrid eigenfunction*, its associated eigenfrequency is called the *hybrid eigenfrequency.* If we are interested in the properties of any given singlet we call that singlet the *target singlet.* Likewise if we are interested in all the singlets of a given multiplet we call that multiplet the *target multiplet.*

c) Quasi-degenerate Perturbation Theory

We introduce quasi-degenerate perturbation theory in order to calculate the hybrid eigenfunctions and eigenfrequencies of non-isolated singlets of a system perturbed about some reference state. We seek a set of eigenvalues of the perturbed system in the neighborhood of a frequency ω_{ref} which we call the reference frequency. Let S

denote the set of all singlets and let K denote the set of singlets with unperturbed frequencies close to ω_{ref} *i.e.*,

$$| \omega_k^2 - \omega_{ref}^2 | \leq \tau \tag{2.75}$$

for each member k of set K, and τ is some small number. Quasi-degenerate perturbation theory is so-named because it is applicable only in a small bandwidth of frequency space as given by equation (2.75).

To obtain the perturbation equations, we perturb the equation of motion of the equilibrium state (47) to first order in ϵ where ϵ is some small number related to the size of the perturbation quantity:

$$(\mathcal{L}_0 + \mathcal{L}_1)(\mathbf{s}_0 + \mathbf{s}_1) = -(\rho_0 + \rho_1)(\omega_{ref}^2 + \omega_1^2)(\mathbf{s}_0 + \mathbf{s}_1), \tag{2.76}$$

where $\mathcal{L}_0$, ρ_0 , and $\mathbf{s}_0$ are, respectively, the Lagrangian, density, and eigenfunction of the equilibrium model each of which are independent of ϵ, and $\mathcal{L}_1$, ρ_1 , and $\mathbf{s}_1$ are the perturbations of the corresponding quantities in the perturbed system to first order in ϵ . The quantity $\omega_{ref}^2 + \omega_1^2$ represents the squared frequency of the perturbed system. The perturbed operator $\mathcal{L}_1$ can include the operators associated with rotational and convective velocity fields derived in the §IV, model perturbations to κ_0 and ρ_0 (and the corresponding perturbations to ϕ_0 and P_0), magnetic fields, and perhaps other effects as well. Collecting the terms independent of ϵ in equation (2.76) yields

$$\mathcal{L}_0 \, \mathbf{s}_0 = -\rho_0 \, \omega_{ref}^2 \mathbf{s}_0 \, . \tag{2.77}$$

The zeroth-order eigenfunction $\mathbf{s}_0$ of the perturbed system is a linear combination of singlets $\mathbf{s}_k$ for $k \in K$. The first-order eigenfunction correction $\mathbf{s}_1$ is a sum of singlets $\mathbf{s}_k$ for $k \in S$. Therefore, the zeroth and first-order hybrid eigenfunctions are written

$$\mathbf{s}_0 = \sum_{k \in K} a_k \mathbf{s}_k, \tag{2.78}$$

$$\mathbf{s}_1 = \sum_{k' \in S} b_{k'} \mathbf{s}_{k'}, \tag{2.79}$$

where the expansion coefficients a_k are independent of ϵ and the $b_{k'}$ are first-order in ϵ. Inserting equation (2.78) into equation (2.77) we obtain

$$\sum_{k \in K} ((\omega_{nl})^2 - \omega_{ref}^2) \rho_0 \, a_k \mathbf{s}_k = 0 \tag{2.80}$$

and consequently $a_k = 0$ for $k \ni K$ to zero order in τ. Collecting the terms first-order in τ or ϵ in equation (2.76) yields

$$(\mathcal{L}_0 + \rho_0 \omega_{ref}^2)\mathbf{s}_1 + (\mathcal{L}_1 + \rho_1 \omega_{ref}^2)\mathbf{s}_0 + \rho_0 \omega_1^2 \mathbf{s}_0 + [(\mathcal{L}_0 + \rho_0 \omega_{ref}^2)\mathbf{s}_0] = 0. \quad (2.81)$$

The last term in equation (2.81) is included because the expression in square brackets leads to terms such as in equation (2.80) which by equation (2.75) are first order in τ. Following the Galerkin method, we substitute equations (2.78) and (2.79) into equation (2.81), project the result on to the basis function $\mathbf{s}_{k''}$, and integrate over the volume of the Sun to obtain

$$\sum_{k' \in S} b_{k'} \int \mathbf{s}_{k''}^* \cdot (\mathcal{L}_0 + \rho_0 \omega_{ref}^2) \cdot \mathbf{s}_{k'} d^3r + \sum_{k \in K} a_k \{ \int \mathbf{s}_{k''}^* \cdot (\mathcal{L}_1 + \rho_1 \omega_{ref}^2) \cdot \mathbf{s}_k d^3r$$

$$+\omega_1^2 \int \rho_0 \mathbf{s}_{k''}^* \cdot \mathbf{s}_k d^3r + \int \mathbf{s}_{k''}^* \cdot (\mathcal{L}_0 + \rho_0 \omega_{ref}^2) \cdot \mathbf{s}_k d^3r \} = 0 \quad (2.82)$$

where each term in equation (2.82) is a scalar.

The first term in equation (2.82) may be reduced to the expression

$$b_{k''}(\omega_{ref}^2 - \omega_{n''l''}^2) N \delta_{n''n'} \delta_{l''l'} \delta_{m''m'} \quad (2.83)$$

where we have used equations (2.21), (2.73), and (2.74). Thus, the expansion coefficient for the first order correction to the zeroth order eigenfunction is given by

$$b_{k''} = \frac{1}{N(\omega_{n''l''}^2 - \omega_{ref}^2)} \sum_{k \in K} a_k \int \{\mathbf{s}_{k''}^* \cdot [\mathcal{L}_1 + \rho_1 \omega_{ref}^2 + \rho_0 \omega_1^2 + \mathcal{L}_0 + \rho_0 \omega_{ref}^2] \cdot \mathbf{s}_k\} d^3r. \quad (2.84)$$

The terms in equation (2.82) are easily reduced to

$$\sum_{k \in K} a_k [\int \mathbf{s}_{k''} \cdot (\mathcal{L}_1 + \rho_1 \omega_{ref}^2) \cdot \mathbf{s}_k d^3r + (\omega_1^2 + \omega_{ref}^2 - \omega_{nl}^2) N \delta_{n''n} \delta_{l''l} \delta_{m''m}] = 0 \quad (2.85)$$

where we have discarded the terms in $b_{n''l''m''}$ for reasons explained below. Equation (2.85) represents the principle result of quasi-degenerate perturbation theory. The eigenfrequency perturbations ω_1^2 are the eigenvalues of the supermatrix whose elements are

$$\frac{1}{N} \left\{ \int \mathbf{s}_{k''} \cdot (-\mathcal{L}_1 - \rho_1 \omega_{ref}^2) \cdot \mathbf{s}_k d^3r - (\omega_{ref}^2 - \omega_{nl}^2) N \delta_{n''n} \delta_{l''l} \delta_{m''m} \right\} \quad (2.86)$$

for $k'', k \in K$.

Had we included the $b_{k''}$ terms for $k'' \ni K$ in the supermatrix, they would have decoupled in an eigenvalue-eigenvector decomposition from the singlets $k \in K$ since the $b_{k''}$ terms fall only on the diagonal. The $b_{k''}$ terms with $k'', k \in K$ do not decouple but become second order in small quantities since they include the factor $\omega_{ref}^2 - \omega_{n''l''}^2$ which becomes $\mathcal{O}(\tau)$ for $k'' \in K$ and since the coefficient $b_{k''}$ is $\mathcal{O}(\epsilon)$ by definition.

We define the general matrix element to be

$$H_{n''n,l''l}^{m''m} = \int \mathbf{s}_{k''} \cdot (-\mathcal{L}_1 - \rho_1 \omega_{ref}^2) \cdot \mathbf{s}_k d^3r \tag{2.87}$$

for $-l'' \leq m'' \leq l''$ and $-l \leq m \leq l$ and where $H_{n''n,l''l}^{m''m}$ is the (m'', m) component of the general matrix $\mathbf{H}_{n''n,l''l}$. Denoting the supermatrix by $\mathbf{Z}$, the component $Z_{k''k}$ becomes

$$Z_{k''k} = \frac{1}{N}\left\{H_{n''n,l''l}^{m''m} - (\omega_{ref}^2 - \omega_{nl}^2) N \delta_{n''n} \delta_{l''l} \delta_{m''m}\right\} \tag{2.88}$$

for $k'', k \in K$. The squared frequencies of the perturbed system are given by

$$\omega_i^2 = \omega_{ref}^2 + (\omega_1^2)_i \tag{2.89}$$

and the range of i is the dimension of the supermatrix. If desired, the approximation

$$(\omega_1^2)_i = 2\omega_{ref} \delta\omega_i \tag{2.90}$$

may be used so that

$$\omega_i = \omega_{ref} + \frac{(\omega_1^2)_i}{2\omega_{ref}}. \tag{2.91}$$

The zeroth-order eigenfunction of the perturbed system is given by equation (2.78) and the expansion coefficients a_k are simply the components of the eigenvectors associated with each eigenfrequency ω_i. If there are factors of frequency such as ω or ω_{nl} which appear in the $H_{n''n,l''l}^{m''m}$ or in $\mathcal{L}_1$, we replace that frequency with ω_{ref}.

Degenerate perturbation theory can be recovered from equation (2.85) by choosing $\omega_{ref} = \omega_{nl}$, setting $n'' = n$, $l'' = l$, and by spanning the entire eigenspace of the multiplet ${}_nS_l$.

To visualize the geometric structure of the coupling problem, it is helpful to examine in matrix notation the block elements contributing to the supermatrix $\mathbf{Z}$. Using the approximation of equation (2.90), the hybrid eigenfrequencies $\delta\omega_i$ are given by the eigenvalues of the matrix $\mathbf{Z}/2\omega_{ref}$. The matrix $\mathbf{Z}$ is assembled from the prescription given in equation (2.88). Suppose we are interested in all the singlets of a target multiplet ${}_nS_l$. We now introduce a small notational change and denote the self-coupling matrix for that multiplet by $\mathbf{H}_{00}$. The singlets of ${}_nS_l$ may also couple to the singlets of other multiplets ${}_{n'}S_{l'}$. The symbol $\mathbf{H}_{ij}$ denotes the general matrix governing interaction between singlets from ${}_{n'}S_{l'}$ and ${}_{n''}S_{l''}$. The index i is chosen to be positive or negative depending on whether $\omega_{n'l'}$ is greater than or less than the reference frequency $\omega_{ref} = \omega_{nl}$. Similarly j is > 0 or < 0 if $\omega_{n''l''} > \omega_{nl}$ or $\omega_{n''l''} < \omega_{nl}$, respectively. Finally, let us denote the reference frequency by ω_0 With this notation, the matrix $\mathbf{Z}$ may be written

$$\mathbf{Z} = \begin{bmatrix} \ddots & & & & \\ & (\omega_{-1}^2 - \omega_0^2)\mathbf{I}_{-1-1} & & & \\ & & \mathbf{0} & & \\ & & & (\omega_1^2 - \omega_0^2)\mathbf{I}_{11} & \\ & & & & \ddots \end{bmatrix} + \frac{1}{N} \begin{bmatrix} & \vdots & & \vdots & \\ \cdots & \mathbf{H}_{-1-1} & \mathbf{H}_{-10} & \mathbf{H}_{-11} & \cdots \\ & \mathbf{H}_{0-1} & \mathbf{H}_{00} & \mathbf{H}_{01} & \\ \cdots & \mathbf{H}_{1-1} & \mathbf{H}_{10} & \mathbf{H}_{11} & \cdots \\ & \vdots & & \vdots & \end{bmatrix}. \tag{2.92}$$

We note that the supermatrix can become quite large if all singlets contributing to the $\mathbf{H}$ matrices are retained. We discuss in §IX the practical details of assembling $\mathbf{Z}$, and provide a criterion which can be used to retain only those singlets which significantly contribute to $\mathbf{Z}$.

d) The Perturbation Equation for Convection

We presently specialize quasi-degenerate perturbation theory to the model parameter and velocity field perturbations associated with convection. The operator for these perturbations in the observers frame to first order in the bulk roation rate and

the flow field is given by equation (2.70). We may rewrite this equation as

$$(\mathcal{L}_0 + \delta\mathcal{L} - \rho_0 \mathbf{B})(\mathbf{s}_0 + \mathbf{s}_1) = -(\rho_0 + \rho_1)(\omega_{ref}^2 + \omega_1^2)(\mathbf{s}_0 + \mathbf{s}_1) \tag{2.93}$$

where $\delta\mathcal{L}$ is given by equation (2.69) and where we have allowed for a general density perturbation ρ_1 . Comparing this to equation (2.76), we may make the identifications

$$\mathcal{L}_1(\mathbf{s}) = \delta\mathcal{L}(\mathbf{s}) - \rho_0 \mathbf{B}(\mathbf{s}) \tag{2.94}$$

and

$$\rho_1 = \delta\rho_0 . \tag{2.95}$$

Substituting equations (2.94) and (2.95) into equation (2.87) gives

$$H^{m''m}_{n''n,l''l} = \int \mathbf{s}_{k''} \cdot (\rho_0 \mathbf{B} - \delta\mathcal{L} - \delta\rho_0 \omega_{ref}^2) \cdot \mathbf{s}_k d^3r. \tag{2.96}$$

VI. THE GENERAL MATRIX ELEMENT FOR CONVECTION

In this section we derive the general matrix for convective perturbations. The scalar and vector perturbations are expanded, respectively, in terms of spherical and vector spherical harmonics. The general matrix which governs the interaction between two modes is given by equation (2.96). It includes contributions from the operators $\mathbf{B}$ and $\delta\mathcal{L}$, and from the perturbation $\delta\rho_0$. The operator $\mathbf{B}$ includes terms linear in Ω and $\mathbf{u}_0$. The operator $\delta\mathcal{L}$ includes terms linear in $\delta\rho_0$ and $\delta\kappa_0$. In §VI.b we derive the general matrix for the term in operator $\mathbf{B}$ which is linear in $\mathbf{u}_0$ for a velocity field without the anelastic constraint. We denote that matrix by $\mathbf{G}_{n'n,l'l}$. We show that $\mathbf{G}_{n'n,l'l}$ does not lead to a hermtian supermatrix. In §VI.c we incorporate the anelastic condition into $\mathbf{G}_{n'n,l'l}$, denote that general matrix by ${}_{an}\mathbf{G}_{n'n,l'l}$, and show that it does lead to a hermitian supermatrix. In §VI.d we present the general matrix for the operator $\mathbf{B}$ whose contributions include terms linear in Ω and $\mathbf{u}_0$ and denote that matrix by $\mathbf{B}_{n'n,l'l}$. In §VI.e we derive the general matrix for the operator $\delta\mathcal{L}$ and denote that general matrix by $\mathbf{L}_{n'n,l'l}$. Finally, in §VI.f we assemble these general matrices and denote the sum by the general matrix $\mathbf{K}_{n'n,l'l}$.

a) The Flow Field and the Thermodynamic Variables

A general, time-independent velocity field can be represented as the sum of vector spherical harmonics

$$\mathbf{u}_0(\mathbf{r}) = \sum_{s=0}^{\infty}\sum_{t=-s}^{s}[u_s^t(r)Y_s^t(\theta,\phi)\hat{\mathbf{r}} + v_s^t(r)\nabla_1 Y_s^t(\theta,\phi) - w_s^t(r)\hat{\mathbf{r}}\times\nabla_1 Y_s^t(\theta,\phi)]. \quad (2.97)$$

The first two terms in equation (2.97) compose the poloidal flow and the last term represents the toroidal flow. The anelastic condition can be incorporated into the Lagrangian describing the oscillating system by combining the anelastic condition with the reality of the flow field to yield a relationship between the poloidal spherical harmonic coefficients u_s^t and v_s^t. The anelastic condition is given by

$$\nabla\cdot(\rho_0\,\mathbf{u}_0) = 0. \quad (2.98)$$

Equation (2.98) implies that

$$\partial_r(r^2\rho_0\,u_s^t) = \rho_0\,rs(s+1)v_s^t \quad (2.99)$$

for each s and t in $\mathbf{u}_0$. The reality of the flow fields implies that each coefficient in equation (2.97) satisfies a condition like $u_s^{-t} = (-1)^t u_s^{t*}$. In addition, the radial component of the velocity field must vanish at the surface. Therefore, we require

$$u_s^t(R_\odot) = 0 \;\; \forall\, s,\, t. \quad (2.100)$$

The scalar model parameters of the reference model are given by

$$\begin{aligned}\kappa(r,\theta,\phi) &= \kappa_0(r) + \delta\kappa_0(r,\theta,\phi)\\ \rho(r,\theta,\phi) &= \rho_0(r) + \delta\rho_0(r,\theta,\phi)\end{aligned} \quad (2.101)$$

where the perturbations to the adiabatic bulk modulus and density are prescribed by

$$\delta\kappa_0 = \delta\kappa_0^e\,Y_2^0(\theta,\phi) + \sum_{s=0}^{\infty}\sum_{t=-s}^{s}\delta\kappa_s^t Y_s^t(\theta,\phi), \quad (2.102)$$

$$\delta\rho_0 = \delta\rho_0^e\,Y_2^0(\theta,\phi) + \sum_{s=0}^{\infty}\sum_{t=-s}^{s}\delta\rho_s^t Y_s^t(\theta,\phi). \quad (2.103)$$

The superscript e denotes the structural perturbation due to the ellipticity induced by the bulk rotation. The ellipticity $\epsilon(r)$ is the solution of Clairauts's equation (see

Tassoul (1978) for a derivation of $\epsilon(r)$). The ellipticity perturbations to κ_0 and ρ_0 are given in Woodhouse and Dahlen (1978):

$$[\delta\kappa_0^e\,,\delta\rho_0^e\,]=\left(\frac{4\pi}{5}\right)^{\frac{1}{2}}\frac{2}{3}r\epsilon(r)\,[\partial_r\kappa_0\,,\partial_r\rho_0\,] \tag{2.104}$$

where

$$\epsilon(r)=\epsilon(R_\odot)\exp\left[-\int_r^{R_\odot}x^{-1}\eta(x)dx\right], \tag{2.105}$$

$$\eta(r)=\frac{25}{4}\left[1-\frac{3}{2}z(r)\right]^2-1, \tag{2.106}$$

$$z(r)=\frac{2}{3}r^{-2}\left(\int_0^r\rho_0\,(x)x^4dx\right)/\left(\int_0^r\rho_0\,(x)x^2dx\right), \tag{2.107}$$

$$\epsilon(R_\odot)=15\Omega^2/[8\pi G\bar{\rho}_0\,(\eta(R_\odot)+2)], \tag{2.108}$$

$$\bar{\rho}_0\;=3{R_\odot}^{-3}\int_0^{R_\odot}\rho_0\,(x)x^2dx. \tag{2.109}$$

b) The General Matrix for a General Flow Field

The contribution $\mathbf{G}_{n'n,l'l}$ to the general matrix $\mathbf{H}_{n'n,l'l}$ for terms first order in $\mathbf{u}_0$ may be obtained from equations (2.61), (2.62), and (2.96):

$$\mathbf{G}_{n'n,l'l}=2i\omega_{ref}\int\rho_0\,\mathbf{s}'^*\cdot\mathbf{u}_0\;\cdot\nabla\mathbf{s}\,d^3\mathbf{r}. \tag{2.110}$$

This is the only term first order in the perturbation quantity which is constrained by the anelastic condition. The components $G^{m'm}_{n'n,l'l}$ of $\mathbf{G}_{n'n,l'l}$ can be derived with the formalism in Appendix 2B. We obtain:

$$G^{m'm}_{n'n,l'l}=2\omega_{ref}4\pi\gamma_{l'}\gamma_l(-1)^{m'}\sum_{s=0}^{\infty}\sum_{t=-s}^{s}\gamma_s\begin{pmatrix}l' & s & l\\ -m' & t & m\end{pmatrix}\times$$

$$\{\int\rho_0 iu_s^t(r)R_s(r)r^2dr+\int\rho_0 iv_s^t(r)H_s(r)rdr+\int\rho_0 w_s^t(r)T_s(r)rdr\} \tag{2.111}$$

where the kernels $R_s(r)$, $H_s(r)$, and $T_s(r)$ are given by

$$R_s=U'\dot{U}B^{(0)+}_{l'sl}+V'\dot{V}B^{(1)+}_{l'sl}, \tag{2.112}$$

$$H_s=[UU'-VU']B^{(1)+}_{sl'l}+(1+(-1)^{(l'+s+l)})\frac{V'V}{r}\Omega_0^{l'}\Omega_0^s\Omega_0^l\Omega_2^l\begin{pmatrix}l' & s & l\\ 1 & 1 & -2\end{pmatrix}$$

$$+[V'U - V'V]\Omega_0^l\Omega_0^l B_{sll'}^{(1)+}, \tag{2.113}$$

$$T_s = [UU' - VU']B_{sl'l}^{(1)-} + [V'U - V'V]\Omega_0^l\Omega_0^l B_{sll'}^{(1)-} -$$

$$(1-(-1)^{(l'+s+l)})\frac{V'V}{r}\Omega_0^{l'}\Omega_0^s\Omega_0^l\Omega_2^l \begin{pmatrix} l' & s & l \\ 1 & 1 & -2 \end{pmatrix}, \tag{2.114}$$

for $-l \le m \le l$, $-l' \le m' \le l'$, and where the overdot indicates the radial derivative. The γ_k and Ω_N^k factors are given by

$$\gamma_k = \sqrt{\frac{2k+1}{4\pi}} \quad \text{and} \quad \Omega_N^k = \sqrt{\frac{(k+N)(k-N+1)}{2}}. \tag{2.115}$$

The $B_{l'l''l}^{(N)\pm}$ coefficients are defined

$$B_{l'l''l}^{(N)\pm} = \frac{1}{2}(1 \pm (-1)^{(l'+l''+l)})\left[\frac{(l'+N)!(l+N)!}{(l'-N)!(l-N)!}\right]^{\frac{1}{2}}(-1)^N \begin{pmatrix} l' & l'' & l \\ -N & 0 & N \end{pmatrix}. \tag{2.116}$$

There are several useful identities which the B coefficients satisfy (see Woodhouse 1980, eqs. (A43) and (A46)):

$$B_{l'sl}^{(1)+} = \frac{1}{2}[l'(l'+1) + l(l+1) - s(s+1)]B_{l'sl}^{(0)+}, \tag{2.117}$$

$$B_{l'sl}^{(1)-} = \frac{1}{2}\left\{\frac{(\Sigma+2)(\Sigma+4)}{\Sigma+3}(\Sigma+1-2l)(\Sigma+1-2l')(\Sigma+1-2s)\right\}^{\frac{1}{2}} \times B_{l'+1,s+1,l+1}^{(0)+} \tag{2.118}$$

where $\Sigma = l' + s + l$. The phase and normalizations of the Wigner 3-j symbols are those of Edmonds 1960. A numerical algorithm for calculating the symbols is given in Appendix 2C. The decomposition of general matrix element of equation (2.119) into a product of a reduced matrix element independent of m and m' times a Clebsch-Gordon coefficient is a consequence of the Wigner-Eckart theorem (see Edmonds 1960).

The general matrix in equation (2.111) does not lead to a hermitian splitting problem. In general, a general matrix is not a square matrix and therefore cannot be hermitian. However, as can be seen from equations (2.85) and (2.86), the splitting problem reduces to performing an eigenvalue-eigenvector decomposition of the

supermatrix in equation (2.86). The supermatrix is an assemblage of block diagonal splitting matrices and block off-diagonal general matrices. The entire assemblage is a square matrix whose dimension is the number of singlets contributing to the coupling. In order for the supermatrix to be hermitian we require that the real terms of the general matrix remain unchanged and that the imaginary quantities be skew-symmetric after the primed and unprimed quantities are interchanged. The w_s^t term in equation (2.111) satisfies this requirement but the terms in u_s^t and v_s^t do not. The w_s^t coefficients are the expansion coefficients for the toroidal velocity field which by definition is a solenoidal field and therefore the anelasticity condition does not constrain them. To obtain a hermitian supermatrix, we must incorporate the anelastic constraint of equation (2.98) into the poloidal kernels.

c) The General Matrix with the Incorporation of the Anelastic Constraint

The anelastic version of the general matrix $G_{n'n,l'l}$ is denoted by ${}_{an}G_{n'n,l'l}$ and is derived in Appendix 2D. The final result is

$$\begin{aligned} {}_{an}G^{m'm}_{n'n,l'l} &= 2\omega_{ref} 4\pi \gamma_{l'}\gamma_l (-1)^{m'} \sum_{s=0}^{\infty}\sum_{t=-s}^{s} \gamma_s \begin{pmatrix} l' & s & l \\ -m' & t & m \end{pmatrix} \\ &\times \{\int \rho_0 i u_s^t(r) R_s^{an}(r) r^2 dr + \int \rho_0 i v_s^t(r) H_s^{an}(r) r dr \\ &+ \int r\rho_0 w_s^t(r) T_s^{an}(r) dr\} \end{aligned} \tag{2.119}$$

where the radial kernels $R_s^{an}(r)$, $H_s^{an}(r)$, and $T_s^{an}(r)$ are given by

$$R_s^{an}(r) = \frac{1}{2}(U'\dot{U} - \dot{U}'U)B_{l'sl}^{(0)+} + \frac{1}{2}(V'\dot{V} - \dot{V}'V)B_{l'sl}^{(1)+}, \tag{2.120}$$

$$H_s^{an}(r) = \frac{1}{2}[l(l+1) - l'(l'+1)]\,[(U'U)B_{l'sl}^{(0)+} + (V'V)B_{l'sl}^{(1)+}\,] + V'UB_{l'ls}^{(1)+} - U'VB_{ll's}^{(1)+}, \tag{2.121}$$

$$T_s^{an}(r) = \{U'V + V'U - U'U - \frac{1}{2}V'V[l(l+1) + l'(l'+1) - s(s+1)]\}B_{l'sl}^{(1)-}. \tag{2.122}$$

The superscript *an* of the kernels $R_s^{an}(r)$, $H_s^{an}(r)$, and $T_s^{an}(r)$ denotes that they are the anelastic version of the kernels $R_s(r)$, $H_s(r)$, and $T_s(r)$ in equations (2.112)-(2.114).

The general matrix ${}_{an}G^{m'm}_{n'n,l'l}$ in equation (2.119) leads to a hermitian splitting problem. This can be seen by noting that the poloidal kernels are multiplied by

the imaginary number i, and that swapping the primed and unprimed quantities in those kernels leads to kernels skew-symmetric with respect to the original ones and performing the same operation on the toroidal kernel $T_s^{an}(r)$ leaves that kernel unchanged. We have also used the reality condition of the expansion coefficients ($u_s^{-t} = (-1)^t u_s^{t*}$, $v_s^{-t} = (-1)^t v_s^{t*}$, $w_s^{-t} = (-1)^t w_s^{t*}$), and the permutation relation for Wigner 3-j symbols in equation (2B.19) of Appendix 2B. In Appendix 2E we show that the operators $\mathbf{B}$ in equation (2.62) is hermitian provided that the anelastic condition is enforced and that the velocity field $\mathbf{u}_0$ satisfies the boundary condition in equation (2.100). If desired, the integral kernels in equation (2.119) may be reduced to expressions involving 3-j symbols of the form:

$$\begin{pmatrix} l' & s & l \\ 0 & 0 & 0 \end{pmatrix},$$

by making use of identities in equations (2.117) and (2.118).

d) The General Matrix for Terms Linear in $\mathbf{u}_0$ *and* Ω

The general matrix $\mathbf{B}_{n'n,l'l}$ valid to first order in Ω and $\mathbf{u}_0$ may be obtained from equations (2.61), (2.62), (2.96) and equation (2.119) to yield

$$\mathbf{B}_{n'n,l'l} = 2i\omega_{ref} \int \mathbf{s}'^* \cdot \mathbf{\Omega} \times \mathbf{s}\, d^3\mathbf{r} + 2i\omega_{ref} \int \mathbf{s}'^* \cdot \mathbf{\Omega} \times \mathbf{r} \cdot \nabla \mathbf{s}\, d^3\mathbf{r} + {}_{an}\mathbf{G}_{n'n,l'l} \quad (2.123)$$

where we have used the anelastic version of $\mathbf{G}_{n'n,l'l}$. Noting that

$$\mathbf{\Omega} \times \mathbf{r} \cdot \nabla \mathbf{s} = \Omega \frac{\partial \mathbf{s}}{\partial \phi} = im\Omega \mathbf{s} + \mathbf{\Omega} \times \mathbf{s}, \quad (2.124)$$

the general matrix becomes

$$\mathbf{B}_{n'n,l'l} = -2m\omega_{ref}\Omega \int \rho_0\, \mathbf{s}'^* \cdot \mathbf{s} d^3\mathbf{r} + 4i\omega_{ref} \int \mathbf{s}'^* \cdot \mathbf{\Omega} \times \mathbf{s} d^3\mathbf{r} + {}_{an}\mathbf{G}_{n'n,l'l}. \quad (2.125)$$

The first two integrals are easily reduced using the technique described in Appendix 2B and ${}_{an}\mathbf{G}_{n'n,l'l}$ is given by equation (2.119). We obtain then,

$$\mathbf{B}^{m'm}_{n'n,l'l} = -2m\Omega\omega_{ref}\delta_{ll'}\delta_{nn'}\delta_{mm'}N + 4m\Omega\omega_{ref}\delta_{ll'}\delta_{mm'} \int_0^{R_\odot} C(r) r^2 dr + {}_{an}G^{m'm}_{n'n,l'l}, \quad (2.126)$$

where the normalization integral N is given by equation (2.74), and

$$C(r) = \rho_0 \, (UV' + U'V + VV'). \tag{2.127}$$

e) The General Matrix for Perturbations to the Thermodynamic Variables

We now present the general matrix for perturbations to the thermodynamic variables. The general matrix for a general aspherical perturbation to the model parameters of the earth has been derived by Woodhouse(1980). The appropriate general matrix for the corresponding model parameters in Sun may be inferred from his work. The required general matrix may be obtained from equation (2.69). Its components are given by

$$L^{m'm}_{n'n,l'l} = -\int \mathbf{s}_{k''} \cdot (\delta\mathcal{L} + \delta\rho_0 \, \omega^2_{ref}) \cdot \mathbf{s}_k \tag{2.128}$$

and

$$\begin{aligned} L^{m'm}_{n'n,l'l} &= E^m_l \int_0^{R_\odot} E(r) r^2 dr + 4\pi\gamma_{l'}\gamma_l(-1)^{m'} \sum_{s=0}^{\infty} \sum_{t=-s}^{s} \gamma_s \begin{pmatrix} l' & s & l \\ -m' & t & m \end{pmatrix} \\ &\times \int_0^{R_\odot} [\delta\kappa^t_s K_s + \delta\rho^t_s R^{(2)}_s] r^2 dr \end{aligned} \tag{2.129}$$

where

$$E^m_l = \delta_{m'm}(T_{lm}\delta_{l'l} + \frac{3}{2} S_{lm} S_{l'+1,m} \delta_{ll'+2} + \frac{3}{2} S_{l'm} S_{l+1,m} \delta_{l'l+2}), \tag{2.130}$$

$$E(r) = \frac{2}{3}[\kappa_0 \, (\bar{K} - (\eta+1)\tilde{K}) + \rho_0 \, (\bar{R} - (\eta+3)\tilde{R})], \tag{2.131}$$

$$K_s(r) = (\dot{U}' + F')(\dot{U} + F) B^{(0)+}_{l'sl}, \tag{2.132}$$

$$\begin{aligned} R^{(2)}_s &= R^{(1)}_s + \frac{4\pi G}{2s+1} \{ r^s \int_r^{R_\odot} r^{-s} [(s+1) G^{(2)}_s - r G^{(1)}_s] dr \\ &- r^{-s-1} \int_0^r r^{s+1} [s G^{(2)}_s + r G^{(1)}_s] dr \}, \end{aligned} \tag{2.133}$$

$$\begin{aligned} R^{(1)}_s &= [-\omega^2_{ref} V\dot{V}' + r^{-1}(\phi_1' \, V + \delta\phi V') + \frac{1}{2} g_0 \, r^{-1}(U'V + V'U)] B^{(1)+}_{l'sl} \\ &+ [8\pi G\rho_0 \, UU' + \delta\dot{\phi}' U + \delta\dot{\phi} U' - \omega^2_{ref} UU' \\ &- \frac{1}{2} g_0 \, (4r^{-1} UU' + U'F + UF')] B^{(0)+}_{l'sl}, \end{aligned} \tag{2.134}$$

$$
\begin{aligned}
G_s^{(1)} &= \frac{1}{2}\rho_0\, r^{-1}(U\dot{V}' + r^{-1}UV' - \dot{U}V' - 2FV')B_{l'ls}^{(1)+} \\
&+ \frac{1}{2}\rho_0\, r^{-1}(U'\dot{V} + r^{-1}U'V - \dot{U}'V - 2F'V)B_{ll's}^{(1)+} \\
&+ \rho_0\, r^{-2}UU's(s+1)B_{l'sl}^{(0)+}, \qquad (2.135)
\end{aligned}
$$

$$
G_s^{(2)} = \frac{1}{2}\rho_0\, r^{-1}UV'B_{l'ls}^{(1)+} + \frac{1}{2}\rho_0\, r^{-1}U'VB_{ll's}^{(1)+} - \rho_0\,(F'U + U'F)B_{l'sl}^{(0)+}, \qquad (2.136)
$$

$$
\begin{aligned}
\bar{K} &= -(\dot{U} + F)(\dot{U}' + \frac{1}{2}(l'(l'+1) - l(l+1) + 6)r^{-1}V') \\
&- (\dot{U}' + F')(\dot{U} + \frac{1}{2}(l(l+1) - l'(l'+1) + 6)r^{-1}V), \qquad (2.137)
\end{aligned}
$$

$$
\begin{aligned}
\bar{R} &= F(r\delta\dot{\phi}' + 4\pi G\rho_0\, rU' + g_0\, U') \\
&+ \frac{1}{2}(l'(l'+1) - l(l+1) + 6)UV'(\omega_{ref}^2 - r^{-1}g_0\,) + 3r^{-1}g_0\, UU' \\
&+ r^{-1}\delta\phi'[\frac{1}{2}(l'(l'+1) + l(l+1) - 6)V - l'(l'+1)U] \\
&+ F'(r\delta\dot{\phi} + 4\pi G\rho_0\, rU + g_0\, U) + \frac{1}{2}(6 + l(l+1) - l'(l'+1))U'V(\omega_{ref}^2 - r^{-1}g_0\,) \\
&+ 3r^{-1}g_0\, U'U + r^{-1}\delta\phi[\frac{1}{2}(l(l+1) + l'(l'+1) - 6)V' - l(l+1)U'], \qquad (2.138)
\end{aligned}
$$

$$
\begin{aligned}
\tilde{K} &= \frac{1}{2}(\dot{U} + F)(-\dot{U}' + F' + (l'(l'+1) - l(l+1) + 6)r^{-1}V') \\
&+ \frac{1}{2}(\dot{U}' + F')(-\dot{U} + F + (l(l+1) - l'(l'+1) + 6)r^{-1}V), \qquad (2.139)
\end{aligned}
$$

$$
\begin{aligned}
\tilde{R} &= \frac{1}{4}(l(l+1) + l'(l'+1) - 6)(2r^{-1}V'\delta\phi - \omega_{ref}^2 VV') \\
&+ \frac{1}{2}U'[2\delta\dot{\phi} + 8\pi G\rho_0\, U - \omega_{ref}^2 U - (l(l+1) \\
&- l'(l'+1) + 6)g_0\, r^{-1}V] + \frac{1}{4}(l(l+1) + l'(l'+1) - 6)(2r^{-1}V\delta\phi' - \omega_{ref}^2 VV') \\
&+ \frac{1}{2}U[2\delta\dot{\phi}' + 8\pi G\rho_0\, U' - \omega_{ref}^2 U' - (l'(l'+1) - l(l+1) + 6)g_0\, r^{-1}V'], \qquad (2.140)
\end{aligned}
$$

$$
F = r^{-1}(2U - l(l+1)V), \quad F' = r^{-1}(2U' - l'(l'+1)V'), \qquad (2.141)
$$

and

$$
S_{lm} = \left[\frac{(l+m)(l-m)}{(2l+1)(2l-1)}\right]^{\frac{1}{2}}, \quad T_{lm} = \frac{l(l+1) - 3m^2}{(2l-1)(2l+3)}. \qquad (2.142)
$$

We have used the notation $\delta\phi$ and $\delta\dot{\phi}$ instead of Woodhouse's notation ϕ_1 and $\dot{\phi}_1$. The variables $\delta\phi$, $\delta\dot{\phi}$, U and V are the eigenfunctions of the solar oscillations. Perturbations in P_0 and ϕ_0 have been incorporated into the density perturbation kernel. The integral in $E(r)$ represents the contribution from the ellipticity.

f) The General Matrix

Finally, we collect the results from the previous sections to obtain the general matrix which governs the interaction between two singlets to first order in Ω, $\mathbf{u}_0$, $\delta\kappa_0$ and $\delta\rho_0$. We denote this general matrix by $\mathbf{K}_{n'n,l'l}$. From equations (2.119), (2.126), and (2.128) we obtain

$$K^{m'm}_{n'n,l'l} = -2m\Omega\omega_{ref}\delta_{ll'}\delta_{nn'}\delta_{mm'}N + 4m\Omega\omega_{ref}\delta_{ll'}\delta_{mm'}\int_0^{R_\odot}\rho_0\, C(r)r^2dr$$
$$+E^m_l\int_0^{R_\odot}E(r)r^2dr +$$
$$4\pi\gamma_{l'}\gamma_l(-1)^{m'}\sum_{s=0}^{\infty}\sum_{t=-s}^{s}\gamma_s\begin{pmatrix} l' & s & l \\ -m' & t & m\end{pmatrix}\times\int_0^{R_\odot}[\delta\kappa^t_s(r)K_s(r) + \delta\rho^t_s(r)R^{(2)}_s(r) +$$
$$\rho_0 i u^t_s(r)R^{an}_s(r) + \rho_0 i v^t_s(r)\frac{H^{an}_s(r)}{r} + \rho_0 w^t_s(r)\frac{T^{an}_s(r)}{r}]r^2dr \qquad (2.143)$$

where the Coriolis kernel $C(r)$, the ellipticity kernel $E(r)$, the bulk modulus perturbation kernel $K_s(r)$, the density perturbation kernel $R^2_s(r)$, the poloidal flow kernels $R^{an}_s(r)$ and $H^{an}_s(r)$, and the toroidal flow kernel $T^{an}_s(r)$ are given, respectively, by equations (2.127), (2.131), (2.132), (2.133), (2.120), (2.121), and (2.122). The velocity field expansion coefficients $u^t_s(r)$, $v^t_s(r)$, and $w^t_s(r)$ are defined by equation (2.97), and the thermodynamic expansion coefficients $\kappa^t_s(r)$ and $\rho^t_s(r)$ are defined, respectively, by equations (2.102) and (2.103)

VII. QUALITATIVE INTERPRETATION OF QUASI-DEGENERATE PERTURBATION THEORY

The determination of modal frequencies and amplitudes for an aspherical Sun requires application of quasi-degenerate perturbation theory as we now argue. Rotation and convection in the Sun lift the degeneracy of each eigenfrequency ω_{nl}. Coupling

can take place between singlets $\mathbf{s}_k$ and $\mathbf{s}_{k'}$ when the difference $\omega_{nl} - \omega_{n'l'}$ is comparable to the predicted total splitting widths of ${}_nS_l$ and ${}_{n'}S_{l'}$ in an ordinary degenerate perturbation theory calculation. Bulk rotation perturbs singlet frequencies of ${}_nS_l$ to the new value $\omega_{nl}^m \sim \omega_{nl} + m\Omega$. Therefore, given the near-degeneracy of many of the p modes (see the $\omega - k$ dispersion diagram in Figure (1) of Libbrecht and Kaufman 1988) and the above criterion, many singlets may couple. In §VII.a we list the selection rules which determine the possible coupling partners. A discussion of the qualitative sensitivity of the p modes to a convective velocity field is given in §VII.b, and in §VII.c we discuss the significance of the hybrid eigenfunctions.

a) Selection Rules

The condition for coupling given by the quasi-degenerate criterion in equation (2.75) is necessary, but not sufficient. For a singlet $\mathbf{s}_k$ to contribute to the supermatrix $\mathbf{Z}$ in equation (2.88) the quantum numbers k must also satisfy selection rules so that $\mathbf{s}_k$ has a nonzero interaction with at least one of the other singlets in the eigenspace. Angular integrations over the sphere are insensitive to the radial order n, and therefore any selection rules on n and n' must be inferred from the radius dependent coupling kernels. The range in l and l' over which modes k and k' can couple depends on the range in harmonic degree s of the spherical harmonic basis functions representing the aspherical perturbation. The harmonic degrees l, l', and s must satisfy the following triangle inequalities:

$$\begin{aligned} | \, l' - s \, | &\leq l, \\ | \, s - l \, | &\leq l', \\ | \, l - l' \, | &\leq s. \end{aligned} \tag{2.144}$$

The azimuthal orders m, m' and t of the singlets must satisfy the selection rule

$$-m' + t + m = 0. \tag{2.145}$$

These selection rules apply for each aspherical perturbation we have considered and may be deduced from equation (2B.22).

b) Qualitative Discussion of Sensitivity

We examine the advection kernels R_s^{an}, H_s^{an}, and T_s^{an} (see equations (2.120)-(2.122)) in detail to obtain insight into mode coupling in the presence of a velocity field which satisfies the anelastic condition. The most important selection rule can be obtained from the kernels R_s^{an} and H_s^{an} by noting they vanish for the case of self-coupling ($l' = l, n' = n$). Therefore, in the anelastic approximation, poloidal flow fields do not split isolated multiplets. The poloidal kernels contain only B^+ terms (see eq. 2.116) which are nonzero only if the sum $l' + l + s$ is even. The toroidal kernel T_s^{an} contains only B^- terms (see eq. 2.116) which are nonzero only if the sum $l' + l + s$ is odd. Therefore, in the self-coupling approximation, only odd degree toroidal expansion coefficients w_s^t induce coupling. Both toroidal and poloidal flows can contribute to coupling when $n' \neq n$ or $l' \neq l$. If the sum $l' + l$ is odd, only odd degree poloidal fields and even degree toroidal fields contribute to coupling. If the sum $l' + l$ is even, only even degree poloidal fields and odd degree toroidal fields lead to coupling. The component of the velocity field with azimuthal order t which contributes to the coupling between modes k and k' is given by $t = m' - m$.

The strength of coupling between modes k and k' is determined by the magnitude of the general matrix element $K^{m'm}_{n'n,l'l}$, and by the frequency difference $(\omega_k - \omega_{k'})$. The latter condition is true because in general, off-diagonal components of the general matrix attain enhanced significance when the difference $(\omega_k - \omega_{k'})$ is small. The magnitude of $K^{m'm}_{n'n,l'l}$ is controlled by the eigenfunctions and the B coefficients (see eq. 2.116). Generally,the radial eigenfunctions U are considerably larger than the horizontal eigenfunction V. Therefore, terms such as U^2 are far larger than terms such as UV or V^2. As may be seen from figures 3a and 3b, the shape of the eigenfunctions U and V in the upper region of the convection zone are strongly correlated when the modes have nearly degenerate eigenfrequencies ω_{nl}. This implies the radial eigenfunction factors in the kernel $R_s^{an}(r)$ are very small for nearly degenerate modes in the upper regions of the convection zone since the kernel is a function of the differences $U'\dot{U} - \dot{U}'U$ and $V'\dot{V} - \dot{V}'V$. Therefore, the near-surface contribution from

the radial component of a poloidal flow field to the splitting spectrum is small. The contribution from the deeper regions will also be minimized because phase differences in the mode shapes lead to cancellation in the integrated kernels that make up the matrix elements. The poloidal contribution to cross-multiplet coupling will be dominated by the horizontal component since the kernel $H_s^{an}(r)$ includes the large factor UU', and the difference $l(l+1) - l'(l'+1)$ can become quite large when the modes are widely separated in harmonic degree. However, $l - l'$ cannot be arbitrarily large because the triangle inequality must be satisfied. In addition the $B^{(1)}$ coefficients in the horizontal poloidal terms are usually larger by a factor of ~ 100 than the $B^{(0)}$ coefficient in the radial poloidal kernel.

c) The Hybrid Eigenfunctions

In a spherical or axisymmetric solar model, each modal frequency is uniquely associated with a single mode k. More generally, a modal frequency of an aspherical model is associated with a hybrid eigenfunction (a linear combination of modes as in equation (2.78). The complex expansion coefficients a_k are the components of the eigenvectors of the supermatrix. The eigenvector matrix in conjunction with the frequencies of the perturbed system may be used to assess the significance of mode coupling. An eigenfrequency can be uniquely associated with a single mode $\mathbf{s}_k$ if the eigenvector matrix is diagonal. If the perturbation includes departures from axial symmetry, there will be non-zero off-diagonal components in a given eigencolumn. If one of these components is significantly larger than all other components in the eigencolumn, then it is still possible to associate a single $\mathbf{s}_k$ with a given eigenfrequency.

It is usually assumed that orthogonal decompositions of Doppler images isolate the contribution from the target mode plus corruption from modal cross-talk due to the non-orthogonality of the spherical harmonics on the hemisphere. A sequence in time of such decompositions are fourier transformed to yield the frequency resonance function of the target mode. In the presence of a non-axisymmetric asphericity there are also contributions from the resonance functions of other hybrid eigenfunctions.

This is because other hybrid eigenfunctions may contain a contribution from the target mode $\mathbf{s}_k$. The spatial filtering operation will extract not only the resonance function from the target resonance function but the resonance function of other hybrid eigenfunctions in an amount which depends on the size of the expansion coefficient of the common component.

The geometric interpretation of mode displacement for an axisymmetric Sun is clear. The sectoral modes with singlets $m = \pm l$ corresponds to modes traveling prograde or retrograde along the equator of the coordinate system depending on whether the time dependence $e^{-i\omega t}$ or $e^{i\omega t}$ is chosen . Modes with $m = 0$ correspond to propagation paths over the poles, and modes with intermediate values have significant displacements in the mid-latitude regions. The displacement pattern of a hybrid eigenfunction is a linear combination in varying degrees of the end members described above.

VIII. SELF-COUPLING

In this section we specialize the formulae of §§V and VI to the case of self coupling in which $l' = l$ and $n' = n$. This reduction represents a simplification since only the toroidal component of the velocity field contributes to self coupling. In this section we neglect thermodynamic perturbations.

a) General Toroidal Flows

The general matrix element in the case of self coupling for a general velocity field may be obtained from equation (2.143):

$$T^{m'm}_{nn,ll} = -2m\Omega\omega_{ref}\delta_{mm'}N + 4m\Omega\omega_{ref}\delta_{mm'}\int_0^{R_\odot}\rho_0\, C(r)r^2dr +$$

$$4\pi\gamma_l\gamma_l(-1)^{m'}\sum_{s=0}^{\infty}\sum_{t=-s}^{s}\gamma_s\begin{pmatrix} l & s & l \\ -m' & t & m \end{pmatrix}\int_0^{R_\odot}\rho_0 w^t_s(r)\frac{T^{an}_s(r)}{r}r^2dr. \quad (2.146)$$

In this special case, the integral kernels $C(r)$ and $T^{an}_s(r)$ are given by

$$T^{an}_s(r) = \{2UV - U^2 - \frac{1}{2}V'V[2l(l+1) - s(s+1)]\}B^{(1)-}_{lsl}, \quad (2.147)$$

$$C(r) = \rho_0\,(2UV + V^2). \quad (2.148)$$

Using equation (2.85) and setting $\omega_{ref} = \omega_{nl}$, the eigenvalue-eigenvector problem becomes

$$\mathbf{Ta} = 2\delta\omega_{nl} N \mathbf{Ia} \tag{2.149}$$

where N is given by equation (2.74), $\mathbf{a}$ represents one of the $(2l+1)$ eigenvectors, $\mathbf{I}$ is the identity tensor, and $2\omega_{nl}\delta\omega$ are the eigenfrequencies of the $(2l+1) \times (2l+1)$ general matrix $\mathbf{T}$.

b) Differential Rotation

The general matrix for differential rotation is a special case of equation (2.146). The differential rotation is an axially symmetric, even function about the equatorial plane. Therefore, the latitude-dependent scalar rotation rate can be expanded in even degree spherical harmonics:

$$\Omega(r,\theta) = \Omega + \sum_{k=0,2,4,\ldots}^{\infty} \Omega_k(r) Y_k^0(\theta,\phi) \tag{2.150}$$

where Ω is the bulk rotation rate and the $\Omega_k(r)$ are radially dependent expansion coefficients representing the differential rotation. The coefficient $\Omega_1(r)$ represents purely radial perturbations to Ω. The rotation rate vector is given by

$$\mathbf{\Omega}(r,\theta) = \Omega(r,\theta)\hat{\mathbf{r}}\cos(\theta) - \Omega(r,\theta)\sin(\theta)\hat{\theta} \tag{2.151}$$

so that the velocity $\mathbf{v}_{rot}$ due to rotation can be written

$$\mathbf{v}_{rot} = \mathbf{\Omega}(r,\theta) \times \mathbf{r} = \Omega r \sin(\theta)\hat{\phi} + \sum_{k=0,2,4,\ldots}^{\infty} \Omega_k(r) r \sin(\theta) Y_k^0(\theta,\phi)\hat{\phi}. \tag{2.152}$$

The expansion coefficients $\Omega_k(r)$ can be obtained by equating $\mathbf{v}_{rot}$ with the toroidal axially symmetric part of $\mathbf{u}_0$ in equation (2.97):

$$\sum_{k=0,2,4,\ldots}^{\infty} \Omega_k(r) r \sin(\theta) Y_k^0(\theta,\phi)\hat{\phi} = -\sum_{s=1,3,5,\ldots}^{\infty} w_s^0 \partial_\theta Y_s^0(\theta,\phi)\hat{\phi}. \tag{2.153}$$

To determine Ω_1, Ω_3, and Ω_5, we take the sum over s and k for $s = 0,2,4$, and $k = 1,3,5$, expand the spherical harmonics in terms of *sin* and *cos* functions, and

equate coefficients sharing the same trigonometric basis function. This operation yields

$$w_1^0(r) = \frac{r}{\gamma_1}\left[\gamma_0\,\Omega_0\,(r) - \frac{\gamma_2\Omega_2(r)}{5} + \frac{\gamma_4\Omega_4(r)}{12}\right], \tag{2.154}$$

$$w_3^0(r) = \frac{r}{\gamma_3}\left[\frac{\gamma_2\Omega_2(r)}{5} - \frac{\gamma_4\Omega_4(r)}{18}\right], \tag{2.155}$$

$$w_5^0(r) = \frac{r}{\gamma_5}\left[\frac{\gamma_4\Omega_4(r)}{9}\right], \tag{2.156}$$

where

$$\gamma_s = \sqrt{\frac{2s+1}{4\pi}}. \tag{2.157}$$

The general matrix for the multiplet ${}_nS_l$ including the effects of bulk rotation, the Coriolis force, and degrees 0, 2 and 4 differential rotation of equation (2.150) may be obtained by substituting the coefficients in equations (2.154), (2.155), and (2.156) into the general matrix for terms first order in Ω and $\mathbf{u}_0$ to yield the splitting matrix $\mathbf{D}_{nn,ll}$ with components

$$\begin{aligned} D_{nn,ll}^{m'm} &= -2m\Omega\omega_{nl}\delta_{mm'}\int \rho_0\,(U^2 + l(l+1)V^2)r^2dr \\ &+4m\Omega\omega_{nl}\delta_{mm'}\int \rho_0\,(2UV + V^2)r^2dr + \\ &2\omega 4\pi\gamma_l^2(-1)^{m'}\sum_{s=1,3,5}\gamma_s\begin{pmatrix} l & s & l \\ -m' & 0 & m \end{pmatrix}\int_0^{R_0}\rho w_s^0(r)T_s^{an}(r)rdr \end{aligned} \tag{2.158}$$

where in this special case,

$$T_s^{an}(r) = [2UV - (U^2 + l(l+1)V^2) + \frac{1}{2}s(s+1)V^2]B_{lsl}^{(1)-}. \tag{2.159}$$

The differential rotation kernel may be further reduced for low harmonic degrees s by using analytic expression for the Wigner 3-j symbols. For the case $s = 1$ we have

$$\begin{pmatrix} l & 1 & l \\ -m' & 0 & m \end{pmatrix} = (-1)^{l-m}\frac{m\delta_{m'm}}{[(2l+1)(l+1)l]^{\frac{1}{2}}}. \tag{2.160}$$

For $s = 2$ we have

$$\begin{pmatrix} l & 2 & l \\ -m' & 0 & m \end{pmatrix} = (-1)^{l-m}\frac{2[m^2 - l(l+1)]\delta_{m'm}}{[(2l+3)(2l+2)(2l+1)(2l)(2l-1)]^{\frac{1}{2}}}. \tag{2.161}$$

Higher order terms ($s = 3, 4, 5, 6, ...$) can also be reduced analytically by using recursion relationships in Edmonds (1960).

IX. NUMERICAL RESULTS

We have performed self and full coupling calculations to assess the influence of a realistic convective flow field on p mode amplitudes and frequencies. The flow field was computed by Dr. Gary Glatzmaier. A description of the anelastic modal equations governing convection and the numerical technique used to solve them is given in Glatzmaier (1984). The convection and differential rotation models used in our calculations are described in §IX.a. We illustrate the effect of convection on frequencies of singlets with dispersion-type diagrams which show the magnitudes of the frequency differences ($\omega_m^{self} - \omega_m^{d.r.}$) and ($\omega_m^{full} - \omega_m^{self}$). The notation ω_m^{self} denotes the frequency of the hybrid eigenfunction associated with the singlet (n, l, m) computed in the self coupling approximation, ω_m^{full} is the frequency of the same hybrid eigenfunction using full coupling theory, and $\omega_m^{d.r.}$ is the frequency of the singlet (n, l, m) calculated in the self coupling approximation with a simple differential rotation model. Only toroidal flow fields contribute to self coupling whereas both poloidal and toroidal fields contribute to full coupling. The eigenspace of a hybrid eigenfunction in the self coupling approximation is always $(2l+1)$ dimensional and is known *a priori*. The eigenspace of a hybrid eigenfunction in the full coupling theory is theoretically infinite dimensional; those elements which contribute significantly must be discovered by numerical experiment. Practical details concerning the numerical implementation of the full coupling theory are given in §IX.b. The effect of convection on the frequencies and the a_i coefficients (see eq. 2.168) is described in §§IX.c and IX.d. In §IX.e. we describe the character of the hybrid eigenfunctions.

a) The Velocity Models

All of our numerical results depend on Glatzmaier's velocity model. Glatzmaier ran his code until the differential rotation matched the observed solar rotation rate.

His velocity field is given by

$$\rho \mathbf{v} = \sum_{s=1}^{42} \sum_{t=-s}^{s} [\nabla \times \nabla \times (W_s^t \hat{\mathbf{r}}) + \nabla \times (Z_s^t \hat{\mathbf{r}})]. \tag{2.162}$$

Since $\rho \mathbf{v}$ is solenoidal it automatically satisfies the anelastic condition $\nabla \cdot (\rho \mathbf{v}) = 0$. The relationship between Glatzmaier's expansion coefficients (W_s^t, Z_s^t) and the expansion coefficients (u_s^t, v_s^t, w_s^t) in equation (2.97) can be obtained by equating the components of equation (2.162) to the components of equation (2.97). The components of the latter are given in equations (2B.12)-(2B.14). This procedure yields

$$u_s^t(r) = \frac{s(s+1)}{\rho_o r^2} W_s^t(r), \tag{2.163}$$

$$v_s^t(r) = \frac{1}{\rho_o r} \frac{\partial W_s^t(r)}{\partial r}, \tag{2.164}$$

$$w_s^t(r) = \frac{Z_s^t(r)}{\rho_o r}. \tag{2.165}$$

We have used capital letters to distinguish Glatzmaier's coefficients from ours. Glatzmaier expanded the radial dependence of the velocity field in terms of Chebyshev polynomials $T_n(r)$ for degrees $0 \leq n \leq 33$. The expansion coeffcient $W_s^t(r)$, for example, is given by

$$W_s^t(r) = \left(\frac{2}{N}\right)^{1/2} \sum_{n=0}^{N} W_{sn}^t T_n(r) \tag{2.166}$$

where the $n = 0$ and $n = N$ terms should be multiplied by $1/2$. The (θ, ϕ) dependence is parameterized in terms of spherical harmonics Y_s^t to harmonic degree $s = 42$. In our numerical calculations we often truncated the velocity field at degree $s = 25$ since there is very little power in the expansion coefficients for $s > 25$. The spherical shell in which convection is modelled extends from $r = 0.65 R_\odot$ to $0.97 R_\odot$.

The solar model we used in our numerical computations was calculated with a solar evolution code written by Ron Gilliland (see Gilliland 1985). The model contains 408 radial knots, 206 of which are located in the convection zone. We interpolated Glatzmaier's velocity coefficients onto 142 radial knots in the range $0.65 R_\odot \leq r \leq 0.97 R_\odot$. Convective motions in the range $0.65 R_\odot \leq r \leq 0.71 R_\odot$ correspond to convective overshoot. We describe in the folowing the differential rotation and convection models.

i) The Differential Rotation Model

The differential rotation model was adapted from the differential rotation law of Libbrecht *et.al.* (1988). The velocity field is given by

$$\mathbf{v} = \begin{cases} [462 - 58\cos^2(\theta) - 84\cos^4(\theta)]r\sin(\theta) & 0.65R_\odot \leq r \leq R_\odot \\ 430\, r\sin(\theta) & 0 \leq r < 0.65R_\odot \end{cases}$$

where θ is the colatitude, and the temporal dependence is in nhz.

ii) The Convection Model

The convection model includes the differential rotation model and the toroidal and poloidal velocity fields calculated by Glatzmaier:

$$\mathbf{v} = \begin{cases} [462 - 58\cos^2(\theta) - 84\cos^4(\theta)]r\sin(\theta) & 0.97R_\odot \leq r \leq R_\odot \\ 462\, r\sin(\theta) + \sum_{s=1}^{42}\sum_{t=-s}^{s}[u_s^t Y_s^t \hat{\mathbf{r}} + v_s^t \nabla_1 Y_s^t - w_s^t \hat{\mathbf{r}}\times\nabla_1 Y_s^t] & 0.65R_\odot \leq r \leq 0.97R_\odot \\ 430\, r\sin(\theta) & 0 \leq r < 0.65R_\odot. \end{cases}$$

To make instructive comparisons of frequency splittings, we replaced the w_1^0, w_3^0, and w_5^0 coefficients calculated by Glatzmaier with coefficients that mimic the velocity field of the first model by using equations (2.154), (2.155), and (2.156). This operation requires running a regression on the first model to obtain the rotation rate in terms of the expansion coefficients Ω_0, Ω_2, and Ω_4 in equation (2.150).

In figure 4 we show the geometrical character of a sectoral flow field. Figure 5 contains the horizontal poloidal component and toroidal component of Glatzmaier's flow field for degrees $1 \leq s \leq 20$ and all azimuthal orders t inclusive. Plots of the magnitude of the velocity expansion coefficients u_s^t, v_s^t, and w_s^t at radial level $r = 0.96R_\odot$ are given respectively in figures 6a, 6b, and 6c. The size of each hexagon in these figures is proportional to the magnitude of the expansion coefficient. The relative amplitude of the expansion coefficients do not change greatly with radius. The power of the expansion coefficients is dominantly in the sectoral ($s = t$) components. These components dominantly perturb the eigenfrequencies and eigenfunctions of the modes.

b) The Numerical Implementation of Self and Full Coupling

The numerical implementation of self coupling is straightforward since the modes contributing to the eigenspace of the hybrid eigenfunction associated with a given target singlet is composed solely of the singlets sharing the same n and l of the target singlet. Thus, the eigenspace is known *a priori* and is $(2l+1)$ dimensional. The poloidal kernels vanish in the self coupling approximation and therefore coupling is caused only by the toroidal component of the velocity field. The coupling is completely specified by the eigenvalue-eigenvector decomposition of equation (2.149).

The purpose of the full coupling calculation is to determine the hybrid eigenfrequency and eigenfunction associated with a target singlet in the presence of poloidal and toroidal flows. The required numerical effort is considerably more burdensome than in the self coupling case since the eigenspace must be discovered by numerical experiment, and a large number of general matrices must be computed. To minimize the computational expense of constructing and decomposing the supermatrix, some sensible criteria must be used to determine a cutoff of the modes that span the eigenspace of hybrid eigenfunctions. Some modes may couple with the target singlet more strongly than others; the criteria should eliminate the modes which do not significantly contribute to the coupling.

i) The Determination of the Eigenspace

The eigenfrequency of a given singlet $k = (n, l, m)$ is predicted to a high degree of accuracy for small (m/l) by a simple bulk rotation model and to ~ 10 % accuracy for $(m/l) \sim 1$. Splitting due to differential rotation, convection, and all other effects lead only to very small perturbations about the frequencies predicted by bulk rotation alone. Thus, the differential rotation model predicts with accuracy sufficient for our purposes the frequencies ω_k in the quasi-degenerate criteria (see eq. 2.75). Let us rewrite that criteria as

$$| \omega_k - \omega_{ref} | \leq \tau'. \tag{2.167}$$

where τ' is a small number. By varying the size of τ' we were able to determine the sensitivity of the hybrid eigenfrequencies to the dimension of the eigenspace of the hybrid eigenfunctions. We used the velocity field of the differential rotation model to calculate all singlet frequencies for p modes that have been observed by Duvall *et.al.* (1988) with degrees $1 \leq l \leq 100$ and with degenerate frequencies ω_{nl} that fall in the range $1.5mhz \leq \omega_{nl} \leq 5mhz$. This window on the ω-k dispersion diagram yielded 1698 modes. The frequency splittings can be parameterized in terms of the splitting coefficients a_i (e.g. Brown and Morrow 1987) where

$$\omega_k = \omega_{nl} + l \sum_{i=0}^{N} a_i P_i(-m/l) \tag{2.168}$$

and the P_i are Legendre Polynomials. We determined the a_i coeffcients by performing a regression analysis on the frequency spectrum for each multiplet. In applying equation (2.167), we used the a_i coefficients from the differential rotation model to calculate ω_{ref} of the target singlet and ω_k of all other singlets.

The minimum dimension eigenspace can be determined by calculating the hybrid frequency for a variety of choices of τ'. We implement equation (2.167) to determine all possible modes k which satisfy the quasi-degenerate criteria for the chosen value of τ'. We then construct and decompose the supermatrix (we describe how to do this in the next subsection) and retain only the hybrid eigenfunction and hybrid eigenfrequency associated with the target singlet. We then perform the same operation for another value of τ'. The value of τ' associated with the minimum dimension eigenspace is defined to be the point where the hybrid eigenfrequency of the target singlet ceases to change significantly as τ' is increased. Alternatively, we could choose τ' at the value where the quantity

$$\sum_k \mid a_k \mid^2 / \mid a_{k_{target}} \mid^2 \quad \text{for } k \neq k_{target} \tag{2.169}$$

levels off as the tolerance τ' is increased. In practice, one need only perform one of the two procedures for just a few singlets, and use the estimated value of τ' for all other singlets. We found it often suffices to use a value of 5.5 μhz.

The singlets that contribute to the eigenspaces of target singlets immediately adjacent in m for a given multiplet are very similar. The eigenspaces are quite different for target singlets with widely different frequencies. For $\tau' = 5.5$ μhz, and a maximum harmonic degree $s = 25$ in the velocity field expansion, the typical dimension of an eigenspace for a target singlet with harmonic degree l varies from ~ 50 to ~ 125 for $10 \leq l \leq 90$.

ii) Assembling the Supermatrix

The supermatrix for each target singlet can be assembled once the appropriate eigenspace is obtained. To determine which general matrices are required, we initially assume that each of the singlets couple with the target singlet and with each other as well. Not all singlets will couple since by equation (2.144), the difference $l - l'$ of the singlets k and k' must not exceed the maximum value of s in the velocity field expansion. General matrices should be computed for all possible $(n'l', nl)$ combinations which satisfy the above selection rules. In addition, splitting matrices should be computed for each (n, l) in the eigenspace. From each general and splitting matrix the subblock which contains matrix elements $K^{m'm}_{n'l',n'}$ describing the interaction between two singlets that are members of the eigenspace should be extracted and incorporated into the supermatrix in a fashion analogous to that illustrated in equation (2.92). The general matrices fill the off-diagonal blocks and the splitting matrices fill the diagonal blocks. The general matrix subblocks will always be square or rectangular and those of the splitting matrix will be square. Since the supermatrix is hermitian, we need only retain the full lower triangles of the splitting matrix and we emplace the subblocks of the general matrices only in the strict lower triangle of the supermatrix. For each target singlet we assemble the supermatrix, decompose it, and save only the hybrid eigenfrequency and hybrid eigenfunction associated with that singlet. We use the double precision complex hermitian path in EISPACK to decompose the supermatrix.

c) The Effect of the Flow Field on Frequencies

We calculated in the self coupling approximation frequencies of all singlets observed by Duvall *et. al.* (1988) whose n and l values lie in the range ($4 \leq l \leq 99$, $2 \leq n \leq 26$). We used the full range in harmonic degree s of the toroidal component convection model and all t inclusive so that ($1 \leq s \leq 42$, $-s \leq t \leq s$). We used the toroidal component only, since in self coupling approximation, frequencies are not affected by the poloidal component of the field. We also calculated the frequency splittings for the same set of multiplets under the self coupling approximation for the differential rotation model. Due to computational expense, we performed full coupling calculations only for a limited set of singlets. The frequencies were computed for every third l in the range ($10 \leq l \leq 90$) along the overtone branches ($2 \leq n \leq 20$) for the azimuthal order $m = -.8l$. We also calculated the frequencies for all singlets of the multiplets ${}_3S_{59}$, ${}_3S_{70}$, ${}_5S_{45}$, ${}_8S_{35}$, ${}_{18}S_{70}$, and ${}_9S_{65}$ using the self coupling approximation, and the full coupling theory. The purpose of the latter computation was to examine how the a_i coefficients are affected by full coupling induced by both toroidal and poloidal velocity fields.

The full coupling calculations for the multiplets listed above were performed with a tolerance of $\tau' = 5.5$ μhz (see eq. 2.167), and maximum s value given by $s = 25$. The results are shown in figures (7a)-(7f). From each frequency $\omega^m_{n,l}$ we subtracted the degenerate frequency of the multiplet and the linear trend induced by the average rotation ($0.46m$). The frequency differences $\omega^{full} - \omega^{d.r}$ and $\omega^{self} - \omega^{d.r}$ are greatest for the sectoral and nearly sectoral singlets and smallest for the zonal and nearly zonal singlets. The reason for this can be deduced from figures 6a, 6b, and 6c. The dominant contribution to Glatzmaier's flow field comes from the sectoral components; there is very little power in the zonal components. A wave that propagates along a line of longitude (which corresponds to a zonal mode) tends not to be advected in that direction. The frequency profile of the full coupling calculations sometimes display abrupt jumps. This is a complicated effect which depends on the structure of the $\omega - k$ dispersion diagram, and on the character of the velocity field. As the azimuthal order m of the target singlets varies, the potential coupling partners change, and

the components of the velocity field which may couple the target singlet with other singlets changes. The eigenspace between two adjacent target singlets is usually quite similar but since the tolerance τ' is finite and since the unperturbed frequencies of the target singlets are about .46 μhz apart, there are differences in the eigenspaces of the adjacent singlets. When a new member is introduced it could happen that it couples particularly strongly with other singlets that couple to the target singlet. This changes the structure of the supermatrix and hence, several of its eigenfrequencies can be quite different than those of the supermatrix for the adjacent singlet.

The hierarchy of coupling among modes in the Sun can be viewed in the following way. The most basic structure is the axisymmetric flow field. In this case, singlets split, but do not couple, and the supermatrix is purely diagonal. In this case, one ususally considers the split singlets of a single multiplet and so the supermatrix consists of a single diagonal block. The next step up is the inclusion of a toroidal velocity field. In this instance, singlets of a single multiplet can split and couple. The splitting block of a particular multiplet may be sparse, but is no longer diagonal. It is possible for singlets from several multiplets to couple. Ignoring this effect leads to the self coupling approximation. In the self coupling approximation, poloidal flows do not induce splitting or coupling. The next step up is the inclusion of toroidal and poloidal velocity fields and to allow for coupling among singlets from different multiplets. We call this full coupling. There are several approximations to full coupling which we call first order coupling, second order coupling and so on. First order coupling consists of identifying those singlets which may couple with the target singlet and only including those in the construction of the supermatrix. Second order coupling consists of including those singlets which may couple to the target singlet, and of including those singlets which may couple to the singlets that couple to the target singlet. The approximations we have described are in order of increasing accuracy. To date, helioseismologists have considered only the axisymmetric case. The abrupt jumps in figures (7a)-(7f) show where the first order coupling theory is inadequate. We only carried the full coupling calculations to first order. If we had unlimited computer

resources, we would include all possible multiplets in the full coupling calculations; this would correspond to a treatment without approximation.

We have found in these full coupling calculations that there can be significant hybridization of the target singlets. For some target singlet-coupling partner pairs, the frequencies can be totally degenerate (or nearly so) which leads to particularly strong coupling. Though the amplitudes are strongly affected, the frequencies are not since the frequency difference between the two singlets must be small in order for this effect to be important. The frequency differences are determined by the structure of the $\omega - k$ diagram. Nevertheless, we can think of the strong hybridization as being due to 'accidental degeneracies'.

We performed a regression analysis to determine the a_i expansion coefficients of the multiplets listed above. The results are tabulated in Table 1. We also provide in Table 1 the a_i coefficients Libbrecht (1988b) has determined from his data. In the full coupling case aspherical convection generates a frequency spectrum with an even component about ω_{nl}. Thus, an expansion of the spectrum in terms of Legendre Polynomials requires even-ordered expansion coefficients. In the self coupling approximation, frequency splitting of a multiplet is purely odd about the degenerate frequency ω_{nl}, and thus requires only odd expansion coefficients. For some of the multiplets, the a_2 coefficients predicted by the flow field are comparable in magnitude to Libbrechts a_2 coefficients. It has been conventional wisdom to ascribe even-ordered expansion coefficients required by actual data to large-scale axisymmetric magnetic fields. Our finding that convection can also contribute to the even coefficients can be understood ray theoretically. In an axisymmetric Sun, frequencies are uniquely associated with one mode, but this does not hold for an aspherical Sun. Instead the displacement pattern, is a linear combination of modes. The set of modes which couple to the mode $(n, l, |m|)$ in the full coupling case, is quite different from the set of modes which couple to the mode $(n, l, -|m|)$. Thus the hybrid eigenfunctions associated with these modes no longer possess the symmetry in the n, l, and m quantum numbers that they did in the self coupling approximation. They sample the Sun in a

manner quite different from the axisymmetric case. It is this non-symmetric sampling which introduces the even component to the frequency splitting.

The frequency difference $(\omega^{self} - \omega^{d.r})$ for the sectoral singlet $(m = l)$ is plotted in figure 8a. Each symbol in the figure is proportional to the size of the frequency difference. The differences tend to increase with increasing l and the largest difference is .65μhz for the singlet $(n = 3, l = 99, m = 99)$. The differences display zones of extinction as a function of the degenerate frequency of the multiplets. This extinction takes place at frequencies where the toroidal sensitivity kernels of the multiplets become nearly orthogonal with the radial variation of the velocity model. As such, their location is a strong function of the convective flow field.

The frequency difference $(\omega^{full}_{m=-.8l} - \omega^{self}_{m=-.8l})$ is shown in figure 8b. The difference is not a completely monotonic function of l but does tend to increase with l. The largest difference is .27 μhz for the singlet $(n = 2, l = 89, m = -72)$. The purpose of the computation was to test the accuracy of the self coupling approximation over a wide range of n and l.

d) The Effect of the Flow Field on the a_i Coefficients

We performed a regression to obtain the a_1, a_3, and a_5 coeffcients for the multiplets corresponding to each sectoral singlet shown in figure 8a. In the self coupling approximation, splitting is odd about the degenerate frequency (it depends on odd azimuthal order only) and it therefore suffices to parameterize frequency splitting with odd a_i only. The differences $(a_1^{d.r} - a_1^{self})$ and $(a_3^{d.r} - a_3^{self})$ are shown respectively in figures 9a and 9b. The size of each symbol is proportional to the magnitude of the coeffcient difference; the largest a_1 coefficient difference is 7.8 nhz for the multiplet ${}_{18}S_{48}$, and the largest a_3 coefficient difference is .27 nhz for the multiplet ${}_3S_{97}$. The extinction pattern of both sets of differences precisely mimics the extinction pattern of the frequency differences in figure 8a. The toroidal flow field reduces the size of the a_i coefficients from the corresponding coefficients of the differential rotation model.

Observers such as Brown and Morrow (1987) and Libbrecht *et. al.* (1988) have

collected and reduced data in order to determine the a_i coefficients and make inferences concering differential rotation. Figure 9c is a reproduction of the a_1, a_3, and a_5 coefficients determined by Brown and Morrow (1987). The dashed lines on the plots indicate the expected values if the surface latitudinal differential rotation prevailed through out the Sun. The coefficients are averaged over the radial overtone n. In figure 9d we plot the difference between a_1^{self} and $a_1^{d.r.}$ for overtone branch $n = 8$. In figure 9e we plot the same difference except we have averaged over all n in the our forward calculations, and performed a running mean average in l. In both cases, we observe that the fluctuations are comparable in magnitude and pattern to the data of Brown and Morrow (1987). One implication is that interpretation of a_1 coefficients in terms of a radially varying rotation profile is likely to be biased by long-wavelength convection. The signal in the a_1 data of Brown and Morrow (1987) is evidently about the same size of the signal due to convection in the self coupling approximation. The same result will no doubt hold true in the full coupling case.

e) The Effect of the Flow Field on the Eigenfunctions

The principal asphericity in the sun is the bulk rotation. This lead to a diagonally dominant splitting matrix for every multiplet and therefore the hybrid eigenfunctions are dominated by a single component (which is the component present in the axisymmetric case). In some cases, there can be strong hybridization if the frequencies of the target singlet and a coupling partner are completely degenerate (or nearly so). When there is complete degeneracy, the size of the diagonal component of the supermatrix is down-weighted and the off-diagonal components assume enhanced relative significance which leads to stronger coupling. Even without degeneracy, for a sufficiently white velocity coefficient spectrum, there is always some coupling present.

The frequencies of 445 target singlets are shown in figure 8b. We can use expansion coefficients a_k (see eq. 2.78; these should not be confused with the frequency expansion coeffcients in eq. 2.168) which completely specify the hybrid eigenfunctions to assess the influence of convection on the corresponding eigenfunctions of the

axisymmetric Sun. The coefficients are normalized so that

$$\sum_{k=1}^{N} \mid a_k \mid^2 = 1 \tag{2.170}$$

where N is the dimension of the eigenspace. The azimuthal order t that contributes to the expansion coefficient a_k can be determined by comparing the azimuthal order of k to the azimuthal order of the target singlet and by using the selection rule $-m' + m + t = 0$ (see eq. 2.145). Without knowledge of the flow model, we cannot distinguish which s is associated with the particular t. However, from figures 7b and 7c, it is clear that the w_s^t and v_s^t expansion coefficients are often the largest for t=s; we can deduce the associated s value with this information. Once we know s, we can also distinguish whether a_k comes from the poloidal or the toroidal part of the field by adding the harmonic degrees l' of the target singlet l of the component $k = (n, l, m)$, and s of the flow field, and by using the fact that the poloidal and toroidal kernels are respectively proportional to $(1 + (-1)^{(l+l'+s)})$ and $(1 - (-1)^{(l+l'+s)})$.

We used the above procedure to assign t values to each a_k coefficient. Figure 10a is a histogram plot of this information. The vertical axis contains the number of coefficients a_k from the 445 target singlets shown in figure 8a that correspond to the absolute value of the associated azimuthal order t. We included only those coefficients which satisfied $|a_k| \geq 0.01$. This figure clearly shows which components of the velocity field primarily contribute to the coupling. We can safely assume the radial poloidal component does not contribute since the radial poloidal kernels are so small. Therefore, by the argument in the preceding paragraph, the contributions to the histogram count come primarily from the $w_s^{\pm s}$ and $v_s^{\pm s}$ components. There are several clear correlations between the histogram count for each t value and the size of the sectoral expansion coefficients in figures 6b and 6c. The largest count is for the $t = \pm 1$ value which corresponds to the $w_1^{\pm 1}$ component. The next largest peak is for $t = \pm 2$ which corresponds to the $v_2^{\pm 2}$ component. The contributions from both poloidal and toroidal fields for $t = \pm 3$ are rather small which accounts for the small histogram count for that t value. There are large contributions at $t = \pm 4$ and $t = \pm 7$ which come respectively from the $v_4^{\pm 4}$ and $v_7^{\pm 7}$ expansion coefficients. Continuing this

sort of analysis for $-8 \leq t \leq 25$, we find a rough correlation between the histogram counts and the size of the $v_s^{\pm s}$ expansion coefficients.

To assess the strength of the coupling for each target singlet shown in figure 8b we again use a histogram plot. Figure 10b contains on the horizontal axis the quantity $|a_k|/|a_{k_{target}}|$ where a_k is the second largest eigenvector component. In every case the largest eigenvector component corresponds to the k of the target singlet. This is the only component which contributes to the eigenfunction for a spherical or an axisymmetric Sun. The vertical axis is the number count of eigenvector component ratios with the values prescribed on the horizontal axis. We truncated the horizontal axis at 0.6 in order to provide enhanced horizontal resolution. The counts for ratios between 0.6 and 0.9 is similar qualitatively to the counts for the range 0.3 to 0.6. We that for a few singlets there is almost complete hybridization but that for most singlets, the largest $|a_k|$ is $\sim .1$.

APPENDIX 2A

THE EQUATIONS OF MOTION IN THE SOLAR FRAME

In this appendix we present the equations of motion governing oscillations in the Sun's frame. We seek to write the momentum equation in a form resembling Newton's equation which at the same time is valid in a noninertial reference frame. This is achieved by adding the fictitious accelerations in equation (2.15) to the acceleration of an object as perceived by an observer in the Sun's frame. Let the subscript *sun* indicate that the local time derivative $\frac{\partial}{\partial t}$ is taken by an observer in the Sun's frame. The momentum equation becomes

$$\left(\frac{D\mathbf{v}_s}{Dt}\right)_{sun} + 2\boldsymbol{\Omega} \times \mathbf{v}_s + \boldsymbol{\Omega} \times \boldsymbol{\Omega} \times \mathbf{r} = -\frac{\nabla P}{\rho} - \nabla\Phi, \tag{2A.1}$$

where

$$\frac{D}{Dt} = \frac{\partial}{\partial t} + \mathbf{v}_s \cdot \nabla \tag{2A.2}$$

and $\mathbf{v}_s$ has the same meaning as in equation (2.14). The perturbed Euler equation is obtained by taking the Lagrangian variation of equation (2A.1) so that

$$\left(\frac{D\Delta\mathbf{v}_R}{Dt}\right)_{sun} + 2\boldsymbol{\Omega}\times\Delta\mathbf{v}_s + \boldsymbol{\Omega}\times\boldsymbol{\Omega}\times\Delta\mathbf{r} - \frac{\Delta\rho}{\rho^2}\nabla P + \frac{\Delta(\nabla P)}{\rho} + \Delta(\nabla\phi) = 0. \quad (2A.3)$$

Noting that $\Delta\mathbf{v}_s = \left(\frac{D\mathbf{s}}{Dt}\right)_{sun}$ and $\Delta\mathbf{r} = \mathbf{s}$, equation (2A.3) can be written

$$\left(\frac{D^2\mathbf{s}}{Dt^2}\right)_{rot} + 2\boldsymbol{\Omega}\times\left(\frac{D\mathbf{s}}{Dt}\right)_{sun} + \boldsymbol{\Omega}\times\boldsymbol{\Omega}\times\mathbf{s} - \frac{\Delta\rho}{\rho^2}\nabla P + \frac{\Delta(\nabla P)}{\rho} + \Delta(\nabla\phi) = 0, \quad (2A.4)$$

where

$$\left(\frac{D^2\mathbf{s}}{Dt^2}\right)_{sun} = \left(\frac{\partial^2\mathbf{s}}{\partial t^2}\right)_{sun} + 2\mathbf{v}_s\cdot\nabla\left(\frac{\partial\mathbf{s}}{\partial t}\right)_{sun} + \left(\frac{\partial\mathbf{v}_s}{\partial t}\right)_{sun}\cdot\nabla\mathbf{s} + \mathbf{v}_s\cdot\nabla\left(\mathbf{v}_s\cdot\nabla\mathbf{s}\right). \quad (2A.5)$$

Equation (2A.4) may be reduced to its final form by using (2.35), equating $\mathbf{v}_s$ with $\mathbf{u}_0$, noting that $\dot{\mathbf{e}}_i = 0$ (since we are in the sun's frame), that the convective flow is steady state, and that the treatment of the pressure and gravity terms is the same as in the inertial case. We obtain then

$$-\rho\omega^2\mathbf{s} + \rho\mathbf{B}_{sun}(\mathbf{s}) + \rho\mathbf{C}_{sun}(\mathbf{s}) + \rho\mathbf{D}_{sun}(\mathbf{s}) + \rho\mathbf{E}_{sun}(\mathbf{s}) = \mathcal{L}(\mathbf{s}) \quad (2A.6)$$

where

$$\mathbf{B}_{sun}(\mathbf{s}) = 2i\omega\boldsymbol{\Omega}\times\mathbf{s} + 2i\omega\mathbf{u}_0\cdot\nabla\mathbf{s}, \quad (2A.7)$$

$$\mathbf{C}_{sun}(\mathbf{s}) = \boldsymbol{\Omega}\times\boldsymbol{\Omega}\times\mathbf{s}, \quad (2A.8)$$

$$\mathbf{D}_{sun}(\mathbf{s}) = 2\boldsymbol{\Omega}\times\mathbf{u}_0\cdot\nabla\mathbf{s}, \quad (2A.9)$$

$$\mathbf{E}_{sun}(\mathbf{s}) = \mathbf{u}_0\cdot\nabla(\mathbf{u}_0\cdot\nabla\mathbf{s}), \quad (2A.10)$$

and $\mathcal{L}(\mathbf{s})$ is given by equation (2.59). Finally, defining $\mathbf{T}_{sun}$ by

$$\mathbf{T}_{sun}(\mathbf{s}) = \mathbf{B}_{sun}(\mathbf{s}) + \mathbf{C}_{sun}(\mathbf{s}) + \mathbf{D}_{sun}(\mathbf{s}) + \mathbf{E}_{sun}(\mathbf{s}), \quad (2A.11)$$

equation (2A.6) becomes

$$-\rho\omega^2\mathbf{s} + \rho\mathbf{T}_{sun}(\mathbf{s}) = \mathcal{L}(\mathbf{s}). \quad (2A.12)$$

APPENDIX 2B

CALCULATING THE GENERAL MATRIX

The matrix elements presented in this paper were calculated using a formalism developed by Burridge (1969) and Phinney and Burridge (1973). A tensor of arbitrary rank may be expanded in terms of generalized spherical harmonics (GSH's) $Y_l^{Nm}(\theta\,\phi)$ where N is the generalized index, l is the harmonic degree, and m is the azimuthal order. The above authors describe a formalism which involves transforming to a new set of canonical coordinates. The rules of vector-differential calculus are then appropriately transformed. These rules represent a simplification of traditional methods used to calculate quantities in spherical geometry. However, the rules themselves are unfamiliar and counterintuitive and thus the procedure is prone to error. We have found it convenient to use a hybrid technique adapted from Phinney and Burridge's results which considerably simplifies the use of generalized spherical harmonics in computations and we describe this procedure below.

The generalized spherical harmonics are the matrix elements of the finite rotation operator in spherical coordinates. In the notation of Edmonds (1960) they are given by

$$Y_l^{Nm}(\theta,\phi) = \mathcal{D}^l_{Nm}(\phi,\theta,0) = d^l_{Nm}(\theta)e^{im\phi}. \tag{2B.1}$$

A scalar spherical harmonic is given by

$$Y_l^m(\theta\,\phi) = \gamma_l Y_l^{0m}(\theta,\phi), \tag{2B.2}$$

where

$$\gamma_l = \sqrt{\frac{2l+1}{4\pi}}. \tag{2B.3}$$

The utility of the generalized spherical harmonics derives from the fact that they may be used to transform calculus operations into simple algebraic operations. Further, their products are easily integrated on the unit sphere by using Wigner 3-j symbol relations. The useful identities are:

$$\Omega^l_N Y_l^{N-1,m}(\theta,\phi) - \Omega^l_{N+1} Y_l^{N+1,m}(\theta,\phi) = \sqrt{2}\frac{d}{d\theta}Y_l^{Nm}(\theta,\phi), \tag{2B.4}$$

$$\Omega^l_{N+1} Y_l^{N+1,m}(\theta,\phi) + \Omega^l_N Y_l^{N-1,m}(\theta,\phi) = \sqrt{2}\frac{N\cos(\theta) - m}{\sin(\theta)} Y_l^{Nm}(\theta,\phi), \tag{2B.5}$$

where

$$\Omega^l_N = \sqrt{\frac{(l+N)(l-N+1)}{2}}. \tag{2B.6}$$

Consider now the vector spherical harmonic

$$\mathbf{s} = U^t_s Y^t_s \hat{\mathbf{r}} + V^t_s \nabla_1 Y^t_s - W^t_s \hat{\mathbf{r}} \times \nabla_1 Y^t_s, \tag{2B.7}$$

where

$$\nabla_1 = \hat{\theta}\frac{\partial}{\partial\theta} + \frac{\hat{\phi}}{\sin(\theta)}\frac{\partial}{\partial\phi}. \tag{2B.8}$$

In component form, $\mathbf{s}$ is given by

$$s_r = U^t_s Y^t_s, \tag{2B.9}$$

$$s_\theta = V^t_s \partial_\theta Y^t_s + \frac{W^t_s}{\sin(\theta)}\partial_\phi Y^t_s, \tag{2B.10}$$

$$s_\phi = -W^t_s \partial_\theta Y^t_s + \frac{V^t_s}{\sin(\theta)}\partial_\phi Y^t_s. \tag{2B.11}$$

Using the above identities, it easy to show that

$$s_r = \gamma_s U^t_s Y^{0t}_s, \tag{2B.12}$$

$$s_\theta = \frac{\gamma_s \Omega^s_0}{\sqrt{2}} V^t_s (Y^{-1t}_s(\theta,\phi) - Y^{1t}_s(\theta,\phi)) - i\frac{\gamma_s \Omega^s_0}{\sqrt{2}} W^t_s (Y^{1t}_s(\theta,\phi) + Y^{-1t}_s(\theta,\phi)), \tag{2B.13}$$

$$s_\phi = -i\frac{\gamma_s \Omega^s_0}{\sqrt{2}} V^t_s (Y^{1t}_s(\theta,\phi) + Y^{-1t}_s(\theta,\phi)) - \frac{\gamma_s \Omega^s_0}{\sqrt{2}} W^t_s (Y^{-1t}_s(\theta,\phi) - Y^{1t}_s(\theta,\phi)). \tag{2B.14}$$

With this representation, it is very convenient to perform standard vector differential operations by repeated application of identities (2B.4) and (2B.5). Higher derivatives in θ are easily calculated. For instance,

$$\partial^2_\theta Y^{0t}_s(\theta,\phi) = \frac{\Omega^s_0}{2}[\Omega^s_2 (Y^{-2t}_s(\theta,\phi) + Y^{2t}_s(\theta,\phi)) - 2\Omega^s_0 Y^{0t}_s(\theta,\phi)]. \tag{2B.15}$$

It may be necessary to take derivatives of the spherical unit vectors. The relations

$$\frac{\partial\hat{\mathbf{r}}}{\partial\theta} = \hat{\theta},\ \frac{\partial\hat{\mathbf{r}}}{\partial\phi} = \hat{\phi}\sin(\theta),\ \frac{\partial\hat{\theta}}{\partial\theta} = -\hat{\mathbf{r}},\ \frac{\partial\hat{\theta}}{\partial\phi} = \hat{\phi}\cos(\theta),\ \frac{\partial\hat{\phi}}{\partial\theta} = 0,\ \frac{\partial\hat{\phi}}{\partial\phi} = -\hat{\mathbf{r}}\sin(\theta) - \hat{\theta}\cos(\theta) \tag{2B.16}$$

should be used. The real advantage of calculating matrix elements with generalized spherical harmonics is the simplicity of the angular integration formula. The integral of the product of three generalized spherical harmonics is given by

$$\frac{1}{4\pi}\int_0^{\pi}\int_0^{2\pi} Y_{l'}^{*N'm'}(\theta,\phi)Y_{l''}^{N''m''}(\theta,\phi)Y_{l}^{Nm}(\theta,\phi)d\Omega = (-1)^{(N'-m')}\begin{pmatrix} l' & l'' & l \\ -N' & N'' & N \end{pmatrix}\begin{pmatrix} l' & l'' & l \\ -m' & m'' & m \end{pmatrix}. \tag{2B.17}$$

Below we list properties of the Wigner 3-j symbols which have proven useful in the derivation of the general matrix elements. The 3-j symbols are invariant under even permutation of columns *i.e.*,

$$\begin{pmatrix} j_1 & j_2 & j_3 \\ m_1 & m_2 & m_3 \end{pmatrix} = \begin{pmatrix} j_2 & j_3 & j_1 \\ m_2 & m_3 & m_1 \end{pmatrix} = \begin{pmatrix} j_3 & j_1 & j_2 \\ m_3 & m_1 & m_2 \end{pmatrix}, \tag{2B.18}$$

and for odd permutations of columns they satisfy the relations

$$\begin{aligned}(-1)^{(j_1+j_2+j_3)}\begin{pmatrix} j_1 & j_2 & j_3 \\ m_1 & m_2 & m_3 \end{pmatrix} &= \begin{pmatrix} j_2 & j_1 & j_3 \\ m_2 & m_1 & m_3 \end{pmatrix} \\ &= \begin{pmatrix} j_1 & j_3 & j_2 \\ m_1 & m_3 & m_2 \end{pmatrix} \\ &= \begin{pmatrix} j_3 & j_2 & j_1 \\ m_3 & m_2 & m_1 \end{pmatrix}. \end{aligned} \tag{2B.19}$$

The symbols also possess the properties

$$\begin{pmatrix} j_1 & j_2 & j_3 \\ -m_1 & -m_2 & -m_3 \end{pmatrix} = (-1)^{j_1+j_2+j_3}\begin{pmatrix} j_1 & j_2 & j_3 \\ m_1 & m_2 & m_3 \end{pmatrix}, \tag{2B.20}$$

$$\begin{pmatrix} j_1 & j_2 & j_3 \\ 0 & 0 & 0 \end{pmatrix} = 0 \text{ if } j_1+j_2+j_3 \text{ is odd}, \tag{2B.21}$$

$$\begin{pmatrix} j_1 & j_2 & j_3 \\ m_1 & m_2 & m_3 \end{pmatrix} \neq 0 \text{ only if } m_1+m_2+m_3=0,\ m_1 \leq j_1,\ m_2 \leq j_2,\ m_3 \leq j_3,$$
$$\text{and } |\, j_1-j_2 \,| \leq j_3,\ |\, j_2-j_3 \,| \leq j_1,\ |\, j_3-j_1 \,| \leq j_2. \tag{2B.22}$$

The first selection rule in equation (2B.22) states that the integral over azimuth of the product of the three azimuthal eigenfunctions $e^{im_k\phi}$ for $k = 1, 2, 3$ vanishes unless $m_1 + m_2 + m_3 = 0$. The second selection rule is a statement that the projection of a momentum state onto the polar axis cannot exceed the magnitude of the momentum. The third selection rule is also known as the triangle inequality and is a statement of the conservation of angular momentum.

We have consistently used the notation, normalization, and phase relations of Edmonds (1960) for all angular functions in this paper with the exception of the notational change defined in equation (2B.1)

APPENDIX 2C

AN ALGORITHM FOR THE CALCULATION OF WIGNER 3-j SYMBOLS

The numerical calculation of the general matrix element in equation (2.143) requires an efficient algorithm to calculate 3-j symbols. There are formulae providing closed expressions for the symbols (e.g. Landau and Lifshitz 1958) but the implementation of such formulae are computationally expensive compared to methods which use judiciously chosen recursion relationships.

The recursion relationships can be derived from equation (6.2.8) in Edmonds (1960) which is given by

$$\sum_{\mu_1\mu_2\mu_3} (-1)^{\alpha} \begin{pmatrix} j_1 & l_2 & l_3 \\ m_1 & \mu_2 & -\mu_3 \end{pmatrix} \begin{pmatrix} l_1 & j_2 & l_3 \\ -\mu_1 & m_2 & \mu_3 \end{pmatrix} \begin{pmatrix} l_1 & l_2 & j_3 \\ \mu_1 & -\mu_2 & m_3 \end{pmatrix} = \begin{pmatrix} j_1 & j_2 & j_3 \\ m_1 & m_2 & m_3 \end{pmatrix} \begin{Bmatrix} j_1 & j_2 & j_3 \\ l_1 & l_2 & l_3 \end{Bmatrix} \tag{2C.1}$$

where $\alpha = l_1 + l_2 + l_3 + \mu_1 + \mu_2 + \mu_3$. The quantity in curly brackets is a 6-j symbol and is defined in Edmonds (1960). Analytic expressions for 3-j and 6-j symbols for numerous special cases are given in the appendices of Edmonds(1960). These in conjunction with equation (2C.1) can be used to obtain analytic representations for more general 3-j symbols and to derive recursion relationships among them. The sum

in equation (2C.1) is taken over all possible combinations of μ_1, μ_2, and μ_3 which satisfy the selection rules in equation (2B.22). In practice, it is necessary to sum over just one of the μ_i since the values of the remaining μ_i are constrained by the requirement that the sum of the bottom row of indices in each 3-j symbol is zero. The range of the μ_i over which the sum is performed must not exceed exceed the harmonic degree associated with it (which is the corresponding l_i value) and therefore it is most convenient to sum over that μ_i which has the smallest associated l_i value. With this choice, equation (2C.1) generates a recursion relation among $(2 * min\{l_1, l_2, l_3\} + 1)$ 3-j symbols where $min\{l_1, l_2, l_3\}$ denotes the smallest l_i integer of that set. Thus if the smallest l_i is simply unity, the values of at least two of the three Wigner 3-j symbols in the recursion must be known *a priori* to initiate the recursive algorithm. For an arbitrary triplet $\{j_1, j_2, j_3\}$, it is simplest to choose the values to be the corner value (for which a closed expression from Edmonds (1960) is available) and a 'ghost' element immediately adjacent to the corner value but outside the allowed bounds of the m_i so that its associated 3-j symbol vanishes.

The corner value (on the upper left) is defined by $(m_1 = -j_1', m_3 = -j_3)$ where m_1 and m_3 are, respectively, the row and column indices of the 3-j symbol on the right hand side of equation (2C.1). It may be calculated by setting $m_3 = j_3$ in equation (3.7.11) of Edmonds (1960) and by applying equations (2B.20) and (2B.19) to the resulting equation to obtain

$$\begin{pmatrix} j_1 & j_2 & j_3 \\ -j_1 & j_1 + j_3 & -j_3 \end{pmatrix} = (-1)^{j_3 + m_3} \times$$

$$\left[\frac{(2j_1)!(-j_1 + j_2 + j_3)!(j_1 + j_2 + j_3)!}{(j_1 + j_2 + j_3 + 1)!(j_1 - j_2 + j_3)!(j_1 + j_2 - j_3)!(-j_1 + j_2 - j_3)!(2j_3)!} \right]^{\frac{1}{2}} \quad \text{(2C.2)}$$

A recursion relation to iterate across rows can be obtained from equation (2C.1) by setting $l_1 = 1$, $l_2 = j_3$, and $l_3 = j_2$. We choose to sum over μ_1 which has a range of $\{-1, 0, 1\}$. If $\mu_1 = 1$, then $\mu_2 = 1 + m_3$, and $\mu_3 = 1 - m_2$. If $\mu_1 = 0$, then $\mu_2 = m_3$, and $\mu_3 = -m_2$. If $\mu_1 = -1$, then $\mu_2 = -1 + m_3$, and $\mu_3 = -1 - m_2$. Performing the sum in (2C.1) and using various analytic reductions of Wigner 3-j and 6-j symbols

from the appendices of Edmonds (1960), we obtain

$$[(j_2 - m_2)(j_2 + m_2 + 1)(j_3 + m_3)(j_3 - m_3 + 1)]^{\frac{1}{2}} \begin{pmatrix} j_1 & j_2 & j_3 \\ m_1 & m_2 + 1 & m_3 - 1 \end{pmatrix} +$$

$$[(j_2 + m_2)(j_2 - m_2 + 1)(j_3 - m_3)(j_3 + m_3 + 1)]^{\frac{1}{2}} \begin{pmatrix} j_1 & j_2 & j_3 \\ m_1 & m_2 - 1 & m_3 + 1 \end{pmatrix}$$

$$= (j_1(j_1 + 1) - j_2(j_2 + 1) - j_3(j_3 + 1) - 2m_2m_3) \begin{pmatrix} j_1 & j_2 & j_3 \\ m_1 & m_2 & m_3 \end{pmatrix}. \qquad (2C.3)$$

Our procedure is to iterate from left to right across successive rows. To do so we use for starting values a 'ghost' column with $m_3 = -j_3 - 1$ for $-j_1 \leq m_1 \leq j_1$ for which the 3-j symbols are zero and, 3-j symbols for the left column with $m_3 = -j_3$ and $-j_1 \leq m_1 \leq j_1$.

A recursion relation which yields the left column values starting from the corner value and the ghost value ($m_1 = -j_1 - 1, m_3 = -j_3$) can be derived from equation (2C.3) by making the index exchanges $j_1 \rightarrow j_3$, $j_3 \rightarrow j_1$, $m_3 \rightarrow m_1$ and, $m_1 \rightarrow m_3$. Performing this operation and applying the identity in equation (2B.19) to the resulting equation yields

$$[(j_2 - m_2)(j_2 + m_2 + 1)(j_1 + m_1)(j_1 - m_1 + 1)]^{\frac{1}{2}} \begin{pmatrix} j_1 & j_2 & j_3 \\ m_1 - 1 & m_2 + 1 & m_3 \end{pmatrix} +$$

$$[(j_2 + m_2)(j_2 - m_2 + 1)(j_1 - m_1)(j_1 + m_1 + 1)]^{\frac{1}{2}} \begin{pmatrix} j_1 & j_2 & j_3 \\ m_1 + 1 & m_2 - 1 & m_3 \end{pmatrix}$$

$$= (j_3(j_3 + 1) - j_2(j_2 + 1) - j_1(j_1 + 1) - 2m_2m_1) \begin{pmatrix} j_1 & j_2 & j_3 \\ m_1 & m_2 & m_3 \end{pmatrix}. \qquad (2C.4)$$

In summary, the procedure involves three steps. (1) Use equation (2C.2) to calculate the corner value. (2) Initiate the recursion relationship in equation (2C.4) with the corner value and the 'ghost' value ($m_1 = -j_1 - 1, m_3 = -j_3$) to calculate all of the elements in the left column. (3) To initiate the recursion relation on each row ($m_1, -j_3 \leq m_3 \leq j_3$), use the previously calculated value ($m_1, -j_3$) and the ghost

value $(m_1, -j_3 - 1)$. Finally, we note the computational time can be halved by computing only the full lower triangle of the desired 3-j symbol (*i.e.*, iterate the m_3 value of the 3-j symbol from the left column to the diagonal element only) and by using the identity in equation (2B.20) to compute the strict upper triangle of the 3-j symbol.

APPENDIX 2D

INCORPORATING THE ANELASTIC CONSTRAINT INTO THE GENERAL MATRIX

The derivation of the general matrix given by equation (2.119) is the purpose of this appendix. The general matrix for a general flow field $\mathbf{u}_0$ is given by equation (2.111); equation (2.119) is its anelastic counterpart. The anelastic condition $\nabla \cdot (\rho_0 \, \mathbf{u}_0) = 0$ imposes a constraint on the expansion coefficients of the poloidal components of the velocity field $\mathbf{u}_0$ (see eq. 2.99). The incorporation of this constraint into the kernels $R_s(r)$ and $H_s(r)$ (equations (2.112) and (2.113)) leads to a general matrix with the required hermitian properties detailed in section *VI*.

The transformation of the general matrix into its anelastic counterpart requires two identities involving the Wigner 3-j symbols. The first identity can be derived by setting $m_1 = -1$, $m_2 = 0$, $m_3 = 1$, $j_1 = l'$, $j_2 = s$, and $j_3 = l$ in equation (2C.3) which yields

$$\Omega_0^s \, \Omega_0^l \begin{pmatrix} l' & s & l \\ 1 & -1 & 0 \end{pmatrix} + \Omega_0^s \, \Omega_2^l \begin{pmatrix} l' & s & l \\ 1 & 1 & -2 \end{pmatrix}$$
$$= \frac{1}{2}[l'(l'+1) - l(l+1) - s(s+1)] \begin{pmatrix} l' & s & l \\ 1 & 0 & -1 \end{pmatrix}. \qquad \text{(2D.1)}$$

Equation (2.116) can be used to rewrite equation (2D.1) in terms of the B coefficients (see eq. 2.116) :

$$-\frac{1}{2}\Omega_0^l \Omega_0^l B_{sll'}^{(1)+} + (1 + (-1)^{(l'+s+l)}) \Omega_0^s \, \Omega_2^l \Omega_0^l \, \Omega_0^{l'} \begin{pmatrix} l' & s & l \\ 1 & 1 & -2 \end{pmatrix}$$
$$\times \frac{1}{4}[s(s+1) + l(l+1) - l'(l'+1)] B_{l'sl}^{(1)+} \qquad \text{(2D.2)}$$

which is our first required identity. From equations (2D.1) and (2.116) we may show that

$$\frac{1}{2}\Omega_0^l\Omega_0^l B_{sll'}^{(1)-} + (1-(-1)^{(l'+s+l)})\Omega_0^s\,\Omega_2^l\Omega_0^l\,\Omega_0^{l'}\begin{pmatrix} l' & s & l \\ 1 & 1 & -2 \end{pmatrix}$$
$$= \frac{1}{4}[l'(l'+1) - l(l+1) - s(s+1)]B_{l'sl}^{(1)-}. \tag{2D.3}$$

Adding the quantity $\frac{1}{2}l(l+1)B_{l'ls}^{(1)-}$ to both sides of equation (2D.3) and recognizing that $B_{l'ls}^{(1)-} = B_{l'sl}^{(1)-}$ (which follows from the symmetry properties of equation (2.118)), we obtain the second required identity which is

$$\frac{1}{2}(1-(-1)^{(l'+s+l)})\Omega_0^s\,\Omega_2^l\Omega_0^l\,\Omega_0^{l'}\begin{pmatrix} l' & s & l \\ 1 & 1 & -2 \end{pmatrix} - \frac{1}{2}\Omega_0^l\Omega_0^l B_{sll'}^{(1)-}$$
$$= \frac{1}{4}[l(l+1) + l'(l'+1) - s(s+1)]B_{l'sl}^{(1)-}. \tag{2D.4}$$

Returning to the general matrix in equation (2.111), we note that the integral kernel for the radial part of the velocity field (eq. 2.112) may be written as a sum of symmetric and antisymmetric parts *i.e.*,

$$\int r^2\rho_0\,(r)iu_s^t(r)\,[\,\frac{1}{2}(U'\dot{U}+U\dot{U}')B_{l'sl}^{(0)+} + \frac{1}{2}(V'\dot{V}+V\dot{V}')B_{l'sl}^{(1)+}\,]\,dr +$$
$$\int r^2\rho_0\,(r)iu_s^t(r)\,[\,\frac{1}{2}(U'\dot{U}-U\dot{U}')B_{l'sl}^{(0)+} + \frac{1}{2}(V'\dot{V}-V\dot{V}')B_{l'sl}^{(1)+}\,]\,dr. \tag{2D.5}$$

The first integral in (2D.5) is a symmetric quantity multiplied by i and is thus anti-hermitian while the second integral is skew-symmetric and is multiplied by i and is therefore hermitian. The symmetric term can be integrated by parts to give

$$-\int \partial_r(r^2\rho_0 iu_s^t(r))\,[\,\frac{1}{2}U'UB_{l'sl}^{(0)+} + \frac{1}{2}V'VB_{l'sl}^{(1)+}\,]\,dr. \tag{2D.6}$$

Substituting the anelastic relation (2.99) into (2D.6) and adding the result to the antisymmetric term in (2D.5) the total contribution from kernel in u_s^t in equation (2.111) may be written

$$\int r^2\rho_0\,(r)iu_s^t(r)[\frac{1}{2}(U'\dot{U}-U\dot{U}')B_{l'sl}^{(0)+} + \frac{1}{2}(V'\dot{V}-V\dot{V}')B_{l'sl}^{(1)+}]dr -$$
$$\int r\rho_0 iv_s^t(r))s(s+1)[\frac{1}{2}U'UB_{l'sl}^{(0)+} + \frac{1}{2}V'VB_{l'sl}^{(1)+}]dr. \tag{2D.7}$$

Using identity (2D.2) the kernel in v_s^t in equation (2.111) may be replaced with the expression

$$\int r\rho_0 i v_s^t(r)\,[\frac{1}{2}[s(s+1)+l(l+1)-l'(l'+1)]VV'B_{l'sl}^{(1)+} \\ +U'UB_{sl'l}^{(1)+}+V'UB_{l'ls}^{(1)+}-VU'B_{ll's}^{(1)+}]dr. \tag{2D.8}$$

Using identity (2D.4) the kernel w_s^t terms in equation (2.111) may be replaced by

$$\int r\rho_0 w_s^t(r)\{(U'V-U'U)B_{sl'l}^{(1)-}+V'UB_{l'ls}^{(1)-} \\ -\frac{1}{2}V'V[l(l+1)+l'(l'+1)-s(s+1)]B_{l'sl}^{(1)-}\}dr. \tag{2D.9}$$

Recognizing that $B_{l'sl}^{(1)-}=B_{sl'l}^{(1)-}=B_{l'ls}^{(1)-}$ (from eq. (2.118)), equation (2D.9) reduces to

$$\int r\rho_0 w_s^t(r)\{U'V+V'U-U'U-\frac{1}{2}V'V[l(l+1)+l'(l'+1)-s(s+1)]\}B_{l'sl}^{(1)-}dr. \tag{2D.10}$$

The integral kernels (2D.7), (2D.8), and (2D.10) represent, respectively, the anelastic versions of the integral kernels for the components u_s^t, v_s^t, and w_s^t of the velocity field. In fact, the w_s^t has remained unchanged, we have merely written it in a more convenient manner. The anelastic constraint does not constrain toroidal flow fields. The anelastic version of the integral kernels general matrix for a general flow field given in equation (2.119) may be derived by summing the integral kernels (2D.7), (2D.8), and (2D.10) and by noting that the terms in UU' that multiply the v_s^t coefficient can be combined by using the identity

$$B_{sl'l}^{(1)+}=\frac{1}{2}[s(s+1)+l(l+1)-l'(l'+1)]B_{l'sl}^{(0)+}, \tag{2D.11}$$

which follows from equation (2.117).

APPENDIX 2E

THE HERMITICITY OF THE GENERAL MATRIX

We must prove the general matrix

$$\mathbf{H}=\int \rho_o \mathbf{s}'^{*}\cdot\mathbf{B}(\mathbf{s})d^3r \tag{2E.1}$$

is Hermitian where $\mathbf{B}(\mathbf{s})$ is given by equation (2.62). Let $\mathbf{s}' = \eta$ and $\mathbf{s} = \xi$, then to be hermitian, the operator $\mathcal{O}$ must satisfy

$$\int \eta^* \cdot \mathcal{O}(\xi) d^3r = \left[\int \xi^* \cdot \mathcal{O}(\eta) d^3r \right]^* \tag{2E.2}$$

where $*$ denotes complex conjugate.

The first term in $\mathbf{B}$ yields

$$\int 2i\omega\rho_o \eta^* \cdot \mathbf{\Omega} \times \xi d^3r = \int 2i\omega\rho_o \mathbf{\Omega} \cdot (\xi \times \eta^*) d^3r, \tag{2E.3}$$

where we have used the identity $\mathbf{a} \cdot (\mathbf{b} \times \mathbf{c}) = \mathbf{b} \cdot (\mathbf{c} \times \mathbf{a})$ The right hand side of (2E.3) clearly passes the Hermiticity test. The second term in $\mathbf{B}$ yields

$$\int 2i\omega\rho_o \eta^* \cdot \mathbf{\Omega} \times \mathbf{r} \cdot \nabla \xi d^3r. \tag{2E.4}$$

Noting that

$$\nabla \cdot (\rho_o \mathbf{\Omega} \times \mathbf{r}) = 0, \tag{2E.5}$$

equation (2E.4) may be written as

$$\int 2i\omega \nabla \cdot (\rho_o \mathbf{\Omega} \times \mathbf{r}\, \eta^* \cdot \xi) d^3r - \int 2i\omega\rho_o \mathbf{\Omega} \times \mathbf{r} \cdot \xi \cdot \nabla \eta^* d^3r. \tag{2E.6}$$

The divergence term in (2E.6) may be converted into a surface integral through application of the divergence theorem. The surface integral vanishes because the unperturbed fluid velocity is orthogonal to the unperturbed surface *i.e.*,

$$\mathbf{\Omega} \times \mathbf{r} \cdot d\mathbf{S} = 0, \tag{2E.7}$$

where $d\mathbf{S}$ is an element of surface area. The remaining term in (2E.6) clearly satisfies the hermiticity condition. The third term in $\mathbf{B}$ yields

$$\int 2i\omega\rho_o \eta^* \cdot \mathbf{u}_0 \cdot \nabla \xi d^3r. \tag{2E.8}$$

Using the anelasticity condition

$$\nabla \cdot (\rho_o \mathbf{u}_0) = 0 \tag{2E.9}$$

we find (2E.8) reduces to

$$\int 2i\omega\nabla\cdot(\rho_o\mathbf{u}_0\,\eta^*\cdot\xi)d^3r-\int 2i\omega\rho_o\xi\cdot\mathbf{u}_0\cdot\nabla\eta^*d^3r \qquad (2E.10)$$

The divergence term vanishes since

$$\mathbf{u}_o\cdot d\mathbf{S}=0 \qquad (2E.11)$$

and the remaining term satisfies the hermiticity condition.

ACKNOWLEDGEMENTS

We thank Juri Toomre and Robert Noyes for continuous support and encouragement. We are grateful to Ad Van Ballegoijegen for pointing out the importance of the anelastic condition and for providing a modified version of Ron Gilliland's stellar evolution code. We appreciate John Woodhouse's crucial assistance in the derivation of Appendix D, and for providing us with his eigenfunction code and a Wigner 3-j symbol code. We thank Edmund Bertschinger and Pawan Kumar for conversations and (P.K.) for providing a preprint prior to publication. The computer support and use of Sun 4's provided to us by Jeremy Bloxham and Richard O'Connell at a critical juncture in this study is greatly appreciated. We thank Philipp Podsialwonski for his solar model and Ken Libbrecht for giving us his splitting coefficients. The numerical results reported in this paper were made possible by Gary Glatzmaier. We are particularly grateful to him for generating a convective flow model for us and for providing a program to read the coefficients.

REFERENCES

Ballegooijen, A.A. van. 1986, *Ap. J.*, **304**, 828.

Bogdan, T. 1989, preprint.

Bray, R.J., Loughhead, R.E., and Durrant 1984, *The Solar Granulation* (Cambridge: Cambridge University Press)

Brown, T.M. 1981, in *Solar Instrumentation: What's next?* ed. R.B. Dunn, (Sunspot:

N.M.).

Brown, T.M., 1984, *Science*, **226**, 687.

Brown, T.M. 1985, *Nature*, **317**, 591.

Brown, T.M., and Gilman, P.A. 1984, *Ap. J.*, **286**, 804.

Brown, T.M., and Morrow, C.A. 1987, *Ap. J.*, **314**, L21.

Brown, T.M., Christensen-Dalsgaard, J., Dziemowski, W.A., Goode, P., Gough D.O., and Morrow, C.A. 1989, preprint.

Christensen-Dalsgaard, J. and Fransden, S., 1982, *Solar Phys.*, **82**, 165.

Christensen-Dalsgaard, J., Duvall, T.L., Jr., Gough, D.O., Harvey, J.W., and Rhodes, E.J., Jr. 1985, *Nature*, **315**, 378.

Christensen-Dalsgaard, J., Dappen, W., and Lebreton, Y. 1988, *Nature*, **336**, 634.

Cox, J.P., and Giuli, R.T. 1968, *Principles of Stellar Structure* (New York: Gordon and Breach).

Cuypers, J. 1980, *A. Ap.*, **89**, 207.

Dahlen, F.A. 1969, *Geophys.J.R.astr.Soc.*, **18**, 397.

Dappen, W., and Gough, D.O. 1986, in *Seismology of the Sun and Distant Stars* ed. D.O. Gough (Reidel) 275.

Duvall T.L., Jr., and Harvey, J.W. 1984, *Nature*, **310**, 19.

Duvall T.L., Jr., and Harvey, J.W., and Pomerantz, M.A. 1986 *Nature*, **321**, 500.

Dziembowski, W., and Goode P. 1988, in *Advances in Helio- and Asteroseismology, IAU Symp. 123,*, ed. J. Christensen-Dalsgaard, (Dordrecht: Reidel), 171.

Edmonds, A.R. 1960, *Angular Momentum in Quantum Mechanics* (Princeton: Princeton University Press).

Gilman P.A., 1987, in *Physics of the Sun* ed. P.A. Sturrock, (Reidel), 95.

Gilman P.A., and Glatzmaier, G.A. 1981, *Ap. J. Suppl.*, **45**, 335.

Gilman, P.A. and Miller, J. 1986. *Ap. J. Supp.* **61**, 585.

Glatzmaier, G.A., and Gilman P.A. 1981, *Ap. J. Suppl.*, **45**, 351.

Glatzmaier, G.A., and Gilman P.A. 1982, *Ap. J.*, **256**, 316.

Glatzmaier, G.A. 1984 *J. Comp. Phys.*, **55**, 461.

Goldreich, P., and Keeley, D.A. 1977, *Ap. J.*, **211**, 934.

Goldreich, P., and Kumar, P. 1988, *Ap. J.*, **326**, 462.

Goldreich, P., and Kumar, P. 1989, preprint.

Goldreich, P., and Kumar, P. 1989, *Ap. J.*, July 1.

Gough, D.O. 1969, *J. Atmos. Sci.* **26**, 448.

Gough, D.O., Moore, D.R., Spiegel, E.A., and Weiss, N.O. 1976, *Ap. J.*, **206**, 536.

Gough, D.O., and Toomre, J. 1983, *Solar Phys.* **82**, 401.

Gough, D.O., and Weiss, N.O. 1976, *M.N.R.A.S.*, **176**, 589.

Hill, F., Gough D.O., and Toomre, J. 1984, *Mem. Soc. Astron. Ital.* **55**, 153.

Korzennik, S., and Ulrich, R.K. 1988, *Ap. J.*, **218**, 521.

Kumar, P., and Goldreich, P. 1989, *Ap. J.*, **342**, 558.

Labonte, B.J., Howard,R., and Gilman, P.A. 1981, *Ap. J.*, **250**, 796.

Latour, J., Spiegel, E.A., Toomre, J., and Zahn, J.-P. 1976, *Ap. J.*, **207**, 233.

Latour, J., Toomre, J., and Zahn, J.-P. 1981, *Ap. J.*, **248**, 1081.

Libbrecht, K.G. 1988a, Caltech Astrophysics Preprint, BBSO no. 0281.

Libbrecht, K.G. 1988b, Caltech Astrophysics Preprint, BBSO no. 0287.

Libbrecht, K.G., Woodard, M., and Kaufman, J. 1988, Caltech Astrophysics Preprint, BBSO no. 0293.

Libbrecht, K.G., and Kaufman, J.M. 1988, *Ap. J.*, **324**, 1172.

Libbrecht, K.G., Popp, B.D., Kaufman, J.M., and Penn, M.J. 1986 *Nature*, **323**, 235.

Libbrecht, K.G., and Zirin, H. 1986. *Ap. J.*, **308**, 413.

Luh, P.C. 1974, *Geophys.J.R.astr.Soc.*, **38**, 187.

Mathews J., and Walker, R.L. 1970, *Mathematical Methods of Physics* (Benjamin Cummings).

Phinney, R.A., and Burridge, R. 1973, *Geophys.J.R.astr.Soc.*, **34**, 451.

Podsiadlowski, P., 1989 Ph.D thesis, Massachussetts Institute of Technology

Stix, M. 1981, *Solar Phys.* **74**, 79.

Tassoul, J-L. 1978, *Theory of Rotating Stars* (Princeton: Princeton University Press).

Tomczyk, S., 1988 Ph.D thesis, University of California, Los Angeles

Toomre, J., Zahn, J.-P., Latour, J., and Spiegel, E.A. 1976, *Ap. J.*, **207**, 545.

Ulrich, R.K., and Rhodes, E.J., Jr. 1977, *Ap. J.*, **218**, 521.

Woodhouse, J.H., and Dahlen, F.A. 1978, *Geophys.J.R.astr.Soc.*, **53**, 335.

Woodhouse, J.H., 1980, *Geophys.J.R.astr.Soc.*, **61**, 261.

TABLE 1
THE a_i COEFFICIENTS FOR SEVERAL MULTIPLETS IN THE CASES OF SELF COUPLING, FULL COUPLING, AND DIFFERENTIAL ROTATION

coupling case for ${}_3S_{59}$	a_1	a_2	a_3	a_4	a_5
full coupling	438.38	-1.25	24.09	0.33	-3.86
self coupling	438.27	0.0	24.05	0.0	-3.84
differential rotation	439.46	0.0	24.12	0.0	-3.85
Libbrecht's data	441.7	0.3	23.0	3.2	-7.9
coupling case for ${}_3S_{70}$	a_1	a_2	a_3	a_4	a_5
full coupling	437.55	-1.85	24.07	0.323	-3.91
self coupling	437.59	0.0	24.05	0.0	-3.85
differential rotation	439.76	0.0	24.16	0.0	-3.87
Libbrecht's data	N.A.	N.A.	N.A.	N.A	N.A
coupling case for ${}_5S_{45}$	a_1	a_2	a_3	a_4	a_5
full coupling	435.37	-0.10	23.71	-0.06	-3.73
self coupling	435.34	0.0	23.84	0.0	-3.85
differential rotation	439.54	0.0	24.07	0.0	-3.81
Libbrecht's data	442.8	-0.1	22.3	0.9	-5.1
coupling case for ${}_8S_{35}$	a_1	a_2	a_3	a_4	a_5
full coupling	438.15	-0.42	23.22	-0.18	-3.55
self coupling	438.17	0.0	23.26	0.0	-3.54
differential rotation	439.09	0.0	23.30	0.0	-3.55
Libbrecht's data	437.0	2.7	25.0	4.2	-4.9
coupling case for ${}_{18}S_{70}$	a_1	a_2	a_3	a_4	a_5
full coupling	437.91	-0.87	23.05	0.02	-3.44
self coupling	438.05	0.0	23.00	0.0	-3.49
differential rotation	440.03	0.0	23.11	0.0	-3.51
Libbrecht's data	N.A.	N.A	N.A.	N.A.	N.A.
coupling case for ${}_9S_{65}$	a_1	a_2	a_3	a_4	a_5
full coupling	436.76	-1.0	24.03	0.1477	-3.82
self coupling	436.72	0.0	23.98	0.0	-3.84
differential rotation	440.54	0.0	24.20	0.0	-3.87
Libbrecht's data	N.A.	N.A	N.A.	N.A.	N.A.

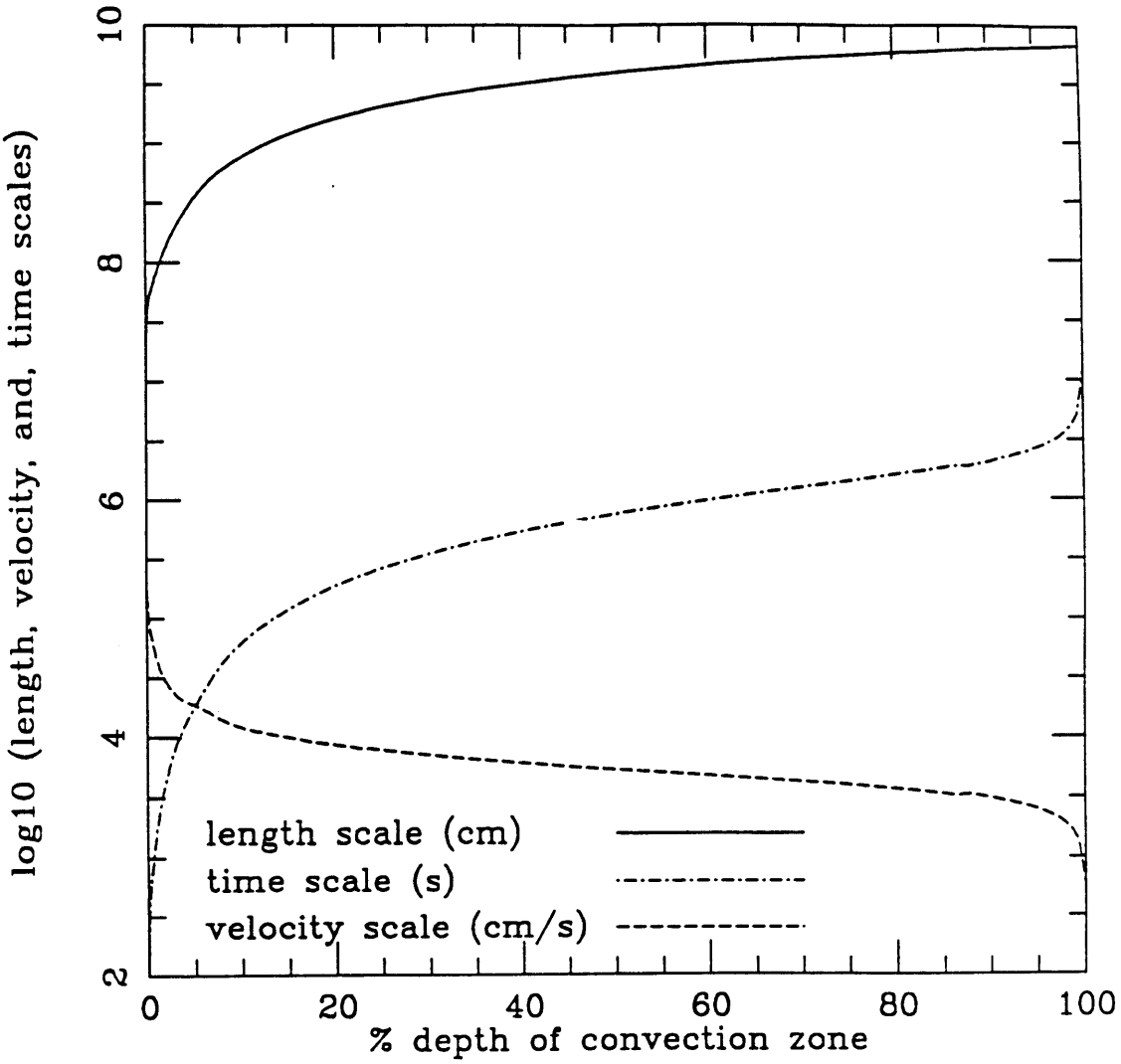

Fig. 1a. - Characteristic length, time, and velocity scales of convective eddies as predicted by mixing length theory (see eqs. (2.4), (2.5) and (2.6)) plotted as a function of depth. The solar model of Podsiadlowski (1989) was used to calculate these quantities.

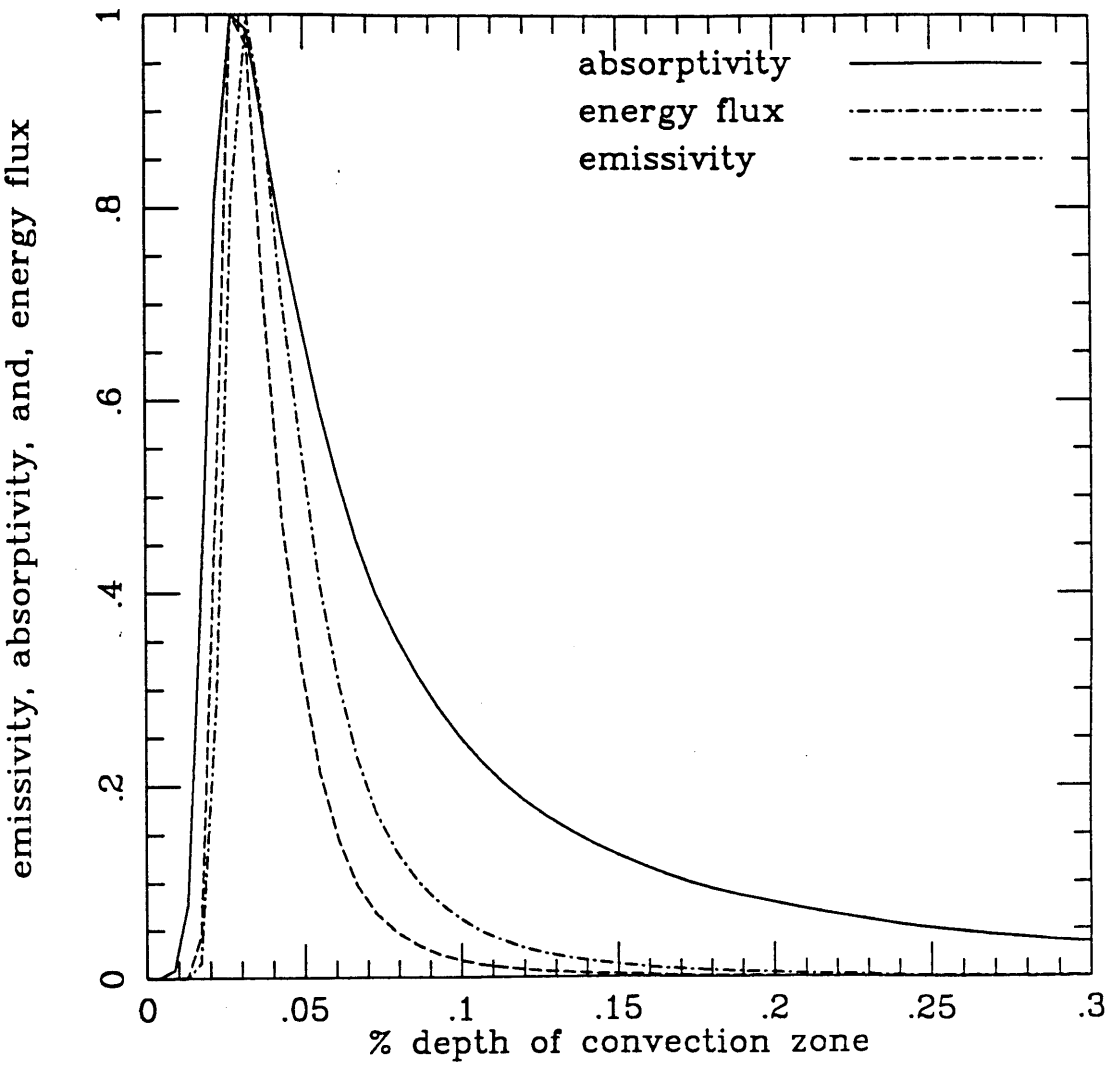

Fig. 1b. - The emissivity $\epsilon(\omega)$ (eq. 2.1), absorptivity $\alpha(\omega)$ (eq. 2.2), and the energy of convective flux flowing into the p modes F_p (eq. 2.3). The quantities have been normalized by their peak values. For $r < 0.99 R_\odot$, $\epsilon(\omega)$, $\alpha(\omega)$, and F_p are many orders of magnitude smaller than the values plotted here. We use the shape of these quantities to argue that coupling between convection and p modes is significant only in the top $\sim 0.15\%$ of the convection zone.

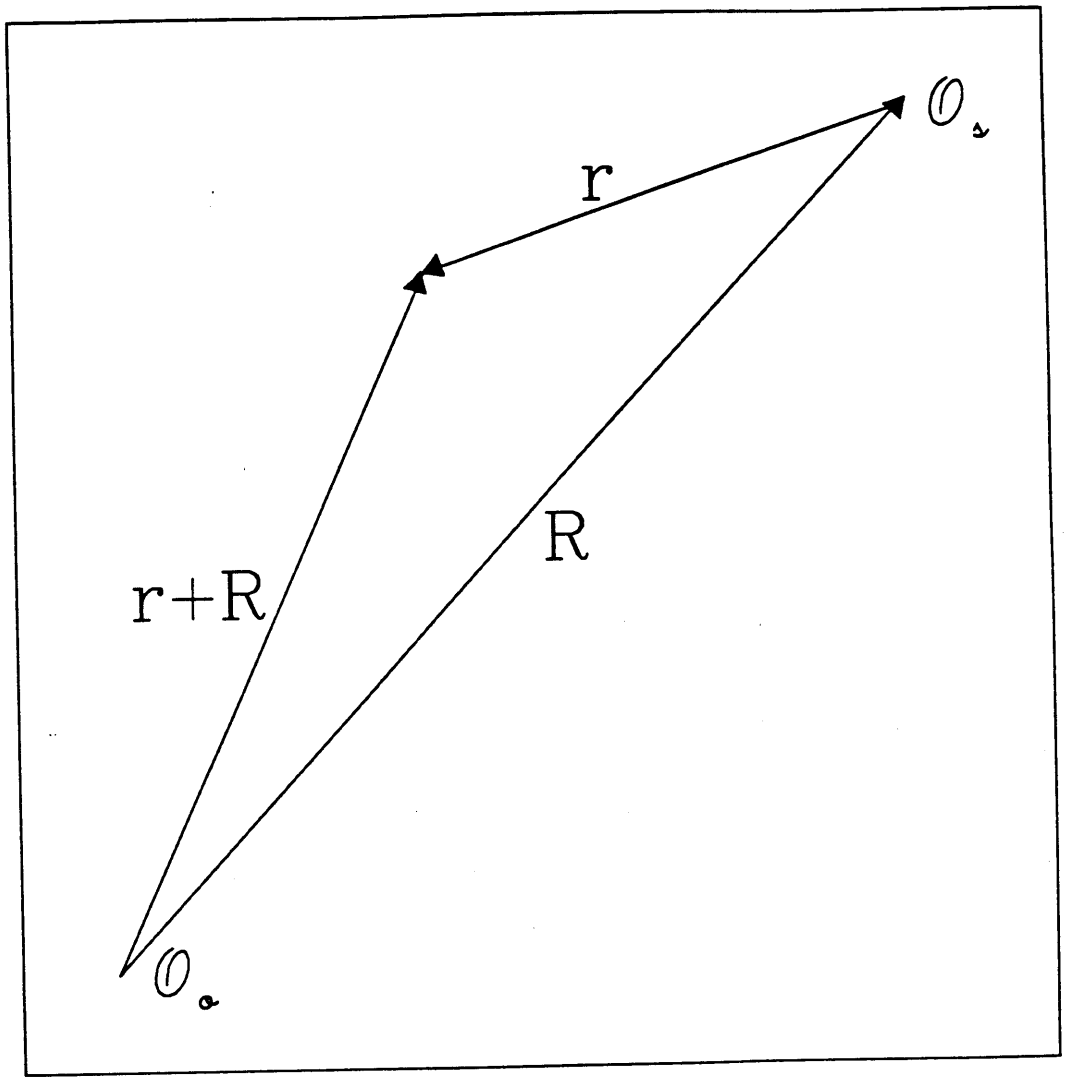

Fig. 2. - This figure illustrates the relationship between the observer's frame and the Sun's frame. The origin of the observer's and Sun's frames are, respectively, $\mathcal{O}_o$ and $\mathcal{O}_s$.

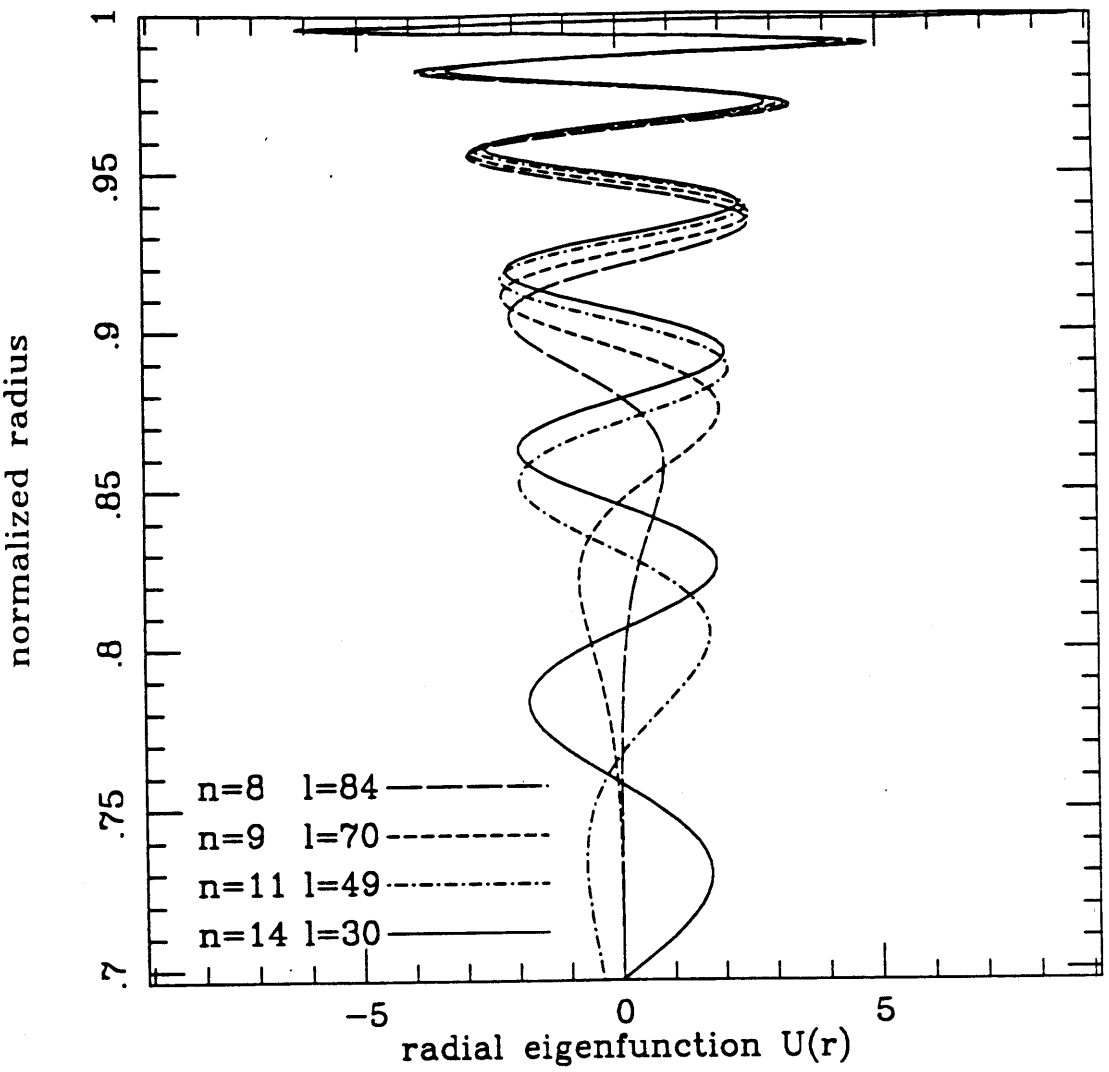

Fig. 3a. - Square root of the kinetic energy density of the radial eigenfunction (*i.e.*, $\rho^{1/2}U$) plotted for the multiplets ${}_{14}S_{30}$ (3.25013 mhz), ${}_{11}S_{49}$ (3.25001 mhz), ${}_{9}S_{70}$ (3.24938 mhz), and ${}_{8}S_{84}$ (3.24786 mhz). The shapes of the eigenfunctions U and V (see Fig. 3b) in the upper region of the convection zone depend primarily on the degenerate frequencies of the multiplets. Eigenfunction shapes at a constant frequency are similar even for widely differing harmonic degree l.

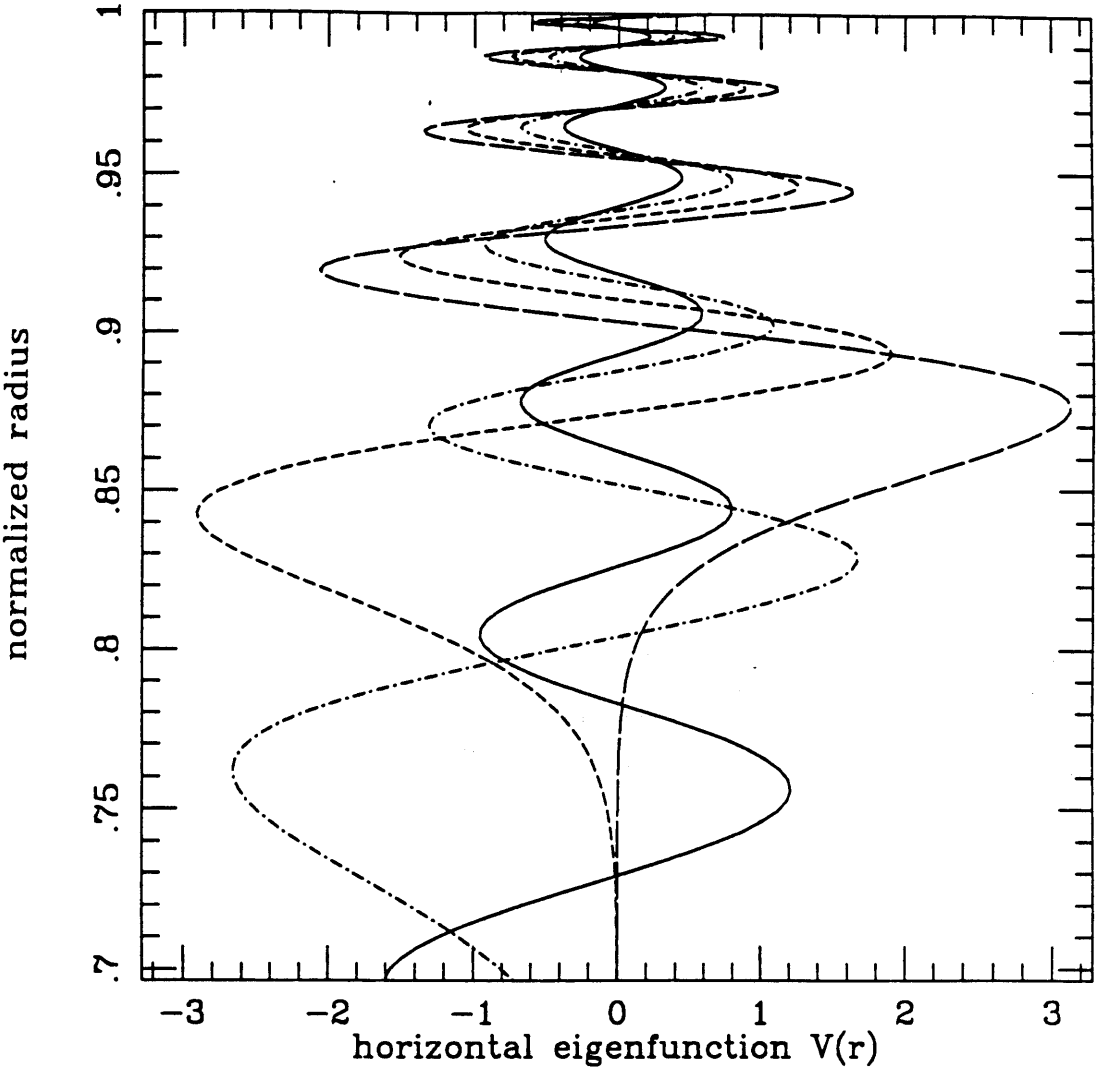

Fig. 3b. - Square root of the kinetic energy density of the horizontal eigenfunction (*i.e.*, $(\rho l(l+1))^{1/2}V$) plotted for the same multiplets as in Fig. 3a. This plot illustrates that the phases of eigenfunctions V which have nearly degenerate frequencies correlate well in the upper region of the convection zone but are phase shifted relative to one another in the deeper regions.

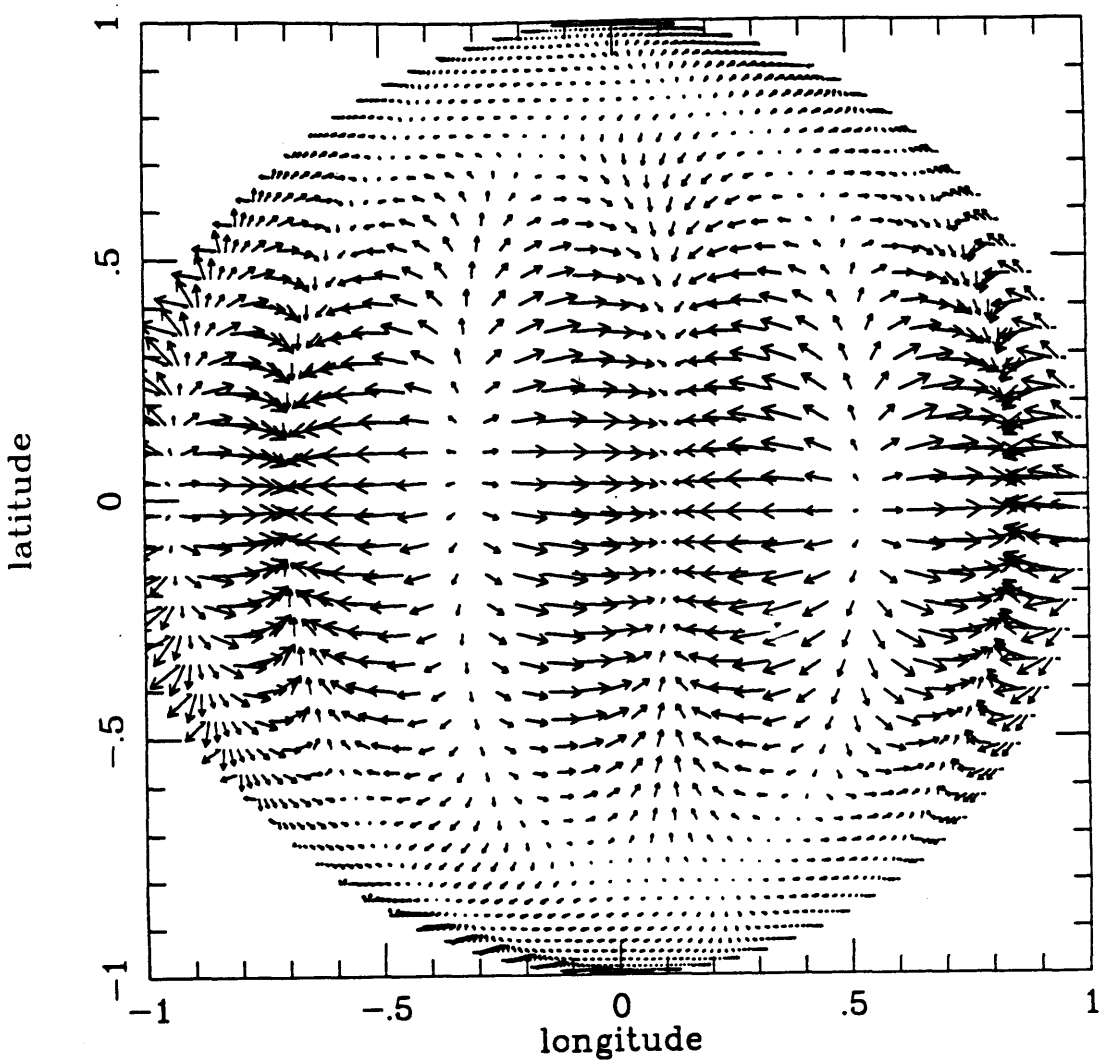

Fig. 4. - The horizontal component of the poloidal flow field for ($s = 7, -7 \leq t \leq 7$) at radial level $r = 0.96 R_{\odot}$. Inspection of the v_s^t expansion coefficients in Fig. 6b reveals that the field is dominated by the sectoral component $t = 7$. The horizontal flow illustrated here has alternating zones of divergence and convergence which corresponds to the well known banana cells. Figs. 6a and 6b illustrate that the power of the poloidal component of horizontal flow is contained primarily in the large wavenumber, sectoral, convective modes of the type shown in this figure and that the vertical flow is principally in the small wave number radial convective modes.

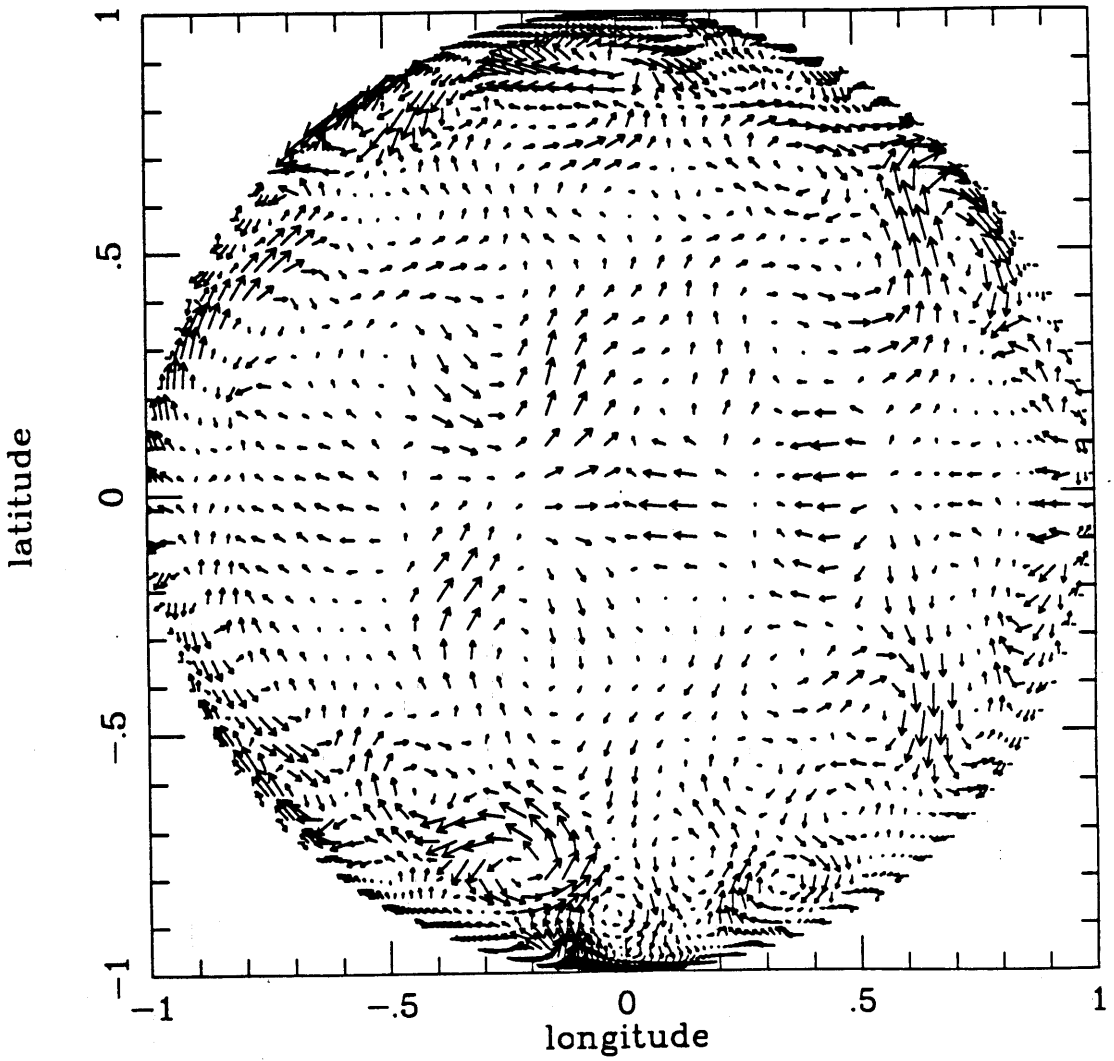

Fig. 5. - The horizontal component of the poloidal and toroidal velocity fields for ($1 \leq s \leq 20$, $-s \leq t \leq s$) at radial level $r = 0.96 R_\odot$. The large magnitude of the differential rotation velocity field would obscure the features of this figure and we therefore removed the w_3^0 and w_5^0 components.

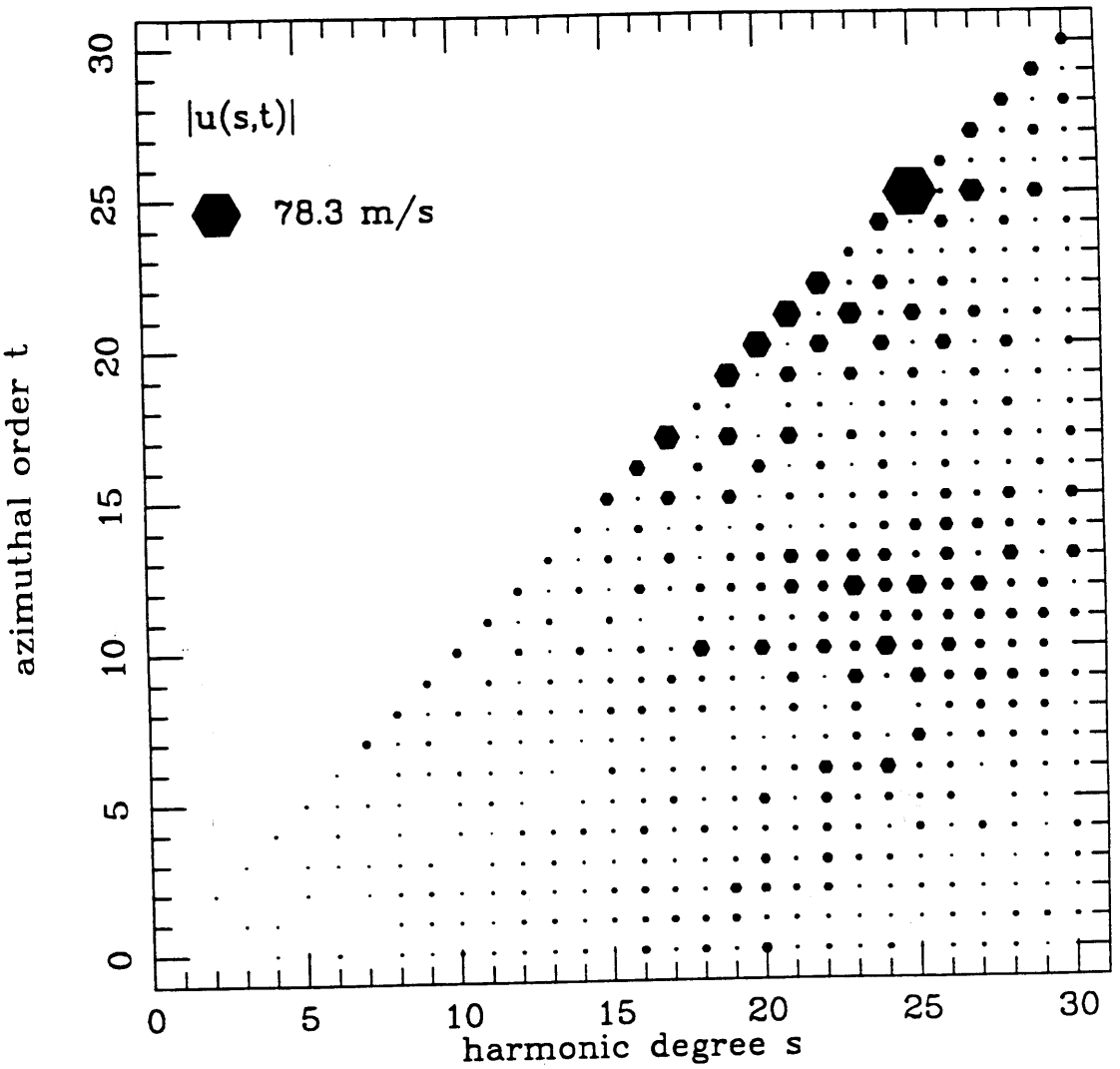

Fig. 6a. - The modulus of the complex expansion coefficient u_s^t of the radial component of the convective velocity field ($\mathbf{v}_{t,s}^{rad} = u_s^t Y_s^t(\theta,\phi)\hat{\mathbf{r}}$) at radial level $r = .96R_\odot$ for harmonic degrees $0 \leq s \leq 30$ and positive azimuthal orders t. The size of each hexagon is proportional to the modulus of u_s^t with units of m/s. Much of the power is concentrated in the sectoral components between $s = 17$ and $s = 25$ peaking at $(s = 25, t = 25)$ with a value of 78.3 m/s. The power in the flow field in the large s components is enriched relative to the power of the small s components which implies the radial flow is composed primarily of narrow updrafts and downdrafts.

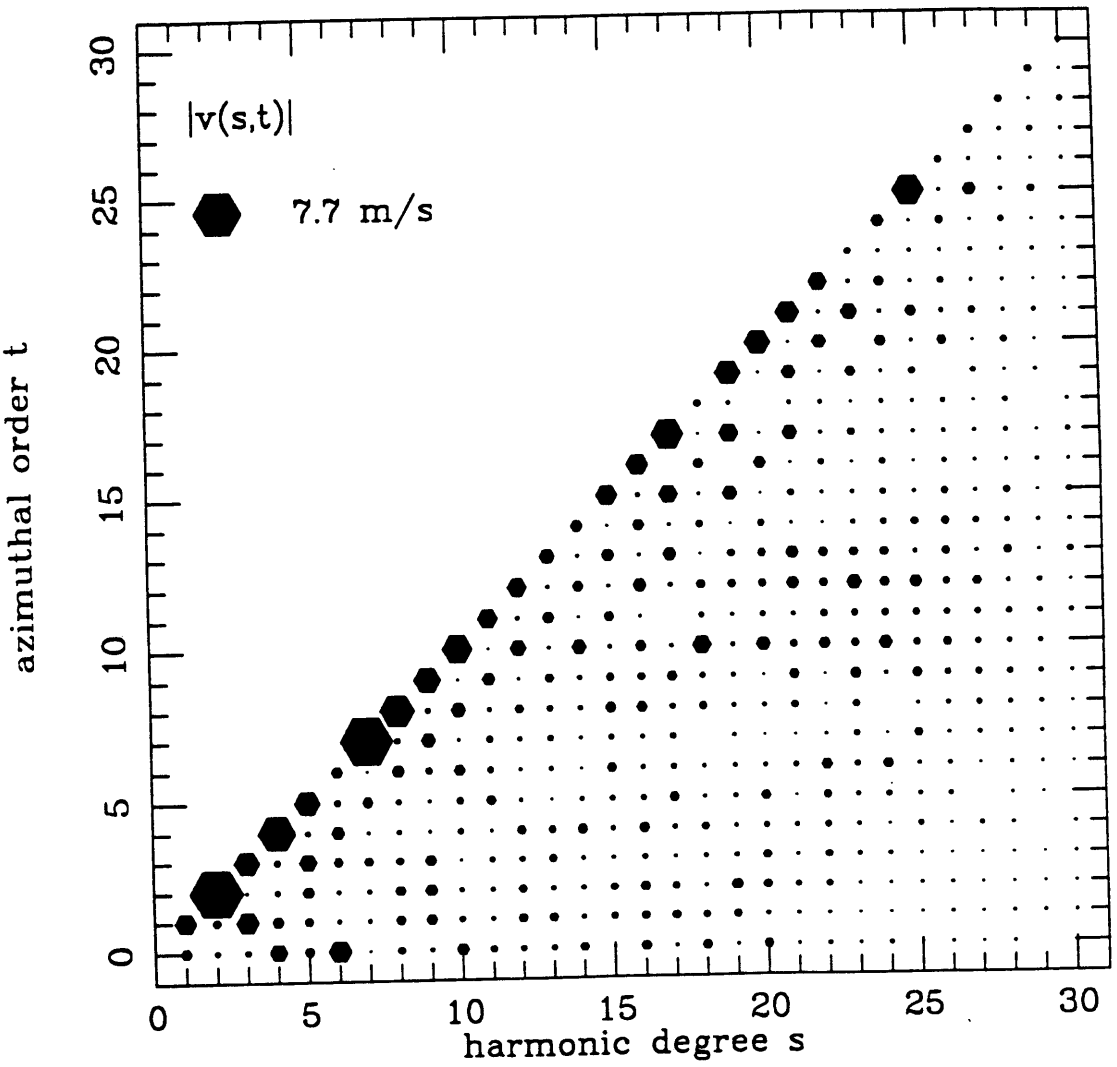

Fig. 6b. - The modulus of the complex expansion coefficient v_s^t of the horizontal contribution to the poloidal component of the convective velocity field (${}_{pol}\mathbf{v}_{t,s}^{hor} = v_s^t \nabla_1 Y_s^t(\theta,\phi)$) at radial level $r = .96 R_\odot$ for harmonic degrees $0 \leq s \leq 30$ and positive azimuthal orders t. See Fig. 6a for a description of the symbols. Much of the power is concentrated in the sectoral components with prominent peaks at ($s = 2, 4, 7, 8, 10, 17$, and 25) which corresponds to the horizontal motions associated with banana cell type convection.

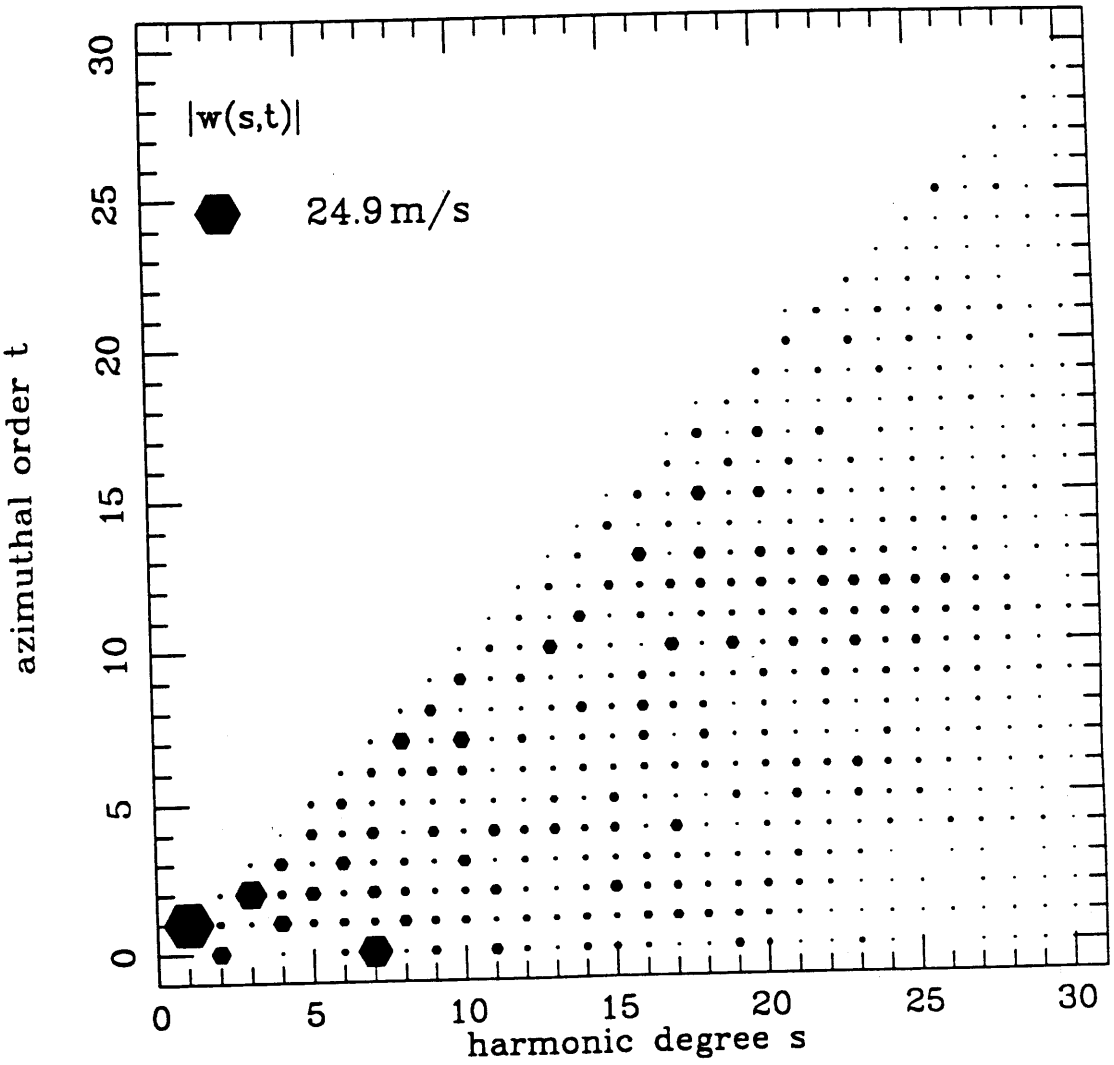

Fig. 6c. - The modulus of the complex expansion coefficient w_s^t of the toroidal component of the convective velocity field ($_{tor}\mathbf{v}_{t,s}^{hor} = -w_s^t(r)\hat{\mathbf{r}}\times\nabla_1 Y_s^t(\theta,\phi)$) at radial level $r = .96R_\odot$ for harmonic degrees $0 \leq s \leq 30$ and of positive azimuthal orders t. See Fig. 6a for a description of the symbols. The zonal (t=0) expansion coefficients for (s=1,3,5) which correspond to bulk rotation (s=1) and differential rotation have been omitted since their large size would overwhelm the features of this plot. There is very little power in the toroidal field for large s and most of the power (excepting the axially symmetric velocity field components) is in the ($s = 1$, $t = 1$) and, ($s = 3$, $t = 2$) components.

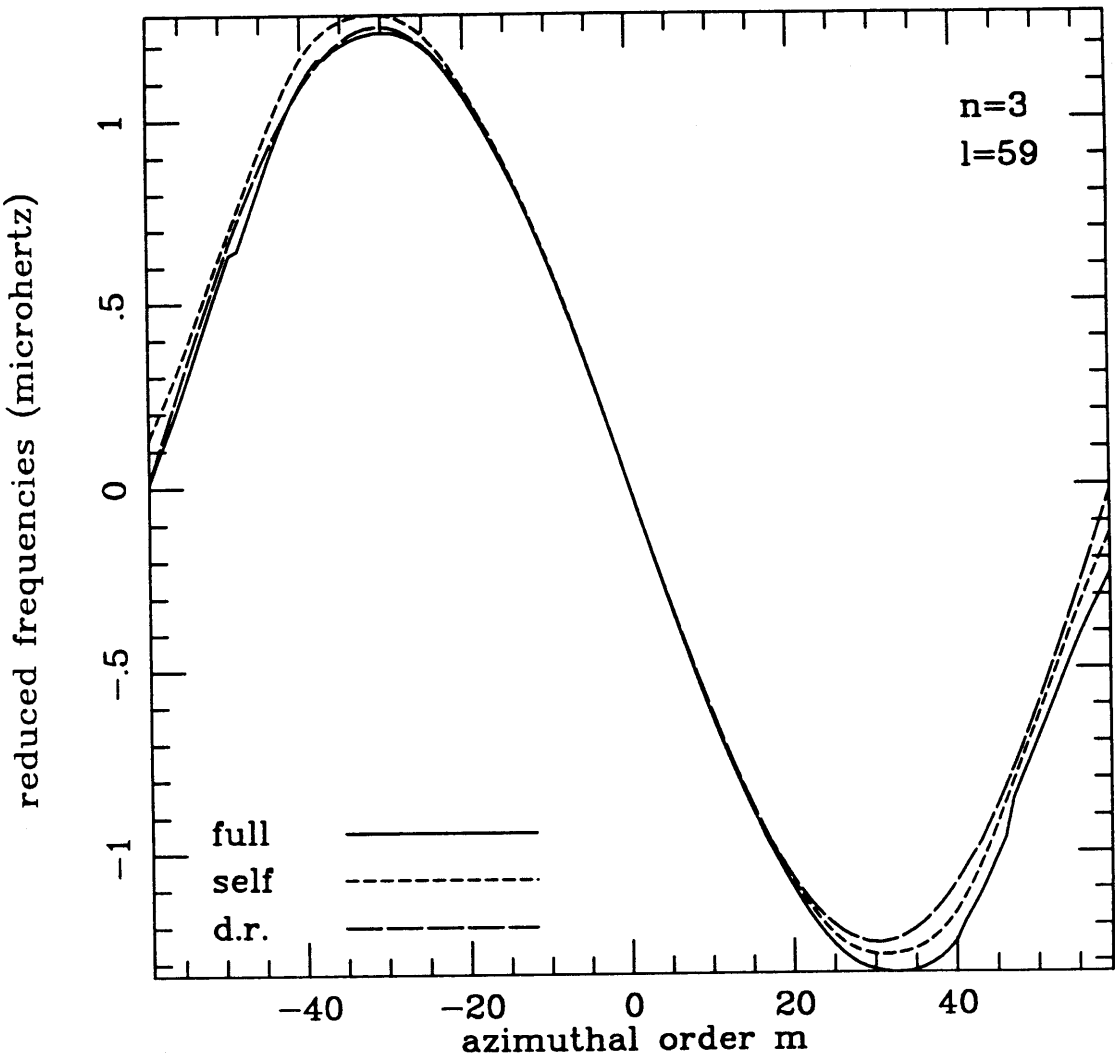

Fig. 7a. - The frequency splittings $[\omega^m_{3,59} - (\omega_{3,59} + 0.46m)]$ in μhz, of multiplet ${}_3S_{59}$ (1.76331 mhz) for the three cases listed in Table 1. The degenerate frequency and the linear trend (the bulk rotation splitting) have been removed from each of the profiles.

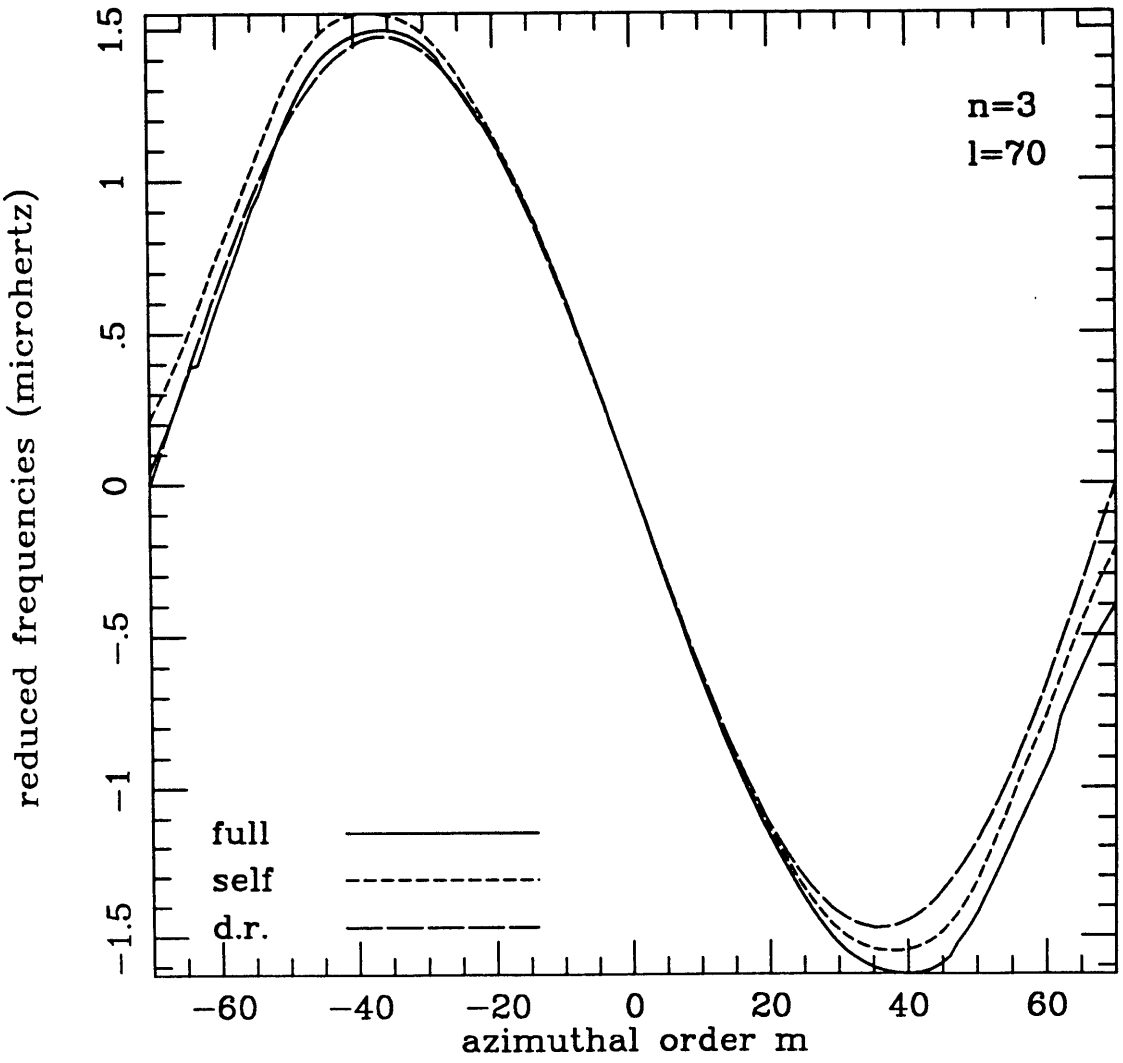

Fig. 7b. - The frequency splittings $[\omega^m_{3,70} - (\omega_{3,70} + 0.46m)]$ in μhz, of multiplet ${}_3S_{70}$ (1.87906 mhz) for the three cases listed in Table 1. The degenerate frequency and the linear trend (the bulk rotation splitting) have been removed from each of the profiles.

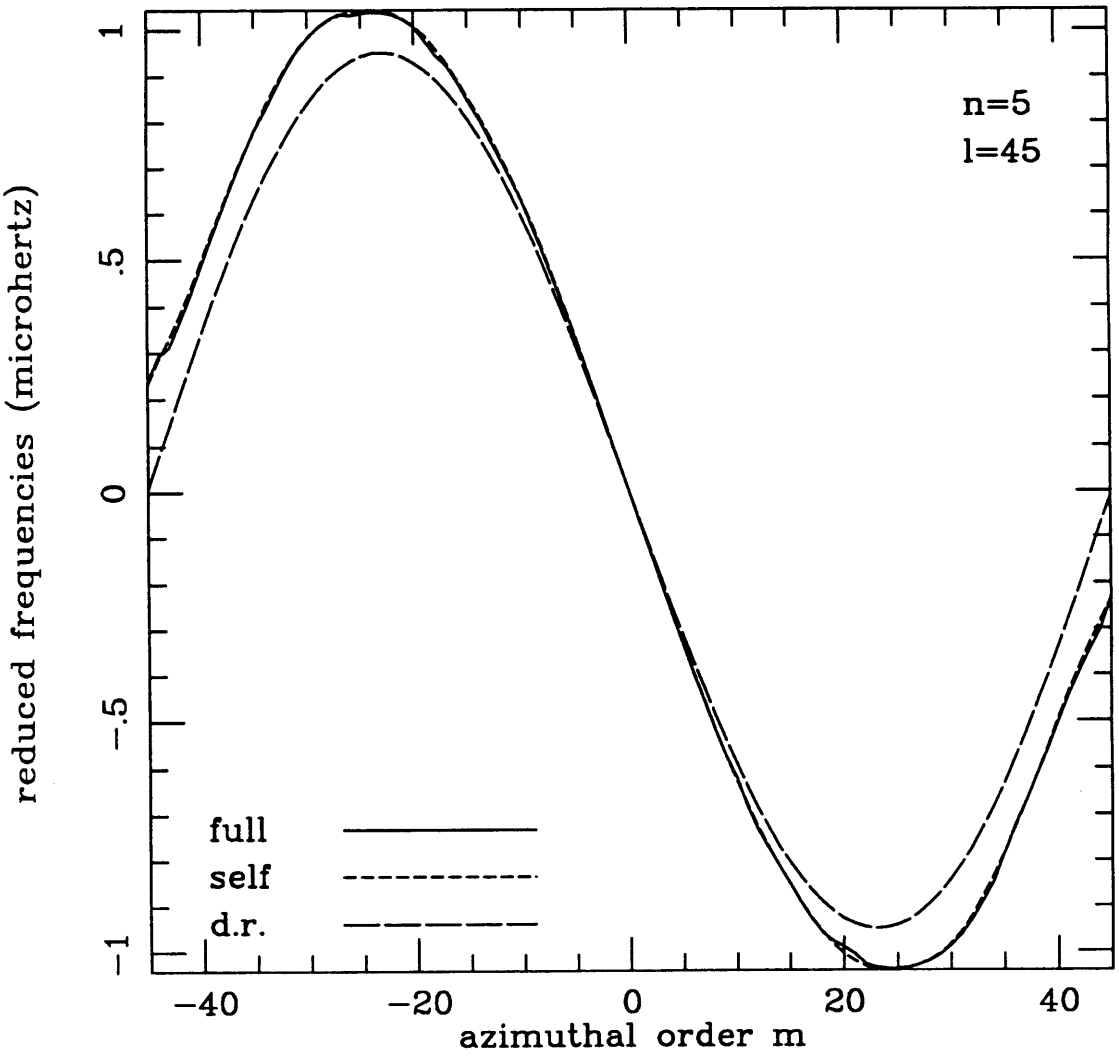

Fig. 7c. - The frequency splittings $[\omega^m_{5,45} - (\omega_{5,45} + 0.46m)]$ in μhz, of multiplet ${}_5S_{45}$ (1.02423 mhz) for the three cases listed in Table 1. The degenerate frequency and the linear trend (the bulk rotation splitting) have been removed from each of the profiles.

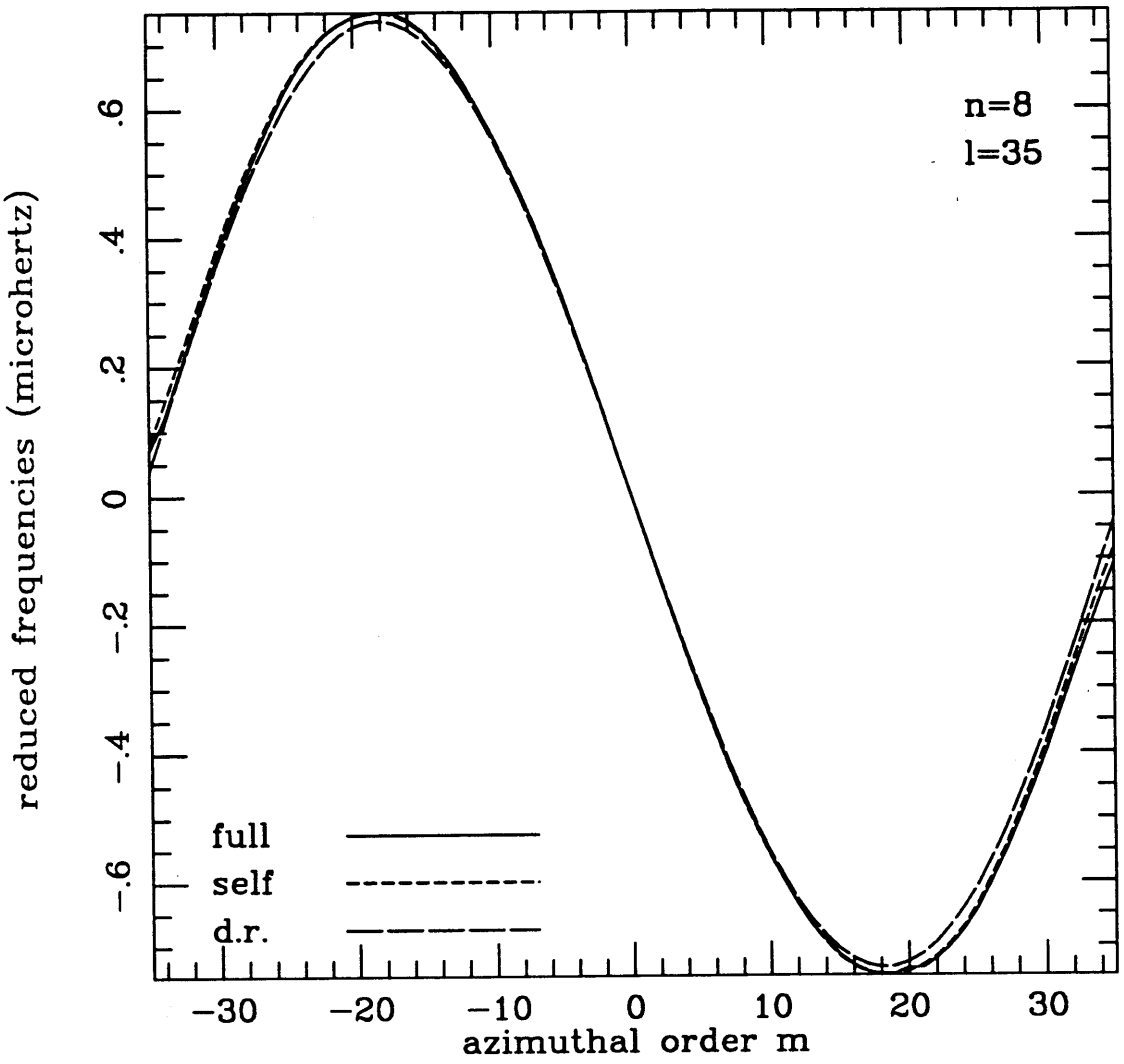

Fig. 7d. - The frequency splittings $[\omega^m_{8,35} - (\omega_{8,35} + 0.46m)]$ in μhz, of multiplet ${}_8S_{35}$ (2.41115 mhz) for the three cases listed in Table 1. The degenerate frequency and the linear trend (the bulk rotation splitting) have been removed from each of the profiles.

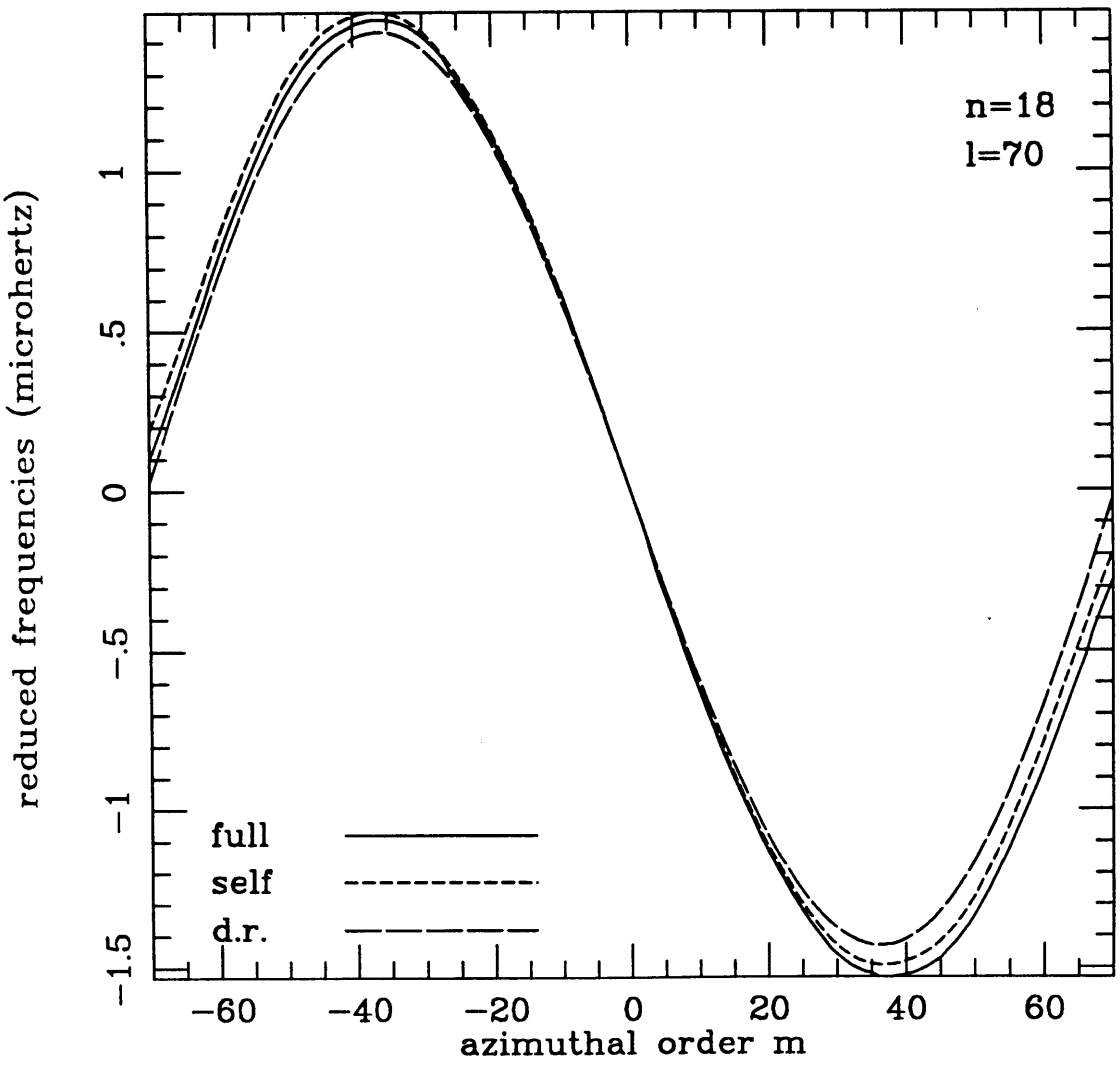

Fig. 7e. - The frequency splittings $[\omega^m_{18,70} - (\omega_{18,70} + 0.46m)]$ in μhz, of multiplet ${}_{18}S_{70}$ (4.99514 mhz) for the three cases listed in Table 1. The degenerate frequency and the linear trend (the bulk rotation splitting) have been removed from each of the profiles.

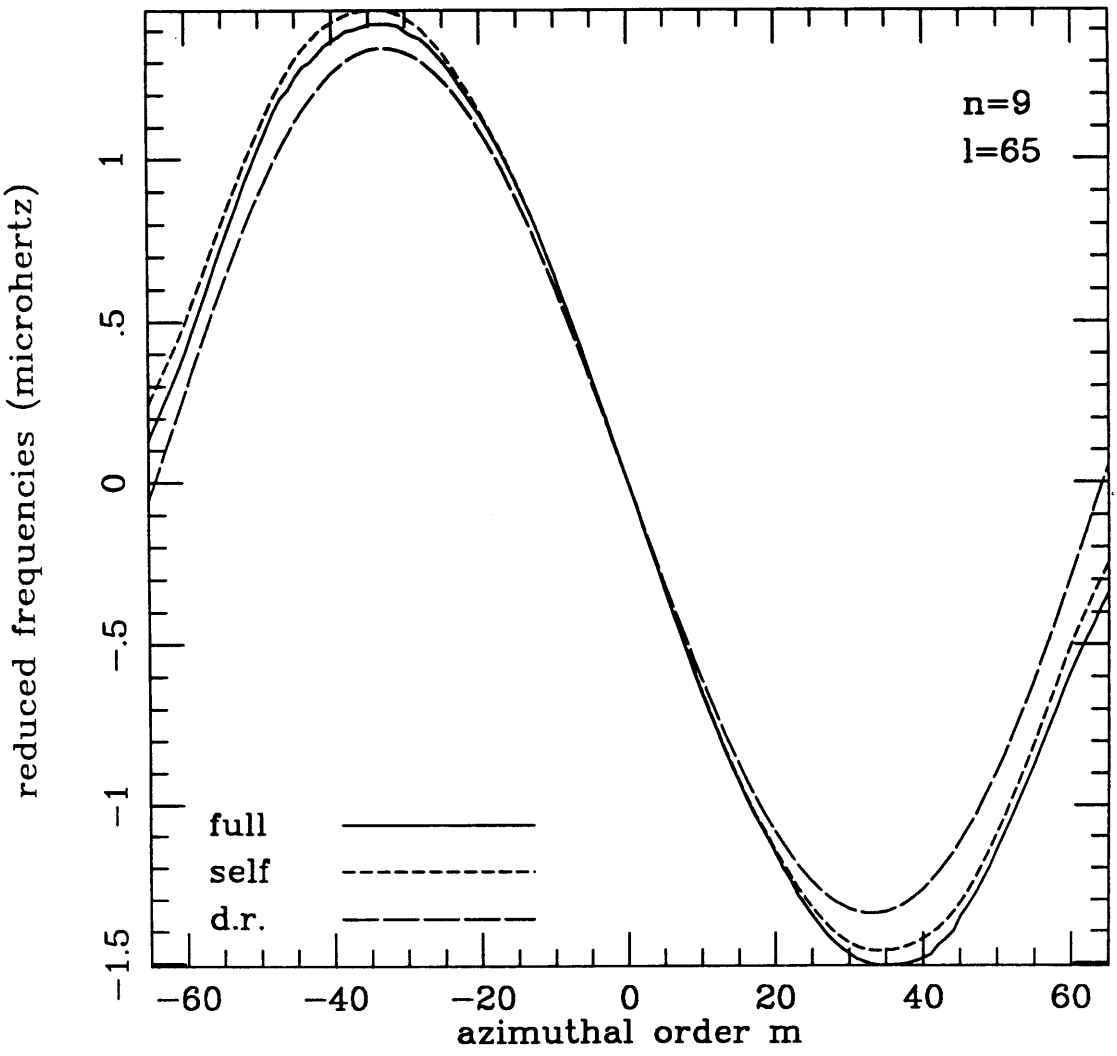

Fig. 7f. - The frequency splittings $[\omega^m_{9,65} - (\omega_{9,65} + 0.46m)]$ in μhz, of multiplet ${}_9S_{65}$ (3.16578 mhz) for the three cases listed in Table 1. The degenerate frequency and the linear trend (the bulk rotation splitting) have been removed from each of the profiles.

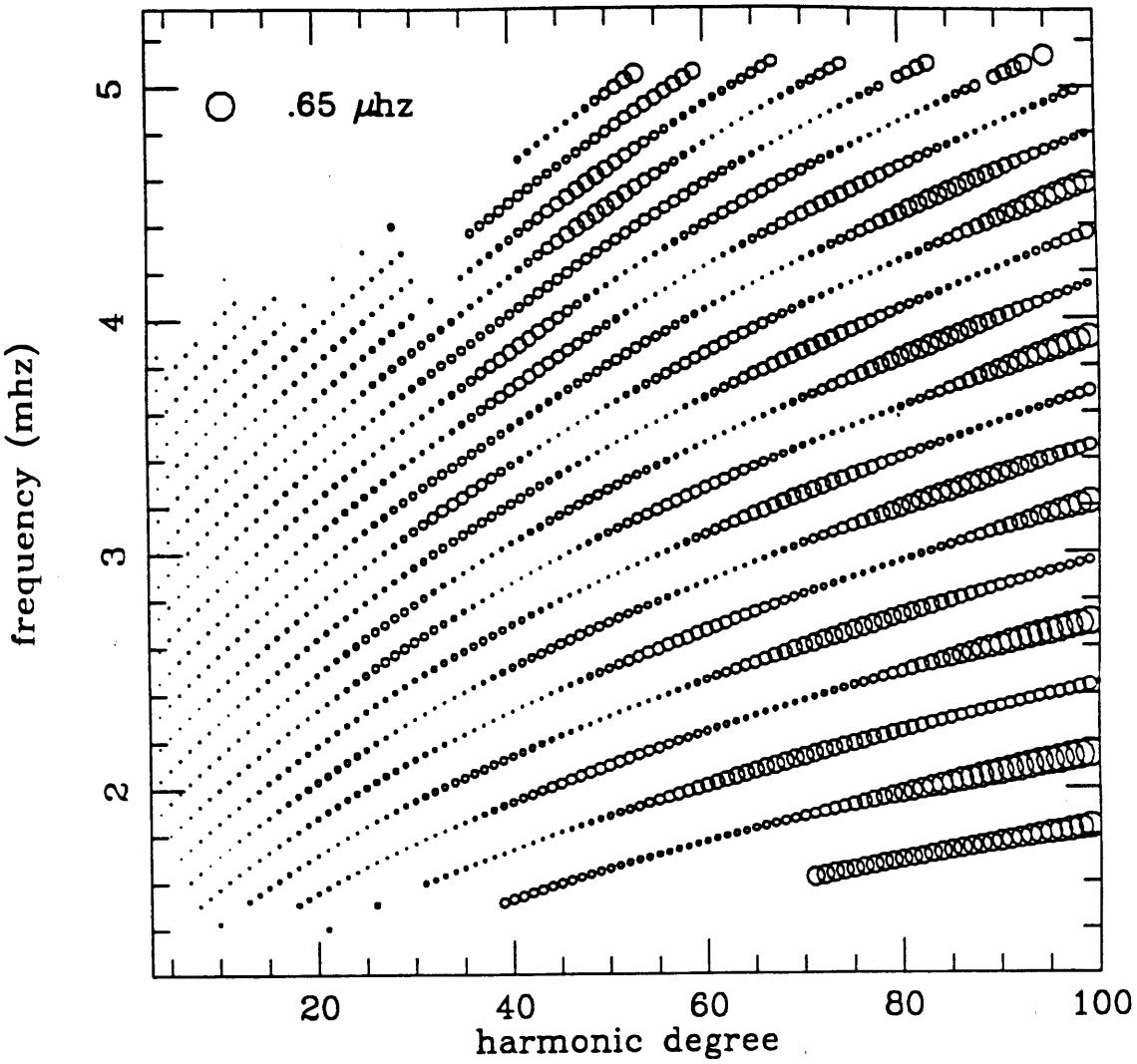

Fig. 8a. - The differences $(\omega^{self}_{m=l} - \omega^{d.r.}_{m=l})$ in frequency of the sectoral singlet $(m = l)$ for two velocity models. The first model includes the components corresponding to differential rotation $(s = 1, 3, 5, t = 0)$ and the second model includes the complete toroidal velocity field $(1 \leq s \leq 42, -s \leq t \leq s)$ with frequencies calculated in the self coupling approximation. In every case, the frequencies of the sectoral singlets for the full toroidal velocity field model are smaller than the associated singlet of the axisymmetric model. The size of each symbol is proportional to the magnitude of the difference, the largest being .65 μhz for $(n = 3, l = 99, m = 99)$. The differences tend to increase with increasing l and display zones of extinction as a function of the degenerate frequency of the multiplets. This extinction takes place at frequencies where the radial eigenfunctions of the multiplets become nearly orthogonal with the radial variation of the velocity model. As such, their location is a strong function of the convective flow field.

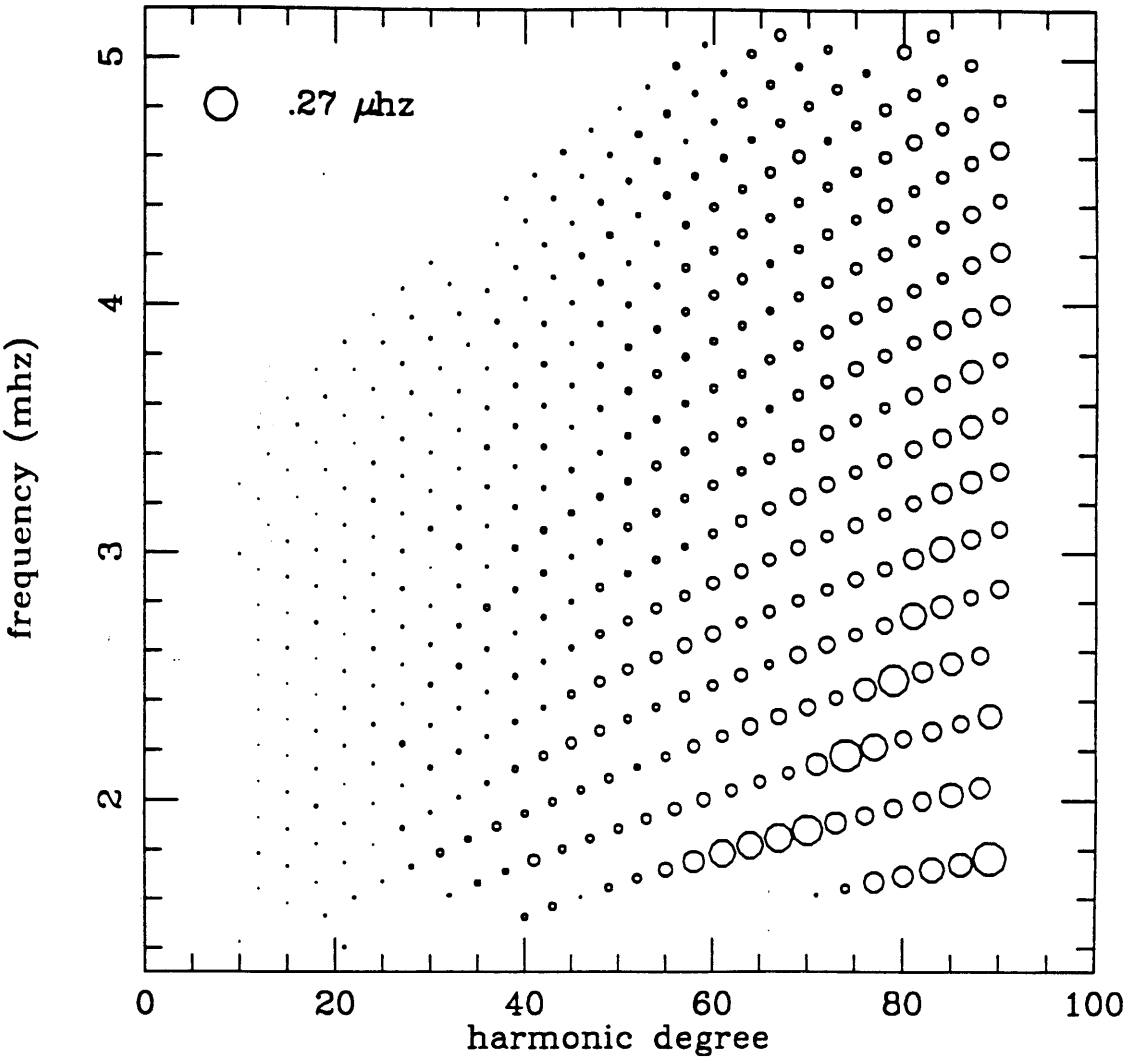

Fig. 8b. - The differences $(\omega^{full} - \omega^{self})$ in frequency of the singlet $(n, l, m = -.8l)$ where ω^{self} and ω^{full} denote, respectively, the frequencies predicted by self coupling (toroidal flows only) and full coupling (poloidal and toroidal flows) using degrees $1 \leq s \leq 30$ of Glatzmaier's flow field. The differences were computed for every third l in the range $(10 \leq l \leq 90)$ along the overtone branches $(2 \leq n \leq 20)$. The eigenspace of the full coupling calculation consisted of all singlets with frequencies $\omega^{d.r.}_{m=-.8l}$ in a ± 3.5 μhz bandwidth about each target singlet. The average dimension of the eigenspace was ~ 200. The size of each symbol is proportional to the magnitude of the residual, the largest being .27 μhz for $(n = 2, l = 89, m = -72)$. The residuals tend to increase with increasing l.

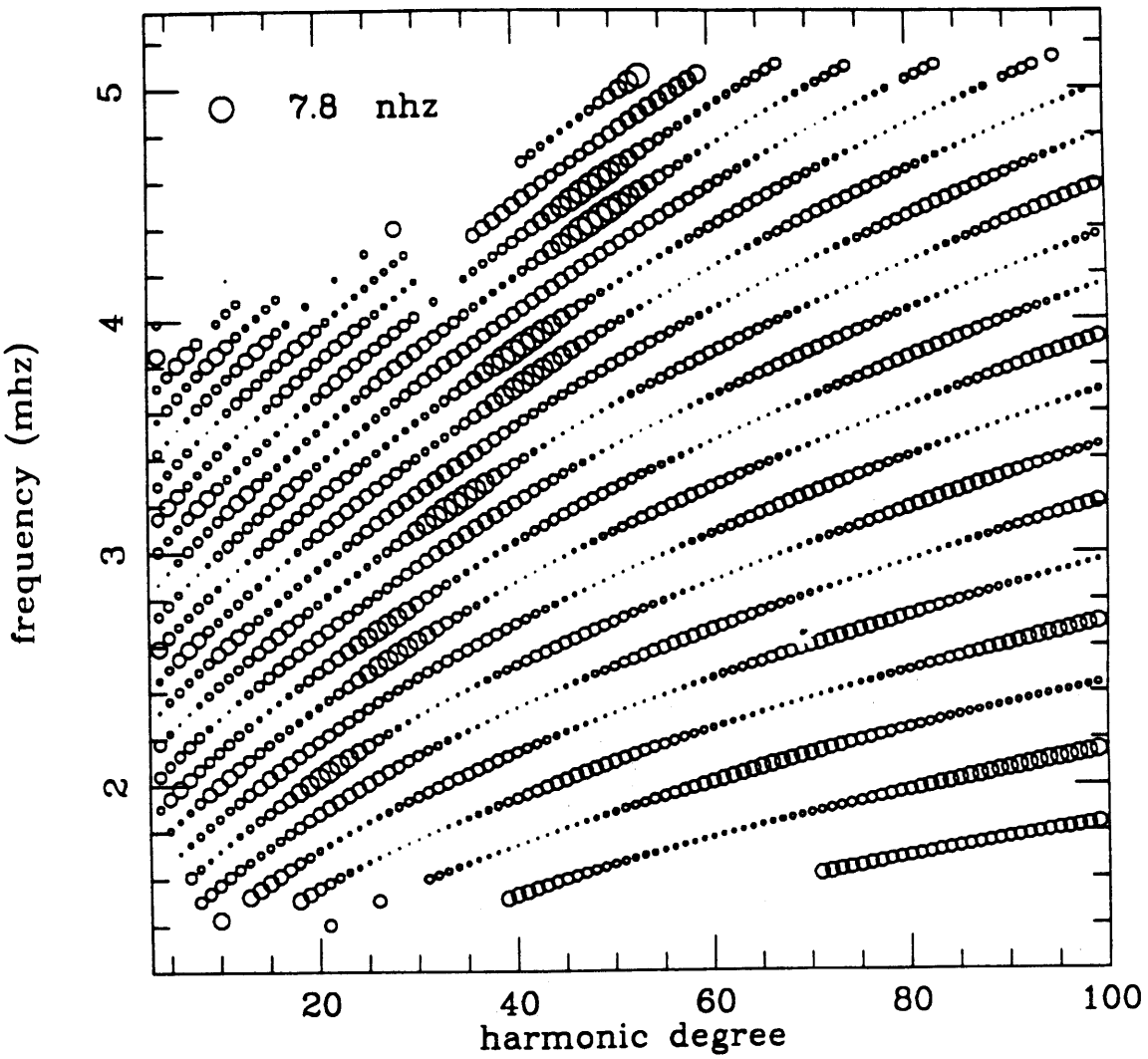

Fig. 9a. - The differences $(a_1^{d.r} - a_1^{self})$ of the a_1 coefficients for the two velocity models described in Fig. 8a for a suite of multiplets. We performed a regression using the frequency splittings of the two models to determine the a_1, a_3, and a_5 coeffcients. In the self coupling approximation, it suffices to parameterize the frequencies of a given multiplet with only odd a_i coefficients since splitting is purely odd in azimuthal order m about the degenerate frequency. The size of each symbol is proportional to the magnitude of the coeffcient difference, the largest being 7.8 nhz for $(n = 18, l = 48)$. The differences $(a_1^{d.r} - a_1^{self})$ display zones of extinction that precisely mimic the extinction pattern of the frequency differences in Fig. 8a.

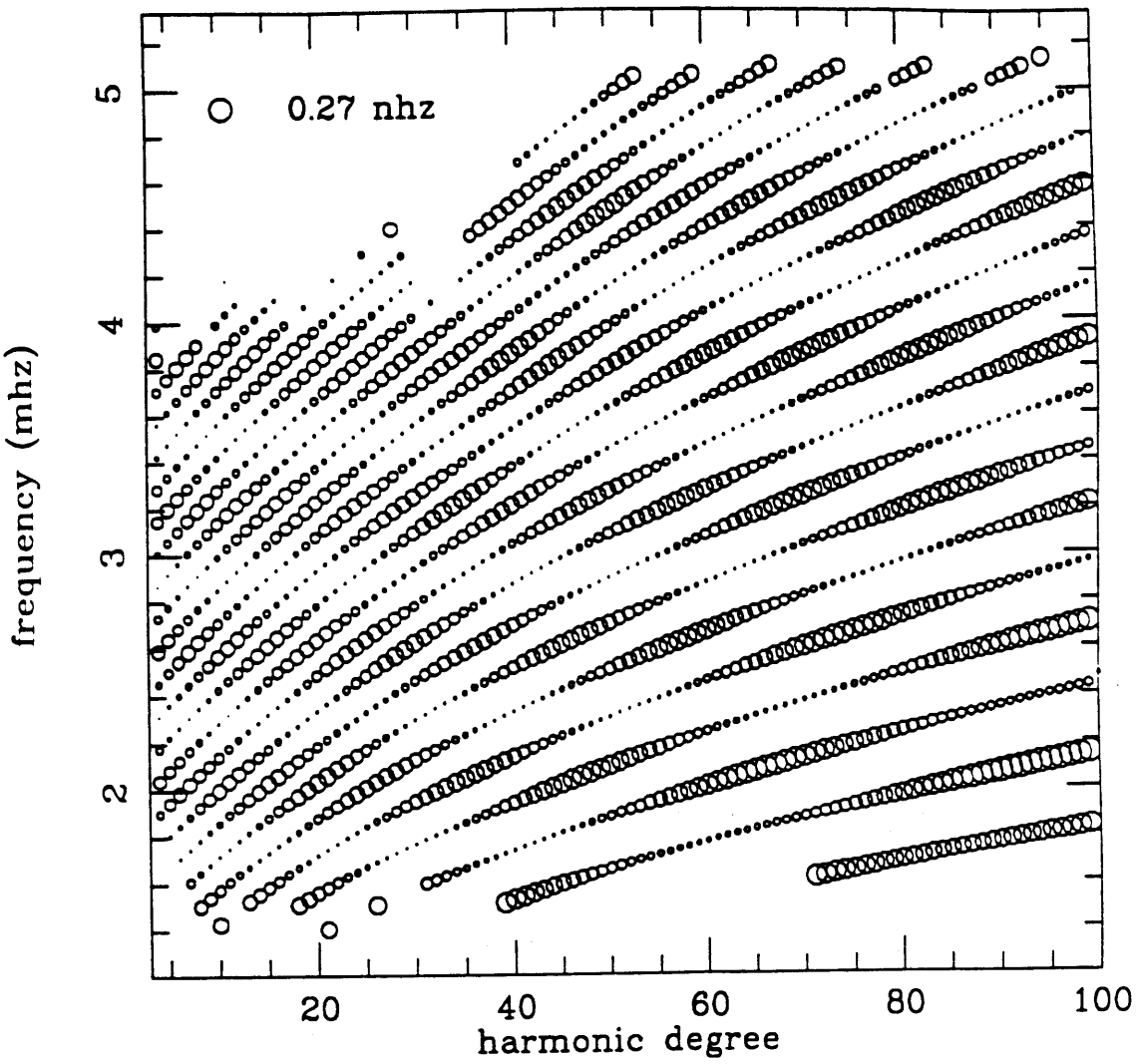

Fig. 9b. - The differences $(a_3^{d.r} - a_3^{self})$ of the a_3 coefficients for the two velocity models described in Fig. 8a. The largest difference is .27 nhz for $(n = 3, l = 97)$. The differences display zones of extinction which mimic the extinction patterns in Figs. 8a and 9a.

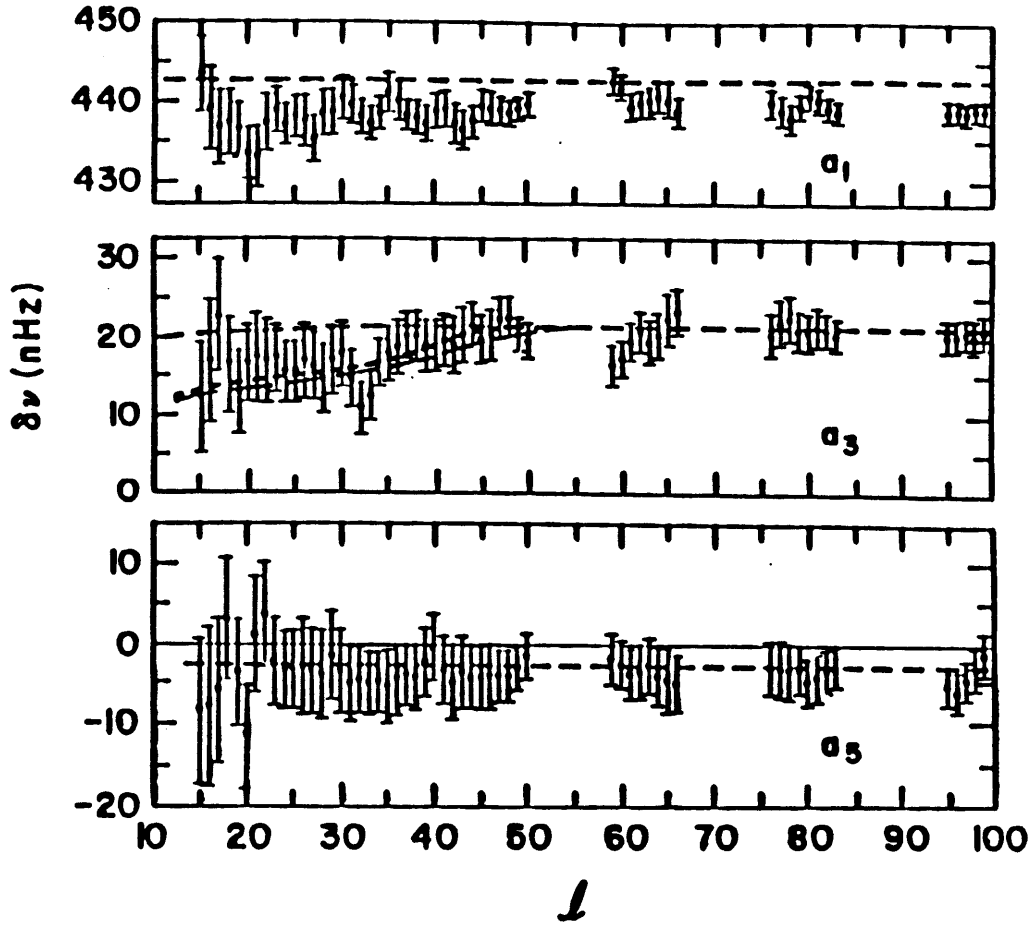

Fig. 9c. - Data from Brown and Morrow (1987). The three figures are the a_1, a_3, and a_5 coefficients. The horizontal lines represent the values the coefficients would have if the observed surface differential rotation rate prevailed through out the Sun.

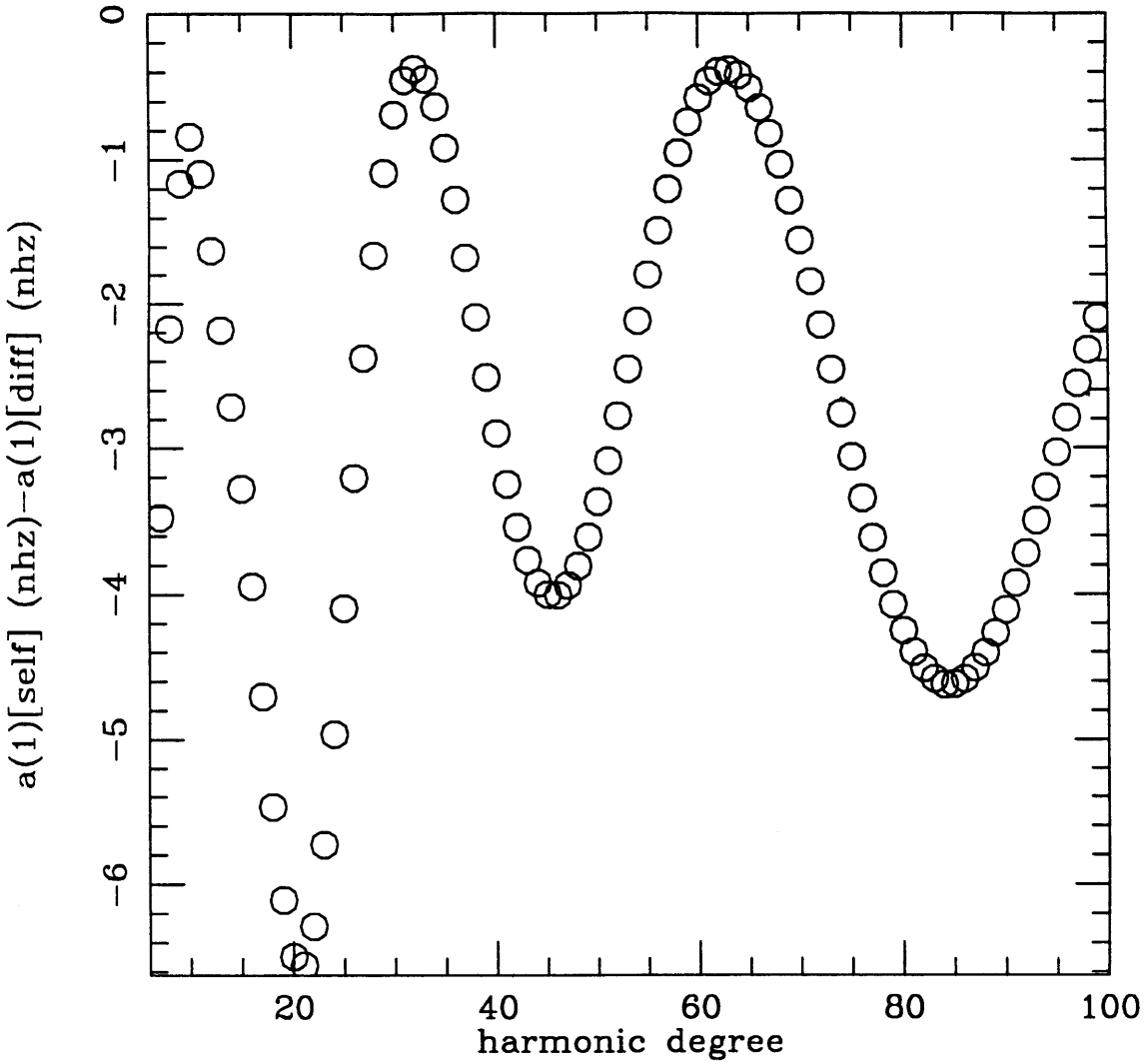

Fig. 9d. - The differences $(a_1^{self} - a_1^{d.r.})$ of the a_1 coefficients for harmonic degrees $4 \leq l \leq 99$, and overtone branch $n = 8$, in units of nanohertz. This should be compared to the corresponding plot of actual data in figure 9c.

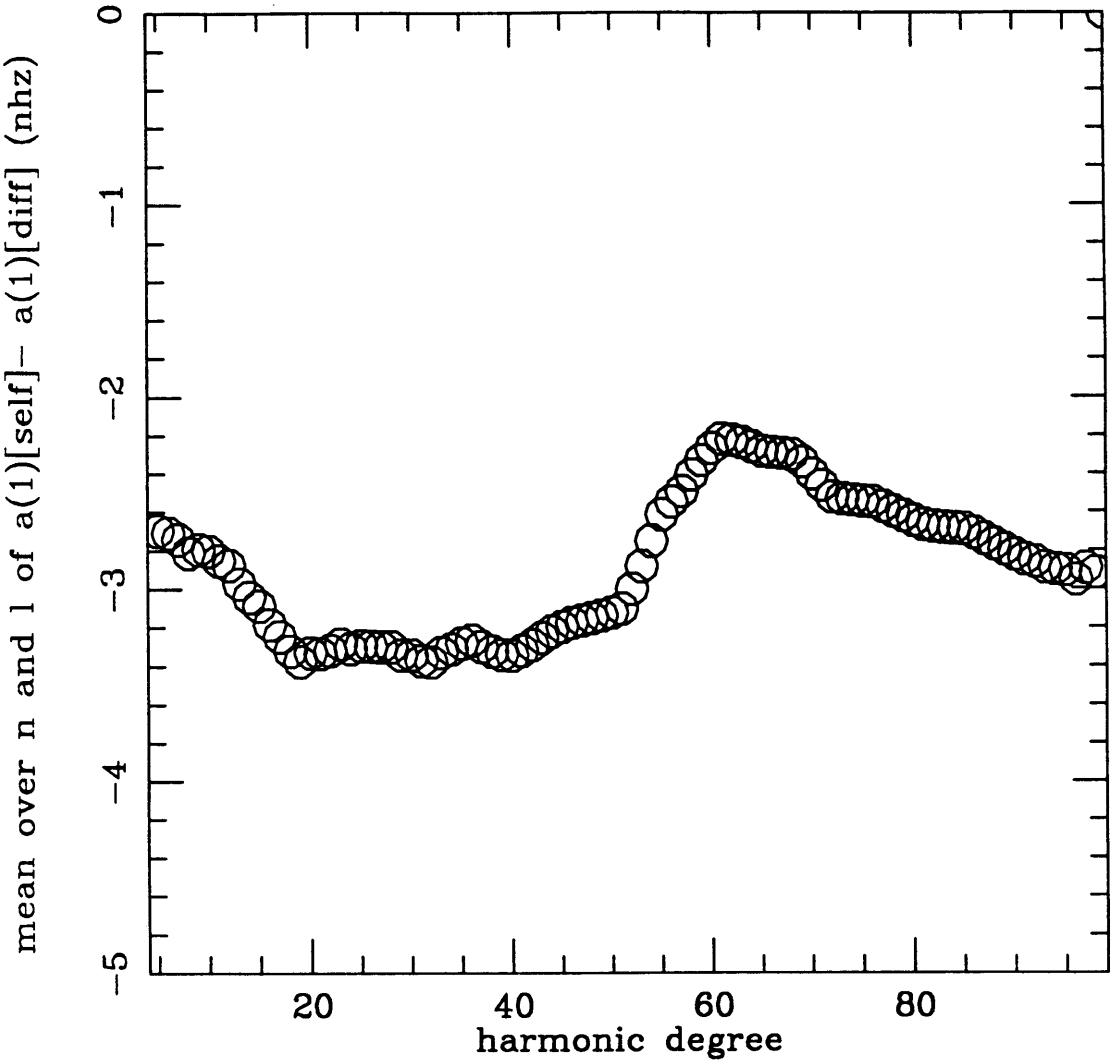

Fig. 9e. - The differences $(a_1^{self} - a_1^{d.r.})$ of the a_1 coefficients for harmonic degrees $4 \leq l \leq 99$ averaged over all overtone branches. In addition, we performed a running mean average in l. The units are in nanohertz. This should be compared to the corresponding plot of actual data in figure 9c.

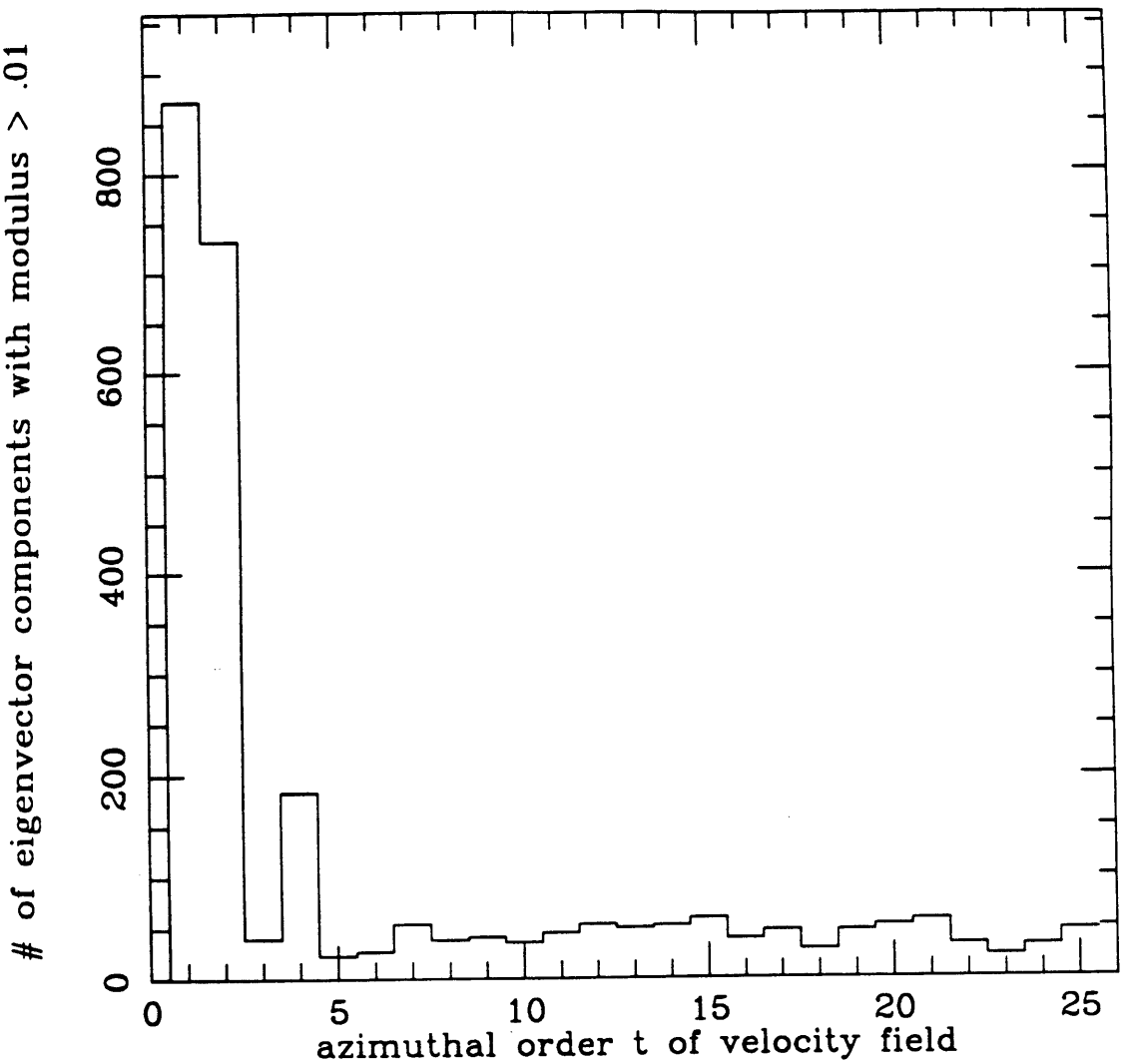

Fig. 10a. - Histogram plot showing the number of eigenvector components a_k that are generated by a toroidal or poloidal component of the flow field which has azimuthal order t. Only coefficients with modulus greater than .1 were used. The coefficients were obtained from the 445 hybrid eigenfunctions corresponding to the modes shown in figure 8a. We argue that the radial poloidal component makes virtually no contribution to a_k and that the primary components of the velocity field responsible for these coefficients can be identified with the horizontal sectoral components $w_s^{\pm s}$ and $v_s^{\pm s}$. For example, the peaks at $(t = 1, 2, 4, 7)$ are due to the components $w_1^{\pm 1}$, $v_2^{\pm 2}$, $v_4^{\pm 4}$, and $v_7^{\pm 7}$.

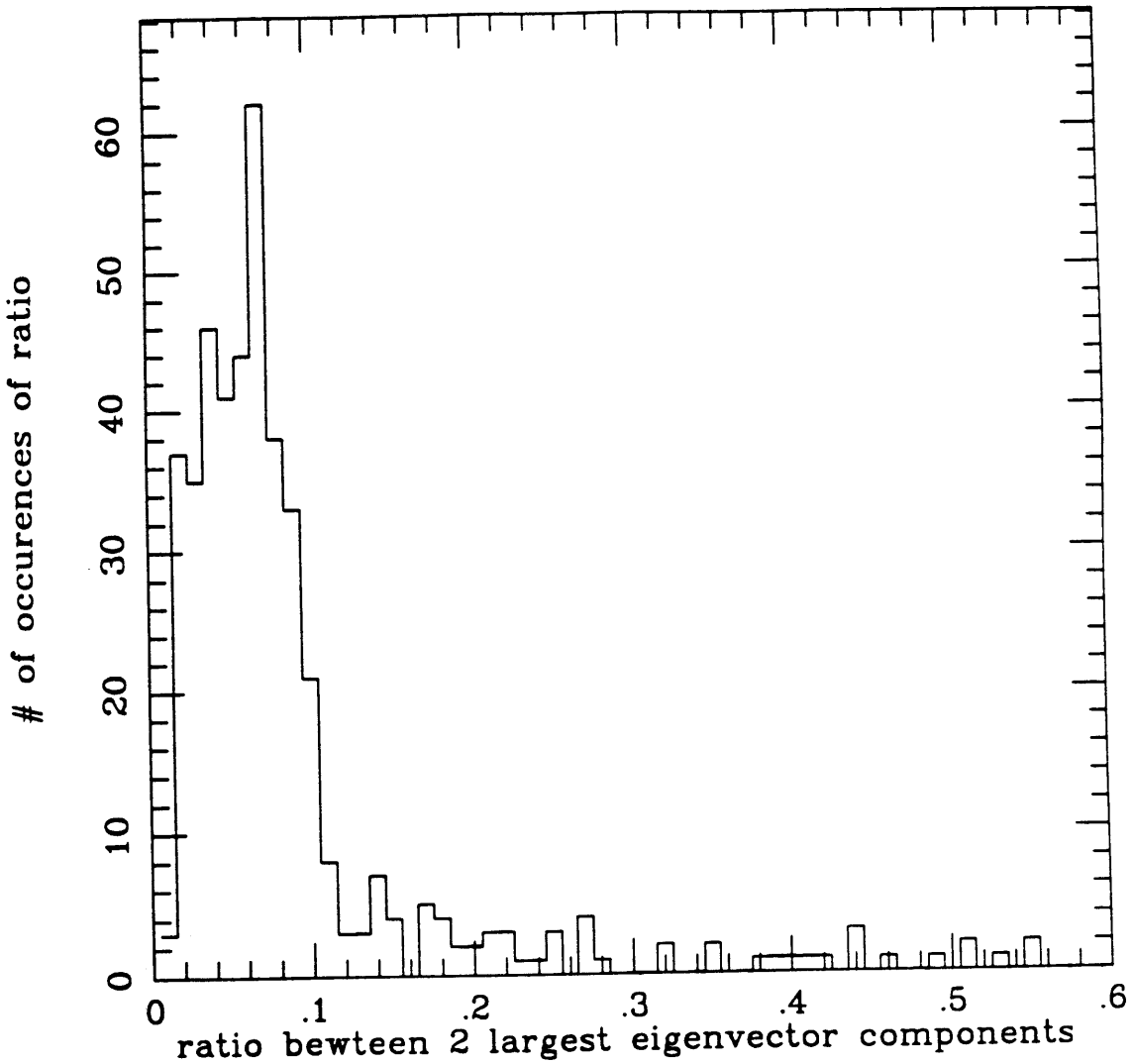

Fig. 10b. - A convenient measure of coupling strength is the ratio between the two largest expansion coefficients a_k of a given hybrid eigenfunction. The target singlet always has the largest a_k. We have plotted in histogram form the numerical value of the modulus of these ratios on the horizontal axis and the number of occurences for each ratio on the vertical axis. The coefficients were taken from the same sample of modes used in the construction of fig 10a. The horizontal axis was truncated at .6 to provide enhanced horizontal resolution; there are ratios which extend up to .9.

CHAPTER 3

THREE MODE COUPLING OF SOLAR OSCILLATIONS 1. THEORY

Some stars, such as the Cepheids, are Capitalist stars since one mode dominates all the others. Other stars, such as the Sun, are Communist stars since all modes share the same low level.

Comments overheard at a colloquium (1988)

Peter Goldreich

THREE MODE COUPLING OF SOLAR OSCILLATIONS 1. THEORY

EUGENE M. LAVELY

Massachusetts Institute of Technology, Department of Earth, Atmospheric, and Planetary Sciences

ABSTRACT

We derive in spherical geometry a theory to calculate energy transfer rates of p modes due to three mode couplings among them. Three mode coupling can alter the power spectrum of modes, limit the growth of overstable modes, contribute to mode linewidths, and slightly alter the apparent frequencies of the modes.

The principal results are the kinetic equation and an expression for the time rate of change of the modal phases. The nonlinear interaction strength scales as M^2, where M is the acoustic Mach number. For the Sun, modal amplitudes reach their peak value near the photosphere, and therefore, the most significant coupling takes place in this region. The collective motion of the resonant modes leads to a velocity field with a non-negligible M near the solar surface. The velocity of each individual mode is $\sim$ 15 cm/s and the collective motion is $\sim$ 0.5 km/s (the sound speed c near the solar surface is $\sim$ 10 km/s). The lowest order nonlinear coupling is three mode coupling which follows from retaining terms in the equation of motion to second order only. Thus, modes can couple in resonant triads provided the interaction conserves energy and angular momentum. A given triad is composed of the modes k, k', and k''. The index k, for example, represents the quantum numbers (n, l, m) which denote respectively the radial overtone, harmonic degree, and azimuthal order of mode k. For the nonlinear interaction to conserve angular momentum, the harmonic degrees must satisfy the triangle inequalities $|l - l'| \leq l''$, $|l' - l''| \leq l$, and $|l - l''| \leq l'$. In addition, l, l', and l'' must sum to an even number. These selection rules can be deduced from the Wigner 3-j symbols which appear in the nonlinear interaction coefficient $V_{kk'k''}$.

To conserve energy, the frequencies ω_k, $\omega_{k'}$, and $\omega_{k''}$ of the modes must satisfy the resonance condition $\omega_k - \omega_{k'} - \omega_{k''} \sim 0$. The coefficient $V_{kk'k''}$ averages to zero over the nonlinear interaction time if the frequency resonance condition is not satisfied. The nonlinear interaction time is the e-folding time for a change in the energy of a mode. The coupling leads to a change of the modal energies on a time scale which is long compared to the periods of oscillation. The selection rules on frequencies and harmonic degrees vastly truncate the multitude of possible coupling partners. The structure of the $\omega - k$ (frequency-wavenumber) dispersion diagram in conjunction with the frequency resonance condition imply that low l modes ($l \leq 100$) with typical periods of ~ 5 minutes can couple with very large l modes ($1000 \leq l \leq 2500$) where the spacings between the fundamental branch and overtone branches are ~ 5 minutes.

The derivation of the energy rate change equation (the kinetic equation) was simplified by application of the random phase approximation (RPA). In this approximation, one assumes the phases of the modes change many times during the nonlinear interaction time. The counterpoint to the RPA is the coherent mode coupling theory which is intended for situations in which the phases of the modes vary only slightly during the nonlinear interaction time. The nonlinear interaction coefficient was reduced to a product of a reduced matrix element times a Wigner 3-j symbol, the latter of which contains all of the azimuthal order dependence, by application of the Wigner-Eckart theorem. The summation over the modes which enter into the kinetic equation was simplified by application of Wigner 3-j symbol orthogonality relations. Highly accurate asymptotic approximations to the Wigner 3-j symbols are provided to make numerical computations practical.

I. INTRODUCTION

We apply weak turbulence theory from plasma physics (*e.g.*, Galeev and Karpman 1963, Davidson 1972) to calculate the energy transfer rates of modes due to three mode couplings. Kumar and Goldreich (1989) have addressed this problem analytically and numerically. Their calculation is for a plane parallel envelope with an adiabatic

convection zone, and an isothermal atmosphere which extends through the optically thin region above the photosphere to the temperature minimum. They show that the theory of three mode coupling indirectly bears on the question of solar p mode excitation. The excitation of the p modes, and the energies and amplitudes they should attain is an area of active study in helioseismology, but has received much less attention than the influence of the internal structure and dynamics on the modal frequencies. The modes are thought to be excited either by turbulent fluctuations, or by an overstability mechanism. Stars with large-amplitude variations such as the Cepheids are thought to be driven by the κ-mechanism. This is an overstable process since during the compression phase, the increased opacity leads to absorption of radiation energy . This mechanism has been discussed in the solar context by Ando and Osaki (1975), and Goldreich and Keeley (1977a). Other authors who have examined the linear stability of p modes include Christensen-Dalsgaard and Fransden (1982), Kidman and Cox (1984), and Anita, Chitre and Narashima (1986). The driving of p modes by the κ-mechanism in the Sun is thought to be weak, and whether it is significant or not depends sensitively on the dissipative effects of turbulence.

A linear overstability calculation can be performed to derive an equation of the form

$$\dot{E}_p = \alpha_p E_p \tag{3.1}$$

where E_p is the energy of a p mode. The mode is overstable if α is greater than zero. The numerical value of α depends on the particular overstability mechanism (the κ mechanism, for instance). It can be shown (*e.g.* Davidson 1972) that energy rate equations for three mode mode coupling depend linearly on the modal energy if the modes that couple are phase coherent. If the modes have random phases, the rate equation has quadratic dependence on the modal energy. In our derivation of the rate equation, we will assume the random phase approximation is valid. Thus the rate equation for modal energies is of the form

$$\dot{E}_p = -\beta_p E_p^2, \quad \beta_p > 0. \tag{3.2}$$

We have taken β_p greater than zero since Kumar and Goldreich (1989) have shown that three mode coupling generally damps modal energies. If three mode coupling and the κ mechanism are simultaneously operative, the rate equation becomes

$$\dot{E}_p = \alpha_p E_p - \beta E_p^2, \tag{3.3}$$

and the steady state energy is given by $E_p = \alpha/\beta$. Kumar and Goldreich (1989) have shown that the dominant coupling process is between a p mode, an f mode, and a propagating wave. Energy can be drained from the trapped modes to the propagating waves by three mode coupling. The f modes couple most dominantly with one another so that the rate equation for f modes is given approximately by

$$\dot{E}_f = \alpha_f E_f - \beta_f E_f E_{f'}, \tag{3.4}$$

and the rate equation for p modes is given approximately by

$$\dot{E}_p = \alpha_p E_p - \beta_p E_p E_f. \tag{3.5}$$

Thus, we see the f mode energies are roughly independent of the p mode energies, and if anything, are damped by the p modes through couplings with the propagating waves. Furthermore, α_f is approximately zero since the f modes have virtually no compression which renders the κ-mechanism inoperative. The f modes and p modes at the same frequencies are observed to have similar energies. Since the f modes cannot be excited by the κ-mechanism or by nonlinear transfer of energy, Kumar and Goldreich (1989) concluded that they must be excited by turbulence. Three mode coupling is thought to be a leading candidate to damp overstable modes. It would have been a more direct argument against overstability to show conclusively via equation (3.5) that three mode coupling cannot damp overstable modes. The reasoning is that the p modes have observed finite amplitudes and energies; if three mode coupling cannot quench the growth of the modes, it is unlikely they are overstable. Unfortunately, such a proof requires accurate knowledge of the energies of modes at large harmonic degree and these are not yet available. In their numerical work, Kumar and

Goldreich (1988) using plausible assumptions, find energy transfer rates which range from 10 to 100 percent of the products of the mode energies and linewidths. If their calculations had conclusively shown that three mode couplings are unimportant, it would have made a strong argument against the overstability mechanism. It is for this reason they used the f mode argument described above to argue against overstability. The driving of p modes by stochastic fluctuations associated with turbulence has been considered by Goldreich and Keeley (1977b) and by Goldreich and Kumar (1988).

As a first step toward addressing these issues for a spherically symmetric Sun with a realistic thermal and density stratification, we apply methodologies from weak turbulence theory of plasma physics to derive the kinetic equation for p modes. We seek to derive an equation of the form given in equation (3.2). The dynamical equation has been derived previously by Vandakurov (1979) and Dziembowski (1982). To derive the kinetic equation, we work directly from the equation of motion whereas Kumar and Goldreich (1989) use a Hamiltonian formalism. These equations are coupled first order differential equations which govern the time rate of change of the amplitudes and energies of the modes. The theory derived here takes explicit account of the effects of spherical geometry and can be applied to a star with arbitrary thermal stratification *i.e.*, the atmosphere need not be isothermal or adiabatic. The effect of the ionization zones and the superadiabatic layer in the sub-photospheric region on nonlinear coupling coefficients is naturally accounted for. The perturbations in gravitational potential are included. The most important result is the kinetic equation (which specifies the energy transfer rate for a given mode). The p modes can nonlinearly interact if the interaction conserves energy and angular momentum. These requirements are embodied by a frequency resonance condition and by selection rules on the Wigner 3-j symbols (which enter into the nonlinear interaction coefficient). Three mode coupling can also systematically shift the phases of the modes and thus slightly alter their apparent frequencies. An expression quantifying this effect is derived. This paper contains theoretical results only; numerical results will be presented

in a future paper.

The outline of the paper is as follows. In §II we derive the dynamical equation, the frequency resonance condition, and the form of the nonlinear interaction coefficient. In §III we discuss the random phase approximation, and apply weak turbulence theory to derive the kinetic equation, and an expression for the frequency shift of the modes. In §IV we derive the equation of motion to second order in the mode displacement, calculate second order perturbation to the thermodynamic variables, and explicitly calculate the nonlinear interaction coefficient in terms of the eigenfunctions of the modes. In Appendix 3A, we provide highly accurate, easily calculated, asymptotic approximations to the Wigner 3-j symbol which appears in the kinetic equation.

II. COHERENT MODE COUPLING

a) Derivation of the Dynamical Equation

In a spherically symmetric Sun, the normal modes of oscillation are uncoupled provided the modal amplitudes are sufficiently small. In this case, the linearized equation of motion is valid and the time-varying displacement field is written

$$\mathbf{s}(\mathbf{r},t) = \sum_k \mathbf{s}_k(\mathbf{r},t) + \mathbf{s}_k^*(\mathbf{r},t) = \sum_k C_k^{(0)}\mathbf{s}_k(\mathbf{r})e^{i\omega_k t} + C_k^{*(0)}\mathbf{s}_k^*(\mathbf{r})e^{-i\omega_k t} \tag{3.6}$$

where $\mathbf{r}$ denotes the spherical polar coordinates (r,θ,ϕ). The temporal and spatial basis functions of the displacement field are given, respectively, by $e^{i\omega_k t}$ and $\mathbf{s}_k$ where ω_k is the mode eigenfrequency and $\mathbf{s}_k$ is the modal displacement. Each are calculated in the linear approximation. The displacement field of equation (3.6) is written as a standing wave pattern. The complex constants $C_k^{(0)}$ and $C_k^{*(0)}$ are the amplitudes of waves with $k = (n,l,m)$ and $k = (n,l,-m)$. The waves propagate in opposite directions because $\mathbf{s}_k$ and $\mathbf{s}_k^*$ are proportional to $\exp[i(\omega_k t + m\phi)]$, and $\exp[-i(\omega_k t + m\phi)]$, respectively. To maintain constant phase as time increases, a wave described by $\exp[i(\omega_k t \pm |m|\phi)]$ propagates in the $\mp\ \phi$ direction. The amplitude $C_k^{(0)}$ depends on the mode excitation mechanism. The superscript (0) in $C_k^{(0)}$ indicates that mode interaction has been neglected. If modal interaction does take place, the displacements

$\mathbf{s}_k$ can serve as basis functions for the new displacement field with time dependent coefficients $C_k(t)$ to be determined. We must assume that the amplitudes do not become so large that the basis functions $\mathbf{s}_k$ are no longer appropriate. Most of the work in this paper is directed toward calculating the time variation of $C_k(t)$ to determine the time-evolution of the energy of mode k due to modal interactions.

The amplitude coefficients $C_k(t)$ can be expanded in the form

$$C_k(t) = C_k^{(0)} + C_k^{(1)} + C_k^{(2)}. \tag{3.7}$$

The superscripts (1) and (2) indicate that C_k is expanded to first and second order in a small parameter of the system. We take this to be the nonlinear interaction coefficient $V_{kk'k''}$, which is derived in §IV. We will suppose that the nonlinear interaction is turned on at time $t = 0$ so that the amplitude of mode k at $t = 0$ is set by the excitation mechanism and is taken to be the result of either a calculation or an actual measurement.

In general, the displacement field is given by

$$\mathbf{s} = \sum_k \mathbf{s}_k(\mathbf{r},t) + \mathbf{s}_k^*(\mathbf{r},t) = \sum_k \{C_k(t)\mathbf{s}_k(\mathbf{r})e^{i\omega_k t} + C_k^*(t)\mathbf{s}_k^*(\mathbf{r})e^{-i\omega_k t}\}. \tag{3.8}$$

where the sum is taken over all modes. The velocity field is given by

$$\begin{aligned} \mathbf{v} &= \sum_k \mathbf{v}_k(\mathbf{r},t) + \mathbf{v}_k^*(\mathbf{r},t) \\ &= \sum_k \{\dot{C}_k(t)\mathbf{s}_k(\mathbf{r}) + i\omega_k C_k(t)\mathbf{s}_k(\mathbf{r})\}e^{i\omega_k t} \\ &+ \{\dot{C}_k^*(t)\mathbf{s}_k^*(\mathbf{r}) - i\omega_k C_k^*(t)\mathbf{s}_k^*(\mathbf{r})\}e^{-i\omega_k t} \end{aligned} \tag{3.9}$$

where the overdot indicates $\frac{\partial}{\partial t}$. If the nonlinearity is weak, it is reasonable to assume that the time variation of $C_k(t)$ is slow compared to the harmonic behavior of the mode *i.e.*,

$$\frac{\dot{C}_k}{C_k} << \omega_k. \tag{3.10}$$

By equation (3.10), we may neglect the temporal derivatives of C_k which are second order or higher. This approximation should be used in calculating higher order derivatives of $\mathbf{v}$.

In the calculation of second-order terms appearing in the nonlinear equation of motion, it proves convenient to work with time derivatives one order higher than is necessary in the linearized case. Therefore, we write the linearized equation of motion as

$$\partial_t^2 \mathbf{v}_k(\mathbf{r},t) + \mathcal{L}\mathbf{v}_k(\mathbf{r},t) = 0. \tag{3.11}$$

The mode $\mathbf{v}_k$ in the linear approximation is orthogonal to all other modes *i.e.*,

$$-\omega_k^2 \int \mathbf{v}_{k'}^* \cdot \mathbf{v}_k d^3r \delta_{kk'} = \int \mathbf{v}_k^* \cdot \mathcal{L}\mathbf{v}_k d^3r. \tag{3.12}$$

However, modes can couple in the linear approximation if the Sun is aspherical (see Chapter 2).

The equation of motion to second order in the displacement field can be written

$$\partial_t^2 \mathbf{v} + \mathcal{L}\mathbf{v} + \mathcal{N}(\mathbf{s},\mathbf{s}) = 0 \tag{3.13}$$

where $\mathbf{s}$ and $\mathbf{v}$ represent, respectively, the displacement and velocity field of all modes. To keep our discussion as general as possible, we defer the derivation of the operators $\mathcal{L}$ and $\mathcal{N}$ until a later section.

Since $\mathcal{N}$ is second order in the displacement, modes will in general couple in triads. To derive the dynamical equations governing the evolution of such a triad (composed of members k, k', and k'') we substitute equations (3.8) and (3.9) into equation (3.13) to obtain

$$\sum_{j=k,k',k''} \{-2\dot{C}_j(t)\omega_j^2 \mathbf{s}_j(\mathbf{r}) e^{i\omega_j t} - 2\dot{C}_j^*(t)\omega_j^2 \mathbf{s}_j^*(\mathbf{r}) e^{-i\omega_j t} + \mathcal{N}(\mathbf{s}_j,\mathbf{s}_j)\} = 0. \tag{3.14}$$

We have used equation (3.11) to cancel terms and equation (3.10) to justify the neglect of second and third order time derivatives of $C_k(t)$. In addition, since the operator $\mathcal{N}$ is presumed to be small, we have neglected any terms which contain derivatives of $C_j(t)$ in $\mathcal{N}$.

To derive the dynamical equations for $C_k(t)$, $C_{k'}(t)$, and $C_{k''}(t)$, we need only multiply equation (3.14) by $\rho_o \mathbf{s}_k^* \exp^{-i\omega_k t}$, $\rho_o \mathbf{s}_{k'}^* \exp^{-i\omega_{k'} t}$, $\rho_o \mathbf{s}_{k''}^* \exp^{-i\omega_{k''} t}$, respectively, and integrate over the volume of the sun. Using the normalization condition

$$\int_0^{R_\odot} \rho_o(r) \mathbf{s}_j^* \cdot \mathbf{s}_k d^3r = \delta_{jk} \tag{3.15}$$

where $d^3r = r^2 \sin(\theta) dr d\theta d\phi$, and $R_\odot$ is the solar radius, we obtain

$$\dot{C}_k(t) = \frac{1}{2\omega_k^2} \int_0^{R_\odot} \rho_o(r) \mathcal{N}(\mathbf{s}, \mathbf{s}) \cdot \mathbf{s}_k^* \exp^{-i\omega_k t} \, d^3r \tag{3.16}$$

$$\dot{C}_{k'}(t) = \frac{1}{2\omega_{k'}^2} \int_0^{R_\odot} \rho_o(r) \mathcal{N}(\mathbf{s}, \mathbf{s}) \cdot \mathbf{s}_{k'}^* \exp^{-i\omega_{k'} t} \, d^3r \tag{3.17}$$

$$\dot{C}_{k''}(t) = \frac{1}{2\omega_{k''}^2} \int_0^{R_\odot} \rho_o(r) \mathcal{N}(\mathbf{s}, \mathbf{s}) \cdot \mathbf{s}_{k''}^* \exp^{-i\omega_{k''} t} \, d^3r \tag{3.18}$$

and where the displacement fields $\mathbf{s}$ and $\mathbf{v}$ in $\mathcal{N}$ are as in equations (3.8) and (3.9) except the sums in equation (3.8) and equation (3.9) should be taken over the three modes k, k', and k'', and any terms containing derivatives of the $C_k(t)$ in $\mathcal{N}$ should be omitted.

The nonlinear operator $\mathcal{N}$ as written in equations (3.16)-(3.18) contain many different products among members of the temporal basis set. To derive the dynamical equations we average equations (3.16)-(3.18) over the fast time scale associated with the oscillation frequencies. We define all of the frequencies ω_k to be positive. The amplitudes C_k, $C_{k'}$, and $C_{k''}$ may be considered constants in such an average since by assumption $\dot{C}_k << \omega_k C_k$. For arbitrary ω_k, $\omega_{k'}$, and $\omega_{k''}$, each term on the right hand sides of equations (3.16)-(3.18) will vanish. However, when the three oscillation frequencies satisfy a resonance condition, the oscillation rate arising from the product of the temporal basis functions in the nonlinear terms reduces to a time scale more comparable with the time scale for a change in the amplitudes $C_k(t)$; the term with those products will survive the averaging process. We define the frequency resonance condition to be

$$\omega_k - \omega_{k'} - \omega_{k''} = \Delta\omega \sim 0 \tag{3.19}$$

where $\Delta\omega$ is a small quantity. By requiring that the resonance condition in equation (3.19) be satisfied and by performing the averaging process, we obtain the coupled dynamical equations. These are given by

$$\dot{C}_k(t) = \frac{1}{2\omega_k^2} V_{kk'k''} C_{k'}(t) C_{k''}(t) \exp^{-i\Delta\omega t}, \tag{3.20}$$

$$\dot{C}_{k'}(t) = \frac{1}{2\omega_{k'}^2} V_{k'kk''*} C_k(t) C_{k''}^*(t) \exp^{i\Delta\omega t}, \tag{3.21}$$

$$\dot{C}_{k''}(t) = \frac{1}{2\omega_{k''}^2} V_{k''kk'^*} C_k(t) C_{k'}^*(t) \exp^{i\Delta\omega t} . \tag{3.22}$$

The nonlinear interaction coefficient $V_{kk'k''}$ is given by

$$V_{kk'k''} = \int_0^{R_\odot} \rho_o(r) \mathcal{N}(\mathbf{s}_{k''}, \mathbf{s}_{k'}) \cdot \mathbf{s}_k^* d^3r + \int_0^{R_\odot} \rho_o(r) \mathcal{N}(\mathbf{s}_{k'}, \mathbf{s}_{k''}) \cdot \mathbf{s}_k^* d^3r. \tag{3.23}$$

The interaction coefficient $V_{k'kk''^*}$ can be obtained from $V_{kk'k''}$ by interchanging indices k and k' and by replacing $\mathbf{s}_{k''}(\mathbf{r})$ and $\omega_{k''}$ with $\mathbf{s}_{k''}^*(\mathbf{r})$ and $-\omega_{k''}$. The interaction coefficient $V_{k''kk'^*}$ can be obtained form $V_{k'kk''^*}$ by interchanging the indices k' and k''.

III. WEAK TURBULENCE THEORY

a) The Random Phase approximation

To analyze modal interactions, it must first be determined whether the modal phases are random or nonrandom. Nonlinear interactions among modes can alter their mean amplitudes and energies. The qualitative nature of the changes depend on whether the phases of the waves remain coherent or vary randomly during the time over which the nonlinear interaction occurs. If the phases remain coherent during the nonlinear interaction, it can be shown that the energy of a given mode varies linearly with the amplitude expansion coefficients (see Davidson 1972). If, on the other hand, the phases vary randomly, the time evolution of a given mode has a quadratic dependence on the energies of the modes with which it interacts. The principal assumption of coherent mode coupling theory is that the phase of the modes remain coherent during the nonlinear interaction time. The weak turbulence theory on the other hand asserts that the phases change randomly many times during the nonlinear interaction time.

Associated with each mode k is a spectral resonance function. The resonance function has a non-zero bandwidth due to the finite lifetime of the mode. We denote the linewidth of mode k by Γ_k. Since a typical period of oscillation is five minutes, and since the modes have lifetimes on the order of days, it follows that

$$\Gamma_k << \omega_k \tag{3.24}$$

To facilitate our discussion of the nature of modal phases we use the following definitions:

$\tau_n^k = 2\pi n/\omega_k$ where n is an integer,

$\tau_p^k =$ characteristic time for a phase shift of mode k,

$\tau_{n.l.}^k =$ characteristic nonlinear interaction time for mode k .

To determine experimentally whether a wave has a random phase, one need simply measure the amplitude of the wave at the same point in space in successive time intervals at times τ_n^k. If the phase does not change, the measurements would give the same value for the amplitude. Suppose now the phases of the waves vary randomly, then for $\tau_n^k >> \tau_p^k$ completely different values of the amplitude are obtained. If the mean value of the amplitude is zero for time $t_n^k >> \tau_p^k$, the field is random. The apparent randomness of the field depends on the measurement technique. If we take $t_n^k << \tau_p^k$, the measured fields could exhibit regular rather than random values. The appropriate observation time $t_{n.l.}^k$ is determined by the characteristic time of the physical process. In our application, this is the length of time for a significant amount of energy to transfer from one mode to another due to three mode coupling. We define this time to be the e-folding time. Denoting the energy of mode k by E_k, we obtain

$$t_{n.l.}^k = \left(\frac{\dot{E}_k}{E_k}\right)^{-1} . \tag{3.25}$$

The time rate of change of the energy of a given mode is given by the kinetic equation which we derive in a later section.

Any given mode has a finite quality factor Q, due to dissipative processes. In addition the mode can undergo phase shifts due to the source excitation processes. Therefore, the mode has a characteristic spectral width in the frequency domain which can vary in time. Thus, the resonance condition $\Delta\omega = \omega_k - \omega_{k'} - \omega_{k''} = 0$ is generally never met, and instead we require that $\Delta\omega$ is less than the sum of the linewidths of the modes. To determine whether coherent mode coupling theory, or weak turbulence theory be applied, we need only determine $\tau_{n.l.}$ and determine whether the argument

$\Delta\omega t$ in the exponential factors in equations (3.20)-(3.22) with $t = \tau_{n.l.}$ is $<< 1$, or $>> 1$. If

$$t = \tau_{n.l.}^{k} = \left(\frac{\dot{E}_k}{E_k}\right)^{-1} >> \frac{2\pi}{\Delta\omega}, \tag{3.26}$$

then the random phase approximation should be used since only mean-squared quantities have non-zero expectation values. In this case the nonlinear interaction occurs over many periods of the oscillation. The phase of the waves can change repeatedly before the nonlinear effects change the power spectrum or the mean wave amplitude. However, if

$$t = \tau_{n.l.}^{k} = \left(\frac{\dot{E}_k}{E_k}\right)^{-1} << \frac{2\pi}{\Delta\omega}, \tag{3.27}$$

is fulfilled, the nonlinear interaction will be felt before any change in the phase relations of the waves. The coherence condition implies that during the time of interaction, the phase difference between the waves cannot change so much as to allow the sign of the the nonlinear interaction to change. Modes which satisfy the coherence condition must have very narrow line-widths.

The random phase approximation means that the values of the phases $\phi_k^{(0)}$ of $C_k^{(0)}(t)$ in equation (3.7) for all modes k are distributed completely randomly. We can assume the modes are either overstable or are excited by stochastic excitation. Although the phases are initially randomly distributed, phase coherence can develop between some of the modes due to nonlinear interactions. Mathematically, the random phase approximation may be written

$$< C_k^{(0)} C_{k'}^{(0)} >= |C_k^{(0)}|^2 \delta_{k*k'}. \tag{3.28}$$

The time average is the same as the average over the statistical ensemble. The systems in the ensemble differ from one another only in the phase $\phi_k^{(0)}$. The distribution of the phases is completely random so that

$$< C_k >= |C_k|(< cos(\phi_k^{(0)}) > + i < sin(\phi_k^{(0)}) >) = 0, \tag{3.29}$$

since $< cos(\phi_k^{(0)}) > = < sin(\phi_k^{(0)}) > = 0$.

b) Derivation of the Kinetic Equation

In this section we apply the methods of weak turbulence theory to derive an equation which governs the time evolution of the energy of a given mode due to all possible nonlinear interactions which conserve energy and angular momentum. We call this equation the kinetic equation which is the same as the *master equation* in the language of Kumar and Goldreich (1989). The energy density of mode k is given by

$$e_k = \frac{1}{2}\rho_0\omega_k^2|C_k|^2\mathbf{s}_k \cdot \mathbf{s}_k^* \tag{3.30}$$

and its energy is given by

$$E_k = \int_0^{R_\odot} \rho_o(r)e_k d^3r = \frac{1}{2}\omega_k^2|C_k|^2 \tag{3.31}$$

where we have used equation (3.15). Thus, to determine the time evolution of E_k we must determine the time rate of change of $|C_k|^2$. The change in energy from time t_0 to time t due to nonlinear interactions is given by

$$\Delta E_k = \frac{1}{2}\omega_k^2[|C_k(t)|^2 - |C_k(t_0)|^2]. \tag{3.32}$$

Dividing both sides of equation (3.32) by the quantity $t - t_0$, we obtain the differential equation

$$\frac{\partial E_k(t)}{\partial t} = \frac{1}{2}\omega_k^2\frac{\partial|C_k(t)|^2}{\partial t}. \tag{3.33}$$

In §II we derived the dynamical equations for a single resonant triad in which the time evolution of mode k was coupled through two additional time evolution equations to the modes k' and k''. In general, the mode k will couple to any set of modes in which the interaction conserves energy and momentum. Thus, the dynamical equation for mode k generalizes to

$$\dot{C}_k(t) = \frac{1}{2\omega_k^2}\sum_{k'k''} V_{kk'k''}C_{k'}(t)C_{k''}(t)\exp^{-i(\omega_k-\omega_{k'}-\omega_{k''})t}. \tag{3.34}$$

The interaction coefficient can be simplified by application of the Wigner-Eckart theorem (see §5.3 of Edmonds 1960). Provided that the nonlinear operator $\mathcal{N}$ which defines the interaction coefficient $V_{kk'k''}$ contains no terms which break symmetry in the azimuthal orders (m, m', m''), the Wigner-Eckart theorem assures us that $V_{kk'k''}$

can be decomposed into a product of a reduced matrix element (independent of m, m', and m'') and a Wigner 3-j symbol that fully specifies the azimuthal quantum number dependence. Thus, we obtain

$$V_{kk'k''} = V^r_{nl,n'l',n''l''}(-1)^{-m} \begin{pmatrix} l & l' & l'' \\ -m & m' & m'' \end{pmatrix}. \tag{3.35}$$

where $V^r_{nl,n'l',n''l''}$ denotes the reduced matrix element. The reduced matrix element can only be determined by a detailed analytical calculation. Its explicit form is given in §IV. Since we know *a priori* that the reduction in equation (3.35) is possible, we will use this result in the derivation of the kinetic equation.

The requirement that angular momentum be conserved is encapsulated in the selection rules that the 3-j symbol in equation (3.35) must satisfy. These are the triangle inequalities and are given by:

$$\begin{aligned} |l - l'| &\leq l'', \\ |l' - l''| &\leq l, \\ |l'' - l| &\leq l'. \end{aligned} \tag{3.36}$$

In addition, the azimuthal orders must satisfy the relation

$$-m' + m + m'' = 0. \tag{3.37}$$

We use time-dependent perturbation theory to determine the coefficients $C^{(1)}_k(t)$ and $C^{(2)}_k(t)$. Equating terms first order in the nonlinear interaction coefficient in equation (3.34), we obtain

$$\dot{C}^{(1)}_k(t) = \frac{1}{2\omega^2_k} \sum_{k'k''} C^{(0)}_{k'} C^{(0)}_{k''} V_{kk'k''} e^{-i(\omega_k - \omega_{k'} - \omega_{k''})t}. \tag{3.38}$$

Integrating this equation over time, we obtain

$$C^{(1)}_k(t) = \frac{1}{2\omega^2_k} \sum_{q'q''} C^{(0)}_{q'} C^{(0)}_{q''} \int_0^t \bar{V}_{kq'q''}(t')dt', \tag{3.39}$$

where q' and q'' are dummy indices, and we have defined

$$\bar{V}_{kq'q''}(t) = V_{kq'q''} e^{-i(\omega_k - \omega_{q'} - \omega_{q''})t}. \tag{3.40}$$

The coefficients $C_{k'}^{(1)}(t)$ and $C_{k''}^{(1)}(t)$ may be determined in an analogous manner. We find

$$C_{k'}^{(1)}(t) = \frac{1}{2\omega_{k'}^2} \sum_{r'r''} C_{r'}^{(0)} C_{r''}^{*(0)} \int_0^t \bar{V}_{k'r'r''*}(t')dt', \tag{3.41}$$

$$C_{k''}^{(1)}(t) = \frac{1}{2\omega_{k''}^2} \sum_{s's''} C_{s'}^{(0)} C_{s''}^{*(0)} \int_0^t \bar{V}_{k''s's''*}(t'')dt'' \tag{3.42}$$

where r', r'', s', and s'' are dummy indices, and we have defined

$$\bar{V}_{k''s's''*}(t) = V_{k''s's''*} e^{i(\omega_{s'} - \omega_{s''} - \omega_{k''})t} \text{ and } \bar{V}_{k'r'r''*}(t) = V_{k'r'r''*} e^{i(\omega_{r'} - \omega_{r''} - \omega_{k'})t}. \tag{3.43}$$

Equating terms in equation (3.34) with second order dependence on the nonlinear interaction coefficient, we find

$$\dot{C}_k^{(2)}(t) = \frac{1}{2\omega_k^2} \sum_{k'k''} \{C_{k'}^{(0)} C_{k''}^{(1)}(t) + C_{k'}^{(1)}(t) C_{k''}^{(0)}\} \bar{V}_{kk'k''}(t) \tag{3.44}$$

Inserting equations (3.41) and (3.42) into equation (3.44), and integrating over time from $t = 0$ to t, we obtain

$$\begin{aligned} C_k^{(2)}(t) &= \frac{1}{4\omega_k^2} \sum_{k'k''} \int_0^t \{\frac{C_{k'}^{(0)}}{\omega_{k''}^2} \sum_{s's''} C_{s'}^{(0)} C_{s''}^{*(0)} \int_0^t \bar{V}_{k''s's''*}(t'')dt'' \\ &+ \frac{C_{k''}^{(0)}}{\omega_{k'}^2} \sum_{r'r''} C_{r'}^{(0)} C_{r''}^{*(0)} \int_0^t \bar{V}_{k'r'r''*}(t')dt'\} \bar{V}_{kk'k''}(t)dt. \end{aligned} \tag{3.45}$$

The right hand side of equation (3.32) can be simplified by application of the random phase approximation. To second order, we find

$$\begin{aligned} &< C_k(t) C_k^*(t) > - < C_k(0) C_k^*(0) > = < C_k^{(1)}(t) C_k^{*(1)}(t) > \\ &+ < C_k^{(2)}(t) C_k^{*(0)} > + < C_k^{(0)} C_k^{*(2)}(t) > \end{aligned} \tag{3.46}$$

where we have used the random phase approximation to eliminate $< C_k^{(0)}(t) C_k^{*(1)}(t) >$ and $< C_k^{(1)}(t) C_k^{*(0)}(t) >$. The first term on the right hand side of equation (3.46) may be written

$$\begin{aligned} < C_k^{(1)}(t) C_k^{*(1)}(t) > &= \frac{1}{4\omega_k^4} \sum_{k'k''} \sum_{q'q''} < C_{k'}^{(0)} C_{k''}^{(0)} C_{q'}^{*(0)} C_{q''}^{*(0)} > \\ &\times \left[\int_0^t \bar{V}_{kk'k''}(t')dt'\right] \left[\int_0^t \bar{V}_{kq'q''}^*(t'')dt''\right]. \end{aligned} \tag{3.47}$$

The amplitude factor in the above equation may be written

$$\begin{aligned} < C_{k'}^{(0)} C_{k''}^{(0)} C_{q'}^{*(0)} C_{q''}^{*(0)} > &= < C_{k'}^{(0)} C_{k''}^{(0)} >< C_{q'}^{*(0)} C_{q''}^{*(0)} > \\ &+ < C_{k'}^{(0)} C_{q'}^{*(0)} >< C_{k''}^{(0)} C_{q''}^{*(0)} > \\ &+ < C_{k'}^{(0)} C_{q''}^{*(0)} >< C_{k''}^{(0)} C_{q'}^{*(0)} > \\ &= |C_{k'}^{(0)}|^2 |C_{k''}^{(0)}|^2 (\delta_{k'q'}\delta_{k''q''} + \delta_{k'q''}\delta_{k''q'}). \end{aligned} \tag{3.48}$$

Inserting this result into equation (3.47), we obtain

$$\begin{aligned} < C_k^{(1)}(t) C_k^{*(1)}(t) >= \frac{1}{4\omega_k^4} \sum_{k'k''} |C_{k'}^{(0)}|^2 |C_{k''}^{(0)}|^2 \\ \times \left[\int_0^t \bar{V}_{kk'k''}(t')dt'\right] \left[\int_0^t \bar{V}^*_{kk'k''}(t'')dt'' + \int_0^t \bar{V}^*_{kk''k'}(t'')dt''\right]. \end{aligned} \tag{3.49}$$

Noting that $V_{kk'k''} = V_{kk''k'}$, this becomes

$$< C_k^{(1)}(t) C_k^{*(1)}(t) >= \frac{1}{2\omega_k^4} \sum_{k'k''} |C_{k'}^{(0)}|^2 |C_{k''}^{(0)}|^2 \left[\int_0^t \bar{V}_{kk'k''}(t')dt'\right] \left[\int_0^t \bar{V}^*_{kk'k''}(t'')dt''\right]. \tag{3.50}$$

To calculate $< C_k^{(2)}(t) C_k^{*(0)} >$ in equation (3.46), we use the expression for $C_k^{(2)}$ in equation (3.45). This leads to

$$\begin{aligned} < C_k^{(2)}(t) C_k^{*(0)} >= \frac{1}{4\omega_k^2} \sum_{k'k''} \int_0^t \{\frac{1}{\omega_{k''}^2} \sum_{s's''} < C_{k'}^{(0)} C_{s'}^{(0)} C_{s''}^{*(0)} C_k^{*(0)} > \int_0^t \bar{V}_{k''s's''*}(t'')dt'' \\ + \frac{1}{\omega_{k'}^2} \sum_{r'r''} < C_{k''}^{(0)} C_{r'}^{(0)} C_{r''}^{*(0)} C_k^{*(0)} > \int_0^t \bar{V}_{k'r'r''*}(t')dt'\} \bar{V}_{kk'k''}(t)dt. \end{aligned} \tag{3.51}$$

The expectation values of the amplitude coefficients are given by

$$< C_{k'}^{(0)} C_{s'}^{(0)} C_{s''}^{*(0)} C_k^{*(0)} >= |C_k^{(0)}|^2 \delta_{ks'} |C_{k'}^{(0)}|^2 \delta_{k's''}, \tag{3.52}$$

$$< C_{k''}^{(0)} C_{r'}^{(0)} C_{r''}^{*(0)} C_k^{*(0)} >= |C_k^{(0)}|^2 \delta_{kr'} |C_{k''}^{(0)}|^2 \delta_{k''r''}. \tag{3.53}$$

Inserting equations (3.52) and (3.53) into equation (3.51), we obtain

$$\begin{aligned} < C_k^{(2)}(t) C_k^{*(0)} >= \frac{1}{4\omega_k^2} \sum_{k'k''} \int_0^t \{\frac{1}{\omega_{k''}^2} |C_k^{(0)}|^2 |C_{k'}^{(0)}|^2 \int_0^t \bar{V}_{k''kk'*}(t'')dt'' + \\ \frac{1}{\omega_{k'}^2} |C_k^{(0)}|^2 |C_{k''}^{(0)}|^2 \int_0^t \bar{V}_{k'kk''*}(t')dt'\} \bar{V}_{kk'k''}(t)dt. \end{aligned} \tag{3.54}$$

The derivation of $< C_k^{(0)}(t)C_k^{*(2)} >$ in equation (3.46) is similar to the derivation of equation (3.54). We obtain

$$< C_k^{(0)}(t)C_k^{*(2)} >= \frac{1}{4\omega_k^2}\sum_{k'k''}\int_0^t \{\frac{1}{\omega_{k''}^2}|C_k^{(0)}|^2|C_{k'}^{(0)}|^2\int_0^t \bar{V}^*_{k''kk'*}(t'')dt'' +$$
$$\frac{1}{\omega_{k'}^2}|C_k^{(0)}|^2|C_{k''}^{(0)}|^2\int_0^t \bar{V}^*_{k'kk''*}(t')dt'\}\bar{V}^*_{kk'k''}(t)dt. \tag{3.55}$$

Consider the integral

$$I = \left|\int_{t_0}^t V_{kk'k''}(t')dt'\right|^2 = |V_{kk'k''}|^2 \times \left|\int_{t_0}^t e^{-i(\omega_k-\omega_{k'}-\omega_{k''})t'}dt'\right|^2 \tag{3.56}$$

Performing the elementary integral over t' in equation (3.56) and applying several trigonometric identities we obtain

$$I = |V_{kk'k''}|^2 4\frac{\sin^2[(\omega_k-\omega_{k'}-\omega_{k''})(t-t_0)/2]}{(\omega_k-\omega_{k'}-\omega_{k''})^2}. \tag{3.57}$$

Equation (3.56) may be reduced further in in the limit of large t by application of the identity

$$4\frac{\sin^2[(\omega_k-\omega_{k'}-\omega_{k''})(t-t_0)/2]}{(\omega_k-\omega_{k'}-\omega_{k'})^2} \rightarrow 2\pi(t-t_0)\delta(\omega_k-\omega_{k'}-\omega_{k'}) \quad \text{for} \quad t\rightarrow\infty \tag{3.58}$$

which yields

$$I = |V_{kk'k''}|^2 2\pi(t-t_0)\delta(\omega_k-\omega_{k'}-\omega_{k'}) \quad \text{for} \quad t\rightarrow\infty. \tag{3.59}$$

Symmetry arguments can be used to show that

$$\frac{V_{kk'k''}}{\omega_k} = \frac{V_{k'kk''*}}{\omega_{k'}} = \frac{V_{k''kk'*}}{\omega_{k''}}. \tag{3.60}$$

Using equations (3.59) and (3.60), and the identities

$$|C_k^{(0)}|^2 = \frac{2E_k^{(0)}}{\omega_k^2}, \quad |C_{k'}^{(0)}|^2 = \frac{2E_{k'}^{(0)}}{\omega_{k'}^2}, \quad |C_{k''}^{(0)}|^2 = \frac{2E_{k''}^{(0)}}{\omega_{k''}^2}, \tag{3.61}$$

the results in equations (3.50), (3.54), and (3.55) can be reduced to the forms

$$< C_k^{(1)}(t)C_k^{*(1)}(t) >= \frac{4\pi}{\omega_k^3}\sum_{k'k''}\left[\frac{|V_{kk'k''}|^2}{(\omega_k\omega_{k'}\omega_{k''})^2}\right]$$
$$\times\omega_k E_{k'}^{(0)}E_{k''}^{(0)}(t-t_0)\delta(\omega_k-\omega_{k'}-\omega_{k''}), \tag{3.62}$$

$$< C_k^{(2)}(t) C_k^{*(0)} >= \frac{2\pi}{\omega_k^3} \sum_{k'k''} \left[\frac{|V_{kk'k''}|^2}{(\omega_k \omega_{k'} \omega_{k''})^2} \right]$$
$$\times \left[\omega_{k''} E_k^{(0)} E_{k'}^{(0)} + \omega_{k'} E_k^{(0)} E_{k''}^{(0)} \right] (t - t_0) \delta(\omega_k - \omega_{k'} - \omega_{k''}), \tag{3.63}$$
$$< C_k^{(0)}(t) C_k^{*(2)} >= \frac{2\pi}{\omega_k^3} \sum_{k'k''} \left[\frac{|V_{kk'k''}|^2}{(\omega_k \omega_{k'} \omega_{k''})^2} \right]$$
$$\times \left[\omega_{k''} E_k^{(0)} E_{k'}^{(0)} + \omega_{k'} E_k^{(0)} E_{k''}^{(0)} \right] (t - t_0) \delta(\omega_k - \omega_{k'} - \omega_{k''}) \tag{3.64}$$

where we have taken the limit $t \to \infty$. Substituting the right hand side of equation (3.46) into equation (3.32), using the above expressions for the expectation values, dividing the resulting expression by $(t - t_0)$, and taking the limit of $t \to \infty$, we obtain finally the kinetic equation

$$\frac{\partial}{\partial t} < E_k(t) >= \frac{2\pi}{\omega_k} \sum_{k'k''} \frac{|V_{kk'k''}|^2}{(\omega_k \omega_{k'} \omega_{k''})^2}$$
$$\times \left\{ \omega_k E_{k'}^{(0)} E_{k''}^{(0)} + \omega_{k'} E_k^{(0)} E_{k''}^{(0)} + \omega_{k''} E_k^{(0)} E_{k'}^{(0)} \right\} \delta(\omega_k - \omega_{k'} - \omega_{k''}). \tag{3.65}$$

More explicitly, the kinetic equation for the rate of change of energy for the modes $(k = n, l, -l \leq m \leq l)$ can be written

$$\frac{\partial}{\partial t} \sum_{m=-l}^{l} < E_{nlm}(t) >= \sum_{m=-l}^{l} \frac{2\pi}{\omega_{nl}^m} \sum_{n'} \sum_{n''} \sum_{l'} \sum_{l''} \sum_{m} \sum_{m'} \frac{|V^r_{nl,n'l',n''l''}|^2}{(\omega_{nl}^m \omega_{n'l'}^{m'} \omega_{n''l''}^{m''})^2}$$
$$\begin{pmatrix} l & l' & l'' \\ -m & m' & m'' \end{pmatrix}^2 \delta(\omega_{nl}^m - \omega_{n'l'}^{m'} - \omega_{n''l''}^{m''})$$
$$\left\{ \omega_{nl}^m E^{(0)}_{n'l'm'} E^{(0)}_{n''l''m''} + \omega_{n'l'}^{m'} E^{(0)}_{nlm} E^{(0)}_{n''l''m''} + \omega_{n''l''}^{m''} E^{(0)}_{nlm} E^{(0)}_{n'l'm'} \right\}. \tag{3.66}$$

where we have used equation (3.35).

For a spherically symmetric Sun we have the simplifications

$$\omega_{nl}^m = \omega_{nl}, \quad \omega_{n'l'}^{m'} = \omega_{n'l'}, \quad \omega_{n''l''}^{m''} = \omega_{n''l''} \tag{3.67}$$
$$E_{nlm}^{(0)} = \frac{E_{nl}^{(0)}}{2l+1}, \quad E^{(0)}_{n'l'm'} = \frac{E^{(0)}_{n'l'}}{2l'+1}, \quad E^{(0)}_{n''l''m''} = \frac{E^{(0)}_{n''l''}}{2l''+1}, \tag{3.68}$$

so that the left hand side of equation (3.66) becomes

$$\frac{\partial}{\partial t} \sum_{m=-l}^{l} < E_{nlm}(t) >= \frac{\partial}{\partial t} < E_{nl}(t) > . \tag{3.69}$$

Further, the azimuthal quantum number dependence on the right hand side of equation (3.66) separates and may be written

$$\sum_{m}\sum_{m'}\sum_{m''}\begin{pmatrix} l & l' & l'' \\ -m & m' & m'' \end{pmatrix}\begin{pmatrix} l & l' & l'' \\ -m & m' & m'' \end{pmatrix}. \tag{3.70}$$

This summation may be vastly simplified by application of the orthogonality property of the Wigner 3-j symbols from equation (3.7.8) of Edmonds (1960). Rewriting that equation in terms of our notation, we obtain

$$\sum_{m'}\sum_{m''}\begin{pmatrix} l & l' & l'' \\ -m & m' & m'' \end{pmatrix}\begin{pmatrix} l''' & l' & l'' \\ -m''' & m' & m'' \end{pmatrix} = \frac{\delta_{ll'''}\delta_{mm'''}\delta(ll'l'')}{2l+1}. \tag{3.71}$$

where $\delta(ll'l'') = 1$ if the three harmonic degrees l, l', and l'', satisfy the triangle inequalities given in equation (3.36) and is zero otherwise. Using this result to simplify equation (3.70), we obtain

$$\sum_{m}\sum_{m'}\sum_{m''}\begin{pmatrix} l & l' & l'' \\ -m & m' & m'' \end{pmatrix}\begin{pmatrix} l & l' & l'' \\ -m & m' & m'' \end{pmatrix} = \sum_{m=-l}^{l}\frac{1}{2l+1} = 1. \tag{3.72}$$

Using equations (3.68), (3.69), and (3.72), the kinetic equation in equation (3.66) can be written

$$\frac{\partial}{\partial t} < E_{nl}(t) >= \frac{1}{2l+1}\frac{2\pi}{\omega_{nl}}\sum_{n'}\sum_{n''}\sum_{l'}\sum_{l''}\frac{|V^{r}_{nl,n'l',n''l''}|^2}{(\omega_{nl}\omega_{n'l'}\omega_{n''l''})^2}\delta(\omega_{nl}-\omega_{n'l'}-\omega_{n''l''})$$
$$\times\left\{\omega_{nl}g(l',l'')E^{(0)}_{n'l'}E^{(0)}_{n''l''}+\omega_{n'l'}g(l,l'')E^{(0)}_{nl}E^{(0)}_{n''l''}+\omega_{n''l''}g(l,l')E^{(0)}_{nl}E^{(0)}_{n'l'}\right\} \tag{3.73}$$

where the $g(j_1, j_2)$ are weight functions are analogous to statistical weights and are given by

$$g(j_1, j_2) = \frac{1}{2j_1+1} * \frac{1}{2j_2+1}. \tag{3.74}$$

c) Determination of the Frequency Shift

We show in this section that three mode coupling can shift the frequency of a given mode. A differential equation governing the time rate of the change of the phase of a mode due to nonlinear interactions with other modes can be derived by

combining the dynamical equation and kinetic equation. The part of the phase that varies linearly in time is associated with the frequency shift.

The amplitude coefficient $C_k(t)$ can be written

$$C_k(t) = |C_k(t)| \exp^{i\phi_k(t)} \tag{3.75}$$

where

$$\phi_k(t) = \phi_k^{(0)} + \phi_k^{(1)}(t) + \phi_k^{(2)}(t). \tag{3.76}$$

The phase of the mode in the absence of nonlinear interactions is given by $\phi_k^{(0)}$ and the superscripts (1) and (2) in equation (3.76) denote the order of the dependence on the nonlinear interaction coefficient $V_{kk'k''}$. The phase is real-valued and therefore $\phi_k = \phi_k^*$. With the aid of equation (3.75), the dynamical equation as given by equation (3.34) can be written

$$|\dot{C}_k| e^{i\phi_k(t)} + |C_k| i\dot{\phi}_k(t) e^{i\phi_k(t)} = \frac{1}{2\omega_k^2} \sum_{k'k''} V_{kk'k''} C_{k'}(t) C_{k''}(t) \exp^{-i(\omega_k - \omega_{k'} - \omega_{k''})t} \tag{3.77}$$

From the kinetic equation (see eq. 3.33), we have

$$|\dot{C}_k(t)| = \frac{\dot{E}_k}{\omega_k^2 |C_k(t)|}. \tag{3.78}$$

Substituting equation (3.78) into equation (3.77) and solving for $\dot{\phi}_k(t)$, we obtain

$$\dot{\phi}_k(t) = \frac{1}{\omega_k^2 |C_k(t)|} \left\{ \frac{i\dot{E}_k}{|C_k(t)|} + \frac{1}{2} \sum_{k'k''} Im(V_{kk'k''}) C_{k'}(t) C_{k''}(t) e^{-i(\Delta\omega + \phi_k(t))} \right\} \tag{3.79}$$

where $\Delta\omega = \omega_k - \omega_{k'} - \omega_{k''}$. In deriving equation (3.79) we used the result from §IV that $V_{kk'k''}$ is purely imaginary *i.e.*, $V_{kk'k''} = iIm(V_{kk'k''})$. Since the phase $\phi_k(t)$ is real, the imaginary components of equation (3.79) must sum to zero. Using this fact, we can obtain the expression for $\dot{\phi}_k(t)$ by taking the real part of the right hand side of equation (3.79):

$$\dot{\phi}_k(t) = \frac{1}{2\omega_k^2 |C_k(t)|} \sum_{k'k''} Im(V_{kk'k''}) \; \mathcal{R}e \left\{ C_{k'}(t) C_{k''}(t) e^{-i(\Delta\omega t + \phi_k(t))} \right\}. \tag{3.80}$$

Retaining terms to first order in the nonlinear interaction coefficient on the right hand of equation (3.80), and using equation (3.61), we obtain the first order expression for

$\dot{\phi}_k(t)$:

$$\dot{\phi}_k^{(1)}(t) = \sum_{k'k''} \frac{Im(V_{kk'k''})}{\omega_k\omega_{k'}\omega_{k''}} \sqrt{\frac{E_{k'}^{(0)}E_{k''}^{(0)}}{2E_k^{(0)}}} cos(\Delta\omega t + \phi_k^{(0)} - \phi_{k'}^{(0)} - \phi_{k''}^{(0)}). \tag{3.81}$$

Equation (3.81) can be integrated to yield

$$\begin{aligned}\phi_k^{(1)}(t) &= \sum_{k'k''} \frac{1}{\Delta\omega} \frac{Im(V_{kk'k''})}{\omega_k\omega_{k'}\omega_{k''}} \sqrt{\frac{E_{k'}^{(0)}E_{k''}^{(0)}}{2E_k^{(0)}}} \\ &\times [sin(\Delta\omega t + \phi_k^{(0)} - \phi_{k'}^{(0)} - \phi_{k''}^{(0)}) - sin(\phi_k^{(0)} - \phi_{k'}^{(0)} - \phi_{k''}^{(0)})].\end{aligned} \tag{3.82}$$

We note that $< \dot{\phi}_k^{(1)}(t) >$, the expectation value over time of $\dot{\phi}_k^{(1)}(t)$ in equation (3.81) vanishes. Therefore, to calculate the frequency shift, we must retain terms to second order on the right hand side of equation (3.80):

$$\begin{aligned}\dot{\phi}_k^{(2)}(t) &= \frac{1}{2\omega_k^2} \frac{1}{|C_k^{(0)}|} \sum_{k'k''} Im(V_{kk'k''}) \\ &\times \mathcal{R}e \left\{ [C_{k'}^{(0)}C_{k''}^{(1)}(t) + C_{k'}^{(1)}(t)C_{k''}^{(0)}] e^{-i(\Delta\omega t + \phi_k^{(0)})} \right\}\end{aligned} \tag{3.83}$$

where $\Delta\omega = \omega_k - \omega_{k'} - \omega_{k''}$. We can perform the integrations in equations (3.41) and (3.42) to obtain

$$C_{k'}^{(1)}(t) = \frac{1}{2\omega_{k'}^2} \sum_{r'r''} C_{r'}^{(0)}C_{r''}^{*(0)}V_{k'r'r''*} \left[\frac{e^{i(\omega_{r'} - \omega_{r''} - \omega_{k'})t} - 1}{i(\omega_{r'} - \omega_{r''} - \omega_{k'})} \right], \tag{3.84}$$

$$C_{k''}^{(1)}(t) = \frac{1}{2\omega_{k''}^2} \sum_{s's''} C_{s'}^{(0)}C_{s''}^{*(0)}V_{k''s's''*} \left[\frac{e^{i(\omega_{s'} - \omega_{s''} - \omega_{k''})t} - 1}{i(\omega_{s'} - \omega_{s''} - \omega_{k''})} \right]. \tag{3.85}$$

Substituting equations (3.84) and (3.85) into equation (3.83), and taking the temporal expectation value of the resulting quantity, we obtain

$$\begin{aligned}< \dot{\phi}_k^{(2)}(t) > &= \frac{1}{2\omega_k^2} \frac{1}{|C_k^{(0)}|} \sum_{k'k''} Im(V_{kk'k''}) \times \mathcal{R}e \{ \\ &C_{k'}^{(0)} \frac{1}{2\omega_{k''}^2} \sum_{s's''} C_{s'}^{(0)}C_{s''}^{*(0)} Im(V_{k''s's''*}) \frac{< e^{i[(\omega_{s'} - \omega_k) + (\omega_{k'} - \omega_{s''})]t} >}{\omega_{s'} - \omega_{s''} - \omega_{k''}} e^{-i\phi_k^{(0)}} + \\ &C_{k''}^{(0)} \frac{1}{2\omega_{k'}^2} \sum_{r'r''} C_{r'}^{(0)}C_{r''}^{*(0)} Im(V_{k'r'r''*}) \frac{< e^{i[(\omega_{r'} - \omega_k) + (\omega_{k''} - \omega_{r''})]t} >}{\omega_{r'} - \omega_{r''} - \omega_{k''}} e^{-i\phi_k^{(0)}} \}\end{aligned} \tag{3.86}$$

where the temporal expectation values of several of the terms have vanished. Noting that

$$< e^{i[(\omega_{r'} - \omega_k) + (\omega_{k''} - \omega_{r''})]t} > = \delta_{r'k}\delta_{r''k''}, \tag{3.87}$$

$$< e^{i[(\omega_{s'} - \omega_k) + (\omega_{k'} - \omega_{s''})]t} > = \delta_{s'k}\delta_{k's''} \tag{3.88}$$

we obtain

$$< \dot{\phi}_k^{(2)}(t) >= \frac{1}{2\omega_k^2}\frac{1}{|C_k^{(0)}|}\sum_{k'k''} Im(V_{kk'k''}) \times$$
$$\mathcal{R}e\ \{C_{k'}^{(0)}\frac{1}{2\omega_{k''}^2}C_k^{(0)}C_{k'}^{*(0)}\frac{Im(V_{k''kk'^*})}{(\omega_k-\omega_{k'}-\omega_{k''})}e^{-i\phi_k^{(0)}} +$$
$$C_{k''}^{(0)}\frac{1}{2\omega_{k'}^2}C_k^{(0)}C_{k''}^{*(0)}\frac{Im(V_{k'kk''^*})}{(\omega_k-\omega_{k''}-\omega_{k'})}e^{-i\phi_k^{(0)}}\}. \tag{3.89}$$

This result can be reduced to the form

$$< \dot{\phi}_k^{(2)}(t) > = \frac{1}{2\omega_k^2}\sum_{k'k''}\frac{Im(V_{kk'k''})}{(\omega_k-\omega_{k'}-\omega_{k''})}$$
$$\times \left[\frac{|C_{k'}^{(0)}|^2}{2\omega_{k''}^2}Im(V_{k''kk'^*}) + \frac{|C_{k''}^{(0)}|^2}{2\omega_{k'}^2}Im(V_{k'kk''^*})\right]. \tag{3.90}$$

Using the previously derived results $|C_{k'}^{(0)}|^2 = 2E_{k'}^{(0)}\omega_{k'}^{-2}$, $|C_{k''}^{(0)}|^2 = 2E_{k''}^{(0)}\omega_{k''}^{-2}$, $V_{k'kk''^*} = \omega_{k'}\omega_k^{-1}V_{kk'k''}$, and $V_{k''kk'^*} = \omega_{k''}\omega_k^{-1}V_{kk'k''}$, the expression in equation (3.90) simplifies to the form

$$< \dot{\phi}_k^{(2)}(t) >= \frac{1}{2\omega_k^3}\sum_{k'k''}\frac{|V_{kk'k''}|^2}{(\omega_k-\omega_{k'}-\omega_{k''})}\left[\frac{1}{(\omega_{k''}\omega_{k'})^2}\right]\left[\omega_{k''}E_{k'}^{(0)}+\omega_{k'}E_{k''}^{(0)}\right] \tag{3.91}$$

We can use equations (3.35), (3.67), and (3.68) to rewrite this result in the form

$$< \dot{\phi}_{nl}^{(2)}(t) > = \frac{1}{2\omega_{nl}^3}\sum_{n'l'm'n''l''m''}\frac{|V_{nl,n'l',n''l''}^r|^2}{(\omega_{nl}-\omega_{n'l'}-\omega_{n''l''})}\begin{pmatrix} l & l' & l'' \\ -m & m' & m'' \end{pmatrix}^2$$
$$\times \left[\frac{1}{(\omega_{n''l''}\omega_{n'l'})^2}\right]\left[\omega_{n''l''}\frac{E_{n'l'}^{(0)}}{2l'+1}+\omega_{n'l'}\frac{E_{n''l''}^{(0)}}{2l''+1}\right]. \tag{3.92}$$

The summation over the azimuthal orders can be elimated by application of the orthogonality relation for 3-j symbols in equation (3.71), we obtain

$$< \dot{\phi}_{nl}^{(2)}(t) > = \frac{1}{2\omega_{nl}^3}\sum_{n'l',n''l''}\frac{|V_{nl,n'l',n''l''}^r|^2}{(\omega_{nl}-\omega_{n'l'}-\omega_{n''l''})}$$
$$\times \left[\frac{1}{2l+1}\right]\left[\frac{1}{(\omega_{n''l''}\omega_{n'l'})^2}\right]\left[\omega_{n''l''}\frac{E_{n'l'}^{(0)}}{2l'+1}+\omega_{n'l'}\frac{E_{n''l''}^{(0)}}{2l''+1}\right]. \tag{3.93}$$

Equation (3.93) is our final expression for the frequency shift of mode (n,l). It should be understood in the following sense. The resonance function of a mode in

the time domain has the dependence $exp[i(\omega_k t + \phi_k)]$. The phase ϕ_k can be expanded in a Taylor series; the term which varies linearly in time leads to the dependence $exp[i(\omega_k + \dot{\phi}_k)t]$ and this yields the frequency shift.

IV. DERIVATION OF THE NONLINEAR INTERACTION COEFFICIENT

a) Equations of Motion of the Quiescent State

The mass continuity equation, the momentum equation, the conservation of energy equation, and Poisson's equation are given respectively by

$$\frac{\partial \rho}{\partial t} + \nabla \cdot (\rho \mathbf{v}) = 0 \tag{3.94}$$

$$\frac{D\mathbf{v}}{Dt} = -\frac{\nabla P}{\rho} - \nabla \Phi \tag{3.95}$$

$$\rho T \frac{DS}{Dt} = \text{entropy production terms} \tag{3.96}$$

$$\nabla^2 \phi = 4\pi G \rho, \tag{3.97}$$

where P, T, ρ, ϕ, S, and $\mathbf{v}$ are respectivley, the pressure, temperature, density, gravitational potential, specific entropy, and velocity. The material time derivative appearing in equations (3.95) and (3.96) is given by

$$\frac{D}{Dt} = \frac{\partial}{\partial t} + \mathbf{v} \cdot \nabla \tag{3.98}$$

Equations (3.94)- (3.97) must be supplemented by an equation of state which is given by

$$P = P(S, \rho) \tag{3.99}$$

and for our purposes it need not take an explicit form. We now assume that the system is adiabatic so that entropy is conserved along streamlines and the equation (3.96) drops out.

b) The Perturbed Equation of Motion

To discover how the system described by (3.94)- (3.97) responds to a seismic disturbance we need to perturb the momentum equation (3.95), which in turn requires

perturbations in ρ, ϕ, and P. These are obtained by perturbing equations (3.94), (3.97), and (3.99) respectively.

We adopt the perturbation expansions

$$\begin{aligned}\rho(\mathbf{r},t) &= \rho_o(r) + \delta_1\rho(\mathbf{r},t) + \delta_2\rho(\mathbf{r},t)\\ P(\mathbf{r},t) &= P_o(r) + \delta_1 P(\mathbf{r},t) + \delta_2 P(\mathbf{r},t)\\ \phi(\mathbf{r},t) &= \phi_o(r) + \delta_1\phi(\mathbf{r},t) + \delta_2\phi(\mathbf{r},t)\end{aligned} \tag{3.100}$$

where the notation $\delta_1 Q$ and $\delta_2 Q$ denotes, respectively, perturbations of the quantity Q to first and second order in the displacement field of the disturbance.

In the linearized theory, the displacement eigenfunction can be written

$$\mathbf{s}(\mathbf{r},t) = \mathbf{s}(\mathbf{r})e^{i\omega t} \tag{3.101}$$

The momentum equation to second order in $\mathbf{s}$ can be written:

$$\frac{\partial}{\partial t}\mathbf{v} + \mathbf{v}\cdot\nabla\mathbf{v} + \left[\frac{1}{\rho_o} + \delta_1\left(\frac{1}{\rho}\right) + \delta_2\left(\frac{1}{\rho}\right)\right]\nabla[P_o + \delta_1 P + \delta_2 P] + \nabla[\phi_o + \delta_1\phi + \delta_2\phi] = 0. \tag{3.102}$$

Taking the time derivative $\frac{\partial}{\partial t}$ of this equation and separating the first and second order contributions, we obtain

$$\partial_t^2\mathbf{v} + \mathcal{L}\mathbf{v} + \mathcal{N}(\mathbf{s},\mathbf{v}) = 0 \tag{3.103}$$

where

$$\mathcal{L}(\mathbf{v}) = \frac{1}{\rho_o(r)}\nabla\frac{\partial\delta_1 P}{\partial t} - \frac{\nabla P_0}{\rho_o^2(r)}\frac{\partial\delta_1\rho}{\partial t} + \nabla\frac{\partial\delta_1\phi}{\partial t} \tag{3.104}$$

and

$$\mathcal{N}(\mathbf{s},\mathbf{v}) = \frac{\partial}{\partial t}[\mathbf{v}\cdot\nabla\mathbf{v}] + \frac{1}{\rho_o(r)}\nabla\frac{\partial\delta_2 P}{\partial t} - \frac{\nabla\delta_1 P}{\rho_o^2(r)}\frac{\partial\delta_1\rho}{\partial t} - \frac{\nabla P}{\rho_o^2(r)}\frac{\partial\delta_2\rho}{\partial t} - \frac{\delta_1\rho}{\rho_o^2}\nabla\frac{\partial\delta_1 P}{\partial t} + \nabla\frac{\partial\delta_2\phi}{\partial t}. \tag{3.105}$$

c) Calculation of First and Second Order quantities

To determine the Eulerian perturbations to ρ and P, it is convenient to use the relationship

$$\Delta = \delta + \mathbf{s}\cdot\nabla \tag{3.106}$$

where Δ and δ are, respectively, the Lagrangian and Eulerian change operators. It is easy to show that

$$\Delta\rho = -\rho\nabla\cdot\mathbf{s} \tag{3.107}$$

$$\Delta P = -P\Gamma_1\nabla\cdot\mathbf{s} \tag{3.108}$$

where Γ_1 is the first adiabatic exponent. Equation (3.108) follows from the equation of state and the assumption that the modes are adiabatic. The Eulerian perturbation of ϕ is the solution of the perturbed Poisson equation

$$\nabla^2\delta\phi = 4\pi G\delta\rho. \tag{3.109}$$

and is given by

$$\delta\phi = -G\int\frac{\delta\rho(\mathbf{r}')}{|\mathbf{r}-\mathbf{r}'|}d^3\mathbf{r}' = G\int\frac{\rho(\mathbf{r}')\mathbf{s}(\mathbf{r}')}{|\mathbf{r}-\mathbf{r}'|}\cdot d\mathbf{S} - G\int\rho(r')\mathbf{s}(\mathbf{r}')\cdot\nabla'\frac{1}{|\mathbf{r}-\mathbf{r}'|}d^3\mathbf{r}' \tag{3.110}$$

where we have used the divergence theorem. Combining equation (3.106) with equations (3.107) and (3.108), we obtain the first order Eulerian perturbations to ρ and P:

$$\delta_1\rho = -\rho\nabla\cdot\mathbf{s} - \mathbf{s}\cdot\nabla\rho, \tag{3.111}$$

$$\delta_1 P = -P\Gamma_1\nabla\cdot\mathbf{s} - \mathbf{s}\cdot\nabla P. \tag{3.112}$$

We may use the method of successive approximations to show that

$$\frac{\partial\delta_2\rho}{\partial t} = \nabla\cdot(\nabla\cdot(\rho_o\mathbf{s})\mathbf{v}) \tag{3.113}$$

From equation (3.112) we may deduce

$$\delta_2 P = -\delta_1(P\Gamma_1)\nabla\cdot\mathbf{s} - \mathbf{s}\cdot\nabla\delta_1 P \tag{3.114}$$

where

$$\delta_1(P\Gamma_1) = P\delta_1\Gamma_1 + \Gamma_1\delta_1 P. \tag{3.115}$$

To derive $\delta_1\Gamma_1$ we take $\Gamma_1 = \Gamma_1(\rho, T)$. We have chosen ρ and T as the independent variables since derivatives of Γ_1 with respect to ρ and T are available from Dappen (1988). The first variation of Γ_1 is given by

$$\delta_1(\Gamma_1) = \left(\frac{\partial\Gamma_1}{\partial\rho}\right)_T\delta_1\rho + \left(\frac{\partial\Gamma_1}{\partial T}\right)_\rho\delta_1 T. \tag{3.116}$$

To determine $\delta_1 T$ we use

$$\Delta u = \frac{P}{\rho^2}\Delta\rho + T\Delta S = \frac{P}{\rho^2}\Delta\rho = c_v \Delta T \tag{3.117}$$

where u is the internal energy of the gas per unit mass, c_v is the specific heat at constant volume, and where we have assumed the oscillations are adiabatic. Substituting equation (3.107) into equation (3.117), and solving for ΔT, we obtain

$$\Delta T = -\frac{P\nabla\cdot\mathbf{s}}{\rho c_v}. \tag{3.118}$$

The lagrangian change in temperature is given by

$$\Delta T = \delta_1 T + \mathbf{s}\cdot\nabla T = \delta_1 T + s_r \frac{dT}{dr} = \delta_1 T - \frac{T s_r}{H_p}\frac{dlnT}{dlnP} \tag{3.119}$$

where $H_p = P/(\rho g)$ is the pressure scale height. Combining equations (3.118) and (3.119), we obtain

$$\delta_1 T = -\frac{P\nabla\cdot\mathbf{s}}{\rho c_v} + \frac{T s_r}{H_p}\frac{dlnT}{dlnP} \tag{3.120}$$

so that equation (3.116) becomes

$$\delta_1(\Gamma_1) = P\left[\left(\frac{\partial\Gamma_1}{\partial\rho}\right)_T \delta_1\rho + \left(\frac{\partial\Gamma_1}{\partial T}\right)_\rho \left\{-\frac{P\nabla\cdot\mathbf{s}}{\rho c_v} + H_p T s_r \frac{dlnT}{dlnP}\right\}\right]. \tag{3.121}$$

The calculation of $V_{kk'k''}$ requires the explicit form of various quantities in terms of the radial and angular eigenfunctions. These can be calculated using the formalism described in Appendix 2B The angular functions can be reduced to functions of the generalized spherical harmonics Y_l^{Nm}, where N is the generalized index (see Phinney and Burridge 1973). The mode displacement is given by

$$\mathbf{s}_k = s_r^{(k)}(r)\gamma_l Y_l^{0m}\hat{\mathbf{r}} + s_H^{(k)}(r)\frac{\gamma_l\Omega_0^l}{\sqrt{2}}(Y_l^{-1m} - Y_l^{1m})\hat{\theta} - i s_H^{(k)}(r)\frac{\gamma_l\Omega_0^l}{\sqrt{2}}(Y_l^{-1m} + Y_l^{1m})\hat{\phi} \tag{3.122}$$

where

$$s_r^{(k)}(r) = U, \text{ and } s_H^{(k)}(r) = V. \tag{3.123}$$

The divergence of mode k is given by

$$\nabla\cdot\mathbf{s}_k = div^{(k)}(r)\gamma_l Y_l^{0m} \tag{3.124}$$

where

$$div^{(k)}(r) = \dot{U} + F, \tag{3.125}$$

$$F(r) = \frac{2U - l(l+1)V}{r}, \tag{3.126}$$

$$\gamma_l = \left(\frac{2l+1}{4\pi}\right)^{1/2}. \tag{3.127}$$

The first order perturbations to the thermodynamic variables P, ρ, and Γ_1 are given by

$$\delta_1 P(\mathbf{s}_k) = \delta_1 P^{(k)}(r)\gamma_l Y_l^{0m}, \tag{3.128}$$

$$\delta_1 \rho(\mathbf{s}_k) = \delta_1 \rho^{(k)}(r)\gamma_l Y_l^{0m}, \tag{3.129}$$

$$\delta_1 \Gamma_1 = \delta_1 \Gamma_1^{(k)}(r)\gamma_l Y_l^{0m}. \tag{3.130}$$

where

$$\delta_1 P^{(k)}(r) = [-P\Gamma_1(\dot{U} + F) + U\rho g], \tag{3.131}$$

$$\delta_1 \rho^{(k)}(r) = -[\rho(\dot{U} + F) + U\dot{\rho}], \tag{3.132}$$

$$\begin{aligned}\delta_1 \Gamma_1^{(k)}(r) &= [\left(-\frac{\partial \Gamma_1}{\partial \rho}\right)_T (\rho(\dot{U} + F) + U\dot{\rho}) \\ &+ \left(\frac{\partial \Gamma_1}{\partial T}\right)_\rho (H_p T U \frac{dlnT}{dlnP} - \frac{P}{\rho c_v}(\dot{U} + F))].\end{aligned} \tag{3.133}$$

Using the linearized equation of motion, we can show that the gradient of $\delta_1 P$ is given by

$$\begin{aligned}\nabla\delta_1 P &= (\nabla\delta_1 P)_r^{(k)}(r)\gamma_l Y_l^{0m}\hat{\mathbf{r}} + (\nabla\delta_1 P)_H^{(k)}\frac{\gamma_l \Omega_0^l}{\sqrt{2}}(Y_l^{-1m} - Y_l^{1m})\hat{\theta} \\ &- i(\nabla\delta_1 P)_H^{(k)}\frac{\gamma_l \Omega_0^l}{\sqrt{2}}(Y_l^{-1m} + Y_l^{1m})\hat{\phi}\end{aligned} \tag{3.134}$$

where

$$(\nabla\delta_1 P)_r^{(k)}(r) = [\rho U\omega_k^2 + \rho g(\dot{U} + F) + gU\dot{\rho} - \rho\dot{\phi}_1] \tag{3.135}$$

$$(\nabla\delta_1 P)_H^{(k)}(r) = [\rho\omega_k^2 V - r^{-1}\rho\phi_1] \tag{3.136}$$

The gradient of the perturbed gravitational potential ϕ_1 is given by

$$\nabla\phi_1(k) = \dot{\phi}_1\gamma_l Y_l^{0m}\hat{\mathbf{r}} + r^{-1}\phi_1\frac{\gamma_l\Omega_0^l}{\sqrt{2}}(Y_l^{-1m} - Y_l^{1m})\hat{\theta} - ir^{-1}\phi_1\frac{\gamma_l\Omega_0^l}{\sqrt{2}}(Y_l^{-1m} + Y_l^{1m})\hat{\phi}. \tag{3.137}$$

e) The Nonlinear Interaction Coefficient

The nonlinear interaction coefficient $V_{kk'k''}$ is a sum of six terms given by

$$V_{kk'k''} = \sum_{i=j}^{6} V^{(j)}_{kk'k''} \tag{3.138}$$

where

$$\begin{aligned}
V^{(1)}_{kk'k''} &= \int_0^{R_\odot} \rho_o(r) \frac{\partial}{\partial t} [\mathbf{v}_{k'} \cdot \nabla \mathbf{v}_{k''} + \mathbf{v}_{k''} \cdot \nabla \mathbf{v}_{k'}] \cdot \mathbf{s}^*_k d^3r \\
&= -i(\omega^2_{k'} \omega_{k''} + \omega^2_{k''} \omega_{k'}) \int_0^{R_\odot} \rho_o(r) \{\mathbf{s}_{k'} \cdot \nabla \mathbf{s}_{k''} + \mathbf{s}_{k''} \cdot \nabla \mathbf{s}_{k'}\} \cdot \mathbf{s}^*_k d^3r \qquad (3.139) \\
V^{(2)}_{kk'k''} &= \int_0^{R_\odot} \mathbf{s}^*_k \cdot \nabla \left[\frac{\partial}{\partial t} \{\delta_2 P(\mathbf{s}_{k'}, \mathbf{s}_{k''}) + \delta_2 P(\mathbf{s}_{k''}, \mathbf{s}_{k'})\} \right] d^3r \\
&= -i(\omega_{k'} + \omega_{k''}) \int_0^{R_\odot} \nabla \cdot \mathbf{s}^*_k \left[\delta_2 P(\mathbf{s}_{k'}, \mathbf{s}_{k''}) + \delta_2 P(\mathbf{s}_{k''}, \mathbf{s}_{k'})\right] d^3r \qquad (3.140) \\
V^{(3)}_{kk'k''} &= -i \int_0^{R_\odot} \frac{1}{\rho_o(r)} \mathbf{s}^*_k \cdot \{\omega_{k''} \nabla \delta_1 P(\mathbf{s}_{k'}) \delta_1 \rho(\mathbf{s}_{k''}) \\
&+ \omega_{k'} \nabla \delta_1 P(\mathbf{s}_{k''}) \delta_1 \rho(\mathbf{s}_{k'})\} d^3r \qquad (3.141) \\
V^{(4)}_{kk'k''} &= \int_0^{R_\odot} g_0 s^{(r)*}_k [i\omega_{k''} \nabla \cdot (\nabla \cdot (\rho_0 \mathbf{s}_{k'}) \mathbf{s}_{k''}) + i\omega_{k'} \nabla \cdot (\nabla \cdot (\rho_0 \mathbf{s}_{k''}) \mathbf{s}_{k'})] d^3r \\
&= \int_0^{R_\odot} i\omega_{k''} \delta_1 \rho(\mathbf{s}_{k'}) [g_0 \mathbf{s}_{k''} \cdot \nabla s^{(r)*}_k + s^{(r)*}_k s^{(r)}_{k''} (4\pi G\rho - \frac{2g}{r}) d^3r \\
&+ \int_0^{R_\odot} i\omega_{k'} \delta_1 \rho(\mathbf{s}_{k''}) [g_0 \mathbf{s}_{k'} \cdot \nabla s^{(r)*}_k + s^{(r)*}_k s^{(r)}_{k'} (4\pi G\rho - \frac{2g}{r}) d^3r \qquad (3.142) \\
V^{(5)}_{kk'k''} &= -i \int_0^{R_\odot} \frac{1}{\rho_o} \mathbf{s}^*_k \cdot \{\omega_{k''} \delta_1 \rho(\mathbf{s}_{k'}) \nabla \delta_1 P(\mathbf{s}_{k''}) \\
&+ \omega_{k'} \delta_1 \rho(\mathbf{s}_{k''}) \nabla \delta_1 P(\mathbf{s}_{k'})\} \cdot \mathbf{s}^*_k d^3r \qquad (3.143) \\
V^{(6)}_{kk'k''} &= -i\omega_{k''} \int_0^{R_\odot} \nabla \cdot (\rho_0 \mathbf{s}_{k'}) \mathbf{s}_{k''} \cdot \nabla \delta_1 \phi^*_k d^3r \\
&- i\omega_{k'} \int_0^{R_\odot} \nabla \cdot (\rho_0 \mathbf{s}_{k''}) \mathbf{s}_{k'} \cdot \nabla \delta_1 \phi^*_k d^3r \qquad (3.144)
\end{aligned}$$

To calculate the six integrals contributing to the nonlienar interaction coefficient, we repeatedly applied the divergence theorem. In each instance we discarded the surface integrals resulting from such operations. We find that $V_{kk'k''}$ can be written in the form

$$V_{kk'k''} = \sum_{j=1}^{6} 4\pi \gamma_l \gamma_{l'} \gamma_{l''} (-1)^m \begin{pmatrix} l & l' & l'' \\ -m & m' & m'' \end{pmatrix} [K^{(j)}_{nl,n'l',n''l''} + K^{(j)}_{nl,n''l'',n'l'}]. \tag{3.145}$$

Comparing this with equation (3.35), we find that the reduced matrix element is given by

$$V^r_{nl,n'l',n''l''} = \sum_{j=1}^{6} 4\pi\gamma_l\gamma_{l'}\gamma_{l''}[K^{(j)}_{nl,n'l',n''l''} + K^{(j)}_{nl,n''l'',n'l'}]. \tag{3.146}$$

The terms $K^{(j)}_{nl,n'l',n''l''}$ and $K^{(j)}_{nl,n''l'',n'l'}$ in equation (3.145) are independent of the azimuthal orders of the modes, and are given by

$$\begin{aligned}
K^{(1)}_{nl,n'l',n''l''} &= -(\omega^2_{k'}\omega_{k''} + \omega^2_{k''}\omega_{k'})\{\int_0^{R_\odot} \rho_o(r)R^{(1)}(r)r^2dr \\
&+ \int_0^{R_\odot} \rho_o(r)H^{(1)}(r)rdr\}, \qquad (3.147)\\
K^{(2)}_{nl,n'l',n''l''} &= i(\omega_{k'} + \omega_{k''})\int_0^{R_\odot} div^{(k)}(r)div^{(k'')}(r)[P\delta_1\Gamma_1^{(k')}(r) \\
&+ \Gamma_1\delta_1P^{(k')}(r) + s_r^{(k'')}(\nabla\delta_1P)_r^{(k')}(r)]B^{(0)}_{ll'l''}r^2dr \\
&+ i(\omega_{k'} + \omega_{k''})\int_0^{R_\odot} div^{(k)}(r)s_H^{(k'')}(r)(\nabla\delta_1P)_H^{(k')}(r)B^{(1)+}_{ll'l''}r^2dr, \qquad (3.148)\\
K^{(3)}_{nl,n'l',n''l''} &= i\omega_k\int_0^{R_\odot}\{\delta_1\rho^{(k')}(r)s_H^{(k)}(r)(\nabla\delta_1P_H^{(k'')}(r)]B^{(1)+}_{ll'l''} \\
&- \delta_1\rho^{(k')}(r)s_r^{(k)}(r)s_H^{(k)}(r)\nabla\delta_1P_r^{(k'')}(r)B^{(0)+}_{ll'l''}\}r^2dr, \qquad (3.149)\\
K^{(4)}_{nl,n'l',n''l''} &= \int_0^{R_\odot}\{[\delta_1\rho^{(k')}(r)s_r^{(k)}(r)s_r^{(k'')}(r)(4\pi G\rho - 2gr^{-1}) \\
&+ \delta_1\rho^{(k')}(r)gs_r^{(k'')}(r)\dot{s}_r^{(k)}(r)]B^{+(0)}_{ll'l''} \\
&- \delta_1\rho^{(k')}(r)gr^{-1}s_H^{(k'')}(r)s_H^{(k)}(r)B^{+(1)}_{ll'l''}\}r^2dr, \qquad (3.150)\\
K^{(5)}_{nl,n'l',n''l''} &= \omega^{-1}_{k'}\omega_{k''}K^{(3)}_{kk'k''} \qquad (3.151)\\
K^{(6)}_{nl,n'l',n''l''} &= \int_0^{R_\odot}\{\delta_1\rho^{(k')}(r)\dot{\phi}_1^{(k)}(r)s_r^{(k'')}(r)B^{(0)+}_{ll'l''} \\
&- r^{-1}\delta_1\rho^{(k')}(r)s_H^{(k'')}(r)\phi_1^{(k)}(r)B^{(1)+}_{ll'l''}r^2dr, \qquad (3.152)
\end{aligned}$$

where

$$\begin{aligned}
R^{(1)}(r) &= U'U\dot{U}''B^{(0)+}_{l'l''l} + U'V\dot{V}''B^{(1)+}_{ll'l''}, \qquad (3.153)\\
H^{(1)}(r) &= [U''UV' - V''UV']B^{(1)+}_{l'll''} - \frac{VV'V''}{2r}[l(l+1) - l''(l''+1) - l'(l'+1)]B^{(1)+}_{ll'l''} \\
&+ \frac{VV'V''}{r}\Omega_0^{l''}\Omega_0^{l''}B^{(1)+}_{l'l''l} + [V'VU'' - V'VV'']\Omega_0^{l''}\Omega_0^{l''}B^{(1)+}_{l'l''l}, \qquad (3.154)
\end{aligned}$$

and it is understood that $\omega_k = \omega_{nl}$, $\omega_{k'} = \omega_{n'l'}$, and $\omega_{k''} = \omega_{n''l''}$. We have defined

$\Omega_0^l = (l(l+1)/2)^{1/2}$. The $B^{(N)\pm}_{l'l''l}$ coefficients are defined

$$B^{(N)\pm}_{l'l''l} = \frac{1}{2}(1 \pm (-1)^{(l'+l''+l)}) \left[\frac{(l'+N)!(l+N)!}{(l'-N)!(l-N)!}\right]^{\frac{1}{2}} (-1)^N \begin{pmatrix} l' & l'' & l \\ -N & 0 & N \end{pmatrix}. \quad (3.155)$$

A useful identity which the $B^{(1)\pm}_{l'l''l}$ coefficients satisfy is given by equation (A43) of Woodhouse (1980):

$$B^{(1)+}_{l'l''l} = \frac{1}{2}[l'(l'+1) + l(l+1) - l''(l''+1)]B^{(0)+}_{l'l''l}. \quad (3.156)$$

We can replace the $B^{(1)+}$ coefficients in $V_{kk'k''}$ with $B^{(0)+}$ by using equation (3.156). This represents a simplification since we then need only compute Wigner 3-j symbols with zeroes on the bottom row. An accurate and efficient asymptotic method for calculating such symbols is given in Appendix 3A. Should the need arise to use the dynamical equation rather than the kinetic equation, the more general form of the Wigner 3-j symbols must be calculated. An algorithm for this is given in Appendix 2C.

APPENDIX 3A

CALCULATION OF WIGNER 3-j SYMBOLS

The practical implementation of the theory described in this paper requires an efficient method to calculate the Wigner 3-j of the form

$$\begin{pmatrix} l & l' & l'' \\ 0 & 0 & 0 \end{pmatrix} \quad (3A.1)$$

which enters into the kinetic equation. It is possible to calculate this particular symbol by application of equation (3.7.17) in Edmonds (1960). He finds

$$\begin{pmatrix} l & l' & l'' \\ 0 & 0 & 0 \end{pmatrix} = (-1)^{L/2} \left[\frac{(L-2l)!(L-2l')!(L-2l'')!}{(L+1)!}\right]^{\frac{1}{2}} \frac{\left(\frac{L}{2}\right)!}{\left(\frac{L}{2}-l\right)!\left(\frac{L}{2}-l'\right)!\left(\frac{L}{2}-l''\right)!} \quad (3A.2)$$

for L even where $L = l + l' + l''$, and is zero otherwise. There are combinations of the harmonic degrees l, l', and l'' which could lead to large factorials which do not

conveniently cancel. In numerical calculations, this prescription, though exact, could lead to great computational expense.

There are several asymptotic approaches to evaluating equation (3A.1). Each method has restrictions on the range of harmonic degrees l, l', and l''. From Brussaard and Tolhoek (1958) we have

$$\begin{pmatrix} l & l' & l'' \\ 0 & 0 & 0 \end{pmatrix} = \frac{2l''^{1/2}(-1)^{(l+l'+l'')/2}}{[\pi(2l''+1)]^{1/2}} \left\{-(l^4+l'^4+l''^4)+2(l^2l'^2+l'^2l''^2+l''^2l^2)\right\}^{-1/4}. \tag{3A.3}$$

This approximation is valid only for large values of l, l', l''. It is derived by applying Stirling's approximation to Racah's closed expression for Wigner 3-j symbols.

Schulten and Gordon (1975) rewrite Wigner 3-j symbol recursion relationships in terms of difference equations which they then convert to differential equations. They solve the latter using the WKBJ method and obtain asymptotic expression for the symbols in terms of well known functions. They obtain uniform and non uniform solutions in the classical and classically forbidden domains. Their results simplify considerably when the azimuthal orders m, m', and m'' vanish. For given l and l', the classical domain of l'' lies in the range

$$[(l+\tfrac{1}{2})^2+(l'+\tfrac{1}{2})^2-2(l+\tfrac{1}{2})(l'+\tfrac{1}{2})]^{1/2} < l'' < [(l+\tfrac{1}{2})^2+(l'+\tfrac{1}{2})^2+2(l+\tfrac{1}{2})(l'+\tfrac{1}{2})]^{1/2}. \tag{3A.4}$$

The full quantum mechanical domain is

$$|l-l'|-1/2 < l'' < l+l'+1/2. \tag{3A.5}$$

The two nonclassical domains are

$$|l-l'|-\frac{1}{2} \;<\; l'' \;<\; [(l+\tfrac{1}{2})^2+(l'+\tfrac{1}{2})^2-2(l+\tfrac{1}{2})(l'+\tfrac{1}{2})]^{1/2}, \tag{3A.6}$$

$$[(l+\tfrac{1}{2})^2+(l'+\tfrac{1}{2})^2+2(l+\tfrac{1}{2})(l'+\tfrac{1}{2})]^{1/2} \;<\; l'' \;<\; l+l'+\frac{1}{2}. \tag{3A.7}$$

Using the results in Schulten and Gordon (1975), we have derived three expressions for the Wigner 3-j symbol in equation (3A.1). The first solution is nonuniform and

is valid in the classical domain:

$$\begin{pmatrix} l & l' & l'' \\ 0 & 0 & 0 \end{pmatrix} = \frac{(-1)^{\frac{3}{2}(l+l'+l'')}}{(2\pi A)^{1/2}} \tag{3A.8}$$

where

$$A = \frac{1}{4}\left[(l+l'+l''+\frac{3}{2})(l'+l''-l+\frac{1}{2})(l''+l-l'+\frac{1}{2})(l+l'-l''+\frac{1}{2})\right]^{1/2} \tag{3A.9}$$

The second solution is uniformly valid in the classical domain and is given by

$$\begin{pmatrix} l & l' & l'' \\ 0 & 0 & 0 \end{pmatrix} = (-1)^{(l+l'-l''+1)}\frac{\alpha^{1/6}}{(2A)^{1/2}}Bi(-\alpha^{2/3}) \tag{3A.10}$$

where

$$\alpha = \frac{3\pi}{4}(l+l'+l''+\frac{3}{2}), \tag{3A.11}$$

and the function Bi is the complement of the Airy function Ai. The third solution is uniformly valid in the classically forbidden region and is given by

$$\begin{pmatrix} l & l' & l'' \\ 0 & 0 & 0 \end{pmatrix} = (-1)^{(l+l'-l''+1)}\frac{\alpha^{1/6}}{(2A)^{1/2}}Bi(\alpha^{2/3}) \tag{3A.12}$$

We have compared the three solutions obtained from Schulten and Gordon (1975), and the Brussaard and Tolhoek (1958) solution to the exact values for a wide range of harmonic degrees. Theoretically, the nonuniform solution in the classical domain should be accurate only for very large harmonic degrees. However, we have found numerically that it is an accurate approximation, even for small harmonic degrees. Therefore, we recommend this solution be used in practice.

ACKNOWLEDGEMENTS

We thank Dr. Pawan Kumar for useful and stimulating conversations.

REFERENCES

Ando, H. and Osaki, Y., 1975, *Publ. Astro. Soc. Japan*, **27**, 581.

Anita, H.M., Chitre, S.M. and Narashima, D., 1986 *Ap. Sp. Sci.*, **118**, 169.

Brussaard, P.J., and Tolhoek, H.A., 1958, *Physica*, **23**, 955.

Christensen-Dalsgaard, J. and Fransden, S., 1982, *Solar Phys.*, **82**, 165.

Davidson, R.C., 1972 *Methods in Nonlinear Plasma Theory*
(New York: Academic Press).

Dziembowski, W., 1982 *Acta Astr.*, **32**, 147.

Edmonds, A.R. 1960, *Angular Momentum in Quantum Mechanics*
(Princeton: Princeton University Press).

Galeev, A.A. and Karpman, V.I. 1963, *Soviet Phys. JETP*, **17**, 403.

Goldreich, P., and Keeley, D.A. 1977a, *Ap. J.*, **211**, 934.

Goldreich, P., and Keeley, D.A. 1977b, *Ap. J.*, **212**, 243.

Goldreich, P., and Kumar, P. 1988, *Ap. J.*, **326**, 462.

Kumar, P., and Goldreich, P. 1989, *Ap. J.*, July 1.

Libbrecht, K.G., and Kaufman, J.M. 1988, *Ap. J.*, **324**, 1172.

Phinney, R.A., and Burridge, R. 1973, *Geophys.J.R.Astr.Soc.*, **34**, 451.

Schulten, K., and Gordon, R.G. 1975, *J. Math. Phys.*, **16**, 1971.

Vandakurov, Y.V., 1979, *Sov. Astron.*, **23**, 421.

Woodhouse, J.H., 1980, *Geophys.J.R.Astr.Soc.*, **61**, 261.

CHAPTER 4

HELIOSEISMOLOGICAL APPLICATIONS OF RAYLEIGH'S PRINCIPLE

> In the deep discovery of the Subterranean world, a shallow part would satisfie some enquirers; who, if two or three yards were open about the surface, would not care to rake the bowels of *Potosi*, and regions towards the Centre.
>
> *Urn Burial* (1658)
>
> *Sir Thomas Browne*

HELIOSEISMOLOGICAL APPLICATIONS OF RAYLEIGH'S PRINCIPLE

EUGENE M. LAVELY

Massachusetts Institute of Technology, Department of Earth, Atmospheric, and Planetary Sciences

ABSTRACT

The degenerate frequencies of solar p modes are integral measures of the radial structure of the Sun. We apply Rayleigh's principle to derive sensitivity kernels that relate frequency perturbations $\delta\omega$ to small model perturbations $\delta m(r)$. The mechanical properties of the oscillations (their frequencies and eigenfunctions) depend on two independent model parameters. Thus, the perturbations relations are of the form $\delta\omega = \int[K_1(r)\delta m_1(r) + K_2(r)\delta m_2(r)]r^2dr$. These relations can be used as the basis for inverse problems in which model parameter perturbations are adjusted to minimize the differences between observed and predicted frequencies. Possible model parameters $m(r)$ include the sound speed $c(r)$, the density $\rho(r)$, the first adiabatic exponent $\Gamma_1(r)$, the adiabatic bulk modulus $\kappa(r)$ and the stratification parameter $\eta(r)$.

We show $\eta(r)$ is sensitive to the chemical and thermal stratification of a star; it is closely related to the Brunt-Väisälä frequency. A fluid parcel of material in a depth range in which $\eta = 1$, is neutrally stable. The parcel is stable or unstable according to whether η is greater or lesser than one. Several important features of stellar structure that depend on the predictions of mixing-length theory could be examined provided the profile of $\eta(r)$ is known. We show that knowledge of η is equivalent to knowledge of the Ledoux instability criteria. An asymptotically valid relationship (in the limits of low and high convective efficiency) is derived which relates $\eta(r)$ to the mixing length in Bohm-Vitense's mixing length theory.

The variable Γ_1 is sensitive to the He, He^+, and He^{++} fractions in the first and second Helium ionization zones. Application of inverse theory to determine the radial

profile of Γ_1 in these ionization zones could be used to place a constraint on the Helium abundance of the Sun.

Modal frequencies depend nonlinearly on the thermodynamic model parameters of the Sun. Therefore, inferring the Sun's radial structure will require an iterative sequence of forward modeling calculations and nonlinear inversions in which the composition parameters and mixing length ratio are adjusted to better match the observed frequencies. The iterative sequence is continued until a chi-squared criteria is satisfied (the theoretical normal mode frequencies match the observed frequencies to within errors in the data).

I. INTRODUCTION

Helioseismology can be used to probe the internal structure of the Sun. The degenerate frequencies of solar p modes depend on the spherically averaged radial profile of the thermodynamic state variables. It is of interest to infer the variation of these variables since such information could, for example, (1) be used to constrain the thermal and chemical stratification of the Sun, (2) be used to constrain free parameters in stellar evolution theory *i.e.*, the Helium abundance and the entropy jump from the photosphere to the adiabatic part of the convection zone (*e.g.* Ulrich and Rhodes 1977), and (3) be used as a basis to test the physics of the equation of state (*e.g.* Christensen-Dalsgaard *et. al.* 1988).

The most uncertain predictions of stellar structure theory are in the subphotospheric region, where the assumptions of mixing length theory break down, and where p modes attain peak amplitudes. The frequencies of modes that are sensitive to structure in deeper regions depend also on the subphotospheric structure. Thus, it is important to obtain a detailed model of this region to make corrections to all frequencies.

The frequencies of the adiabatic oscillations of a star can be calculated given the radial profile of two independent thermodynamic variables. We calculate the perturbation in frequency due to perturbations of several pairs of thermodynamic

variables including (ρ, κ), (c, κ), (c, ρ), (ρ, Γ_1), (c, Γ_1), (c, η), and (ρ, η), where ρ, κ, c, Γ_1, and η denote, respectively, the density, adiabatic bulk modulus, adiabatic sound speed, first adiabatic exponent, and stratification parameter. The quantities κ and Γ_1 are defined by the relation

$$\frac{1}{\kappa} = -\frac{1}{V}\left(\frac{\partial V}{\partial P}\right)_{s,\mu} = \frac{1}{P\Gamma_1} \tag{4.1}$$

where P is the pressure, V is the specific volume, and the derivative is taken at constant entropy s and mean molecular weight μ. The adiabatic sound speed is given by

$$c^2 = \frac{\kappa}{\rho} = \frac{P\Gamma_1}{\rho}. \tag{4.2}$$

The stratification parameter is given by $\eta = -\Gamma_1 H_p \rho^{-1}(\frac{d\rho}{dr})$ where H_p is the pressure scale height (see eq. 4.23) and is discussed in detail in §II. The parameter η is sensitive to departures from chemical homogeneity and thermal adiabaticity. In particular, η can be related to ∇_μ (see eq. 4.11) and the sub or superadiabatic temperature gradient $\nabla - \nabla_{ad}$. For a typical solar model, the parameter η varies between 0 and 1 in the superadiabatic region, is a nearly constant value very slightly less than 1 in the adiabatic part of the convection zone, and varies between 1 and 2 in the subadiabatic radiation zone and chemically stratified core. The inverse problem for any of the model parameter pairs listed above can be posed as a nonlinear optimization problem. Inversions for these variables will be the subject of future work. We only consider theoretical issues in this paper. The constraint that the mass of the Sun remain unchanged can be imposed if ρ is one of the variables being inverted for. Should we have *a priori* knowledge of the entropy jump from the photosphere to the adiabatic part of the convection zone, we can use the variable η to impose the constraint that the entropy jump remain unchanged. The first adiabatic exponent is sensitive to the degree of ionization in the ionization zones. Hydrogen is almost completely ionized at the depth of the HeI ionization zone so that Γ_1 in this depth range is sensitive to the Helium abundance. Thus, the latter can be constrained by a helioseismic inversion for Γ_1. To obtain a unique solution for any of these variables and to stabilize the inversion,

a priori information must be introduced. The objective function to be minimized is a chi-squared measure of data misfit, and model-roughness (for example). Various non-linear iterative methods can be used including variable metric methods, and the Levenberg-Marquardt method. A data set of 2097 degenerate eigenfrequencies of solar p modes is available (see Duvall *et. al.* 1988; Libbrecht and Kaufman 1988).

The outline of the paper is as follows. In §II we discuss the physical significance of the stratification parameter. In §III we apply Rayleigh's principle to derive various perturbation equations. In §IV we establish an asymptotic connection between the thermal stratification predicted by mixing length theory, and the stratification parameter.

II. ENTROPY AND DENSITY STRATIFICATION

In the following we derive expressions for the entropy and density stratification of the Sun in which we explicitly account for departures from chemical homogeneity and thermal adiabaticity. The well known Bullen stratification parameter from geophysics (see Bullen 1967) is introduced. We show that it may be used as a measure of convective instability, and that it is equivalent to the Ledoux instability criteria. The value of this parameter from the perspective of helioseismology is that it may be inverted for from the solar oscillation frequencies. Masters (1979) has inverted for the terrestrial profile of η to determine the stratification of the Earth's mantle and core.

For a chemically homogeneous system, a thermodynamic state variable depends only on two independent state variables. However, if the system is a multi-component system, or if the system is ionizing, then a general variation of a state variable will depend in addition on changes in mass fractions of the various components. In general, four thermodynamic state variables are required, the ionic molecular weight μ_o, the electronic molecular weight μ_e, and any two additional state variables v_1 and v_2. The mean molecular weight per ion is given by

$$\frac{1}{\mu_o} = \sum_i \frac{X_i}{A_i}, \tag{4.3}$$

where X_i and A_i are the mass fraction and the atomic weight of atomic species i. The electronic molecular weight is given by

$$\frac{1}{\mu_e} = \frac{E}{\mu_o} \tag{4.4}$$

where E is the total number of free electrons. The total molecular weight μ is given by

$$\frac{1}{\mu} = \frac{1}{\mu_e} + \frac{1}{\mu_o}. \tag{4.5}$$

It follows that $d\mu$ is given by

$$d\mu = \frac{\mu^2}{\mu_e^2} d\mu_e + \frac{\mu^2}{\mu_o^2} d\mu_o. \tag{4.6}$$

In general, a thermodynamic state variable F has dependence $F(v_1, v_2, \mu_e, \mu_o)$. However, in certain idealized circumstances, *e.g.*, in nondegenerate regimes where there is full ionization, or where the ideal equation of state applies, $F(v_1, v_2, \mu_e, \mu_o)$ may be simplified to $F(v_1, v_2, \mu)$. Let the specific entropy s be a function of temperature T, pressure P, and mean molecular weight μ so that $s = s(T, P, \mu)$. It follows that the radial stratification of the specific entropy is given by

$$\frac{ds}{dr} = \left(\frac{\partial s}{\partial P}\right)_{T,\mu} \frac{dP}{dr} + \left(\frac{\partial s}{\partial T}\right)_{P,\mu} \frac{dT}{dr} + \left(\frac{\partial s}{\partial \mu}\right)_{P,T} \frac{d\mu}{dr}. \tag{4.7}$$

This result can be rewritten in terms of readily calculated quantities introduced below. The coefficient of thermal expansion is given by

$$Q = \frac{1}{V}\left(\frac{\partial V}{\partial T}\right)_{P,\mu} = -\frac{1}{V}\left(\frac{\partial s}{\partial P}\right)_{T,\mu} = -\frac{1}{\rho}\left(\frac{\partial \rho}{\partial T}\right)_{P,\mu}, \tag{4.8}$$

where V is the specific volume *i.e.* $\rho V = 1$. The specific heat at constant pressure c_p is given by

$$c_p = T\left(\frac{\partial s}{\partial T}\right)_{P,\mu}. \tag{4.9}$$

The hydrostatic support relation is given by

$$\frac{dP}{dr} = -\rho g. \tag{4.10}$$

Inserting equations (4.8), (4.9), and (4.10) into equation (4.7) and using the notation

$$\nabla = \frac{dlnT}{dlnP}, \quad \nabla_{ad} = \left(\frac{dlnT}{dlnP}\right)_s, \quad \nabla_\mu = \frac{dln\mu}{dlnP}, \tag{4.11}$$

and

$$H_P = \frac{P}{\rho g}, \tag{4.12}$$

where H_P is the pressure scale height, we obtain

$$\frac{ds}{dr} = Qg - \frac{c_p}{H_P}\nabla - \left(\frac{\partial s}{\partial \mu}\right)_{P,T} \frac{\mu}{H_P}\nabla_\mu. \tag{4.13}$$

The adiabatic temperature gradient ∇'_{ad} is obtained by setting the radial entropy gradient to zero:

$$\nabla'_{ad} = \frac{gQH_p}{c_p} - \frac{1}{c_p}\left(\frac{\partial s}{\partial \mu}\right)_{P,T} \mu\nabla_\mu. \tag{4.14}$$

The prime in ∇'_{ad} denotes the adiabatic gradient in the presence of a gradient in the mean molecular weight. The gradient can arise where there is an inhomogeneous mixture (as in the core), or in the hydrogen and helium ionization zones where the number of free particles can nearly double. It is common in astrophysics to define the adiabatic gradient for a system in which $\nabla_\mu = 0$ (*e.g.*, Kippenhahn *et.al.* 1967). To be consistent with the notation and usage of Kippenhahn, we define the adiabatic gradient for such a system to be

$$\nabla_{ad} = \frac{gQH_P}{c_p}. \tag{4.15}$$

With these definitions the entropy gradient becomes

$$\frac{ds}{dr} = \frac{c_p}{H_P}\left[\nabla_{ad} - \nabla - \frac{1}{c_p}\left(\frac{\partial s}{\partial \mu}\right)_{P,T} \mu\nabla_\mu\right] \tag{4.16}$$

Now consider the radial derivative of the density which we take to be a function of specific entropy, pressure, and composition *i.e.* $\rho = \rho(s, P, \mu)$. We obtain

$$\frac{d\rho}{dr} = \left(\frac{\partial \rho}{\partial s}\right)_{P,\mu} \frac{ds}{dr} + \left(\frac{\partial \rho}{\partial P}\right)_{s,\mu} \frac{dP}{dr} + \left(\frac{\partial \rho}{\partial \mu}\right)_{P,s} \frac{d\mu}{dr}. \tag{4.17}$$

Again, we seek to rewrite this in terms of easily calculated quantities. Toward this end, it proves convenient to use Jacobians to transform thermodynamic derivatives. Using the identities

$$\frac{\partial(u,v,w)}{\partial(x,y,z)} = \frac{\partial(u,v,w)}{\partial(r,s,t)}\frac{\partial(r,s,t)}{\partial(x,y,z)} \tag{4.18}$$

and

$$\left(\frac{\partial u}{\partial x}\right)_{y,z} = \frac{\partial(u,y,z)}{\partial(x,y,z)} \tag{4.19}$$

the first thermodynamic derivative in equation (4.17) can be written in the form

$$\left(\frac{\partial \rho}{\partial s}\right)_{P,\mu} = \frac{\partial(\rho,P,\mu)}{\partial(T,P,\mu)}\frac{\partial(T,P,\mu)}{\partial(s,P,\mu)} = -\frac{\rho T Q}{c_p} \tag{4.20}$$

where we have used equations (4.8) and (4.9). Substituting equations (4.10), (4.16), and (4.20) into equation (4.17), and using equation (4.2), we obtain

$$\frac{d\rho}{dr} = -\frac{\rho g}{c^2} + \frac{\rho T Q}{H_P}\left[\nabla - \nabla_{ad} + \left[\frac{1}{c_p}\left(\frac{\partial s}{\partial \mu}\right)_{T,P} - \frac{1}{\rho T Q}\left(\frac{\partial \rho}{\partial \mu}\right)_{s,P}\right]\mu\nabla_\mu\right]. \tag{4.21}$$

a) The Stratification Parameter η

The stratification parameter is most naturally introduced by way of the the Adams-Williamson equation, a well known relation in geophysics. Under the assumption of chemical homogeneity and thermal adiabaticity, the derivative of the density can be written

$$\left(\frac{d\rho}{dr}\right)_{s,\mu} = \left(\frac{d\rho}{dP}\right)_{s,\mu}\frac{dP}{dr} = -\frac{\rho g}{c^2}, \tag{4.22}$$

where the last equality follows from equations (4.10) and (4.21). The stratification parameter is defined

$$\eta \equiv -\frac{c^2}{\rho g}\frac{d\rho}{dr} = -H_p \Gamma_1 \rho^{-1}\frac{d\rho}{dr} \tag{4.23}$$

where Γ_1 is the first adiabatic exponent. The motivation for this definition is that

$$\eta = 1, \text{ if } \frac{d\rho}{dr} = \left(\frac{d\rho}{dr}\right)_{s,\alpha}. \tag{4.24}$$

A departure in η from the value 1 signifies either chemical or thermal stratification or both. Inserting equation (4.21) into equation (4.23) we obtain

$$\eta = 1 - \frac{c^2 T Q}{g H_p}\left[\nabla - \nabla_{ad} + \left[\frac{1}{c_p}\left(\frac{\partial s}{\partial \mu}\right)_{T,p} - \frac{1}{\rho T Q}\left(\frac{\partial \rho}{\partial \mu}\right)_{s,p}\right]\mu\nabla_\mu\right]. \tag{4.25}$$

b) The Stratification Parameter as an Instability Criteria

Knowledge of η is equivalent to knowledge of the Ledoux convective instability criteria. See Kippenhahn *et. al.* (1967) for a discussion of the latter. To show this, we begin by deriving the relationship between η and the Brunt-Väisälä frequency. The buoyancy restoring force depends on the thermal and chemical stratification. Consider a small radial displacement ζ of a parcel of material in a time small compared to the diffusion times of heat and matter (the parcel moves with constant entropy and composition). Equation (4.22) can be used to calculate the density change of such a parcel

$$(\delta\rho)_{parcel} = -\frac{\rho g}{c^2}\zeta. \tag{4.26}$$

From equation (4.23), the change in density outside the parcel is

$$(\delta\rho)_{out} = -\frac{\rho g \eta}{c^2}\zeta. \tag{4.27}$$

The restoring force acting on the parcel is given by

$$g[(\delta\rho)_{out} - (\delta\rho)_{parcel}] = -\frac{\rho g^2}{c^2}(\eta - 1)\zeta. \tag{4.28}$$

Equating the restoring force to the inertial reaction of the parcel, we obtain

$$\rho\frac{d^2\zeta}{dt^2} = -\frac{\rho g^2}{c^2}(\eta - 1)\zeta. \tag{4.29}$$

This result can be rewritten as

$$\frac{d^2\zeta}{dt^2} + N^2\zeta = 0 \tag{4.30}$$

where

$$N^2 = \frac{g^2}{c^2}(\eta - 1). \tag{4.31}$$

A fluid parcel oscillates with real frequency N if $\eta > 1$. In such a medium, the stratification is stable. Toroidal motions are allowed (since toroidal displacements are confined to spherical shells), but large scale poloidal motions are excluded. If η is less than 1, the stratification is unstable and a perturbation to a material parcel will

grow with exponential rate N. A medium with $\eta = 1$ is neutrally stratified; a parcel of material, if displaced, will remain at its new position. Using equations (4.2) and (4.10), it follows that N^2 may be rewritten as

$$N^2 = \frac{g}{r}\left[\frac{1}{\Gamma_1}\frac{dlnP}{dlnr} - \frac{dln\rho}{dlnr}\right] \tag{4.32}$$

which is the familiar definition of the Brunt-Väisälä frequency. For chemically homogeneous, non-ionizing regions of the Sun, the expression for N^2 in equation (4.31) reduces to

$$N^2 = -\frac{gTQ}{H_P}(\nabla - \nabla_{ad}). \tag{4.33}$$

To establish the connection of η with the Ledoux instability criteria, we return to the general expression for η in equation (4.25) and rewrite it as

$$(1-\eta)\frac{gH_p}{c^2TQ} = \nabla - \nabla_{ad} - \left[\frac{1}{c_p}\left(\frac{\partial s}{\partial \mu}\right)_{T,p} - \frac{1}{\rho TQ}\left(\frac{\partial \rho}{\partial \mu}\right)_{s,p}\right]\mu\frac{\partial ln\mu}{\partial M_r}\frac{4\pi r^4 P}{GM_r}, \tag{4.34}$$

where we have used equation (4.10) in the form

$$\partial lnP = -\frac{GM_r}{4\pi r^4 P}\partial M_r \tag{4.35}$$

where $\partial M_r = 4\pi\rho r^2 dr$. Using equation (4.34), let us define the critical temperature gradient $\nabla_{cr}(r)$ by the relation

$$\nabla_{cr} - \nabla_{ad} + \left[-\frac{1}{c_p}\left(\frac{\partial s}{\partial \mu}\right)_{T,p} + \frac{1}{\rho TQ}\left(\frac{\partial \rho}{\partial \mu}\right)_{s,p}\right]\mu\frac{\partial ln\mu}{\partial M_r}\frac{4\pi r^4 P}{GM_r} = 0. \tag{4.36}$$

Since the factor multiplying $(1-\eta)$ on the left hand side of equation (4.34) is always positive, the stratification at radius r is unstable, neutrally stable, or stable, depending on whether $\nabla(r) > \nabla_{cr}(r)$, $\nabla(r) = \nabla_{cr}(r)$, or $\nabla(r) < \nabla_{cr}(r)$. According to Kippenhahn *et.al.* (1967), the Ledoux convective instability criteria is embodied by the equation

$$\nabla_{cr} - \nabla_{ad} + \left(\frac{\partial lnT}{\partial ln\mu}\right)_{p,\rho}\frac{\partial ln\mu}{\partial M_r}\frac{4\pi r^4 P}{GM_r}. \tag{4.37}$$

To complete the proof that knowledge of η is equivalent to knowldege of the Ledoux instability criteria, we must show that the thermodynamic derivatives in equations

(4.36) and (4.37) are equivalent. Substituting the rightmost equality in equation (4.8) and the first equality in equation (4.9) into equation (4.36), and equating the resulting expression with equation (4.37), we find that the two criteria are identical if it can be shown that the identity

$$\left(\frac{\partial T}{\partial \mu}\right)_{p,\rho} = -\left[\left(\frac{\partial T}{\partial s}\right)_{p,\mu}\left(\frac{\partial s}{\partial \mu}\right)_{T,p} + \left(\frac{\partial T}{\partial \rho}\right)_{p,\mu}\left(\frac{\partial \rho}{\partial \mu}\right)_{s,p}\right] \tag{4.38}$$

is valid. Since the pressure is taken to be constant in each of the above derivatives, we drop the p subscript notation. The left hand side of equation (4.38) can be rewritten

$$\begin{aligned}
\left(\frac{\partial T}{\partial \mu}\right)_{\rho} &= \frac{\partial(T,\rho)}{\partial(s,\mu)}\frac{\partial(s,\mu)}{\partial(\mu,\rho)} \\
&= \left[\left(\frac{\partial T}{\partial s}\right)_{\mu}\left(\frac{\partial \rho}{\partial \mu}\right)_{s} - \left(\frac{\partial \rho}{\partial s}\right)_{\mu}\left(\frac{\partial T}{\partial \mu}\right)_{s}\right]\left[-\left(\frac{\partial s}{\partial \rho}\right)_{\mu}\right] \\
&= \left[-\left(\frac{\partial T}{\partial s}\right)_{\mu}\left(\frac{\partial \rho}{\partial \mu}\right)_{s}\left(\frac{\partial s}{\partial \rho}\right)_{\mu} + \left(\frac{\partial T}{\partial \mu}\right)_{s}\right] \\
&= \left[\left(\frac{\partial T}{\partial s}\right)_{\mu}\right]\left[-\left(\frac{\partial \rho}{\partial \mu}\right)_{s}\left(\frac{\partial s}{\partial \rho}\right)_{\mu} + \left(\frac{\partial T}{\partial \mu}\right)_{s}\left(\frac{\partial s}{\partial T}\right)_{\mu}\right].
\end{aligned} \tag{4.39}$$

The right hand side of equation (4.38) can be written

$$\begin{aligned}
- &\left[\left(\frac{\partial T}{\partial s}\right)_{\mu}\left(\frac{\partial s}{\partial \mu}\right)_{T} + \left(\frac{\partial T}{\partial \rho}\right)_{\mu}\left(\frac{\partial \rho}{\partial \mu}\right)_{s}\right] \\
&= -\left(\frac{\partial T}{\partial s}\right)_{\mu}\left[\left(\frac{\partial s}{\partial \mu}\right)_{T} + \left(\frac{\partial T}{\partial \rho}\right)_{\mu}\left(\frac{\partial \rho}{\partial \mu}\right)_{s}\left(\frac{\partial s}{\partial T}\right)_{\mu}\right] \\
&= -\left(\frac{\partial T}{\partial s}\right)_{\mu}\left[\left(\frac{\partial s}{\partial \mu}\right)_{T} + \left(\frac{\partial s}{\partial \rho}\right)_{\mu}\left(\frac{\partial \rho}{\partial \mu}\right)_{s}\right]
\end{aligned} \tag{4.40}$$

Comparing the last equalities in equations (4.39) and (4.40), we find the two criteria are equivalent if the identity

$$\left(\frac{\partial T}{\partial \mu}\right)_{s}\left(\frac{\partial s}{\partial T}\right)_{\mu} = -\left(\frac{\partial s}{\partial \mu}\right)_{T} \tag{4.41}$$

is valid. Using the identity

$$\left(\frac{\partial x}{\partial y}\right)_{\psi,z}\left(\frac{\partial y}{\partial z}\right)_{\psi,x}\left(\frac{\partial z}{\partial x}\right)_{\psi,y} = -1, \tag{4.42}$$

(with $x = s, y = \mu, z = T, \psi = P$), we find that equation (4.41) is indeed correct. Therefore, the information contained in the stratification parameter is equivalent to the information contained in the Ledoux instability criteria *i.e.*,

$$\begin{aligned}
\eta < 1 \quad &\rightarrow \quad \nabla_{cr} - \nabla_{ad} + \left(\frac{\partial ln T}{\partial ln \mu}\right)_{p,\rho} \frac{\partial ln \mu}{\partial M_r} \frac{4\pi r^4 P}{G M_r} > 0 \quad \rightarrow \quad \text{instability,} \\
\eta = 1 \quad &\rightarrow \quad \nabla_{cr} - \nabla_{ad} + \left(\frac{\partial ln T}{\partial ln \mu}\right)_{p,\rho} \frac{\partial ln \mu}{\partial M_r} \frac{4\pi r^4 P}{G M_r} = 0 \quad \rightarrow \quad \text{neutral stratification,} \\
\eta > 1 \quad &\rightarrow \quad \nabla_{cr} - \nabla_{ad} + \left(\frac{\partial ln T}{\partial ln \mu}\right)_{p,\rho} \frac{\partial ln \mu}{\partial M_r} \frac{4\pi r^4 P}{G M_r} < 0 \quad \rightarrow \quad \text{stability.} \qquad (4.43)
\end{aligned}$$

We have taken care in defining the stratification parameter because it can be inverted for directly using helioseismology as we show in the next section. The diagnostic capabilities of such a variable are clearly important.

III. THE FORWARD PROBLEM

In this section, we apply Rayleigh's variational principle to obtain the perturbation equations for numerous model parameter combinations including the pairs (ρ, κ), (c, κ), (c, ρ) (ρ, Γ_1), (c, Γ_1), (η, ρ), and (η, c). The displacement of the p modes can be written in the form

$$\mathbf{s}(\mathbf{r}) = [{}_nU_l(r) Y_l^m(\theta, \phi)\hat{\mathbf{r}} + {}_nV_l(r) \nabla_1 Y_l^m(\theta, \phi)] e^{i\omega t} \qquad (4.44)$$

where ${}_nU_l(r)$ and ${}_nV_l(r)$ denote respectively the radial and horizontal eigenfunctions for harmonic degree l and radial order n. The angular frequency of the mode is denoted by ω. The surface gradient operator is given by $\nabla_1 = r(\nabla - \hat{\mathbf{r}} \cdot \nabla)$. The function Y_l^m is a spherical harmonic of of degree l and azimuthal order m defined using the convention of Edmonds 1960:

$$\int_0^{2\pi} \int_0^{\pi} [Y_{l'}^{m'}(\theta, \phi)]^* Y_l^m(\theta, \phi) \sin\theta d\theta d\phi = \delta_{mm'} \delta_{l'l} \qquad (4.45)$$

where the integration is over the unit sphere. The coordinates (r,θ,ϕ) are spherical polar coordinates (where θ is colatitude) and $\hat{\mathbf{r}}, \hat{\theta}, \hat{\phi}$ denote unit vectors in the coordinate directions. Henceforth, we drop the subscripts n and l, in equation (4.44) and

use instead the notation $U = {}_nU_l(r)Y_l^m$, $V = {}_nV_l(r)\nabla_1 Y_l^m$ so that

$$\mathbf{s} = U\hat{\mathbf{r}} + \nabla_1 V = s_r\hat{\mathbf{r}} + s_\theta\hat{\theta} + s_\phi\hat{\phi} \tag{4.46}$$

The equation of motion is given by

$$\mathcal{L}_{ij}s_j = \rho\partial_t^2 s_i \tag{4.47}$$

where

$$\mathcal{L}_{ij}s_j = \nabla_i(P\Gamma_1\nabla_j s_j) - (\nabla_j s_j)\nabla_i P + (\nabla_i s_j)\nabla_j P - \rho s_j\nabla_j\nabla_i\phi - \rho\nabla_i\phi_1 \tag{4.48}$$

where ϕ_1 is the perturbation in gravitational potential due to deismic motions. This operator can be simplified by introducing the Piola-Kirchoff tensor

$$T_{ij}(r,\theta,\phi) = P_0\Gamma_1\partial_j s_j\delta_{ij} + P_0\partial_i s_j - P_0\delta_{ij}\partial_k s_k \tag{4.49}$$

The pressure P vanishes at $r = R_\odot$ and therefore

$$T_{ij}(R_\odot,\theta,\phi) = 0. \tag{4.50}$$

It follows from equations (4.48) and (4.49) that

$$\mathcal{L}_{ij}s_j = \partial_j T_{ij} - \rho_0\partial_i\phi_1 - \rho_0 s_j\partial_i\partial_j\phi_0. \tag{4.51}$$

To construct the variational principle, we begin by multiplying equation (4.51) by s_i' and adding and subtracting the term $\rho_0 s_i\partial_i\phi_1'$ to obtain

$$s_i'\mathcal{L}_{ij}s_j = s_i'\partial_j T_{ij} - \rho_0 s_i'\partial_i\phi_1 - \rho_0 s_i' s_j\partial_i\partial_j\phi_0 + (\rho_0 s_i\partial_i\phi_1' - \rho_0 s_i\partial_i\phi_1'). \tag{4.52}$$

The first term on the right hand side of equation (4.52) can be rewritten

$$s_i'\partial_j T_{ij} = \partial_j(T_{ij}s_i') - T_{ij}\partial_j s_i'. \tag{4.53}$$

The term $\rho_0 s_i\partial_i\phi_1'$ in equation (4.52) can be written

$$\begin{aligned}
\rho_0 s_i\partial_i\phi_1' &= \partial_i(\rho_0 s_i\phi_1') - \phi_1'\partial_i(\rho_0 s_i) \\
&= \partial_i(\rho_0 s_i\phi_1') + \phi_1'\rho_1 \\
&= \partial_i(\rho_0 s_i\phi_1') + \frac{\phi_1'\nabla^2\phi_1}{4\pi G} \\
&= \partial_i(\rho_0 s_i\phi_1' + \frac{1}{4\pi G}\phi_1'\partial_i\phi_1) - \frac{1}{4\pi G}\partial_i\phi_1'\partial_i\phi_1
\end{aligned} \tag{4.54}$$

where the perturbation in density is given by $\rho_1 = -\partial_i(\rho_0 s_i)$. Inserting equations (4.53) and (4.54) into equation (4.52) we obtain

$$s_i' \mathcal{L}_{ij} s_j = \partial_j [s_i' T_{ij} + \phi_1' (\frac{1}{4\pi G} \partial_j \phi_1 + \rho_0 s_j)] -$$
$$[T_{ij} \partial_j s_i' + \rho_0 s_i' \partial_i \phi_1 + \rho_0 s_i \partial_i \phi_1' + \rho_0 s_i s_j' \partial_i \partial_j \phi_0 + \frac{1}{4\pi G} \partial_i \phi_1' \partial_i \phi_1]. \quad (4.55)$$

The terms in the second set of square brackets are unaffected if $\mathbf{s}$ and $\mathbf{s}'$ are interchanged so that

$$s_i' \mathcal{L}_{ij} s_j - s_i \mathcal{L}_{ij} s_j' = \partial_j [s_i' T_{ij} - s_i T_{ij}' + \phi_1' (\frac{1}{4\pi G} \partial_j \phi_1 + \rho_0 s_j) - \phi_1 (\frac{1}{4\pi G} \partial_j \phi_1' + \rho_0 s_j')]. \quad (4.56)$$

The perturbed Poisson's equation is given by

$$\nabla^2 \phi_1 = -4\pi G \partial_k (\rho_0 s_k), \quad (4.57)$$

which implies that

$$\int \nabla \cdot [\nabla \phi_1 + 4\pi \rho_0 G \mathbf{s}] d^3 r = 0. \quad (4.58)$$

Applying the divergence theorem to equation (4.58), we obtain

$$\int [\nabla \phi_1 + 4\pi \rho_0 G \mathbf{s}] \cdot d\mathbf{S} = 0. \quad (4.59)$$

By taking the volume integrals of the terms on the right hand side of equation (4.56), and by applying the divergence theorem, we can show that the volume integral of each term vanishes by using equations (4.50) and (4.59). It follows that the Lagrangian is a symmetric operator *i.e.*,

$$\int s_i' \mathcal{L}_{ij} s_j d^3 r = \int s_i \mathcal{L}_{ij} s_j' d^3 r. \quad (4.60)$$

Inserting equation (4.49) into equation (4.55), integrating the resulting quantity over the volume of the Sun, and recognizing that the first term (the divergence term) vanishes, we obtain

$$\int s_i' \mathcal{L}_{ij} s_j d^3 r = -\int [P \Gamma_1 \partial_j s_j \delta_{ij} \partial_j s_i' + P_0 \{\partial_i s_j - \delta_{ij} \partial_k s_k\} \partial_j s_i' + \rho_0 s_i' \partial_i \phi_1 + \rho_0 s_i \partial_i \phi_1'$$
$$+ \rho_0 s_i s_j' \partial_i \partial_j \phi_0 + \frac{1}{4\pi G} \partial_i \phi_1 \partial_i \phi_1'] d^3 r. \quad (4.61)$$

Consider the quantity

$$\partial_j[P_0(s_i'\partial_i s_j - \delta_{ij}(\partial_k s_k)s_i')] = P_0[\partial_i s_j \partial_j s_i' - \delta_{ij}(\partial_k s_k)\partial_j s_i'] +$$
$$\partial_j P_0[s_i'\partial_i s_j - \delta_{ij}(\partial_k s_k)s_i'] + P_0[s_i'\partial_i\partial_j s_j - \delta_{ij}\partial_j(\partial_k s_k)s_i']. \tag{4.62}$$

We see the last term equation (4.62) is zero, and that by integrating over the volume of the sun the divergence term on the left hand side vanishes by Gauss' theorem so that we obtain

$$\int P_0[\partial_i s_j \partial_j s_i' - \delta_{ij}(\partial_k s_k)\partial_j s_i']d^3r = -\int \partial_j P_0[s_i'\partial_i s_j - \delta_{ij}(\partial_k s_k)s_i']d^3r. \tag{4.63}$$

Inserting this result into equation (4.61) and using $\partial_j P_0 = -\rho_0\partial_j\phi_0$ we obtain the result

$$\int s_i'\mathcal{L}_{ij}s_j d^3r = -\int [P\Gamma_1\partial_j s_j\delta_{ij}\partial_j s_i' + \rho_0\partial_j\phi_0(s_i'\partial_i s_j - s_j'\partial_i s_i) +$$
$$\rho_0 s_i'\partial_i\phi_1 + \rho_0 s_i\partial_i\phi_1' + \rho_0 s_i s_j'\partial_i\partial_j\phi_0 + \frac{1}{4\pi G}\partial_i\phi_1\partial_i\phi_1']d^3r. \tag{4.64}$$

By setting $\mathbf{s}_k(\mathbf{r},t) = \mathbf{s}_k(\mathbf{r})e^{i\omega_k t}$, it follows from equation (4.47) that

$$\omega_k^2\int \rho\mathbf{s}_{k'}^*\cdot\mathbf{s}_k d^3r = \int [P\Gamma_1\partial_j s_j\delta_{ij}\partial_j s_i' + \rho_0\partial_j\phi_0(s_i'\partial_i s_j - s_j'\partial_i s_i) +$$
$$\rho_0 s_i'\partial_i\phi_1 + \rho_0 s_i\partial_i\phi_1' + \rho_0 s_i s_j'\partial_i\partial_j\phi_0 + \frac{1}{4\pi G}\partial_i\phi_1\partial_i\phi_1']d^3r \tag{4.65}$$

which is the final statement of the variational principle. We now set $P\Gamma_1 = \kappa$ and $\mathbf{s}' = \mathbf{s}^*$ (for notational convenience, we henceforth ignore the complex conjugate symbol). Equation (4.65) becomes

$$\omega^2\int_0^{R_\odot}\rho\mathbf{s}\cdot\mathbf{s}\cdot d^3r = \int_0^{R_\odot}[\kappa(\partial_i s_i)^2 + \rho s_i s_j\partial_i\partial_j\phi_0 + \rho\partial_j\phi_0(s_i\partial_i s_j - s_j\partial_i s_i) +$$
$$\frac{1}{4\pi G}|\nabla\phi_1|^2 + 2\rho s_i\partial_i\phi_1]d^3r. \tag{4.66}$$

This is identical to the result stated in the appendix of Backus and Gilbert (1967).

Several of the terms in equation (4.66) can be simplified by application of the chain rule and the relations

$$r^2 = x_1^2 + x_2^2 + x_3^2 \text{ and } \frac{\partial r}{\partial x_j} = \frac{x_j}{r}. \tag{4.67}$$

Thus, the term $\partial_i\partial_j\phi_0$ can be rewritten

$$\partial_i\partial_j\phi_0 = \delta_{ij}r^{-1}\partial_r\phi_0 - r^{-3}x_ix_j\partial_r\phi_0 + r^{-2}x_ix_j\partial_r^2\phi_0. \tag{4.68}$$

The second derivative in the last term can be removed with the relation $\partial_r^2\phi_0 = 4\pi G\rho - 2r^{-1}\partial_r\phi_0$ so that

$$\partial_i\partial_j\phi_0 = r^{-3}(r^2\delta_{ij} - 3x_ix_j)\partial_r\phi_0 + 4\pi G\rho r^{-2}x_ix_j. \tag{4.69}$$

Inserting equation (4.69) and the identity $\partial_j\phi_0 = r^{-1}x_j\partial_r\phi_0$ into the right hand side of equation (4.66), we obtain

$$\begin{aligned}\omega^2\int_0^{R_\odot}\rho_0\mathbf{s}\cdot\mathbf{s}d^3r = \int_0^{R_\odot}[\kappa(\partial_is_i)^2 + \rho_0s_is_jr^{-3}(r^2\delta_{ij} - 3x_ix_j)\partial_r\phi_0 + \\ 4\pi G\rho_0r^{-2}s_is_jx_ix_j + \rho_0r^{-1}\partial_r\phi_0(x_js_i\partial_is_j - x_js_j\partial_is_i) + \\ \frac{1}{4\pi G}|\nabla\phi_1|^2 + 2\rho_0s_i\partial_i\phi_1]d^3r.\end{aligned} \tag{4.70}$$

The terms $x_js_i\partial_is_j$, $x_js_j\partial_is_i$, $s_ix_is_jx_j$, $s_is_j\delta_{ij}$, ∂_is_i, and $s_i\partial_i\phi_1$ in equation (4.70) can be simplified with the identities

$$\begin{aligned} x_js_i\partial_is_j &= s_i\partial_i(s_jx_j) - s_is_j\partial_ix_j = s_i\partial_i(s_jx_j) - s_is_j\delta_{ij} = \mathbf{s}\cdot\nabla(rs_r) - \mathbf{s}\cdot\mathbf{s} \\ &= s_r^2 + r\mathbf{s}\cdot\nabla s_r - \mathbf{s}\cdot\mathbf{s} && (4.71)\\ x_js_j\partial_is_i &= \mathbf{r}\cdot\mathbf{s}\,\nabla\cdot\mathbf{s} = rs_r\nabla\cdot\mathbf{s} && (4.72)\\ s_ix_is_jx_j &= (\mathbf{r}\cdot\mathbf{s})(\mathbf{r}\cdot\mathbf{s}) = r^2s_r^2 && (4.73)\\ s_is_j\delta_{ij} &= \mathbf{s}\cdot\mathbf{s} && (4.74)\\ \partial_is_i &= \nabla\cdot\mathbf{s} && (4.75)\\ s_i\partial_i\phi_1 &= \mathbf{s}\cdot\nabla\phi_1 && (4.76)\end{aligned}$$

Inserting equations (4.71)- (4.76) into equation (4.70), we obtain

$$\begin{aligned}\omega^2\int_0^{R_\odot}\rho\mathbf{s}\cdot\mathbf{s}d^3r = \int_0^{R_\odot}[\kappa(\nabla\cdot\mathbf{s})^2 + \rho\dot{\phi}_0(-2r^{-1}s_r^2 - s_r\nabla\cdot\mathbf{s} + \mathbf{s}\cdot\nabla s_r) + 4\pi G\rho^2s_r^2 \\ + \frac{1}{4\pi G}|\nabla\phi_1|^2 + 2\rho\mathbf{s}\cdot\nabla\phi_1]d^3r.\end{aligned} \tag{4.77}$$

Inserting into equation (4.77) the representation for the displacement field $\mathbf{s}$ given in equation (4.46) and using repeatedly the identity $\nabla_1a\cdot\nabla_1b = -a\nabla_1^2b$ (where a and

b are products between an arbitrary functions of radius and a spherical harmonic), we obtain finally the desired result:

$$\omega^2 \int_0^{R_\odot} \rho[U^2 + l(l+1)V^2]r^2 dr = \int_0^{R_\odot} [\kappa(\dot{U} + F)^2 - 2UF\rho g + 4\pi G\rho^2 U^2 + \frac{l(l+1)\phi_1^2}{4\pi G r^2} + 2\rho\left(U\dot{\phi}_1 + \frac{l(l+1)V\phi_1}{r}\right)]r^2 dr \tag{4.78}$$

where

$$F = \frac{2U - l(l+1)V}{r}, \tag{4.79}$$

and where we have returned to the notation $U = {}_nU_l(r)$, $V = {}_nV_l(r)$, and $\phi_1 = {}_n\phi_{1,l}(r)$.

The modes satisfy an orthogonality condition given by

$$\int \rho \mathbf{s}^*_{k'} \cdot \mathbf{s}_k d^3r = N\delta_{m'm}\delta_{n'n}\delta_{l'l} \tag{4.80}$$

where k denotes the triplet (n, l, m), and

$$N = \int_0^{R_\odot} \rho[U^2 + l(l+1)V^2]r^2 dr. \tag{4.81}$$

Rayleigh's principle states that first order variations of modal frequencies are stationary to first order variations of the eigenfunctions. Thus, in taking the variation of equation (4.78) to determine the frequency variation $\delta\omega^2 = 2\omega\delta\omega$, we can (to first order accuracy) neglect the contributions from the eigenfunction perturbations (δU, δV, $\delta\phi_1$) and consider only the structural variations ($\delta\kappa$, $\delta\phi_0$, $\delta\dot{\phi}_0$, $\delta\rho$). The perturbation equations are derived in Appendix 4A. The final results are:

$$\delta\omega^2 N = \int_0^{R_\odot} [K_\rho^{(1)}(r)\delta\rho(r) + K_\kappa^{(1)}(r)\delta\kappa(r)]r^2 dr, \tag{4.82}$$

$$\delta\omega^2 N = \int_0^{R_\odot} [K_c^{(2)}(r)\delta c(r) + K_\kappa^{(2)}(r)\delta\kappa(r)]r^2 dr, \tag{4.83}$$

$$\delta\omega^2 N = \int_0^{R_\odot} [K_c^{(3)}(r)\delta c(r) + K_\rho^{(3)}(r)\delta\rho(r)]r^2 dr, \tag{4.84}$$

$$\delta\omega^2 N = \int_0^{R_\odot} [K_\rho^{(4)}(r)\delta\rho(r) + K_{\Gamma_1}^{(4)}(r)\delta\Gamma_1(r)]r^2 dr, \tag{4.85}$$

$$\delta\omega^2 N = \int_0^{R_\odot} [K_c^{(5)}(r)\delta c(r) + K_{\Gamma_1}^{(5)}(r)\delta\Gamma_1(r)]r^2 dr, \tag{4.86}$$

$$\delta\omega^2 N = \int_0^{R_\odot} [K_c^{(6)}(r)\delta c(r) + K_\eta^{(6)}(r)\delta\eta(r)]r^2 dr, \tag{4.87}$$

$$\delta\omega^2 N = \int_0^{R_\odot} [K_\rho^{(7)}(r)\delta\rho(r) + K_\eta^{(7)}(r)\delta\eta(r)]r^2 dr \tag{4.88}$$

where

$$
\begin{aligned}
K_\rho^{(1)}(r) &= -\omega^2[U^2 + l(l+1)V^2] - 2UFg + 8\pi G\rho U^2 \\
&+ 2\left[U\dot{\phi}_1 + \frac{l(l+1)V\phi_1}{r}\right] - 4\pi G S^{(1)}(r), && (4.89)\\
K_\kappa^{(1)}(r) &= (\dot{U} + F)^2, && (4.90)\\
K_\kappa^{(2)}(r) &= K_\kappa^{(1)}(r) + \frac{K_\rho^{(1)}(r)}{c^2(r)}. && (4.91)\\
K_c^{(2)}(r) &= \frac{-2\rho(r)K_\rho^{(1)}(r)}{c(r)}, && (4.92)\\
K_\rho^{(3)}(r) &= K_\rho^{(1)}(r) + c^2(r)K_\kappa^{(1)}(r), && (4.93)\\
K_c^{(3)}(r) &= 2\rho(r)c(r)K_\kappa^{(1)}(r), && (4.94)\\
K_{\Gamma_1}^{(4)}(r) &= P(r)K_\kappa^{(1)}(r), && (4.95)\\
K_\rho^{(4)}(r) &= K_\rho^{(1)}(r) + [B^{(4)}(0) - B^{(4)}(r)][\frac{g(r)}{r^2} + \bar{S}^{(4)}(r)], && (4.96)\\
K_c^{(5)}(r) &= -\frac{2\rho(r)}{c(r)}K_\rho^{(4)}(r) + \frac{2\rho(r)}{c(r)}[S^{(5)}(0) - S^{(5)}(r)][\frac{g(r)}{r^2} + \bar{S}^{(5)}(r)], && (4.97)\\
K_{\Gamma_1}^{(5)}(r) &= K_{\Gamma_1}^{(4)}(r) - \frac{c(r)K_c^{(5)}(r)}{2\Gamma_1(r)}, && (4.98)\\
K_\eta^{(6)}(r) &= \frac{g(r)}{r^2c^2(r)}\left[\int_0^r \rho K_\rho^{(3)} r^2 dr - 4\pi G\int_0^r \rho(r)r^2 S^{(6)}(r)dr\right], && (4.99)\\
K_c^{(6)}(r) &= K_c^{(3)}(r) - \frac{2\eta(r)}{c(r)}K_\eta^{(6)}(r), && (4.100)\\
K_\eta^{(7)}(r) &= -K_\kappa^{(2)}(r)\frac{g(r)\rho^2(r)}{\dot{\rho}(r)}, && (4.101)\\
K_\rho^{(7)} &= K_\rho^{(1)}(r) + 2c^2(r)K_\kappa^{(1)}(r) + 4\pi G S^{(7)}(r) \\
&+ \frac{1}{r^2}\left\{2\psi\dot{\psi}\frac{r^2}{\rho^2\eta g} + \psi^2\frac{d}{dr}\left[\frac{r^2}{\rho^2\eta g}\right]\right\} && (4.102)
\end{aligned}
$$

and

$$
\begin{aligned}
S^{(1)}(r) &= \int_r^{R_\odot} 2U(r')F(r')\rho(r')dr', && (4.103)\\
\bar{S}^{(4)}(r) &= \int_r^{R_\odot} \frac{4\pi G\rho(r')}{r'^2}dr', && (4.104)\\
B^{(4)}(r) &= \int_r^{R_\odot} K_\kappa^{(1)}(r')\Gamma_1(r')r'^2 dr', && (4.105)\\
S^{(5)}(r) &= \int_r^{R_\odot} \frac{K_c^{(5)}(r')c(r')}{2P(r')}r'^2 dr', && (4.106)\\
\bar{S}^{(5)}(r) &= \int_r^{R_\odot} \frac{4\pi G\rho(r')}{r'^2}dr', && (4.107)
\end{aligned}
$$

$$S^{(6)}(r) = \int_0^r \frac{\eta(r')K_\eta^{(6)}(r')}{g(r')}dr', \tag{4.108}$$

$$S^{(7)}(r) = \int_r^{R_\odot} \frac{\rho(r')c^2(r').K_\kappa^{(1)}(r')}{g(r')}dr', \tag{4.109}$$

and ψ and $\dot{\psi}$ are given respectively by equations (4A.49) and (4A.50). The kernels $K_c^{(5)}$, $K_\eta^{(6)}$, and $K_\rho^{(7)}$ are the solutions of integral equations. The rest of the kernels in equations (4.89)-(4.102) are in closed form. To solve these integral equations numerically, we use the following procedure. An inital guess for the given kernel is obtained by calculating those terms on the right hand side of the equality which are known *a priori*. This first solution is then substituted into the remaining terms to obtain a second solution for the desired kernel. This procedure is iterated until convergence. Depending on the mode, we have found numerically that the solutions to these equations converge to sufficient accuracy with no less than three but no more than seven iterations.

IV. THE THEORETICAL RELATIONSHIP OF THE STRATIFICATION PARAMETER TO PREDICTIONS OF MIXING LENGTH THEORY

a) Overview of Mixing Length Theory

Mixing length theory (*e.g.*, Cox and Giuli 1968; Gough and Weiss 1976) is the most widely used method to calculate the temperature gradient ∇ in convectively unstable regions. The goals of mixing length theory are to predict the temperature stratification ∇, the convective heat flux F_c, and the convective velocity $\bar{v}$. Below the strongly super-adiabatic boundary layer the Sun convects very efficiently and thus $\nabla = \nabla_{ad}$ to a high degree of accuracy. In the bulk of the convection zone, the high thermal capacity of the gas and the relatively small radiative losses (of the buoyant parcels of material) leads to high convective efficiency and so only slight superadiabaticity is required to transport the heat flux. The entropy in this region is nearly constant (slightly increasing with depth) and the pressure and temperature lie on an adiabat, *i.e.*

$$P = KT^{\frac{\Gamma_2}{\Gamma_2 - 1}} \tag{4.110}$$

where K identifies the particular adiabat under consideration. This relation follows from the definition of the second adiabatic exponent:

$$\nabla = \nabla_{ad} = (\Gamma_2 - 1)/\Gamma_2. \tag{4.111}$$

The quantity K is a constant provided that Γ_2 is a constant, and therefore K assumes different values in each of the ionization zones. The entropy jump from the surface of the star to the nearly adiabatic region determines the value of the constant K. The entropy jump depends on the mixing length theory and the choice of mixing length Λ. The structure of the convection zone is specified by the constant value of the entropy s, the equation of state, and the composition.

In solar evolution calculations, the primary use of mixing length theory is to determine the entropy jump across the superadiabatic region. The entropy jump defines the adiabat of the convection zone and implicitly determines K in equation (4.110). The strength of convective instability is measured by $\nabla_r - \nabla_{ad}$ where ∇_r is the radiative gradient. The radiative opacity κ_r becomes quite large in the H, He, and HeI ionization zones and the pressure increases dramatically compared to the temperature because Γ_2 approaches unity in an ionizing region. Since ∇_r is proportional to $\kappa_r P/T^4$ the radiative gradient becomes very large in these regions. It reaches a peak value at the base of the HeI ionization zone and decreases roughly as $1/T^3$ until the depth where $\nabla_r = \nabla_{ad}$ (the base of the convection zone). Since P and T have been on adiabats since the transition point to efficient convection (just beneath the strongly superadiabatic layer), the peak value of ∇_r depends on the value of P and T at the transition point. These P and T values depend in turn on the entropy jump. Thus only the integrated properties and not the detailed structure of the super-adiabatic region are relevant to the structure of the rest of the Sun. The metal abundance can also affect the depth of the convection zone since metal ionization can become important at high temperatures and thereby raise the radiative temperature gradient.

To gain insight on how mixing length theory determines certain aspects of the structure of the convection zone, we derive asymptotic expressions for the superadi-

abatic temperature gradient in the limit of low and high convective efficiencies, and the expression for the stratification parameter in the corresponding limits. We obtain the well known result that the radial variation of the pressure and temperature in strongly superadiabatic regions has a strong dependence on the value of the mixing length.

Using the radial rate of change of entropy given in equation (4.16), we find the entropy jump from the photosphere to the adiabatic part of the convection zone is given by

$$\Delta S = \int_{r_{ad}}^{R_\odot} \frac{ds}{dr} dr = \int_{r_{ad}}^{R_\odot} \frac{c_p}{H_P} \left[\nabla_{ad} - \nabla - \frac{1}{c_p} \left(\frac{\partial s}{\partial \mu} \right)_{P,T} \mu \nabla_\mu \right] dr \qquad (4.112)$$

where r_{ad} is the depth at which $(\nabla - \nabla_{ad})$ first becomes negligibly small. The radial variation of $(\nabla - \nabla_{ad})$ in the strongly superadiabatic region depends critically on the mixing theory and choice of mixing length (see Gough and Weiss 1976). The most significant contribution to the entropy jump integral comes from the subphotospheric region where the applicability of the mixing length theory is most suspect. The density in this region is small and the radiative losses are large which taken together imply that the thermal capacity of the gas is low. To transport the luminosity, an appreciable superadiabatic gradient and a large convective velocity is required. Approaching the surface, the dominant mode of heat transport switches from convective to radiative since the convective efficiency becomes so low and since the medium becomes optically thin.

We point to the connection between the thermal stratification and the stratification parameter since the helioseismic recovery of the latter could be used for a variety of applications. The radial variation of $\eta(r)$ is sensitive to the superadiabaticity of the sub-photospheric region, the depth at which the convection zone first becomes adiabatic, and the entropy jump from the photosphere to this depth. An empirical determination of $\eta(r)$ would provide data with which to fit the temperature gradient ∇ as a function of density or optical depth to an empirical law (in the manner of the Krishna-Swamy relation for instance). The $\eta(r)$ profile changes abruptly at

the base of the convection zone. In addition, it sensitive to the subadiabaticity and chemical stratification in the core and radiative zone. To make clear the context of our development, we briefly summarize the principal features of mixing theory. Since the asymptotic results we derive in the following depend on the specific form of mixing length theory used, we follow the extremely clear development of Cox and Giuli (1968).

Mixing length theory is to calculate ∇ in convectively unstable regions. In the convectively stable portions of a star, the temperature gradient is set equal to the radiative gradient *i.e.*

$$\nabla = \nabla_r = \frac{3L_r}{16\pi acGM_r}\frac{\kappa P}{T^4}. \tag{4.113}$$

During the evolution calculation, a stability criteria must be evaluated at each radial knot of the stellar model to determine which temperature gradient to use. There are three possible criteria one could choose from (two of which are equivalent). Often, the Schwarzschild criteria is used (the mixing length formalism is employed if $\nabla_r > \nabla$). This criteria takes into account the thermal stratification only. Alternatively, one may use the Ledoux criteria which accounts for the chemical as well as the thermal stratification. Here, the mixing length formalism is used if $\nabla_r > \nabla_{cr}$ where

$$\nabla_{cr} = \nabla_{ad} - \left(\frac{\partial lnT}{\partial ln\mu}\right)_{P,\rho}\frac{\partial ln\mu}{\partial M_r}\frac{4\pi r^4 P}{GM_r} \tag{4.114}$$

The third criteria that one could use is to evaluate the stratification parameter η. The star is convectively unstable at a given radius if

$$\eta = -H_p\Gamma_1\rho^{-1}\frac{d\rho}{dr} \tag{4.115}$$

is less than 1 at that point. We showed in §II this is equivalent to the Ledoux instability criteria.

According to Bohm-Vitense's theory, to calculate ∇ one begins by postulating that the mixing length is given by

$$\Lambda = \alpha H_p \tag{4.116}$$

where α is a constant, typically between one and two. Physical reasoning leads one to the cubic equation

$$\xi^{\frac{1}{3}} + B\xi^{\frac{2}{3}} + a_0 B^2 \xi - a_0 B^2 = 0 \tag{4.117}$$

which must be solved for the unknown variable ξ given by

$$\xi = \frac{\nabla_r - \nabla}{\nabla_r - \nabla_{ad}} = \frac{a_0 \Gamma^2}{1 + \Gamma(1 + a_0 \Gamma)}. \tag{4.118}$$

Here, $a_0 = 9/4$ and Γ is a measure of convective efficiency given by

$$\Gamma = \frac{\nabla - \nabla'}{\nabla' - \nabla_{ad}}. \tag{4.119}$$

The gradient ∇' is the temperature gradient of the convecting element. The quantity B is given by

$$B = \left[A^2(\nabla_r - \nabla_{ad})\right]^{\frac{1}{3}} \tag{4.120}$$

where

$$A = \frac{Q^{1/2} c_p \kappa_r g \rho^{5/2} \Lambda^2}{12\sqrt{2} a c P^{1/2} T^3}, \tag{4.121}$$

and $Q = (4 - 3\beta)\beta^{-1}$ (where β is the ratio of the gas pressure to the total pressure). In this development, ξ is the basic unknown. As $\xi \to 0$, $\Gamma \to 0$ (inefficient convection) and as $\xi \to 1$, $\Gamma \to \infty$ (efficient convection). It can be shown that there is only one real root of equation (4.117) for $0 \leq \xi \leq 1$. Once ξ is determined, the important quantities ∇, $\nabla - \nabla'$, and Γ are given by

$$\nabla = (1 - \xi)(\nabla_r) + \xi \nabla_{ad}, \tag{4.122}$$

$$\nabla - \nabla' = \left[\frac{\xi(\nabla_r - \nabla_{ad})}{A a_0}\right]^{\frac{2}{3}}, \tag{4.123}$$

$$\Gamma = B\xi^{\frac{1}{3}}. \tag{4.124}$$

The ratio of convective flux to the total flux is given by

$$\frac{F_c}{F} = [1 - \frac{\nabla_{ad}}{\nabla_r}]\xi. \tag{4.125}$$

The ratio of the convective velocity to the local sound speed v_s can be written

$$\frac{\bar{v}}{v_s} = \frac{\alpha Q^{1/2} (\nabla - \nabla')^{1/2}}{2\sqrt{2\Gamma_1}}. \tag{4.126}$$

From equation (4.122) we have

$$(\nabla - \nabla_{ad}) = (1 - \xi)(\nabla_r - \nabla_{ad}). \tag{4.127}$$

Thus, $1 - \eta$ can be written

$$1 - \eta = \frac{v_s^2 Q}{H_p g}(\nabla - \nabla_{ad}) = \frac{v_s^2 Q}{H_p g}(1 - \xi)(\nabla_r - \nabla_{ad}). \tag{4.128}$$

From equations (14.83) and (14.84) of Cox and Giuli (1968) we can derive approximate solutions for $(1 - \xi)$ for low ($B << 1$), and high ($B >> 1$) convective efficiencies. We have

$$1-\xi = \begin{cases} 1 - a_0 A^4(\nabla_r - \nabla_{ad})^2[1 - 3A^2(\nabla_r - \nabla_{ad}) + \\ (9 - 3a_0)A^4(\nabla_r - \nabla_{ad})^2] & \text{B} << 1 \\ \frac{1}{[a_0^2 A^2(\nabla_r - \nabla_{ad})]^{1/3}}\left[1 - \frac{2}{3[a_0^2 A^2(\nabla_r - \nabla_{ad})]^{1/3}} + \frac{(1-a_0)}{3[a_0^2 A^2(\nabla_r - \nabla_{ad})]^{2/3}}\right] & \text{B} >> 1 \end{cases} \tag{4.129}$$

Combining this result with equation (4.128), we obtain

$$1-\eta = \begin{cases} \frac{v_s^2 Q}{H_p g}\{(\nabla_r - \nabla_{ad}) - a_0^4 A^4(\nabla_r - \nabla_{ad})^3[1 - 3A^2(\nabla_r - \nabla_{ad}) + \\ (9 - 3a_0)A^4(\nabla_r - \nabla_{ad})^2]\} & \text{B} << 1 \\ \frac{v_s^2 Q}{H_p g}\frac{(\nabla_r - \nabla_{ad})}{[a_0^2 A^2(\nabla_r - \nabla_{ad})]^{1/2}}\left[1 - \frac{2}{3[a_0^2 A^2(\nabla_r - \nabla_{ad})]^{1/3}} + \frac{(1-a_0)}{3[a_0^2 A^2(\nabla_r - \nabla_{ad})]^{2/3}}\right] & \text{B} >> 1 \end{cases} \tag{4.130}$$

Setting

$$A = \alpha^2 E \quad \text{and} \quad E = \frac{Q^{1/2} c_p \kappa g \rho^{5/2} H_p^2}{12\sqrt{2} a c P^{1/2} T^3}, \tag{4.131}$$

the expressions for $1 - \eta$ at low and high convective efficiencies can be written

$$1-\eta = \begin{cases} \frac{v_s^2 Q}{H_p g}\{(\nabla_r - \nabla_{ad}) - a_0^4 \alpha^8 E^4(\nabla_r - \nabla_{ad})^3[1 - 3\alpha^4 E^2(\nabla_r - \nabla_{ad}) + \\ (9 - 3a_0)\alpha^8 E^4(\nabla_r - \nabla_{ad})^2]\} & \text{B} << 1 \\ \frac{v_s^2 Q}{H_p g}\frac{(\nabla_r - \nabla_{ad})^{1/2}}{\alpha^2 a_0 E}\left[1 - \frac{2/3}{\alpha^{4/3}[a_0^2 E^2(\nabla_r - \nabla_{ad})]^{1/3}} + \frac{(1-a_0)}{3\alpha^{8/3}[a_0^2 E^2(\nabla_r - \nabla_{ad})]^{2/3}}\right] & \text{B} >> 1 \end{cases} \tag{4.132}$$

We have ignored mean molecular weight gradients. The necessary correction term can easily be deduced from equation (4.25).

b) Inferring the Mixing Length Ratio from Helioseismic Data

There are several ways in which the mixing length ratio α could be determined from helioseismic data. The first possible approach is deterministic and the second is a monte-carlo technique based upon χ^2 minimization.

In the first approach, the quantity $1-\eta$ is inverted from the oscillation frequencies as a function of radius. The inversion for $1-\eta$ is underdetermined. However, once the radial profile of $1-\eta$ is obtained, α can be estimated by performing a nonliner, least squares fit using equation (4.132). The analytic formulae in equation (4.132), though fairly accurate if the conditions on the convective efficiency measure B are satisfied, are only approximate. The second approach avoids this problem .

In the second approach, a suite of solar models are evolved with various combinations of (X/Z, α), for example, where X is the hydrogen abundance and Z is the metal abundance.. For each model, the mixing length ratio α is held constant and the ratio of the hydrogen to metallic abundance (X/Z) is changed until the solar radius and luminosity are matched. For each model the profile of $(\nabla - \nabla_{ad})$ is retained. We denote this profile by $(\nabla - \nabla_{ad})_i^{theo(\alpha)}$. The superscript indicates the profile is the result of a theoretical forward calculation and depends on the mixing length ratio α. Next, the radial dependence of the quantity $1-\eta$ is inverted from the data and related to $(\nabla - \nabla_{ad})$ from equation (4.128). We denote this profile by $(\nabla - \nabla_{ad})_i^{data}$. Once these profiles are obtained, the χ^2 quantity

$$\chi^2_\alpha = \sum_{i=1}^{K} \frac{[(\nabla - \nabla_{ad})_i^{theo(\alpha)} - (\nabla - \nabla_{ad})_i^{data}]^2}{[(\nabla - \nabla_{ad})_i^{theo(\alpha)}]^2} \tag{4.133}$$

is formed for each theoretical model. The index i indicates the radial grid knot, and K is the total number of grid knots. The model which yields the smallest χ^2_α best fits the data, and is therefore the model with the best choice of mixing length.

The numerical value of the mixing length ratio α depends on the particular mixing length theory implemented (see Gough and Weiss 1976). Much more fundamental is the stratification $(\nabla - \nabla_{ad})$ in the strongly superadiabatic region of the Sun. An inversion for $1-\eta$ would in principle yield the value of $(\nabla - \nabla_{ad})$ and the result

would be independent of mixing length theory. Just as the Krishna Swamy relates temperature to optical depth in stellar atmospheres, an inversion for $\nabla - \nabla_{ad}$ could be used to as the basis of an empirical law relating the thermal stratification to either the temperature or density depth of an atmosphere until the point where the convection is strongly adiabatic.

Appendix 4A

DERIVATION OF PERTURBATION EQUATIONS

In this appendix we present the derivation of equations (4.82)-(4.88).

a) Derivation of equation (4.82)

To derive equation (4.82), we take the variation equation (4.78) and apply Rayleigh's Principle to obtain

$$\delta\omega^2 \int_0^{R_\odot} \rho[U^2 + l(l+1)V^2]r^2dr + \omega^2 \int_0^{R_\odot} \delta\rho[U^2 + l(l+1)V^2]r^2dr =$$
$$\int_0^{R_\odot} [\delta\kappa(\dot{U} + F)^2 - 2UFg\delta\rho - 2UF\rho\delta g + 8\pi GU^2\delta\rho +$$
$$2\delta\rho\left(U\dot{\phi}_1 + \frac{l(l+1)V\phi_1}{r}\right)]r^2dr. \tag{4A.1}$$

We seek to express $\delta\omega^2$ in the above equation in terms of $\delta\rho$ and $\delta\kappa$. The gravity perturbation δg can be expressed in terms of $\delta\rho$ with the identity

$$\delta g(r) = \frac{4\pi G}{r^2} \int_0^r \delta\rho(r')r'^2dr'. \tag{4A.2}$$

In this appendix, we must repeatedly use the rules for differentiation of integrals which are

$$\frac{d}{dx}\int_x^a f(t)dt = -f(x) \text{ and } \frac{d}{dx}\int_a^x f(t)dt = f(x) \tag{4A.3}$$

where x is the independent variable, t is a dummy variable, a is a constant, and $f(t)$ is an arbitrary function of t. Using the first rule in equation (4A.3) we can derive the identity

$$\int_0^{R_\odot} A(r)m(r)dr = -\int_0^{R_\odot} \partial_r S(r)m(r)dr \tag{4A.4}$$

where

$$S(r) = \int_r^{R_\odot} A(r')dr' \tag{4A.5}$$

and $m(r)$ and $A(r)$ are arbitrary functions of radius. To complete the transformation of the integral over δg into one over $\delta\rho$ in equation (4A.1), we set $A(r) = 2UF\rho r^2$, and $m(r) = \delta g(r)$ in equation (4A.4) and perform an integration by parts to obtain

$$\int_0^{R_\odot} 2UF\rho\delta g(r)r^2dr = 4\pi G \int_0^{R_\odot} S^{(1)}(r)\delta\rho(r)r^2dr \tag{4A.6}$$

where

$$S^{(1)}(r) = \int_r^{R_\odot} 2U(r')F(r')\rho(r')dr'. \tag{4A.7}$$

Substituting equation (4A.6) into equation (4A.1), and separating terms in $\delta\rho$ and $\delta\kappa$ yields equation (4.82).

b) Derivation of equation (4.83)

The result in equation (4.83) can be obtained by replacing $\delta\rho$ in equation (4.82) with the expression

$$\delta\rho = \frac{1}{c^2}\delta\kappa - \frac{2\rho}{c}\delta c \tag{4A.8}$$

(which follows from taking the variation of $c^2 = \kappa/\rho$) and separating terms in δc and $\delta\kappa$.

c) Derivation of equation (4.84)

Equation (4.84) can be derived by replacing $\delta\kappa$ in equation (4.82) with $\delta\kappa = c^2\delta\rho + 2\rho c\delta c$ (which follows from eq. 4A.8) and separating the terms in $\delta\rho$ and δc.

d) Derivation of equation (4.85)

To derive equation (4.85) we begin by replacing $\delta\kappa$ in equation (4.82) with the expression

$$\delta\kappa(r) = \Gamma_1(r)\delta P(r) + P(r)\delta\Gamma_1(r), \tag{4A.9}$$

which can be derived by taking the variation of $\kappa = P\Gamma_1$. The pressure is given by

$$P(r) = \int_r^{R_\odot} \rho(r')g(r')dr' \tag{4A.10}$$

so that $\delta P(r)$ is given by

$$\delta P(r) = \int_r^{R_\odot} \left[g(r')\delta\rho(r') + \frac{4\pi G\rho(r')}{r'^2} \int_0^{r'} \delta\rho(r'')r''^2 dr'' \right] dr' \tag{4A.11}$$

which follows from equation (4A.2). Inserting equation (4A.9) into equation (4.82) and using equation (4A.11), we obtain

$$\begin{aligned} \delta\omega^2 N = & \int_0^{R_\odot} \{K_\rho^{(1)}\delta\rho + PK_\kappa^{(1)}\delta\Gamma_1 + \\ & \Gamma_1 K_\kappa^{(1)} \left[\int_r^{R_\odot} [g(r')\delta\rho(r') + \frac{4\pi G\rho(r')}{r'^2} \int_0^{r'} \delta\rho(r'')r''^2 dr'']dr' \right] \} r^2 dr. \end{aligned} \tag{4A.12}$$

The rightmost term in equation (4A.12) can be simplified by setting

$$A(r') = \frac{4\pi G\rho(r')}{r'^2} \quad \text{and} \quad m(r') = \int_0^{r'} \delta\rho(r'')r''^2 dr'' \tag{4A.13}$$

in equation (4A.4), and performing an integration by parts to obtain

$$\begin{aligned} & \int_0^{R_\odot} \left[\Gamma_1(r)K_\kappa^{(1)}(r) \int_r^{R_\odot} \frac{4\pi G\rho(r')}{r'^2} \int_0^{r'} \delta\rho(r'')r''^2 dr'' dr' \right] r^2 dr = \\ & \int_0^{R_\odot} \Gamma_1(r)K_\kappa^{(1)}(r) \int_r^{R_\odot} [\bar{S}^{(4)}(r')\delta\rho(r')r'^2 dr']r^2 dr \end{aligned} \tag{4A.14}$$

where

$$\bar{S}^{(4)}(r') = \int_{r'}^{R_\odot} \frac{4\pi G\rho(r''')}{r'''^2} dr'''. \tag{4A.15}$$

Setting

$$A(r) = \Gamma_1(r)K_\kappa^{(1)}(r)r^2 \quad \text{and} \quad m(r) = \int_r^{R_\odot} \bar{S}^{(4)}(r')\delta\rho(r')r'^2 dr' \tag{4A.16}$$

in equation (4A.4), and performing an integration by parts, we obtain

$$\begin{aligned} & \int_0^{R_\odot} \Gamma_1(r)K_\kappa^{(1)}(r) \int_r^{R_\odot} [\bar{S}^{(4)}(r')\delta\rho(r')r'^2 dr']r^2 dr = \\ & \int_0^{R_\odot} [B^{(4)}(0) - B^{(4)}(r)]\bar{S}^{(4)}(r)\delta\rho(r)r^2 dr \end{aligned} \tag{4A.17}$$

where $B^{(4)}(r)$ is given by

$$B^{(4)}(r) = \int_{r'}^{R_\odot} \Gamma_1(r')K_\kappa^{(1)}(r')r'^2 dr'. \tag{4A.18}$$

Returning to equation (4A.12) we can apply techniques similar to those already used to derive the identity

$$\int_0^{R_\odot} \Gamma_1(r) K_\kappa^{(1)}(r) \int_r^{R_\odot} [\delta\rho(r')g(r')dr'] r^2 dr = \int_0^{R_\odot} [B^{(4)}(0) - B^{(4)}(r)] g(r)\delta\rho(r) dr. \tag{4A.19}$$

Replacing the last two terms in equation (4A.12) with equations (4A.17) and (4A.19), we obtain equation (4.85) which is the desired result.

e) Derivation of equation (4.86)

To derive the kernels $K_c^{(5)}(r)$ and $K_{\Gamma_1}^{(5)}(r)$ in equation (4.86) we begin by postulating the identity

$$\delta\omega^2 N = \int_0^{R_\odot} [K_\rho^{(4)}(r)\delta\rho(r) + K_{\Gamma_1}^{(4)}(r)\delta\Gamma_1(r)] r^2 dr = \int_0^{R_\odot} [K_c^{(5)}(r)\delta c(r) + K_{\Gamma_1}^{(5)}(r)\delta\Gamma_1(r)] r^2 dr. \tag{4A.20}$$

The perturbation $\delta c(r)$ on the right hand side of equation (4A.20) can be replaced with the identity

$$\delta c = \frac{1}{2}\Big[\frac{c(r)}{\Gamma_1(r)}\delta\Gamma_1 - \frac{c(r)}{\rho(r)}\delta\rho + \frac{\Gamma_1(r)}{c(r)\rho(r)}\left\{\int_r^{R_\odot}\left[g(r')\delta\rho(r') + \frac{4\pi G\rho(r')}{r'^2}\int_0^{r'}\delta\rho(r'')r''^2 dr''\right]dr'\right\}\Big]. \tag{4A.21}$$

Equation (4A.21) can be derived by taking the variation of equation (4.2) and replacing δP with the expression in equation (4A.11). Performing this operation and equating the appropriate groups of terms we obtain the identities

$$\begin{aligned} \int_0^{R_\odot} K_\rho^{(4)}(r)\delta\rho(r) r^2 dr &= \int_0^{R_\odot} \frac{c(r)K_c^{(5)}(r)}{2P(r)} \\ &\times \{\int_r^{R_\odot}\left[g(r')\delta\rho(r') + \frac{4\pi G\rho(r')}{r'^2}\int_0^{r'}\delta\rho(r'')r''^2 dr''\right]dr'\} r^2 dr \\ &- \int_0^{R_\odot} \frac{c(r)K_c^{(5)}(r)}{2\rho(r)}\delta\rho r^2 dr, \end{aligned} \tag{4A.22}$$

$$K_{\Gamma_1}^{(4)}(r) = \frac{c(r)K_c^{(5)}(r)}{2\Gamma_1(r)} + K_{\Gamma_1}^{(5)}(r). \tag{4A.23}$$

The first term on the right hand side of equation (4A.22) can be simplified by setting

$$A(r) = \frac{c(r)r^2}{2P(r)} K_c^{(5)}(r) \quad \text{and} \quad m(r) = \int_r^{R_\odot} \delta\rho(r')g(r')dr' \tag{4A.24}$$

in equation (4A.4) and performing an integration by parts, which yields

$$\int_0^{R_\odot} \frac{c(r)K_c^{(5)}(r)}{2P(r)} \left[\int_r^{R_\odot} g(r')\delta\rho(r')dr'\right] r^2 dr = \int_0^{R_\odot} [S^{(5)}(0) - S^{(5)}(r)]g(r)\delta\rho(r)dr \tag{4A.25}$$

where

$$S^{(5)}(r) = \int_r^{R_\odot} \frac{c(r')r'^2 K_c^{(5)}(r')}{2P(r')} dr'. \tag{4A.26}$$

Using a similar methodology, we can show that

$$\int_0^{R_\odot} \frac{c(r)K_c^{(5)}(r)}{2P(r)} \left[\int_r^{R_\odot} \frac{4\pi G\rho(r')}{r'^2} \int_0^{r'} \delta\rho(r'')r''^2)dr''\right] dr'r^2 dr =$$
$$\int_0^{R_\odot} [S^{(5)}(0) - S^{(5)}(r)]\bar{S}^{(5)}(r)\delta\rho(r)r^2 dr. \tag{4A.27}$$

where

$$\bar{S}^{(5)}(r) = \int_r^{R_\odot} \frac{4\pi G\rho(r')}{r'^2} dr'. \tag{4A.28}$$

Inserting the identities in equations (4A.25) and (4A.27) into equation (4A.22), inferring the appropriate equalities, and solving for $K_c^{(5)}$, and $K_{\Gamma_1}^{(5)}$, we obtain

$$K_c^{(5)}(r) = -\frac{2\rho}{c} K_\rho^{(4)}(r) + \frac{2\rho}{c}[S^{(5)}(0) - S^{(5)}(r)][\frac{g(r)}{r^2} + \bar{S}^{(5)}(r)], \tag{4A.29}$$

$$K_{\Gamma_1}^{(5)}(r) = K_{\Gamma_1}^{(4)}(r) - \frac{c(r)K_c^{(5)}(r)}{2\Gamma_1(r)}. \tag{4A.30}$$

Equation (4A.29) is an integral equation for $K_c^{(5)}$. A suggested method of solution is described in §III. Once $K_c^{(5)}$ is obtained numerically, the kernel $K_{\Gamma_1}^{(5)}$ follows immediately.

f) Derivation of equation (4.87)

To derive equation (4.87) we begin by postulating the identity

$$\delta\omega^2 N = \int_0^{R_\odot} [K_\rho^{(3)}(r)\delta\rho(r) + K_c^{(3)}(r)\delta c(r)]r^2 dr = \int_0^{R_\odot} [K_c^{(6)}(r)\delta c(r) + K_\eta^{(6)}(r)\delta\eta(r)]r^2 dr. \tag{4A.31}$$

Taking the variation of $\eta = -c^2\dot{\rho}/(\rho g)$, inserting the resulting expression into $\delta\eta$ of equation (4A.31), and equating the appropriate groups of terms, we obtain the identities

$$K_c^{(6)}(r) = K_c^{(3)}(r) - \frac{2\eta(r)}{c(r)}K_\eta^{(6)}(r), \tag{4A.32}$$

$$\int_0^{R_\odot} K_\rho^{(3)}(r)\delta\rho(r)r^2dr = \int_0^{R_\odot}[-\frac{\eta(r)K_\eta^{(6)}(r)}{\rho(r)}\delta\rho(r) - \frac{c^2(r)}{\rho(r)g(r)}K_\eta^{(6)}(r)\frac{d\delta\rho(r)}{dr} - \eta(r)K_\eta^{(6)}(r)\frac{\delta g(r)}{g(r)}]r^2dr. \tag{4A.33}$$

The δg term in equation (4A.33) can reduced to a term over $\delta\rho$ in a manner similar to the derivation of equation (4A.6). We find

$$-\int_0^{R_\odot}\eta K_\eta^{(6)}\frac{\delta g}{g}r^2dr = \int_0^{R_\odot} 4\pi G S^{(6)}(r)\delta\rho r^2dr \tag{4A.34}$$

where

$$S^{(6)}(r) = \int_0^r \frac{\eta(r')K_\eta^{(6)}(r')}{g(r')}dr'. \tag{4A.35}$$

The integral in equation (4A.33) over $d\delta\rho/dr$ can be integrated by parts to yield

$$\int_0^{R_\odot} -\frac{c^2(r)}{\rho(r)g(r)}K_\eta^{(6)}(r)\frac{d\delta\rho(r)}{dr}r^2dr = -\int_0^{R_\odot}\delta\rho(r)\frac{d}{dr}\left(\frac{r^2c^2(r)K_\eta^{(6)}(r)}{\rho(r)g(r)}\right)dr \tag{4A.36}$$

where we have neglected a surface term. Replacing the appropriate terms in equation (4A.33) with equations (4A.34) and (4A.36), we obtain the identity

$$K_\rho^{(3)} = -\frac{\eta K_\eta^{(6)}}{\rho} + \frac{1}{r^2}\frac{d}{dr}\left(\frac{r^2c^2K_\eta^{(6)}}{\rho g}\right) + 4\pi G S^{(6)}(r). \tag{4A.37}$$

Multiplying equation (4A.37) by ρr^2 and integrating from 0 to r, we obtain

$$\int_0^r \rho K_\rho^{(3)}r^2dr = -\int_0^r \eta K_\eta^{(6)}r^2dr + 4\pi G\int_0^r \rho(r)r^2S^{(6)}(r)dr + \int_0^r \rho\frac{d}{dr}\left(\frac{r^2c^2K_\eta^{(6)}}{\rho g}\right)dr. \tag{4A.38}$$

The last term in equation (4A.38) can be integrated by parts to yield

$$\int_0^r \rho\frac{d}{dr}\left(\frac{r^2c^2K_\eta^{(6)}}{\rho g}\right)dr = \frac{c^2(r)r^2K_\eta^{(6)}(r)}{g} + \int_0^r \eta K_\eta^{(6)}r^2dr. \tag{4A.39}$$

Substituting equation (4A.39) into equation (4A.38) and solving for $K_\eta^{(6)}$ we obtain

$$K_\eta^{(6)}(r) = \frac{g(r)}{r^2c^2(r)}\left[\int_0^r \rho K_\rho^{(3)}r^2dr - 4\pi G\int_0^r \rho(r)r^2S^{(6)}(r)dr\right] \tag{4A.40}$$

which is an integral equation for $K_\eta^{(6)}$(r). A method of solution is suggested in §III.

g) Derivation of equation (4.88)

To derive equation (4.88) we begin by postulating the identity

$$\begin{aligned}\delta\omega^2 N &= \int_0^{R_\odot}[K_\rho^{(1)}(r)\delta\rho(r) + K_\kappa^{(1)}(r)\delta\kappa(r)]r^2dr \\ &= \int_0^{R_\odot}[K_\rho^{(7)}(r)\delta\rho(r) + K_\eta^{(7)}(r)\delta\eta(r)]r^2dr. \qquad (4A.41)\end{aligned}$$

Substituting the relation

$$\delta\kappa = -\frac{g\rho^2\delta\eta}{\dot\rho} + 2c^2\delta\rho + \frac{\rho c^2}{g}\delta g - \frac{\rho c^2}{\dot\rho}\frac{d\delta\rho}{dr} \qquad (4A.42)$$

into the left hand side of equation (4A.41) and equating the appropriate groups of terms, we obtain the identities

$$K_\eta^{(7)}(r) = -K_\kappa^{(1)}(r)\frac{g\rho^2}{\dot\rho}, \qquad (4A.43)$$

$$\int_0^{R_\odot}[K_\rho^{(1)}(r)\delta\rho(r) + K_\kappa^{(1)}(r)\left\{2c^2\delta\rho + \rho c^2\frac{\delta g}{g} - \frac{\rho c^2}{\dot\rho}\frac{d\delta\rho}{dr}\right\}]r^2dr =$$

$$\int_0^{R_\odot} K_\rho^{(7)}(r)\delta\rho(r)(r)r^2dr. \qquad (4A.44)$$

To transform the integral over $\delta g(r)$ in equation (4A.44) to an integral over $\delta\rho(r)$

$$A(r) = \frac{\rho c^2 r^2 K_\kappa^{(1)}(r)}{g} \quad \text{and} \quad m(r) = \delta g(r) \qquad (4A.45)$$

in equation (4A.4), and integrate by parts to obtain

$$\int_0^{R_\odot}\frac{\rho c^2 K_\kappa^{(1)}(r)}{g}\delta g(r)r^2dr = 4\pi G\int_0^{R_\odot} S^{(7)}(r)\delta\rho(r)r^2dr \qquad (4A.46)$$

where

$$S^{(7)}(r) = \int_r^{R_\odot}\frac{\rho(r')c^2(r')K_\kappa^{(1)}(r')}{g(r')}dr'. \qquad (4A.47)$$

Consider the integral in equation (4A.44) over $d\delta\rho/dr$. Performing an integration by parts we obtain

$$\int_0^{R_\odot}\frac{\rho(r)c^2(r)K_\kappa^{(1)}(r)}{\dot\rho(r)}\frac{d\delta\rho(r)}{dr}r^2dr = -\int_0^{R_\odot}\delta\rho\frac{d}{dr}\left[\frac{K_\kappa^{(1)}\kappa r^2}{\dot\rho}\right]dr \qquad (4A.48)$$

We were able to discard the surface contribution by application of the boundary condition $\Delta P = \kappa(\dot{U} + F) = 0$ where ΔP is the Lagrangian pressure variation. Letting

$$\psi = \kappa(\dot{U} + F), \tag{4A.49}$$

we can show from the equation of motion that

$$\frac{d\psi}{dr} = \left(-\rho\omega^2 - \frac{4\rho g}{r} + \frac{\rho l(l+1)g^2}{r^2\omega^2}\right) U - \frac{l(l+1)g}{r^2\omega^2}\psi + \left(\frac{\rho l(l+1)g}{r^2\omega^2} - \frac{(l+1)\rho}{r}\right)\phi_1 + \rho\left(\dot{\phi}_1 + \frac{(l+1)\phi_1}{r} + 4\pi G\rho U\right) \tag{4A.50}$$

Using equations (4A.49) and (4A.50), the right hand side of equation (4A.48) can be written

$$-\int_0^{R_\odot} \delta\rho \frac{d}{dr}\left[\frac{K_\kappa^{(1)}\kappa r^2}{\dot{\rho}}\right] dr = \int_0^{R_\odot} \delta\rho \frac{d}{dr}\left[\psi^2 \frac{r^2}{\rho^2\eta g}\right] dr$$
$$= \int_0^{R_\odot} \delta\rho \left\{2\psi\dot{\psi}\frac{r^2}{\rho^2\eta g} + \psi^2 \frac{d}{dr}\left[\frac{r^2}{\rho^2\eta g}\right]\right\} dr. \tag{4A.51}$$

Substituting equations (4A.46) and (4A.51) into equation (4A.44) we obtain finally, the desired result

$$K_\rho^{(7)} = K_\rho^{(1)} + 2c^2(r)K_\kappa^{(1)}(r) + 4\pi G S^{(7)} + \frac{1}{r^2}\left\{2\psi\dot{\psi}\frac{r^2}{\rho^2\eta g} + \psi^2\frac{d}{dr}\left[\frac{r^2}{\rho^2\eta g}\right]\right\}. \tag{4A.52}$$

ACKNOWLEDGEMENTS

We thank Dr. Philipp Podsiadlowski for assistance in proving equation (4.38), and for sharing his insight into the theory of stellar structure.

REFERENCES

Backus, G., and Gilbert, F. 1967 *Geophys.J.R.Astr.Soc.*, **13**, 247.

Bullen, K.E. 1967 *Geophys.J.R.Astr.Soc.*, **13**, 459.

Christensen-Dalsgaard, J., Duvall, T.L., Jr., Gough, D.O., Harvey, J.W., and Rhodes, E.J., Jr. 1985, *Nature*, **315**, 378.

Christensen-Dalsgaard, J., Dappen, W., and Lebreton, Y. 1988, *Nature*, **336**, 634.

Cox, J.P., and Giuli, R.T. 1968, *Principles of Stellar Structure* (New York: Gordon and

Breach).

Duvall, T.L.Jr., Harvey, J.W., Libbrecht, K.G., Popp, B.D., and Pomerantz, M.A. 1988, *Ap. J.* **324**, 1158.

Edmonds, A.R. 1960, *Angular Momentum in Quantum Mechanics* (Princeton: Princeton University Press).

Kippenhahn, R., Weigert, A., and Hofmeister, E., 1967, in *Methods in Computational Physics,* Vol. **7**, ed. B. Alder, S. Fernback, and M. Rhothenberg (New York: Academic Press), 129-190.

Gough, D.O., and Weiss, N.O. 1976. *M.N.R.A.S.*, **176**, 589.

Libbrecht, K.G., and Kaufman, J.M. 1988, *Ap. J.*, **324**, 1172.

Masters, T.G., 1979, *Geophys.J.R.Astr.Soc.*, **57**, 507.

Phinney, R.A., and Burridge, R. 1973, *Geophys.J.R.Astr.Soc.*, **34**, 451.

Ulrich, R.K., and Rhodes, E.J.Jr., 1977, *Ap. J.* **218**, 521.

CHAPTER 5

CONCLUSION

ESTRAGON: I can't go on like this.

VLADIMIR: That's what you think.

Waiting for Godot (1948)

Samuel Beckett

CONCLUSION

We have carried out three separate investigations in this thesis. Our aim has been to derive new methodologies with which to address important issues confronting helioseismology. These include the influence of the structure and internal dynamics of the Sun on the oscillations, and the influence of nonlinear interactions among the modes on their frequencies and amplitudes.

In Chapter 2, we derived a theory to model the influence of large scale convection on solar oscillations. We implemented the theory with the aid of a realistic convective flow model provided to us by Dr. Gary Glatzmaier. We treated the forward problem only; the inverse problem is much more difficult and will be the subject of future work. However, we obtained several important results from the forward modelling. First, the convective flow appears to be able to generate departures in the a_1 coefficients from the value predicted by bulk rotation alone that are similar in magnitude to observations. Second, the combined effect of poloidal and toroidal flow fields on the frequencies is sufficient to generate a_2 coefficients that are in some cases comparable in magnitude to a_2 coefficients measured by observers.

In Chapter 3, we used weak turbulence theory from plasma physics to derive the kinetic equation for p modes in spherical geometry and an expression for the frequency shift of a mode due to nonlinear interactions. The purpose of the derivation was to provide a theoretical framework with which to address the question of mode excitation. If it can be shown that three mode coupling cannot decisively damp overstable modes, then one would conclude that it is more likely the modes are excited by turbulence rather than by the κ-mechanism. This work is intended to complement the work of Kumar and Goldreich.

In Chapter 4, we applied Rayleigh's Principle to derive perturbation equations relating small model perturbations to differences between theoretical and observed modal frequencies. We showed how these problems can serve as the basis of inverse problems to recover important free parameters of stellar evolution theory such as the *mixing length*.

With the unprecedented amount of helioseismic data soon forthcoming from the GONG network and the SOHO satellite, we are poised to learn a great deal about the physics of the Sun. We hope the work in this thesis will aid in that quest.